
Electronic Thesis and Dissertation Repository

3-28-2019 2:30 PM

Sedimentology, Lithostratigraphy and Geochronology of the Paleoproterozoic Gordon Lake Formation, Huronian Supergroup, Ontario, Canada

Carolyn M. Hill
The University of Western Ontario

Supervisor
Corcoran, Patricia L.
The University of Western Ontario

Graduate Program in Geology

A thesis submitted in partial fulfillment of the requirements for the degree in Doctor of Philosophy

© Carolyn M. Hill 2019

Follow this and additional works at: <https://ir.lib.uwo.ca/etd>



Part of the [Sedimentology Commons](#)

Recommended Citation

Hill, Carolyn M., "Sedimentology, Lithostratigraphy and Geochronology of the Paleoproterozoic Gordon Lake Formation, Huronian Supergroup, Ontario, Canada" (2019). *Electronic Thesis and Dissertation Repository*. 6084.

<https://ir.lib.uwo.ca/etd/6084>

This Dissertation/Thesis is brought to you for free and open access by Scholarship@Western. It has been accepted for inclusion in Electronic Thesis and Dissertation Repository by an authorized administrator of Scholarship@Western. For more information, please contact wlsadmin@uwo.ca.

Abstract

The Gordon Lake Formation of the Paleoproterozoic Huronian Supergroup is a primarily-siliciclastic succession ranging from 300 to 1100 m thick. Lithostratigraphic and sedimentological analysis of the formation in the Bruce Mines and Flack Lake areas, and Killarney and Lady Evelyn-Smoothwater provincial parks revealed 7 lithofacies, which comprise 3 distinct lithofacies associations. The lithofacies associations are subtidal nearshore, subtidal to shallow shelf, and mixed intertidal flat. Microbially-induced sedimentary structures (MISS) related to microbial mat destruction and decay were recognized in the Flack Lake area. The preserved MISS include sand cracks, mat chips, remnant gas domes, and pyrite patches, and iron laminae. A biological origin for the fossil structures is supported by their similarities to modern and ancient documented examples of MISS, the sand-dominated nature of the substrate in which they are preserved, and key microtextures identified in thin section. The identified MISS support the interpretation of a tidal flat depositional environment. The Gordon Lake Formation contains soft-sediment deformation structures (SSDS) in all four study areas. Identified SSDS include load casts, convolute bedding, pseudonodules, ball-and-pillow structures, flame structures, syn-sedimentary faults, and one dewatering pipe. The primary trigger mechanism is interpreted to be storm or tsunami activity, however seismic shock, overloading brought about by density inversions, or a combination of these processes, may have influenced the development of the structures to a lesser degree. Microbial mats may have played a minor role in the formation of the SSDS, but do not appear to have been a prominent driving mechanism. Detrital zircon U-Pb ages from a sandstone provide new evidence for the maximum depositional age of the formation and reinterpretation of the depositional history of the upper Huronian Supergroup. The average age of the youngest zircon grains constrains the age of deposition to sometime after 2315 ± 5 Ma, but prior to intrusion of gabbro (Nipissing) approximately 95 m.y. later.

Keywords

Gordon Lake Formation, Huronian Supergroup, Paleoproterozoic, siliciclastic, carbonate, shallow marine, subtidal, tides, microbially induced sedimentary structures (MISS), soft-sediment deformation structures (SSDS), U-Pb geochronology

Co-Authorship Statement

The following people contributed to the publication of work undertaken as part of this thesis:

Carolyn M. Hill, The University of Western Ontario = **Candidate**

Patricia L. Corcoran, The University of Western Ontario, Supervisor = **Author 1**

Fred J. Longstaffe, The University of Western Ontario = **Author 2**

Rohan D.J. Aranha, The University of Western Ontario = **Author 3**

Don W. Davis, The University of Toronto = **Author 4**

Paper 1; Chapter 3 – *Microbially induced sedimentary structures in the Paleoproterozoic upper Huronian Supergroup, Canada*: Candidate was the primary author and with author 1 contributed to the conception and design of the research project and prepared the paper. Authors 2 and 3 assisted in the field. Published in Precambrian Research 281, 155-165.

Paper 2; Chapter 4 – *Processes responsible for the development of soft-sediment deformation structures (SSDS) in the Paleoproterozoic Gordon Lake Formation, Huronian Supergroup, Canada*: Candidate was the primary author and contributed to the planning, execution, and preparation of the research project and subsequent paper. Author 1 contributed to the conception, design, and execution of the research project and interpretation of the work by critically revising the paper. Published in Precambrian Research 310, 63-75.

Paper 3; Chapter 5 – *New U-Pb geochronology evidence for 2.3 Ga detrital zircon grains in the youngest Huronian Supergroup formations, Canada*: Candidate was the primary author and contributed to the planning, execution, and preparation of the research project and subsequent paper. Author 4 contributed to the analysis and interpretation of the research data, imaged the detrital zircon grains using BSE and CL, and constructed the U-Pb concordia plots and age probability density diagrams. Author 1 contributed to the interpretation of the work by critically revising the paper. Published in Precambrian Research 314, 428-433.

Acknowledgments

First, I would like to extend my deepest thanks to my supervisor, Dr. Patricia Corcoran, for introducing me to the Huronian Supergroup in second year field camp and allowing me to work on this project. Under her guidance and with her unwavering support, my abilities, confidence, and curiosity as a scholar have grown considerably. I am forever grateful for her mentorship and friendship, and will look back particularly fondly on all of our time spent doing fieldwork together. I would also like to thank Dr. Fred Longstaffe and Dr. Burns Cheadle for their sage counsel, suggestions, and support as members of my thesis committee. Thanks are also due to Dr. Darrel Long for his advice, constructive feedback, and for sharing his expertise on the Huronian Supergroup.

I greatly appreciate the field and lab assistance offered by Sara Belontz, Magdalena Kapron, Tim Howe, and Rohan Aranha. This project was supported by a Queen Elizabeth II Graduate Scholarship in Science and Technology, Ontario Graduate Scholarship, and travel grants from the Precambrian Division of the Geological Association of Canada and the International Association of Sedimentologists, for which I am grateful. I would also like to thank my co-author Dr. Don Davis (University of Toronto) for U-Pb data collection and analysis of detrital zircons, Ontario Parks for approving research permits to work in Killarney and Lady Evelyn-Smoothwater provincial parks, the Ontario Geological Survey in Sault Ste. Marie for access to drill core, and everyone in Western's Department of Earth Sciences for creating a welcoming community. A special thank you goes to the examination committee (Dr. Alessandro Ielpi, Dr. Jisuo Jin, Dr. Elizabeth Webb and Dr. Peter Ashmore) for their insightful revisions and thoughtful questions during my defence.

Last but certainly not least, I would like to thank my wonderful husband Dominik for his endless patience, encouragement, and unconditional love over the last five years. This journey would have been much more difficult without him. I am also thankful for the support and diversion offered by my family and friends.

Table of Contents

Abstract	i
Co-Authorship Statement.....	iii
Acknowledgments.....	iv
Table of Contents	v
List of Tables	ix
List of Figures	x
List of Appendices	xix
Chapter 1	1
1 Introduction	1
1.1 Overview	1
1.2 Research questions.....	2
1.3 Geological history of the Huronian Supergroup.....	4
1.3.1 Elliot Lake Group	8
1.3.2 Hough Lake Group	8
1.3.3 Quirke Lake Group.....	9
1.3.4 Cobalt Group.....	9
1.3.5 Flack Lake Group	10
1.3.6 Correlative Successions	11
1.3.7 Composition of the Paleoproterozoic atmosphere	12
1.4 Local geology and access.....	12
1.5 Structure of the dissertation	13
1.6 References.....	14
Chapter 2.....	21

2	The Paleoproterozoic Gordon Lake Formation, Huronian Supergroup, Canada: a macro-tidal to shallow marine shelf, characterized by microbial, tide, and storm activity	21
2.1	Introduction.....	21
2.2	Geological Setting.....	22
2.2.1	Gordon Lake Formation.....	24
2.3	Methodology.....	26
2.4	Lithofacies descriptions and interpretations	27
2.4.1	Very fine- to fine-grained sandstone.....	32
2.4.2	Fine- to medium-grained sandstone.....	38
2.4.3	Carbonate	42
2.4.4	Interlaminated to interbedded mudstone and fine-grained sandstone.....	45
2.4.5	Coarse-grained sandstone	48
2.4.6	Intraformational granular to pebbly sandstone and conglomerate.....	50
2.4.7	Mudstone.....	53
2.5	Discussion.....	56
2.5.1	Paleoenvironmental interpretation and lithofacies associations	56
2.5.2	Basin dynamics	63
2.5.3	Summary of the depositional history of the Gordon Lake Formation	64
2.6	Conclusion	65
2.7	References.....	66
	Chapter 3.....	76
3	Microbially induced sedimentary structures in the Paleoproterozoic, upper Huronian Supergroup, Canada	76
3.1	Introduction.....	76
3.2	Geological Setting.....	77
3.2.1	Flack Lake Group	80

3.3 Upper Huronian Supergroup MISS	82
3.3.1 Mat-Destruction Structures	82
3.3.2 Mat-Decay Structures	84
3.4 Criteria for the biogenicity of MISS in the upper Huronian Supergroup	88
3.5 Discussion	90
3.6 Conclusions	95
3.7 References	95
Chapter 4	104
4 Processes responsible for the development of soft-sediment deformation structures (SSDS) in the Paleoproterozoic Gordon Lake Formation, Huronian Supergroup, Canada	104
4.1 Introduction	104
4.2 Geological Setting	105
4.2.1 Gordon Lake Formation	108
4.3 Bruce Mines area exposure	111
4.3.1 Soft-sediment deformation structures	111
4.3.2 Microbial mats	116
4.4 Discussion	117
4.4.1 Significance of the assemblage of SSDS in the study area	117
4.4.2 SSDS elsewhere in the Gordon Lake Fm	121
4.4.3 Possible triggers for SSD in the Gordon Lake Fm	122
4.4.4 Significance of microbial mats	127
4.5 Conclusion	129
4.6 References	130
Chapter 5	140
5 New U-Pb geochronology evidence for 2.3 Ga detrital zircon grains in the youngest Huronian Supergroup formations, Canada	140

5.1 Introduction.....	140
5.2 Methods.....	143
5.3 Results	144
5.3.1 CH-14-50 Sandstone, Gordon Lake Formation	144
5.3.2 RA-14-79 Claystone, Bar River Formation	145
5.4 Discussion and Conclusion.....	145
5.5 References.....	151
Chapter 6.....	155
6 Conclusions	155
6.1 Lithofacies and lithofacies associations.....	155
6.2 Microbial influence on sedimentation	156
6.3 Other influences on sedimentation.....	157
6.4 Timing of deposition.....	157
6.5 Future studies	158
Appendices.....	159
Curriculum Vitae	235

List of Tables

Table 2.1: Summary, description, and interpretation of lithofacies in the Gordon Lake Formation	33
Table 3.1: Summary of the microbially induced sedimentary structures (MISS) identified in the Gordon Lake and Bar River formations in the Flack Lake area	83
Table 4.1: Summary of soft-sediment deformation structures described in the Huronian Supergroup	107
Table 5.1: Summary of reported upper and lower age limits for the Huronian Supergroup... ..	142

List of Figures

- Figure 1.1:** Simplified geological map showing the distribution of the Huronian Supergroup and locations of the study areas. A) Location of mapping areas in Ontario, Canada. B) General stratigraphy of the Huronian Supergroup. Maximum depositional age (M.D.A.) of the Gordon Lake Formation from Hill et al. (2018) and lower age from Krogh et al. (1984) and Ketchum et al. (2013). C) Simplified geological map of the distribution of the Huronian Supergroup, modified from Young et al. (2001). General locations of the study areas are indicated with black squares. Provincial Park is abbreviated to P.P 5
- Figure 1.2:** Schematic diagram of the basin configuration of the Huronian Supergroup. The Elliot Lake, Hough Lake, and Quirke Lake groups are interpreted to have been deposited in a transform-rift basin, whereas the Cobalt and Flack Lake (unofficial) groups are believed to have been deposited along a passive margin. The syn-volcanic intrusions were likely emplaced during initial rifting. Modified from Young et al. (2001) 7
- Figure 2.1:** General regional geological correlation of the Gordon Lake Formation. Base map modified from Young et al. (2001) 25
- Figure 2.2:** Maps of the Bruce Mines study area. A) Geological map, modified from Giblin et al. (1979). Black box outlines the area in B. B) Outcrop location map with bedding measurements. Figure modified from Google Earth Pro (2018); map data from Google, DigitalGlobe..... 28
- Figure 2.3:** Maps of the Flack Lake study area. A) Geological map, modified from Giblin et al. (1979). Black box outlines the area in B. Legend as in Figure 2.2. B) Outcrop location map with bedding measurements. Figure modified from Google Earth Pro (2018); map data from Google, CNES/Airbus, DigitalGlobe..... 29
- Figure 2.4:** Maps of the Lady Evelyn-Smoothwater Provincial Park study area. A) Geological map, modified from Card and Lumbers (1977). Black boxes outline the areas in B and C. Legend as in Figure 2.2. B) Outcrop location map around McGiffin Lake with bedding measurements. C) Outcrop location map on Smoothwater Lake with bedding

measurements. Figures B and C modified from Google Earth Pro (2018); map data from Google, CNES/Airbus, DigitalGlobe..... 30

Figure 2.5: Maps of the Baie Fine and Killarney Provincial Park study area. A) Geological map, modified from Card (1978b). Black boxes outline the areas in B-E. Legend as in Figure 2.2. B) Outcrop location map of the western end of Baie Fine, with bedding measurements. C) Outcrop location map of the eastern end of Baie Fine, with bedding measurements. D) Outcrop location map between Artist Lake (left) to O.S.A. Lake (right), with bedding measurements. E) Outcrop location map of the eastern part of Killarney Lake, with bedding measurements. Figures B-E modified from Google Earth Pro (2018); map data from Google, CNES/Airbus, DigitalGlobe, TerraMetrics..... 31

Figure 2.6: Representative stratigraphic section for lithofacies 1 from Smoothwater Lake, Lady Evelyn-Smoothwater Provincial Park. Coordinates for the outcrop are 47°23'39.30"N, 80°41'11.58"W..... 35

Figure 2.7: Representative photos of lithofacies 1, very fine- to fine-grained sandstone. A) trough cross-bedded and rippled sandstone with iron stained laminae, from Smoothwater Lake. B) Planar laminated sandstone, from near Flack Lake. C) Mudstone drapes between wavy to low angle cross-bedded sandstone, from Baie Fine. D) Flat-topped ripples with local bifurcations, from Baie Fine. E) Bedding cut by a thick clastic dike. Dashed lines outline the dike margins. Stratigraphically higher than A. F) Small-scale syndimentary fault, with iron staining, in Baie Fine. Pencils are 14.5 cm long and 8 mm wide 36

Figure 2.8: Representative stratigraphic section for lithofacies 2 from Baie Fine. Legend as in Figure 2.6. Coordinates for the outcrop are 46° 2'8.77"N, 81°30'22.25"W 39

Figure 2.9: Representative photos of lithofacies 2 (A-C) and 3 (D-G). A) trough cross-beds in the quartz-rich middle section in Baie Fine (Figure 2.8). Pencil points to top. B) Massive bedded sandstone with thin mudstone interbeds, in Baie Fine near the upper formational contact. Arrow points to top. C) Massive to faintly laminated sandstone with scoured base that tapers out laterally on Artist Lake in Killarney Provincial Park. Interpreted as a tidal channel deposit. Thin adjacent beds contain mudstone pebbles, minor cross laminae, ripples, and minor SSDS. One nodule bed was observed above the channel. Beds generally thin- up

section. Black arrow points to bed termination. Arrow points to top. D) Lenticular bedded fenestral dolostone near Flack Lake. E) Stromatolitic sandy dolostone on Smoothwater Lake. F) Close-up of stratiform stromatolites from E. G) Close-up of laterally-linked, domal stromatolites from E. Pencils are 14.5 cm long and 8 mm wide and camera lens cap is 5.8 cm wide..... 40

Figure 2.10: Representative stratigraphic section for lithofacies 3 from the Flack Lake area. Legend as in Figure 2.6. Coordinates for the outcrop are 46°37'30.97"N, 82°50'1.90"W 43

Figure 2.11: Representative photos of lithofacies 4. A) Interference ripples, near Flack Lake. B) Lenticular bedding, desiccation cracks, rippled sandstone and mudstone drapes in Killarney Provincial Park. C) Oblique view of a reactivation surface in Lady Evelyn-Smoothwater Provincial Park. White arrow points to the erosion surface. D) Complete tidal cycle deposit in Baie Fine. Arrows point to mudstone drapes that were deposited in slack water between both ebb and flood current reversals. Ripple cross laminae support bipolar-opposed tidal currents. E) Interpreted small tidal channel deposit, from Flack Lake area. F) Microbially induced curved and sinuous sand cracks near Flack Lake. Pencils are 14.5 cm long and 8 mm wide..... 46

Figure 2.12: Representative photos of lithofacies 5 and 6. A) Lens of LF5 that tapers out laterally, in the Bruce Mines area. Loading is evident at the base of the bed. B) Photomicrograph of pyrite grain morphologies in A. C) Trough cross-bedding outlined by heavy mineral laminae in Baie Fine. Arrows point to over- and underlying mudstone drapes. Bipolar flow directions were observed in this interval. D) Lithofacies 6a in Lady Evelyn-Smoothwater Provincial Park, interpreted as the base of a fining-upwards storm deposit. E) Lithofacies 6a in Baie Fine. Possible herringbone cross stratification. Note pebbles aligned along foresets. F) Lithofacies 6b in Baie Fine. G) Jasper nodules in thin LF5a bed from Lady Evelyn-Smoothwater Provincial Park. G) Sugary quartz nodules from Baie Fine. Note how bedding was displaced by nodule growth after deposition. Pencils are 14.5 cm long and 8 mm wide..... 49

Figure 2.13: A) Representative stratigraphic section for lithofacies 4 and 7 from the Flack Lake area. Coordinate for the outcrop are 46°35'55.00"N, 82°46'27.30"W. B) Representative

stratigraphic section for lithofacies 6a from Lady Evelyn-Smoothwater Provincial Park. Coordinate for the outcrop are 47°21'48.78"N, 80°31'2.06"W. Legend as in Figure 2.6..... 52

Figure 2.14: Representative photos of lithofacies 7 and bedding types. A) Top of photo shows medium to thick beds of mudstone overlying LF4 in the Flack Lake area. Vertical crack fills and thin lenticular pink sandstone define bedding surfaces. B) Convolute bedding and load structures near Bruce Mines. C) Possible HCS (white arrow) near the top of the formation in Baie Fine. Top to left. D) Thick bedded sandstone near the transition with the overlying Bar River Formation in Baie Fine. Top to right. E) Rapid transition from sandy red beds to fine-grained green mudstone beds in a cliff section (marked by arrow) at Lady Evelyn-Smoothwater Provincial Park. Pencil is 14.5 cm long and 8 mm wide and fieldbook is 19 cm long..... 55

Figure 2.15: Depositional model for the Gordon Lake Formation. A) Deposition of the lower part of the formation, interpreted to have occurred in the subtidal nearshore to shallow shelf zones along a passive margin. B) Deposition of the upper part of the formation, interpreted to have occurred in the subtidal nearshore to mixed intertidal flat zones along a passive margin 62

Figure 3.1: Simplified geologic map of the distribution of the Huronian Supergroup north of Lake Huron. The study area is located 29 km north of Elliot Lake. Modified from Young et al. (2001) and Long (2009) 78

Figure 3.2: General stratigraphy of the Huronian Supergroup. Modified from Long (2004) and Young (2013). Date for Nipissing Diabase from Corfu and Andrews (1986). Date for Copper Cliff Formation from Krogh et al. (1984) and Ketchum et al. (2013) 79

Figure 3.3: Mat-destruction structures identified in the Flack Lake area. Scales include pencil (14.5 cm) and camera lens cap (5.8 cm). (A) Single incipient tears preserved in fine-grained sandstone of the Bar River Formation. (B) Triradiate cracks preserved in fine-grained sandstone of the Gordon Lake Formation. (C) Curved, sinuous sand cracks preserved in siltstone of the Gordon Lake Formation. (D) Curved, corrugated sand cracks preserved in siltstone of the Gordon Lake Formation. (E) Curved sand cracks filled from above preserved in fine-grained sandstone of the Bar River Formation. (F) Curved cracks confined to the

crests of interference ripples preserved in fine-grained sandstone of the Bar River Formation 85

Figure 3.4: Mat-destruction structures identified in the Flack Lake area. Scales include pencil (14.5 cm) and camera lens cap (5.8 cm). (A) Microbial mat chips preserved in iron stained, fine-grained sandstone of the Bar River Formation. (B) Microbial sand and silt chips preserved in fine-grained sandstone of the Gordon Lake Formation. (C) Microbial sand and silt chips preserved in fine-grained sandstone of the Bar River Formation. (D) Microbial sand and silt chips preserved in fine-grained sandstone of the Gordon Lake Formation. Note the frayed margins of the large mat chip and the biolaminations below the pencil. (E) Microbial mat chips preserved in fine-grained sandstone of the Gordon Lake Formation. Note the curled appearance of these chips. (F) Torn mat chip preserved in the same fine-grained sandstone bed as Figure 4-E. Note the mottled appearance of the mat and distinct torn margins..... 86

Figure 3.5: Mat-decay structures identified in the Flack Lake area. Pencil for scale (14.5 cm). (A) Gas domes preserved in fine-grained sandstone of the Gordon Lake Formation. Note the iron staining concentrated around the domes and the shrinkage cracks in the upper left portion of the figure. (B) Close-up of ruptured gas dome preserved in fine-grained sandstone of the Gordon Lake Formation. Note the radial nature of the dome center. (C) Pyrite patches preserved in the troughs of interference ripples in fine- to medium-grained sandstone of the Bar River Formation. (D) Wavy iron laminae preserved in fine- to medium-grained sandstone of the Bar River Formation 87

Figure 3.6: Mat microtextures identified in thin sections from the Gordon Lake Formation. (A) Frayed mat chip preserved in fine-grained sandstone. Note the internal layering and torn margin on the right side of the mat chip. (B) Mat chip preserved in siltstone. Note the iron cement concentrated around the wavy carbonaceous laminae. (C) Mat chips preserved in a granule- to pebble-conglomerate with a siltstone to fine-grained sandstone matrix. (D) Close-up of the center of Figure 6-C showing a layered mat chip (L) and curled mat chip (C). (E) Carbonaceous laminae preserved in siltstone. (F) Oriented quartz grains preserved in mudstone 91

Figure 3.7: Paleoenvironmental setting of upper Huronian Supergroup MISS. Note that the distribution of MISS is related to, but not restricted by, the tidal zones..... 94

Figure 4.1: Simplified geologic map of the distribution of the Huronian Supergroup north of Lake Huron with major fault zones. The study area is located approximately 11.5 km north-northwest of Bruce Mines (small black box). Modified from Young et al. (2001)..... 106

Figure 4.2: Geological map of the Bruce Mines area. The study area is indicated by the white rectangle. Roads not shown for the purpose of clarity. Coordinates for the outcrop are 46°24'08.6"N, 83°49'22.4"W. Modified from Giblin et al. (1979) 110

Figure 4.3: Exposure of the Gordon Lake Formation in the study area. A) Lowest stratigraphic interval exposed along Old Soo Road, composed of mudstone, siltstone, chert, fine-grained sandstone and minor medium-grained sandstone. B) Discontinuous intraformational conglomerate with small-scale load structures indicated by white arrows. C) Large flame (white arrow) and ball-and-pillow structures (black arrow). Note the chaotic nature of the base of this outcrop. Pencil is 14.5 cm long and field book is 19 cm long 113

Figure 4.4: Continuation of the Gordon Lake Formation exposure in the study area. A) Stratigraphic continuation of the outcrop in Figure 4.3a. This section contains thin beds of mudstone, siltstone, fine-grained sandstone and minor medium-grained sandstone. The white circle indicates the start of the stratigraphic section in Figure 4.5. B) Large ball structures and load casts. Note the thin internal laminations. White arrow indicates an internal water-escape structure. Photo colour saturation increased to enhance structures. C) Convolute bedding and load casts. Note the dark microbial mat capping a bedding surface. D) Simple load casts with flame structures. White arrow indicates relatively undeformed laminae. E) Load casts and flame structures. F) Line markings highlighting the main deformation styles in Figure 4e. Person for scale is 178 cm tall, pencil is 14.5 cm long and field book is 19 cm long 114

Figure 4.5: Stratigraphic section illustrating the lower to middle portion of the Gordon Lake Formation exposure on Old Soo Road. Starting interval indicated in Figure 4.4a. Abbreviations: alt., alternating; ms, mudstone; sltst, siltstone; fsst, fine-grained sandstone; msst, medium-grained sandstone 115

Figure 4.6: Pseudonodules and dewatering pipe. A) Small, elongate to circular pseudonodules containing sulphide minerals (white-arrow) and mud rip-up clasts (black arrow). B) Two pseudonodules below a biofilm-bound surface (pencil top). The left structure contains abundant sulphides and mud rip-up clasts, whereas the right structure contains internal laminations and minor sulphides. C) Thin section photomicrograph illustrating the general grain size, sorting, roundness and mineralogy of a pseudonodule. Note the curled, plastic nature of the leftmost mud clast (black arrow). D) Photomicrograph illustrating the general grain size, sorting, roundness and mineralogy of a pseudonodule, and the contact with the surrounding sediment. Note the wispy, soft-sediment deformation patterns that formed in the surrounding sediment during pseudonodule development. E) Small pseudonodules (white arrow) detached from an event layer (oblique section). Note the path of water-escape that successfully pierced through the stabilized layer (thin black arrow) and one that did not (thick black arrow). The bright, undulating bed is interpreted to be biofilm-bound (thick white arrow). F) Cylindrical structure interpreted as a dewatering-pipe. The dashed lines outline the neck of the pipe. Note the chert pebble outlined in black at the base of the pipe and the pseudonodule to the left of the pipe (black arrow). Pencil is 14.5 cm long and 8 mm wide 118

Figure 4.7: Microbial mats and mat chips identified in the Bruce Mines area (oblique sections). A) Laterally and vertically continuous microbial mat with fine, wavy laminations. Note the irregular, undulating surface of the mat and slightly botryoidal horizon (white arrow). B) Close-up of the mat surface from (A) and its botryoidal texture. Photo colour saturation increased to enhance structures. C) Base of microbial mat shown in (A). Note the horizon of sulphide minerals (thick white arrow) and pseudonodules detaching from the base of the biofilm (black arrows). A small, laminated pseudonodule on the right is detached (thin white arrow). D) Fine-grained sandstone bed with wavy laminae and numerous voids (fenestrae?) in the top 2 cm of the bed, interpreted to be a microbial mat. E) Close-up of a second microbial mat displaying wavy to slightly pseudo-columnar appearance. Photo colour saturation increased to enhance structures. F) Small, layered mat-chip with ragged margins. Pencil is 14.5 cm long and 8 mm wide 119

Figure 4.8: Assortment of structures in the middle interval of the outcrop exposure. A) Two examples of load (thin white arrow) and water-escape structures (thin black arrow) in beds

beneath a microbially-stabilized event layer (thick black arrow). The interval immediately above the load structures contains convolute laminae (thick white arrow). B) Small, flat to wavy microbial mats within a fine-grained sandstone bed. C) Large mat-chip surrounded by mudstone and siltstone. Note the ragged margins of the chip and the load structures immediately below. D) Close-up of a large mat-chip showing spongy, irregular texture and mat margins. E) Concave-upward carbonaceous laminae. Note the faint horizontal laminations above and below the laminae, which are often defined by trapped sand and silt sized quartz grains. D) Irregular, wavy, carbonaceous laminae. Note the silt grains bound within the laminae. Pencil is 14.5 cm long 120

Figure 5.1: Distribution and stratigraphy of the Huronian Supergroup north of Lake Huron. A) Location of study area in Ontario, Canada. B) General stratigraphy of the Huronian Supergroup. Location of samples shown with black stars. Maximum depositional ages (M.D.A.) from this study are shown in bold. Lower age from Krogh et al. (1984) and Ketchum et al. (2013). C) Simplified geologic map of the distribution of the Huronian Supergroup, modified from Young et al. (2001). Gordon Lake Formation sample collected at 46°36'17.1"N 82°46'13.2"W and Bar River Formation sample collected at 46°35'52.7"N 82°45'33.7"W 141

Figure 5.2: Backscattered electron (left) and cathodoluminescence (right) images of representative zircon grains from the different age populations in the Gordon Lake and Bar River formations. A) Four zircons from the Bar River Formation. Grains 1, 2 and 4 have an age of ca. 2300 Ma and grain 3 has an age of ca. 2700. B) Four zircons from the Gordon Lake Formation. Grains 21 and 22 have an age of ca. 2700 Ma and grains 23 and 24 have an age of ca. 2500 Ma. C) Three long prismatic zircons from the Gordon Lake Formation with an age of ca. 2300 Ma 146

Figure 5.3: U-Pb data from the Gordon Lake Formation. A) 91 zircon grains, 75 of which were used for radiometric dating. B) U-Pb concordia plot showing data on 75 detrital zircons from quartz-rich sandstone sample CH-14-50 in the Gordon Lake Formation. The inset shows the youngest data..... 147

Figure 5.4: U-Pb data from the Bar River Formation. A) 36 zircon grains, 27 of which were used for radiometric dating. B) U-Pb concordia plot showing data on the detrital zircons from sample BR-14-79 in the Bar River Formation. 148

Figure 5.5: Age probability density diagrams with superimposed histograms for $^{207}\text{Pb}/^{206}\text{Pb}$ ages on detrital zircon grains from sample CH-14-50 of the Gordon Lake Formation (top), and sample BR-14-79 of the Bar River Formation (bottom), Huronian Supergroup 149

List of Appendices

Appendix A: Outcrop locations with coordinates.....	159
Appendix B: Supplementary stratigraphic sections.....	165
Appendix C: Supplementary back-scattered electron (BSE; left) and cathodoluminescence images (CL; right) of detrital zircon grains from the Gordon Lake and Bar River formations	223
Appendix D: Laser-ablation inductively coupled plasma mass spectroscopy (LA-ICP-MS) data from detrital zircons in the Gordon Lake and Bar River formations	228

Chapter 1

1 Introduction

1.1 Overview

The year 2021 will mark the 200th year since the Paleoproterozoic Huronian Supergroup was first the subject of geological research and mapping (Junnila, 1987). In general, the earliest studies dealt with localized mineral exploration and it was not until 1950 that regional investigations and mapping took place. A significant quantity of literature has since been developed on the Huronian Supergroup between industry, government, and academia. The succession is well-known world-wide, particularly for its excellent preservation, economic occurrences, and record of multiple glacial events. The idea that the Huronian Supergroup records multiple glacial periods, the change from an anoxic to oxic early Earth atmosphere, and presents a possibility of global correlation helped renew scientific interest in the succession (Ojakangas, 1988; Kasting and Ono, 2006). This resulted in extensive study of the glacially-influenced formations, such as the Gowganda Formation, and those containing evidence of an anoxic atmosphere, such as the Matinenda Formation, which contains detrital uranium-bearing minerals (Young, 1981a; Hattori et al., 1983).

The Gordon Lake Formation – the focus of this thesis – is the second youngest formation in the Huronian Supergroup and has been poorly studied compared to underlying formations. This has resulted in insufficient understanding of the sedimentological history of the formation, potential indications of early life, and possible evidence for the rise in atmospheric oxygen. The difficulties in conducting a regional study of the Gordon Lake Formation stem from its overall discontinuous outcrop exposure both locally and across the preserved basin, which is over 300 km wide. Despite this, Eisbacher and Bielenstein (1969) recognized vertical trends in the formation and subdivided it into three units. In general, previous studies of the Gordon Lake Formation have focused on individual sedimentary structures or single mapping areas and units (e.g. Wood, 1973; Chandler, 1988; Bekker et al., 2006). The lack of regional studies produced a knowledge

gap concerning the paleodepositional and atmospheric conditions of the upper Huronian Supergroup at the time of deposition (Pavlov et al., 2000; Young et al., 2001; Bekker et al., 2005).

1.2 Research questions

The aim of this thesis project is to investigate the extent to which early life and the lack of vegetation affected sedimentary processes and controlled the composition and overall depositional environment of the Paleoproterozoic Gordon Lake Formation, Huronian Supergroup. A number of aspects are addressed, including fossil evidence of life, the stratigraphy and distribution of lithofacies for paleodepositional reconstruction, and detrital zircon geochronology.

Various depositional environments have been proposed for the Gordon Lake Formation, such as tidal flat, sabkha, lagoon, and deep offshore (Wood, 1973; Card, 1978; Rust and Shields, 1987; Chandler, 1988), however no comprehensive sedimentological study has been reported in the literature. A regional approach was taken herein to evaluate the paleodepositional setting of the Gordon Lake Formation. This thesis contains the first publicly described regional lithofacies analysis of the Gordon Lake Formation and provides new insight into pre-vegetated, Paleoproterozoic surficial environments, as related to early life, Earth's rise in atmospheric oxygen and the break-up of the supercontinent Kenorland. In order to assess the knowledge gap addressed above, four questions were proposed:

(1) Which depositional environment(s) is represented by the Gordon Lake Formation?

In order to address this first, over-arching question, regional and detailed lithostratigraphic and sedimentological investigations were undertaken in four regions where the Gordon Lake Formation is best exposed: north of Bruce Mines (southeast of Sault Ste. Marie), around Flack Lake (north of Elliot Lake), around McGiffin and Smoothwater lakes and along the Lady Evelyn River in Lady Evelyn-Smoothwater Provincial Park, and between Killarney Lake and Baie Fine (inclusive) in Killarney

Provincial Park. Fifty exposed sections and five diamond drill cores through the Gordon Lake Formation were studied, which involved detailed measurement of stratigraphic sections, bedding measurements, and regular sampling of representative rock types. Samples collected from the study areas were used for lithofacies and petrographic analyses, as outlined in Chapter 2.

This question prompted focused inquiries on two groups of sedimentary structures that are recognized in the Gordon Lake Formation. These structures provide information on the sedimentological and tectonic conditions at the time of and shortly following deposition, and are crucial in making an informed interpretation of the conditions at the time of deposition. Within this context, the next two research questions were advanced:

(2) Does the Gordon Lake Formation contain fossil evidence of life?

Recognition of fossil evidence of life in the Gordon Lake Formation was accomplished through lithostratigraphic, sedimentological, and petrographic analysis. Rocks that contain surface textures morphologically similar to modern day microbial mats and microbially induced sedimentary structures (MISS) were described and analyzed under a petrographic microscope in order to identify mat micro-textures in thin section. The descriptions of MISS, microbial mat fragments, and stromatolites are outlined in Chapters 2, 3, and 4.

(3) Which processes and trigger mechanisms led to the formation and distribution of soft-sediment deformation structures (SSDS) in the formation, and what implications does that have for paleodepositional setting and basin tectonism?

The processes and trigger mechanisms that led to the formation of various types of SSDS preserved throughout the Gordon Lake Formation were assessed in consideration of the structural setting and stratigraphic context of the formation. The descriptions of SSDS are outlined in Chapter 4.

The last section of this thesis involves determining whether or not the depositional age of the Gordon Lake Formation can be refined in order to understand its deposition in a stratigraphic and global sense. This led to the fourth research question:

(4) Can the depositional age of the Gordon lake Formation be refined?

Detrital zircon geochronology was used to investigate the maximum depositional age of the formation and to compare it to a depositional age reported from purported tuffs. The radiometric results are outlined in Chapter 5.

1.3 Geological history of the Huronian Supergroup

The Huronian Supergroup is a succession of primarily siliciclastic sedimentary rocks that were deposited between ca. 2455 Ma (Krogh et al., 1984; Ketchum et al., 2013; Bleeker et al., 2013) and 2215 Ma (Corfu and Andrews, 1986; Bleeker et al., 2015), which overlaps with the rise of atmospheric oxygen at ca. 2300 Ma during the Great Oxidation Event (GOE). Minor carbonate and basal volcanic rocks are also preserved in the stratigraphy. The rocks of the Huronian Supergroup are exposed north of Lake Huron and trend roughly east-west from Sault Ste. Marie, Ontario, to the Ontario-Québec border, and north into the Cobalt area (Long, 1978) (Figure 1.1). The Huronian succession thickens to the south where it reaches a thickness of approximately 12 km (Young and Nesbitt, 1999; Long, 2004a). The Huronian Supergroup unconformably overlies Archean rocks of the Superior Province in the north and west, and is bounded by the Grenville Province in the east and Paleozoic strata in the south (Young et al., 2001). Large-scale mapping for this thesis was completed in four areas across the preserved basin (Figure 1.1). In the western (Bruce Mines and Flack Lake) and northern (Lady Evelyn-Smoothwater Provincial Park) study areas, the rocks have been metamorphosed to lower greenschist grade, whereas in the southern study area (Baie Fine and Killarney Provincial Park), the rocks have been metamorphosed to amphibolite grade (Card, 1978). The prefix “meta” is herein omitted for simplicity.

The tectonic setting of the Huronian Supergroup has been thoroughly debated (Young, 1983; Long 2004a). Several tectonic models have been suggested for the southward-

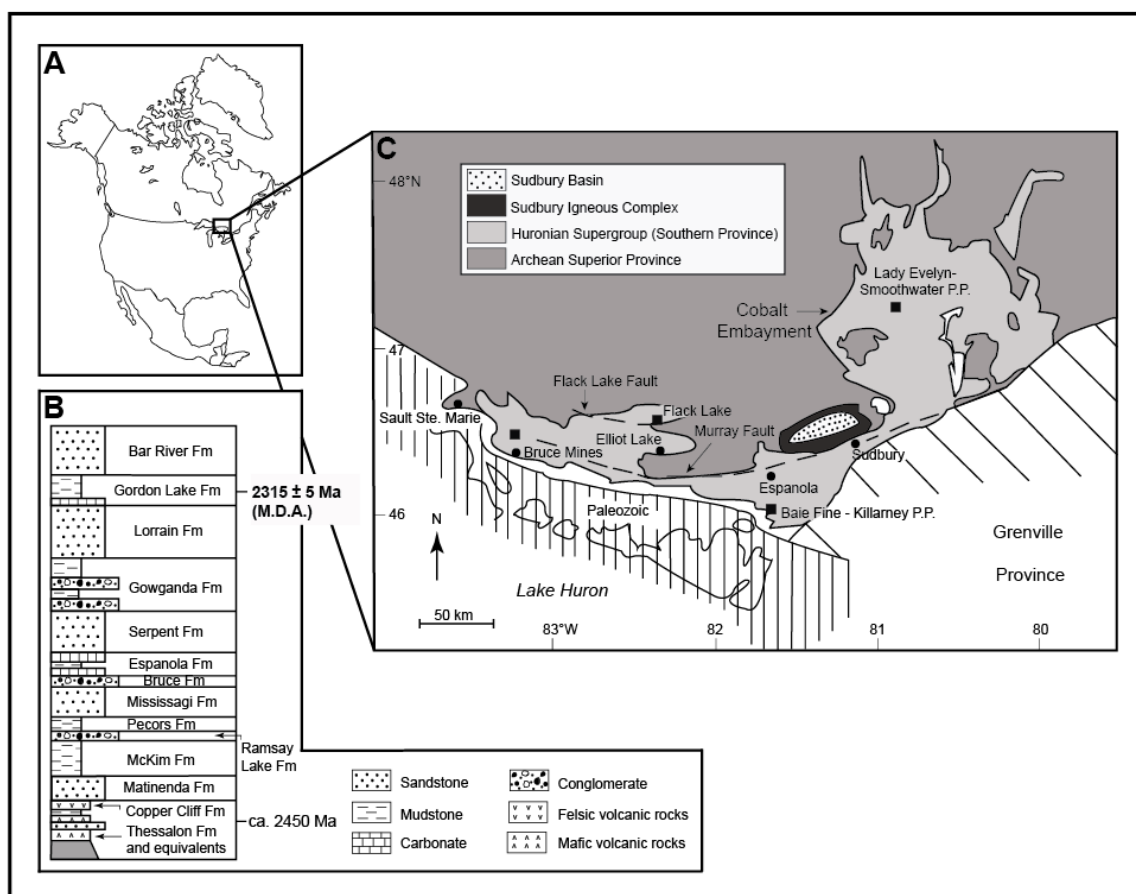


Figure 1.1. Simplified geological map showing the distribution of the Huronian Supergroup and locations of the study areas. A) Location of mapping areas in Ontario, Canada. B) General stratigraphy of the Huronian Supergroup. Maximum depositional age (M.D.A.) of the Gordon Lake Formation from Hill et al. (2018) and lower age from Krogh et al. (1984) and Ketchum et al. (2013). C) Simplified geological map of the distribution of the Huronian Supergroup, modified from Young et al. (2001). General locations of the study areas are indicated with black squares. Provincial Park is abbreviated to P.P.

thickening succession, including rift basin (Parviainen, 1973), aulacogen (Young, 1983), divergent continental margin (Roscoe and Card, 1993), transtensional extensional basins to passive margin (Long and Lloyd, 1983; Long, 2004a), and a passive margin (Bennett et al., 1991). Overall, restricted deposition of the lowermost formations (Serpent Formation and older) is supported by limited areal extent, thickness changes across faults, a lack of marine indicators, and preservation of seismites (Zolnai et al., 1984; Young and Nesbitt, 1985; Long, 2004a; Young, 2014). Conversely, the greater areal extent, evidence of marine conditions, overall uniform paleoflow patterns, and thick deposits of the Gowganda and overlying formations suggests that deposition occurred post-rifting along a subsiding continental margin (Zolnai et al., 1984; Young and Nesbitt, 1985; Long, 1995; Young et al., 2001). However, establishment of a passive margin may have occurred sometime before deposition of the Gowganda Formation (Young, 1970; Young et al., 2001). A transform-rift to passive margin model has largely been adopted by recent authors (e.g. Ojakangas et al., 2001; Young et al., 2001; Long, 2004a; 2009; Hill et al., 2016; Hill and Corcoran, 2018) (Figure. 1.2). Intrusion of Nipissing gabbro dikes and sills through the entire Huronian succession occurred at ca. 2.22 Ga (Corfu and Andrews, 1986; Bleeker et al., 2015). Evidence of incomplete consolidation of Huronian sediments at the time of intrusion of some gabbro bodies suggests that deposition took place until ca. 2.2 Ga (Young et al., 2001). Huronian strata were folded during at least one event known as the Penokean orogeny, which is associated with ocean closure at ca. 1.875 to 1.825 Ga (Van Schmus, 1976; Schulz and Cannon, 2007).

The Huronian Supergroup is composed of four official groups, which are in ascending order: the Elliot Lake, Hough Lake, Quirke Lake and Cobalt groups. However, a fifth, unofficial group, named the Flack Lake Group, has been suggested for the two uppermost formations (Wood, 1973; Long, 2004a; 2009). Three tripartite cycles consisting of a lower paraconglomerate overlain by a fine-grained unit and capped by sandstone are displayed in the Hough Lake, Quirke Lake and Cobalt groups. These cycles are interpreted to represent cycles of glaciation and associated eustatic sea level changes, and reflect the transition from glacially-generated deposits to deeper water deltaic deposits and finally subaerial, predominantly fluvial or shallow marine deposits (McDowell, 1957; Roscoe, 1957; Card et al., 1977; Rice, 1986; Robertson and Card, 1988; Young et al.,

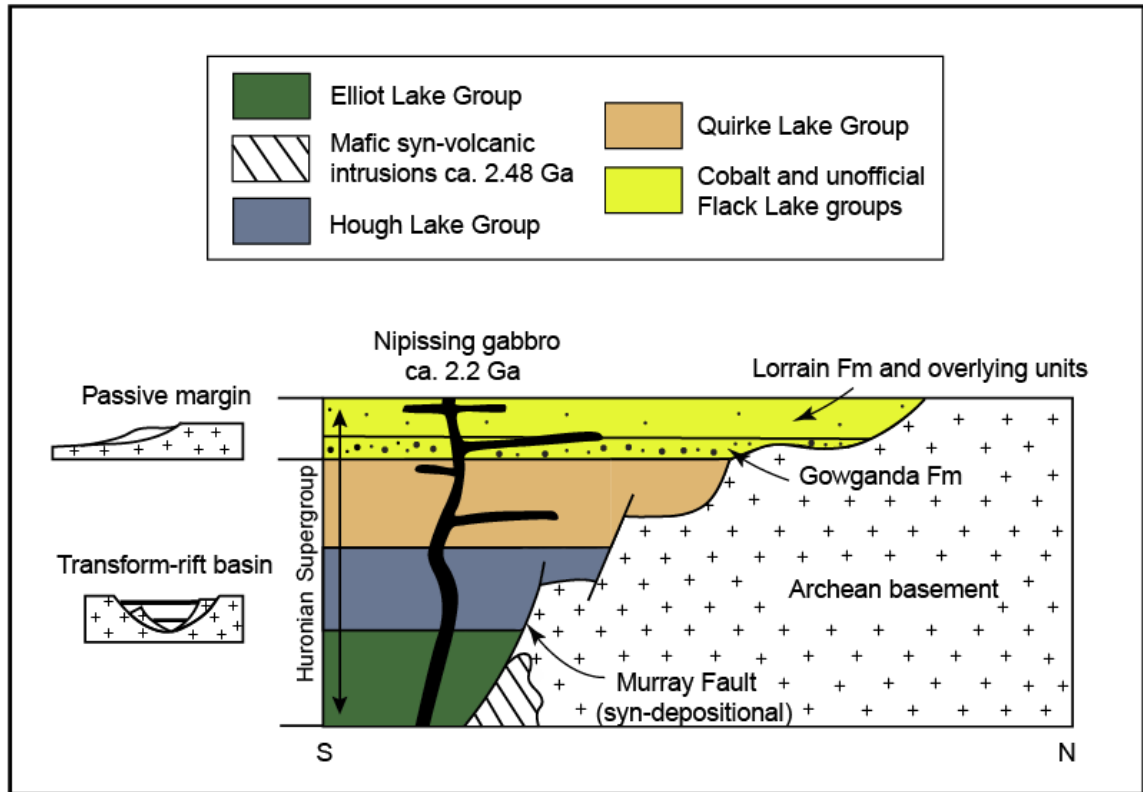


Figure 1.2. Schematic diagram of the basin configuration of the Huronian Supergroup. The Elliot Lake, Hough Lake, and Quirke Lake groups are interpreted to have been deposited in a transform-rift basin, whereas the Cobalt and Flack Lake (unofficial) groups are believed to have been deposited along a passive margin. The syn-volcanic intrusions were likely emplaced during initial rifting. Modified from Young et al. (2001).

2001; Long, 1978; 2004a; 2009).

The Espanola Formation, which represents the fine-grained interval of the Quirke Lake Group tripartite cycle, is unique in that it is the only carbonate-rich formation in the Huronian Supergroup (Young, 2002; Al-Hashim, 2016). Initiation of the Huronian glaciations was likely related to formation of the supercontinent Kenorland (Williams et al., 1991; Aspler and Chiarenzelli, 1998). Enhanced weathering associated with increased exposure of continental material may have drawn down a large enough quantity of atmospheric carbon dioxide to result in global cooling, which would have subsequently initiated the process of glaciation. Alternatively, the rise of atmospheric oxygen levels may have contributed to a drop in temperature due to the elimination of methane and reduced greenhouse effects (Pavlov et al., 2000; Tang and Chen, 2013).

1.3.1 Elliot Lake Group

The Elliot Lake Group is composed of the Livingstone Creek, Matinenda, and McKim formations, which are underlain by local basal volcanic units. The Livingstone Creek Formation is the oldest unit in the Huronian Supergroup and consists of cross-bedded arkosic sandstone with minor carbonate, polymictic conglomerate, siltstone, and wackes (Young et al., 2001). In the western portion of the basin (Thessalon area) the basal volcanic units consist of felsic and mafic rocks, whereas in the central and eastern portions of the basin (Sudbury and Cobalt areas) they are intercalated with rocks of the Matinenda Formation (Bennett et al., 1991; Young et al., 2001). The Matinenda Formation is characterized by pyritic-, quartz-, and uranium-bearing pebble conglomerate and cross-bedded arkosic sandstone (Long, 2009). It is interpreted to have been deposited as alluvial fans and braided rivers (Card and Jackson, 1995; Long et al., 1999). The McKim Formation is composed primarily of mudstone and represents offshore deposition from turbidity currents and prodeltaic suspension deposition (Card et al., 1977; Long, 2009).

1.3.2 Hough Lake Group

The Hough Lake Group is composed of the Ramsay Lake, Pecors, and Mississagi formations. The Ramsay Lake Formation is characterized by sandy, clast-rich

paraconglomerate with minor sandstone and siltstone beds and is interpreted to represent deposition as sub-glacial melt-out (Card et al., 1977; Long, 2009). This first glacial deposit of the Huronian Supergroup is overlain by the Pecors Formation, which is composed of laminated mudstone and wackes of prodeltaic origin (Long, 2009). The Pecors Formation is overlain by shallow braided river deposits of the Mississagi Formation (Long, 1978; 2009). This formation is comprised primarily of cross-bedded arkosic to subarkosic sandstone, with conglomerate and mudstone intervals preserved locally (Long, 1978; 2009). Long (2009) proposed a lacustrine setting for a 120 m-thick muddy sandstone interval in the Cobalt area.

1.3.3 Quirke Lake Group

The Quirke Lake Group is represented by the Bruce, Espanola, and Serpent formations. This tripartite cycle is interpreted to represent the second glaciation during deposition of the Huronian Supergroup. The Bruce Formation is composed of clast-rich, matrix-supported, sandy paraconglomerate that is interpreted to have been deposited beneath a floating ice-shelf (Young, 1981b). The middle, fine-grained unit of the Quirke Lake Group is represented by the Espanola Formation, which is composed mainly of limestone, siltstone, and calcareous siltstone (Long, 2009). Deltaic, lacustrine, and tidally-influenced shallow marine settings have been proposed as paleoenvironmental settings (Bernstein and Young, 1990; Veizer et al., 1992; Junnila and Young, 1995; Card and Jackson, 1995; Al-Hashim, 2016). Stromatolites are described locally in the Espanola Formation (e.g. Hofmann et al., 1980; Al-Hashim, 2016). The overlying Serpent Formation is characterized by cross-bedded arkosic sandstone with local conglomerate and minor siltstone and shale and is generally agreed to have a fluvial origin (Fedo et al., 1997; Long, 2009). The feldspathic nature of the Serpent Formation distinguishes it from the other thick sandstone units of the Huronian Supergroup and it has been attributed to less intense weathering at the time of deposition (Fedo et al., 1997).

1.3.4 Cobalt Group

The Cobalt Group is divided into the Gowganda and Lorrain formations. The Gowganda Formation is composed of two members: the lower Coleman Member, containing

laminated paraconglomerate and mudstone with dropstones, and the upper Firstbrook Member, composed largely of interbedded sandstone and mudstone (Junnila and Young, 1995). Overall, at least two major glacial advances are recognized in the Gowganda Formation, and deposition is interpreted to have occurred beneath a continental ice sheet with periods of deep-water conditions during glacial retreat (Coleman member), followed up-section by a prodeltaic setting (Firstbrook Member) (Young and Nesbitt, 1985; Long and Leslie, 1986). The overlying Lorrain Formation is thick, widespread and characterized by arkosic to quartz-rich sandstone with minor mudstone and quartz-jasper conglomerate. A number of paleoenvironments have been suggested for the Lorrain Formation, including fluvial and shallow marine settings, however the bulk of the formation is generally agreed to have a fluvial origin (Young, 1973a; Lowey, 1985; Chandler, 1986; Roussell and Long, 1998; Long, 2004a).

1.3.5 Flack Lake Group

The unofficial Flack Lake Group is composed of the Gordon Lake and Bar River formations. The Gordon Lake Formation appears to have a gradational contact with the underlying Lorrain Formation, however Wood (1973) described a sharp, unconformable contact between the two formations in drill core. Overall, the formation is characterized by interbedded sandstone, mudstone, and intraformational conglomerate with local basal carbonate (Wood, 1973; Card et al., 1977; Chandler, 1986; 1988; Hill et al., 2016; Hill and Corcoran, 2018). Sedimentary structures indicative of wave, tide, and storm processes are preserved throughout the formation and include various types of ripples, flaser and lenticular bedding, SSDS, and graded beds (Wood, 1973; Hill et al., 2016; Hill and Corcoran, 2018). Evidence of microbial colonization at the time of deposition has been described from two areas where the formation is exposed (Hofmann et al., 1980; Hill et al., 2016; Hill and Corcoran, 2018). Multiple settings have been suggested for the Gordon Lake Formation, from shallow marine to tidal flat to deep marine (Wood, 1973; Frarey, 1977; Card, 1978; Rust and Shields, 1987; Hill et al., 2016; Hill and Corcoran, 2018). The youngest formation of the Huronian Supergroup is the Bar River Formation, which is composed primarily of cross-bedded quartz arenite with minor mudstone interbeds (Wood, 1973; Card et al., 1977; Aranha, 2015). Although most workers agree

that the Gordon Lake and Bar River formations were deposited along a passive margin, there is currently no consensus on the depositional setting represented by either formation. The settings proposed for the Bar River Formation include fluvial, beach with aeolian influence, nearshore to shallow marine, sand shoals, and tidal channel (e.g. Frarey and Roscoe, 1970; Pettijohn, 1970; Wood, 1973; Card, 1978; Chandler, 1984; Rust and Shields, 1987; Aranha, 2015).

1.3.6 Correlative Successions

The Kona Dolomite of the Chocolay Group, Marquette Range Supergroup, Michigan, U.S.A., is interpreted to be broadly correlative with the Gordon Lake Formation (Young, 1983; Ojakangas et al., 2001b; Bekker et al., 2006; Bennett, 2006). It is characterized by dolostone with relatively minor mudstone and sandstone (Larue, 1981). Reported sedimentary features include desiccation cracks, domal and stratiform stromatolites, red beds, evaporite pseudomorphs, ooids, cross-bedding, and ripples (Taylor, 1972; Larue, 1981). Young (1983) suggested that variances in clastic influx may account for the sedimentological differences between the Gordon Lake Formation and Kona Dolomite. He proposed that the Chocolay Group was deposited in a failed rift basin that formed to the west of the area occupied by the Huronian Supergroup.

In terms of sedimentology and stratigraphy, the Snowy Pass Supergroup, Wisconsin, U.S.A., has long been considered similar to the Huronian Supergroup (Young, 1973b; Roscoe and Card, 1993). The Lookout Formation, Lower Libby Creek Group, which is characterized by laminated and rippled sandstone, phyllite, and dolostone, is interpreted to be equivalent to the Gordon Lake Formation (Roscoe and Card, 1993). In Europe, the upper Jatulian subgroup of the Karelian Supergroup, Fennoscandian Shield, has also been generally correlated with the Gordon Lake and Bar River formations (Marmo and Ojakangas, 1984; Ojakangas, 1988; Ojakangas et al., 2001a). This subgroup is composed of mixed chemical-siliciclastic sedimentary rocks and is proposed to have had a marine origin (Ojakangas et al., 2001a). Young (1973) proposed that the Snowy Pass Supergroup may represent a displaced and rotated block of the Huronian basin, whereas Roscoe and Card (1993) suggested that the Huronian Supergroup and the Snowy Pass Supergroup

were contiguous and that the Karelian craton formed at ca. 2.1 Ga during breakup of Kenorland.

1.3.7 Composition of the Paleoproterozoic atmosphere

Evidence of the transition from an anoxic to oxic Earth atmosphere is recorded in the Huronian Supergroup. Evidence for an oxygen-poor atmosphere includes detrital uranium-bearing minerals and pyrite in the Matinenda (Elliot Lake Group) and Mississagi (Hough Lake Group) formations, respectively (Long, 2009), and a lack of red beds in the lower formations. Evidence for an oxygenated atmosphere include red beds in the Gowganda (Cobalt Group) and stratigraphically younger formations, and evaporite minerals in the Gordon Lake Formation (Flack Lake Group) (Wood, 1973; Chandler, 1988). Recognition of stromatolites in the Espanola Formation, microbial mat fragments and stromatolites in the Gordon Lake Formation, and MISS in the Bar River Formation support locally oxygenic conditions at the time of deposition of the upper Huronian Supergroup (Hoffman, et al., 1980; Hill et al., 2016; Al-Hashim, 2016; Hill and Corcoran, 2018).

1.4 Local geology and access

Field investigation of the Gordon Lake Formation was conducted in the summers and falls of 2014, 2015, 2016, 2017 and 2018. The Flack Lake and Bruce Mines areas were mapped in 2014 with overall easy access to outcrop exposures. A boat was required to access the outcrops on Flack Lake. The McGiffin Lake study area in Lady Evelyn-Smoothwater Provincial Park was mapped in 2015. Access to this area was by foot or canoe. In addition, the area was heavily vegetated. In 2016, Baie Fine and a small portion of the western side of Killarney Provincial Park were mapped. Access to this area required a boat or canoe, but it was otherwise easy to navigate between exposures. In 2017, the area from Baie Fine to Killarney Lake was studied and also required the use of a canoe with relatively easy access between both exposures and lakes. Smoothwater Lake in Lady Evelyn-Smoothwater Provincial Park was investigated in the fall of 2017. Access to the lake was gained by float plane and a canoe was used to reach outcrop exposures. In addition to outcrop mapping, five diamond drill cores were logged in the summer of

2018, totaling approximately 725 m of core. Access was granted by the Ontario Geological Survey office in Sault Ste. Marie.

1.5 Structure of the dissertation

This thesis is divided into four main chapters, in addition to introductory (Chapter 1) and concluding (Chapter 6) chapters. Chapter 2 investigates the sedimentology and stratigraphy of the Gordon Lake Formation through detailed regional lithofacies analysis. Lithofacies are described and organized into lithofacies associations based on stratigraphic relationships. The results are compared with modern and ancient examples of similar depositional environments, and a depositional model is proposed for the formation.

Chapter 3 recognizes a previously unidentified group of sedimentary structures in the Gordon Lake and Bar River formations in the Flack Lake area, and reassesses the origin of several types of crack structures from the Gordon Lake Formation. Fossil evidence of microbial mats and MISS are presented and used to aid in paleoenvironmental reconstruction.

Chapter 4 evaluates the origin and possible trigger mechanisms responsible for the formation of SSDS in the Gordon Lake succession and investigates the role that microbial mats played in their formation. The conclusions provide information on conditions during and shortly following deposition, in addition to providing insight into basin tectonics.

Chapter 5 contributes to the understanding of the depositional history of the Huronian Supergroup by providing new U-Pb detrital zircon data for the Gordon Lake and Bar River formations. The data reveal a maximum depositional age of the uppermost formations and associated reinterpretation of the origin of the zircon grains.

Attached appendices include a table listing outcrop locations and coordinates (Appendix A), supplementary stratigraphic sections not included in Chapter 2 (Appendix B), supplementary back-scattered electron (BSE) and cathodoluminescence (CL) images of detrital zircon grains (Appendix C), and geochronological data (Appendix D).

1.6 References

- Al-Hashim, M.H., 2016. Sedimentology and geochemistry of the mixed carbonate-siliciclastic Espanola Formation, Paleoproterozoic Huronian Supergroup, Bruce Mines-Elliot Lake Area, Ontario, Canada (PhD Thesis), The University of Western Ontario. Electronic Thesis and Dissertation Repository, 4350.
- Aranha, R.D.J., 2015. Factors controlling the composition and Lithofacies characteristics of the Paleoproterozoic Bar River Formation, Huronian Supergroup (MSc Thesis), The University of Western Ontario. Electronic Thesis and Dissertation Repository, 3321.
- Aspler, L.B., Chiarenzelli, J.R., 1998. Two Neoproterozoic supercontinents? Evidence from the Paleoproterozoic. *Sed. Geol.* 120, 75-104.
- Bekker, A., Karhu, J.A., Kaufman, A.J., 2006. Carbon isotope record for the onset of the Lomagundi carbon isotope excursion in the Great Lakes area, North America. *Precambrian Res.* 148, 145-180.
- Bekker, A., Kaufman, A.J., Karhu, J.A., Eriksson, K.A., 2005. Evidence for Paleoproterozoic cap carbonates in North America. *Precambrian Res.* 137, 167-206.
- Bennett, G., 2006. Geological features and correlation of a dolostone unit in Fenwick Township, northeast of Sault Ste Marie, Ontario. In: *The Huronian Supergroup between Sault Ste Marie and Elliot Lake, Field Trip Guidebook, Part 4*, 49-50.
- Bennett, G., Dressler, B.O., Robertson, J.A., 1991. The Huronian Supergroup and associated intrusive rocks. In: Thurston, P.C., Williams, H.R., Sutcliffe, R.H., Stott, G.M. (Eds.) *Geology of Ontario, special volume 4, Part 1*. Ontario Geological Survey, Toronto, 549-591.
- Bernstein, L.M., Young, G.M., 1990. Depositional environments of the early Proterozoic Espanola Formation, Ontario, Canada. *Can. J. Earth Sci.* 27, 539-551.
- Bleeker, W., Kamo, S., Ames, D., 2013. New field observations and U-Pb age data for footwall (target) rocks at Sudbury: towards a detailed cross-section through the Sudbury Structure. *Large Meteorite Impacts and Planetary Evolution V. Geol. Soc. Am. Special Papers* 3112.
- Bleeker, W., Kamo, S.L., Ames, D.E., Davis, D., 2015. New field observations and U-Pb ages in the Sudbury area: toward a detailed cross-section through the deformed Sudbury Structure. In: *Targeted Geoscience Initiative 4: Canadian Nickel-Copper Platinum Group Elements-Chromium Ore Systems – Fertility. New and Revised Models*, Geological Survey of Canada Open File, Pathfinders, 153–166.
- Card, K.D., 1978. *Geology of the Sudbury-Manitoulin area, districts of Sudbury and Manitoulin*. Ontario Geological Survey, Geoscience Report 166, 238p.

- Card, K.D., Innes, D.G., Debicki, R.L., 1977. Stratigraphy, Sedimentology, and Petrology of the Huronian Supergroup of the Sudbury-Espanola Area. Ontario Division of Mines, Geoscience Study 16, 99p.
- Card, K.D., Jackson, S.L., 1995. Tectonics and metallogeny of the Early Proterozoic Huronian fold belt and the Sudbury Structure of the Canadian Shield. Geological Survey of Canada Field Trip Guidebook, Open File 3139, 55p.
- Chandler, F.W., 1984. Sedimentary setting of an early Proterozoic copper occurrence in the Cobalt Group, Ontario; A preliminary assessment. In: Current Research, Part A, Geological Survey of Canada Paper 84-1A, 185–192.
- Chandler, F.W., 1986. Sedimentology and paleoclimatology of the Huronian (Early Aphebian) Lorrain and Gordon Lake Formations and their bearing on models for sedimentary copper mineralization. In: Geological Survey of Canada Paper 86-1A, 121–132.
- Chandler, F.W., 1988. Diagenesis of sabkha-related, sulphate nodules in the early Proterozoic Gordon Lake Formation, Ontario, Canada. Carbonates Evaporites 3, 75–94.
- Corfu, F., Andrews, A.J., 1986. A U–Pb age for mineralized Nipissing diabase, Gowganda, Ontario. Can. J. Earth Sci. 23, 107–109.
- Eisbacher, G.H., Bielenstein, H.U., 1969. The Flack Lake depression, Elliot Lake area, Ontario (51 J/10). Geological Survey of Canada Paper 69-1, Part B, 58-60.
- Fedo, C.M., Young, G.M., Nesbitt, H.W., 1997. Paleoclimatic control on the composition of the Paleoproterozoic Serpent Formation, Huronian Supergroup, Canada: a greenhouse to icehouse transition. Precambrian Res. 86, 201-223.
- Frarey, M.J., 1977: Geology of the Huronian Belt Between Sault Ste. Marie and Blind River, Ontario. Geological Survey of Canada, Memoir 383, 87p.
- Frarey, M.J., Roscoe, S.M., 1970. The Huronian supergroup north of Lake Huron. Symposiums on Basins and Geosynclines of the Canadian Shield, Geological Survey of Canada, Paper 70-40, 143-158.
- Hattori, K., Campbell, F.A., Krouse, H.R., 1983. Sulphur isotope abundances in Aphebian clastic rocks: implications for the coeval atmosphere. Nature 302, 323-326.
- Hill, C., Corcoran, P.L., Aranha, R., Longstaffe, F.J., 2016. Microbially induced sedimentary structures in the Paleoproterozoic, upper Huronian Supergroup, Canada. Precambrian Res. 281, 155–165.

- Hill, C.M., Corcoran, P.L., 2018. Processes responsible for the development of soft-sediment deformation structures (SSDS) in the Paleoproterozoic Gordon Lake Formation, Huronian Supergroup, Canada. *Precambrian Res.* 310, 63–75.
- Hill, C.M., Davis, D.W., Corcoran, P.L., 2018. New U-Pb geochronology evidence for 2.3 Ga detrital zircon grains in the youngest Huronian Supergroup formations, Canada. *Precambrian Res.* 314, 428-433.
- Hofmann, H.J., Pearson, D.A.B., Wilson, B.H., 1980. Stromatolites and fenestral fabric in early Proterozoic Huronian Supergroup, Ontario. *Can. J. Earth Sci.* 17 (10), 1351–1357.
- Junnila, R.M., 1987. A bibliography of the Huronian Supergroup: 1821-1987. Ontario Geological Survey, Open File Report 5651, 71p.
- Junnila, R.M., Young, G.M., 1995. The Paleoproterozoic upper Gowganda Formation, Whitefish Falls area, Ontario, Canada; subaqueous deposits of a braid delta. *Can. J. Earth Sci.* 32, 197-209.
- Kasting, J.F., Ono, S., 2006. Palaeoclimates: the first two billion years. *Philosophical Transactions of the Royal Society of London, Series B: Biological Sciences* 361 (1470), 917-929.
- Ketchum, K.Y., Heaman, L.M., Bennett, G., Hughes, D.J., 2013. Age, petrogenesis and tectonic setting of the Thessalon volcanic rocks, Huronian Supergroup, Canada. *Precambrian Res.* 233, 144–172.
- Krogh, T.E., Davis, D.W., Corfu, F., 1984. Precise U–Pb zircon and baddeleyite ages for the Sudbury Structure. In: Pye, E.G., Naldrett, A.J., Giblin, P.E. (Eds.), *Geology and Ore Deposits of the Sudbury Structure*. Ontario Geological Survey, pp. 431–446.
- Larue, D.K., 1981. The Chocoday Group, Lake Superior region, U.S.A: Sedimentologic evidence for deposition in basinal and platform settings on an early Proterozoic craton. *Geol. Soc. Am. Bull.* 92, 7: 417-435.
- Long, D.G.F., 1978. Depositional environments of a thick Proterozoic sandstone; the (Huronian) Mississagi Formation of Ontario, Canada. *Can. J. Earth Sci.* 15, 190-206.
- Long, D.G.F., 1995. Huronian sandstone thickness and paleocurrent trends as a clue to the tectonic evolution of the Southern Province. *Can. Mineral.* 33, Part 4, 922-923.
- Long, D.G.F., 2004a. The tectonostratigraphic evolution of the Huronian basement and subsequent basin fill: geological constraints on impact models of the Sudbury event. *Precambrian Res.* 129, 203–223.

- Long, D.G.F., 2004b. Precambrian Rivers. In: Eriksson, P.G., Altermann, W., Nelson, D.R., Mueller, W.U., Catuneanu, O. (Eds.), *The Precambrian Earth: tempos and events*. *Developments in Precambrian Geology* 12, Elsevier, 660-662.
- Long, D.G.F., 2009. The Huronian Supergroup. In: Rousell, D.H., Brown, G.H. (Eds.), *A Field Guide to the Geology of Sudbury, Ontario*. Ontario Geological Survey, Open File Report 6243, pp. 14–30.
- Long, D.G.F. and Leslie, C.A. 1986. The placer gold potential of the early Aphebian Gowganda Formation along the northern margin of the Cobalt Embayment, with comments on associated concentrations of silver and copper. Ontario Geological Survey, Open File Report 5608, 54p.
- Long, D.G.F., Lloyd, T.R., 1983. Placer gold potential of basal Huronian strata of the Elliot lake Group in the Sudbury Area, Ontario. Ontario Geological Survey, Miscellaneous Paper 116, 256-258.
- Lowey, G.W., 1985. Stratigraphy and sedimentology of the Lorrain Formation, Huronian Supergroup (Aphebian), between Sault Ste. Marie and Elliot Lake, Ontario, and implications for stratiform gold mineralization. Geological Survey of Canada, Open File Report 1154, 60p.
- Marmo, J., Ojakangas, R.W., 1984. Lower Proterozoic glaciogenic deposits, eastern Finland. *Geol. Soc. Am. Bull.* 95, 1055-1062.
- McDowell, J.P., 1957. The sedimentary petrology of the Mississagi quartzite in the Blind River area. Ontario Department of Mines Geological Circular 6, 31p.
- Ojakangas, R.W., 1988. Glaciation; an uncommon mega-event as a key to intracontinental and intercontinental correlation of Early Proterozoic basin fill, North American and Baltic cratons. In: Kleinspehn, K.L., Paola, C. (Eds.), *New Perspectives in Basin Analysis*. Springer, Berlin, pp. 431-444.
- Ojakangas, R.W., Marmo, J.S., Heiskanen, K.I., 2001a. Basin evolution of the Paleoproterozoic Karelian Supergroup of the Fennoscandian (Baltic) Shield. *Sed. Geol.* 141-142, 255-285.
- Ojakangas, R.W., Morey, G.B., Southwick, D.L., 2001b. Paleoproterozoic basin development and sedimentation in the Lake Superior region, North America. *Sed. Geol.* 141-142, 319-341.
- Pavlov, A.A., Kasting, J.F., Brown, L.L., 2000. Greenhouse warming by CH₄ in the atmosphere of early Earth. *J. Geophys. Res.* 105, 11981–11990.
- Parviainen, A.E.U., 1973. The sedimentology of the Huronian Ramsay Lake and Bruce Formations, north shore of Lake Huron, Ontario. Ph.D. thesis, University of Western Ontario, London, Ont., Canada, 426 pp.

- Pettijohn, F.J., 1970. The Canadian Shield; a status report, 1970. In: Baer, A.J. (Ed.), Symposium on Basins and Geosynclines of the Canadian Shield. Geological Survey of Canada Paper 70-40, 239-265.
- Plotnick, R.E., 1986. A fractal model for the distribution of stratigraphic hiatuses. *J. Geol.* 94, 885–890.
- Rice, R.J., 1986. Regional sedimentation in the Lorrain Formation (Aphebian), central Cobalt Embayment. Summary of Field Work and Other Activities: Ontario Geological Survey Miscellaneous Paper 137, 210–216.
- Robertson, J.A., Card, K.D., 1988. Geology and Scenery: North shore of Lake Huron Region. Ontario Geological Survey, Geological Guidebook, 224p.
- Roscoe, S.M., 1957. Stratigraphy, Quirke Lake-Elliot Lake Senior, Blind River area, Ontario. Royal Society of Canada Special Publication Number 6, 54–58.
- Roscoe, S.M., Card, K.D., 1993. The reappearance of the Huronian in Wyoming: rifting and drifting of ancient continents. *Can. J. Earth Sci.* 30, 2475-2480.
- Rousell, D.H., Long, D.G.F., 1998. Are outliers of the Huronian Supergroup preserved in structures associated with the collapse of the Sudbury impact crater? *J. Geol.* 106, 407-419.
- Rust, B.R., Shields, M.J., 1987. The sedimentology and depositional environments of the Huronian Bar River Formation, Ontario. Grant 189, Ontario Geological Survey Open File Report 5672, pp. 37.
- Sadler, P.M. 1999. The influence of hiatuses on sediment accumulation rates. *GeoRes. Forum* 5, 15–40.
- Schulz, K.J., Cannon, W.F., 2007. The Penokean orogeny in the Lake Superior region. *Precambrian Res.* 157, 4-25.
- Sheets, B.A., Hickson, T.A., Paola, C., 2002. Assembling the stratigraphic record: depositional patterns and time-scales in an experimental alluvial basin. *Basin Res.* 14, 287–301.
- Tang, H., Chen, Y., 2013. Global glaciations and atmospheric change at ca. 2.3 Ga. *Geosci. Front.* 4, 583–596.
- Taylor, G.L., 1972. Stratigraphy, sedimentology, and sulfide mineralization of the Kona Dolomite. Ph.D. Thesis. Michigan Technological Institute, Lansing, Michigan, 111 pp.
- Van Schmus, W.R., 1976. Early and middle Proterozoic history of the Great Lakes area, North America. *Philos. Trans. R. Soc. Lond., Ser. A* 280 (1298), 605–628.

- Veizer, J., Clayton, R.N., Hinton, R.W., 1992. Geochemistry of Precambrian carbonates; IV, Early Paleoproterozoic (2.25 + or - 0.25 Ga) seawater. *Geochim. Cosmochim. Ac.* 56, 875-885.
- Williams, H., Hoffman, P.F., Lewry, J.F., Monger, J.W.H., Rivers, T., 1991. Anatomy of North America thematic geologic portrayals of the continent. *Tectonophysics* 187, 117-134.
- Wood, J., 1973. Stratigraphy and depositional environments of Upper Huronian rocks of the Rawhide Lake-Flack Lake area, Ontario. In: Young, G.M. (Ed.) *Huronian stratigraphy and sedimentation*, Geological Association of Canada, Special Paper 12, pp. 73-95.
- Young, G.M., 1970. An extensive Early Proterozoic glaciation in North America? *Palaeogeogr. Palaeoclimatol.* 7, 85-101.
- Young, G.M., 1973a. Origin of carbonate-rich Early Proterozoic Espanola Formation, Ontario, Canada. *Geol. Soc. Am. Bull.* 84, 135-159.
- Young, G.M., 1973b. Tillites and aluminous orthoquartzites as possible time markers for middle Precambrian (Aphebian) rocks of North America. In: Young, G.M. (Ed.) *Huronian stratigraphy and sedimentation*, Geological Association of Canada, Special Paper 12, pp. 97-128.
- Young, G.M., 1981a. Field guidebook to the sedimentary environments and regional tectonic setting of the Huronian Supergroup, north shore of Lake Huron, Ontario, Canada. Univ. West. Ont., London, ON, Canada, 62p.
- Young, G.M., 1981b. Diamictites of the early Proterozoic Ramsay Lake and Bruce formations, north shore of Lake Huron, Ontario, Canada. In: Hambrey, M.J., Harland, W.B. (Eds) *Earth's Pre-Pleistocene Glacial Record*. Cambridge University Press, Cambridge, UK, p. 813-816.
- Young, G.M., 1983. Tectono-sedimentary history of early Proterozoic rocks of the northern Great Lakes Region. *Geol. Soc. Am. Mem.* 160, 15-32.
- Young, G.M., 2002. Stratigraphic and tectonic settings of Proterozoic glaciogenic rocks and banded iron-formations; relevance to the snowball Earth debate. *J. Afr. Earth Sci. Middle East* 35, 451-466.
- Young, G.M., 2014. Contradictory correlations of Paleoproterozoic glacial deposits: local, regional or global controls? *Precambrian Res.* 247, 33-44.
- Young, G.M., Long, D.G.F., Fedo, C.M., Nesbitt, H.W., 2001. Proterozoic Huronian basin: product of a Wilson cycle punctuated by glaciations and a meteorite impact. *Sediment. Geol.* 141-142, 233-254.

- Young, G.M., Nesbitt, H.W., 1985. The lower Gowganda Formation in the southern part of the Huronian outcrop belt, Ontario, Canada: stratigraphy, depositional environments and tectonic setting. *Precambrian Res.* 29, 265–301.
- Young, G.M., Nesbitt, H.W., 1999. Paleoclimatology and provenance of the glaciogenic Gowganda Formation (Paleoproterozoic), Ontario, Canada; a chemostratigraphic approach. *Geol. Soc. Am. Bull.* 111, 264-274.
- Zolnai, A.I., Price, A., Helmstaedt, H., 1984. Regional cross section of the Southern Province adjacent to Lake Huron, Ontario: implications for the tectonic significance of the Murray Fault Zone. *Can. J. Earth Sci.* 21, 447-456.

Chapter 2

2 The Paleoproterozoic Gordon Lake Formation, Huronian Supergroup, Canada: a macro-tidal to shallow marine shelf, characterized by microbial, tide, and storm activity

2.1 Introduction

Precambrian sedimentary systems are notoriously difficult to interpret due to the absence of pronounced biological activity, especially bioturbation (Schopf, 1975; Eriksson et al., 2004 and references therein; Flannery et al., 2018). In addition, the paucity of chronological markers, combined with the lack of modern analogues unaffected by biological activity, pose a significant challenge in evaluating ancient depositional models. As a result, considerable dependence is placed on sedimentary structures as environmental indicators, even though many depositional environments share similar sedimentary characteristics, including “diagnostic” structures, and therefore care must be taken when reconstructing Precambrian paleoenvironments.

Previous studies of the Gordon Lake Formation have tended to base their environment analyses on individual structures, such as nodules (e.g. Chandler, 1988), and typically do not consider regional trends. Much of the existing literature proposes that the Gordon Lake Formation was deposited in shallow water (e.g. Wood, 1973; Frarey, 1977), and that it may have formed part of a back-barrier system, although this has never been proven. Studies of barrier systems older than the Holocene are uncommon as they are inherently transient systems with poor preservation potential (Hoyt and Vernon, 1967; Riggs, 2010). Barrier islands and associated features are also thought to have generally been absent on tidally-influenced Precambrian shelves, but this may be a result of poor preservation or difficulty distinguishing these environments from fluvial and offshore deposits (Eriksson et al., 1998, 2004; and references therein; Donaldson et al., 2002).

Building on the work of Hill et al. (2016), Hill and Corcoran (2018) and Hill et al. (2018), this paper aims to: 1) define the major lithofacies of the Gordon Lake Formation, 2) determine the depositional processes responsible for lithofacies development, and 3) propose a viable depositional model for the formation. Understanding the depositional

environment of a well-preserved succession exposed over an area roughly 280 x 125 km, provides critical information on sedimentary processes that took place on non-vegetated surfaces, with only local development of microbial mats. The present study also attempts to explain the depositional transition between the fine-grained sandstone and mudstone of the Gordon Lake Formation, and the underlying and overlying extensive quartz arenite successions.

2.2 Geological Setting

Several momentous global developments occurred during the Proterozoic Eon, including the rise of atmospheric oxygen, evolution of eukaryotes, and multiple extreme climate shifts (Eriksson et al., 2001, 2004). Evidence of rising atmospheric oxygen levels and glacial periods are well-preserved in rocks of the Huronian Supergroup, which is exposed north of Lake Huron, Canada (Figure 1.1). This primarily siliciclastic succession forms part of the Southern Geological Province and unconformably overlies Archean basement of the Superior Province. Basal volcanic units are present locally. Uranium-lead zircon dating of volcanic rocks near the base of the Huronian succession yielded a lower age limit of ca. 2450 Ma (Krogh et al., 1984; Ketchum et al., 2013; Bleeker et al., 2013), whereas an upper age limit of ca. 2220 Ma (Corfu and Andrews, 1986; Bleeker et al., 2015) was determined from U-Pb dating of zircons and baddeleyite from a gabbro (Nipissing) intrusion. A maximum depositional age of 2315 ± 5 Ma was determined for the Gordon Lake and Bar River formations from detrital zircon in a sandstone and claystone bed, respectively (Hill et al., 2018); this date constrains the time of deposition of the upper Huronian Supergroup to between 2315 ± 5 Ma and emplacement of the gabbro intrusions ca. 2215 Ma (Bleeker et al., 2015). Depositional ages of 2308 ± 8 Ma and 2311 ± 1 Ma were reported by Rasmussen et al. (2013) from purported tuff beds in the Gordon Lake Formation. Although the youngest ages of the detrital zircons analyzed by Hill et al. (2018) coincide with those of Rasmussen et al. (2013), it is impossible to prove a volcanic origin for the grains. In general, the rounded nature of the zircon grains and the high-energy setting of the upper Huronian Supergroup suggest a decreased likelihood of preserving a tuff. In addition, the period from 2450 and ca. 2100 Ma is

interpreted to have been quiet in terms of magmatic activity in continental areas (Condie, 1998).

According to Wood (1973) and Long (2009), five groups comprise the Huronian Supergroup: the Elliot Lake, Hough Lake, Quirke Lake and Flack Lake groups, from oldest to youngest. Other workers divide the succession into four groups by incorporating the Flack Lake Group into the Cobalt Group. The maximum thickness of the Huronian succession is approximately 12 km in the southern part of the Huronian belt (Young et al., 2001), and sandstone, mudstone, and paraconglomerate are the dominant lithologies. The lower three groups are allocyclic in nature and consist of a lower paraconglomerate unit overlain by mudstone-carbonate and sandstone units, interpreted respectively as glacial deposits, deeper-water deltaic deposits, and fluvial-marine deposits (Card et al., 1977; Rice, 1986; Robertson and Card, 1988; Young et al., 2001; Long, 2004a, 2009). Huronian strata were folded during at least one event known as the ca. 1.875-1.825 Ga Penokean orogeny (Van Schmus, 1976; Schulz and Cannon, 2007) and have been regionally subject to low greenschist grade metamorphism (Card, 1978a; Young et al., 2001). In contrast, Huronian strata in the Killarney area, have been subject to low amphibolite grade metamorphism (Card, 1978a). The prefix “meta” has been omitted in the present study for simplicity.

The Huronian Supergroup is interpreted to reflect the transition from a transform-rift to passive margin during the breakup of the Archean Supercontinent Kenorland (Aspler and Chiarenzelli, 1998; Long, 2004a). The two major influences on the evolution of the Huronian basin were tectonism and paleoclimate cyclicity (Eriksson et al., 2001). The presence of a reducing atmosphere during deposition of the lower Huronian formations is supported by detrital uranium-bearing minerals in the Matinenda Formation (Elliot Lake Group) and sulphur isotope data from the Mississagi Formation (Zhou et al., 2017). The establishment of a partially-oxygenated atmosphere midway through the succession is supported by red beds, which first appear in the Gowganda Formation (Cobalt Group), and are present throughout stratigraphically higher formations, as are local evaporite minerals (Wood, 1973), microbial mat fragments (Hill et al., 2016; Hill and Corcoran, 2018) in the Gordon Lake Formation (Flack Lake Group), MISS in the Gordon Lake and

Bar River formations (Hill et al., 2016), and stromatolites in the Espanola Formation (Hofmann et al. 1980; Al-Hashim, 2016).

2.2.1 Gordon Lake Formation

Strata now assigned to the Gordon Lake Formation were originally recorded as fine-grained sandstone and minor limestone (Murray, 1858, p. 76), or “banded cherty quartzite” (Collins, 1925, p.111), in the upper part of the Huronian succession. The formation was formally defined by Frarey (1967), and has received relatively little attention compared to the older formations of the Huronian Supergroup. The formation was re-examined because it: 1) records the final stages of transition from an anoxic to oxic early Earth atmosphere (Great Oxidation Event), 2) contains significant and convincing evidence of fossilized microbial life in the Huronian Supergroup, 3) contains the only carbonates in the upper Huronian Supergroup, 4) represents complex deposition of a significant quantity of fine-grained material on a passive margin lacking evidence of burrowing organisms and marine plants, and 5) is part of an economic and historically significant succession that spans the Siderian and early Rhyacian periods.

In the preserved Huronian basin, the Gordon Lake Formation thickens southward, from approximately 300 m near Flack Lake, to approximately 1100 m in the Killarney area (Figure 2.1). It is composed primarily of very fine- to fine-grained sandstone, mudstone, and intraformational conglomerate. Three units have previously been suggested for the Gordon Lake Formation and are described as upper and lower sandy red members and a middle finer-grained, green member (Eisbacher and Bielenstein, 1969; Card et al., 1977; Card, 1978a). The lower upward-fining unit was described as containing interbedded rippled white and red sandstone and siltstone, intraformational breccia and nodular anhydrite. The middle unit was considered a mixture of dark green argillite, chert and fine-grained grey sandstone, with a variety of sedimentary structures, including cross-laminae, ripples, graded beds and SSDS. The upward-coarsening top unit was described as containing red, mudcracked siltstone, argillite and sandstone. The contacts with the underlying Lorrain Formation and overlying Bar River Formation are conformable. Environmental interpretations of the Gordon Lake Formation include lagoon (Rust and

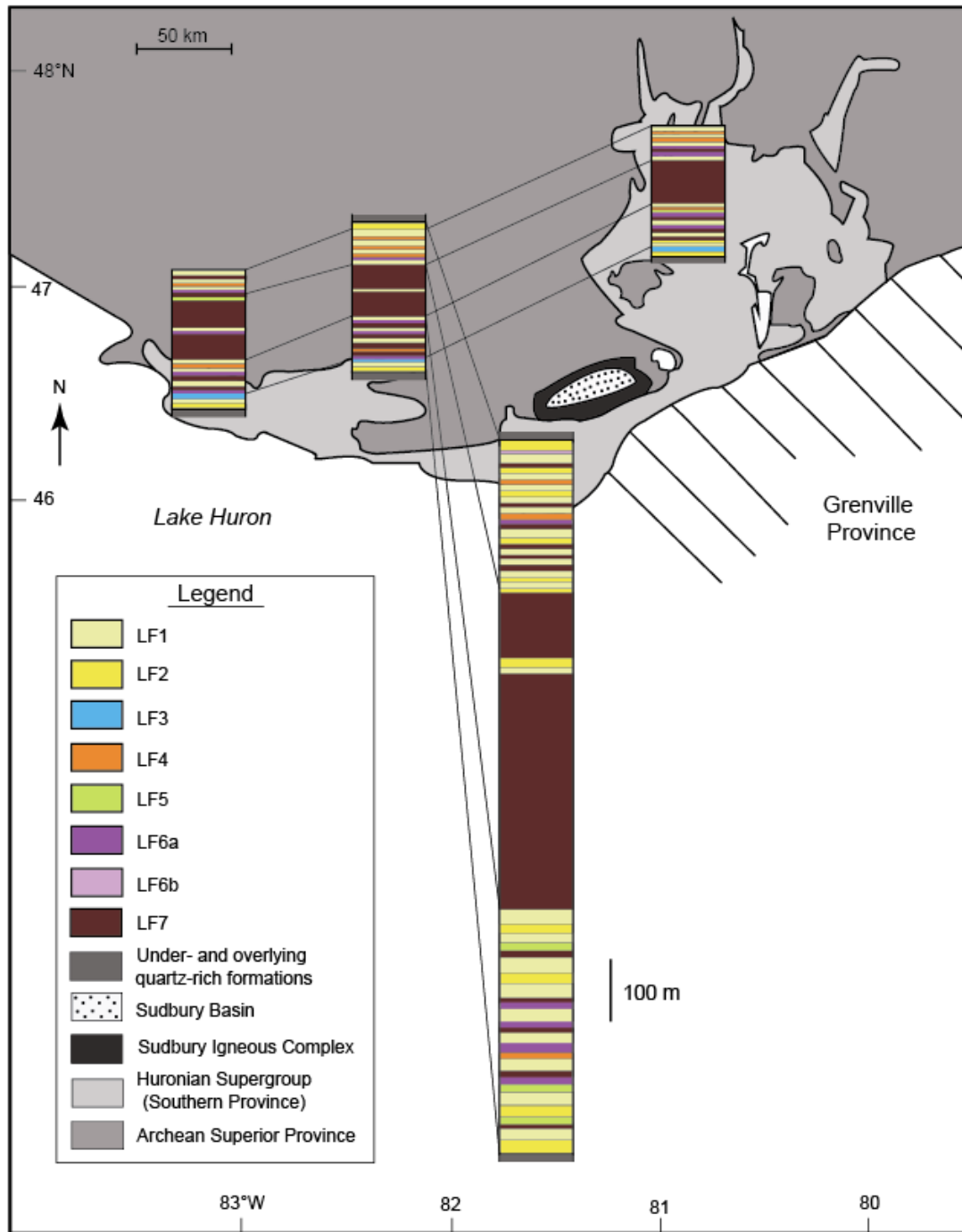


Figure 2.1. General regional geological correlation of the Gordon Lake Formation. Base map modified from Young et al. (2001).

Shields, 1987), tidal flat (Wood 1973; Card, 1976; Siemiatkowska, 1978), storm influenced shallow marine (Chandler, 1984), and deep water turbidite settings (Card, 1978a). Casshyap (1966) suggested a deeper-water equivalent to the Lorrain Formation. Wood (1973) identified hematite oolites and anhydrite-gypsum nodules in the Flack Lake area, and interpreted silt grains to be glacial loess, transported by wind. This led to his interpretation of deposition in a tidal flat setting in a relatively arid, subarctic climate. Alternatively, Chandler (1988) proposed a hot, generally dry coastal sabkha environment for the lower Gordon Lake Formation, based on the evaporite nodules near the base, and suggested a storm-dominated shelf setting for overlying strata. Wood (1973) and Chandler (1986) observed minor strata-bound copper mineralization at the base of the Gordon Lake Formation at Welcome Lake and concluded that this was sabkha-related. Chandler (1986) also observed possible chamosite oolites and “glauconite-like” peloids in the middle of the formation.

Hofmann et al. (1980) observed fenestral dolostone in the Bruce Mines area, which they interpreted as primary voids possibly indicating localized microbial mat activity. An approximately 30 m thick dolostone unit with wavy, irregular laminae “suggestive of algal mats” was also identified in the Goulais Bay area of Ontario, approximately 60 km north of Gordon Lake (Bennett et al., 1989). Hill et al. (2016), and Hill and Corcoran (2018) recognized MISS and microbial mat fragments in the Gordon Lake Formation in the Flack Lake and Bruce Mines areas, significantly increasing the known occurrences of biosignatures in the Huronian Supergroup.

2.3 Methodology

Four field areas were selected for lithostratigraphic and sedimentological analysis, based on the availability and accessibility of exposure of the Gordon Lake Formation. The study areas are located north-northwest of Bruce Mines (Figure 2.2), around Flack Lake (Figure 2.3), around McGiffin Lake and at Smoothwater Lake in Lady Evelyn-Smoothwater Provincial Park (Figure 2.4), and between Baie Fine and Killarney Lake in Killarney Provincial Park (Figure 2.5). Diamond drill core from the Flack Lake area, now stored at the Ontario Geological Survey Core Library in Sault Ste. Marie, Ontario, was

also logged. This included hole 68-1 from Canadian Johns Manville Ltd., and holes 063-83-1, 063-83-2, 063-83-3 and 063-83-9 from Canamax Resources Ltd.

Detailed stratigraphic sections were established in all four study areas. At each location, lithology, grain size, and sedimentary and potential biogenic structures were documented. Representative rock samples were collected for petrographic analysis and analyzed in thin section. Point counting was completed on thin sections of sandstone samples using the Indiana method in which polymineralic grains are characterized as lithic fragments (Ingersoll et al., 1984). A minimum of 400 grains were counted on each sample using 1 mm step increments. The process of lithofacies analysis entailed describing rock samples and units, interpreting sedimentary processes that occurred at the time of deposition, and grouping the lithofacies into associations, which reflect paleodepositional environment. In this thesis, each depositional process is represented by a distinct package of rock types called lithofacies. The Munsell Rock Color Book (2019 year revised, 2017 production) was used to describe lithofacies colours. Munsell colour notation combines the values for hue, value, and chroma to form the colour designation.

2.4 Lithofacies descriptions and interpretations

Seven distinct lithofacies were identified in the Gordon Lake Formation. These are: 1) very fine- to fine-grained sandstone, 2) fine- to medium-grained sandstone, 3) carbonate, 4) interlaminated to interbedded mudstone and fine-grained sandstone, 5) coarse-grained sandstone, 6) intraformational granule- to pebbly sandstone and conglomerate, and 7) mudstone. The strata can be broadly correlated between different areas based on observed units and details of the stratigraphy. Specific marker beds (event beds) were not identified, however distinctive marker “intervals” were identified. Lateral interfingering of Gordon Lake Formation facies with strata of the Lorrain and Bar River formations was not observed, and although the formation contacts in places appear gradational, uninterrupted coeval deposition is not proven. A summary of lithofacies and accompanying descriptions and interpretations is presented in Table 2.1.

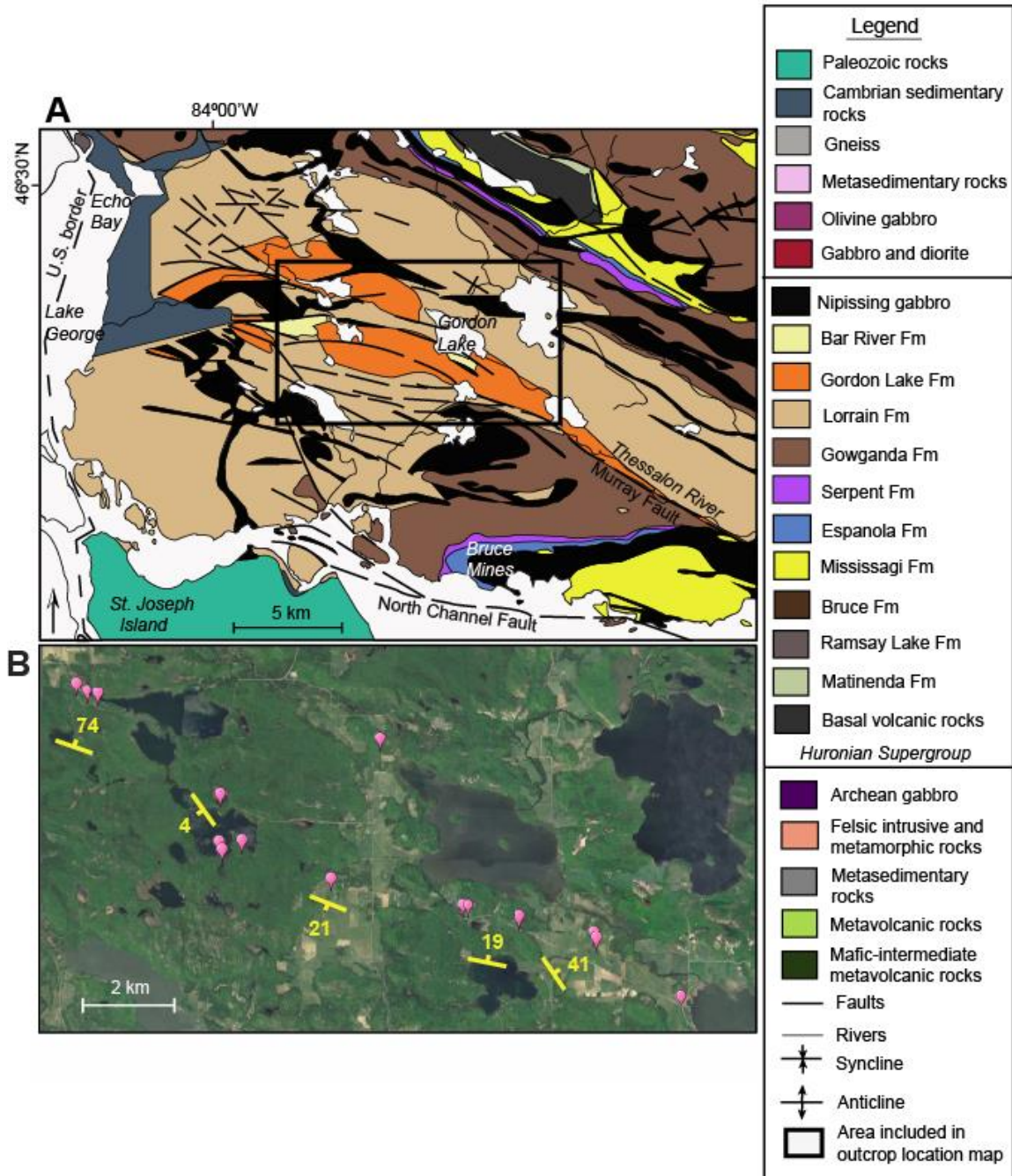


Figure 2.2. Maps of the Bruce Mines study area. A) Geological map, modified from Giblin et al. (1979). Black box outlines the area in B. B) Outcrop location map with bedding measurements. Figure modified from Google Earth Pro (2018); map data from Google, DigitalGlobe.

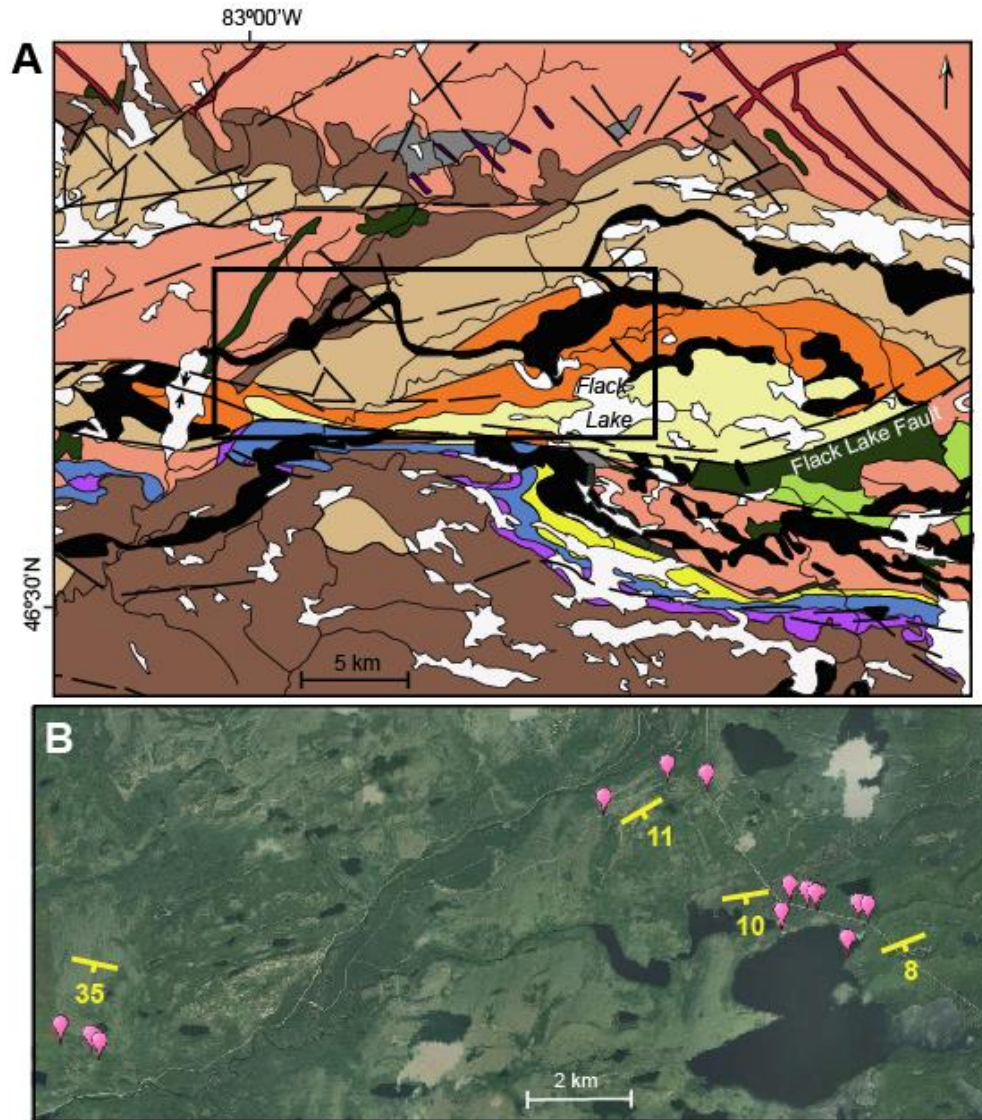


Figure 2.3. Maps of the Flack Lake study area. A) Geological map, modified from Giblin et al. (1979). Black box outlines the area in B. Legend as in Figure 2.2. B) Outcrop location map with bedding measurements. Figure modified from Google Earth Pro (2018); map data from Google, CNES/Airbus, DigitalGlobe.

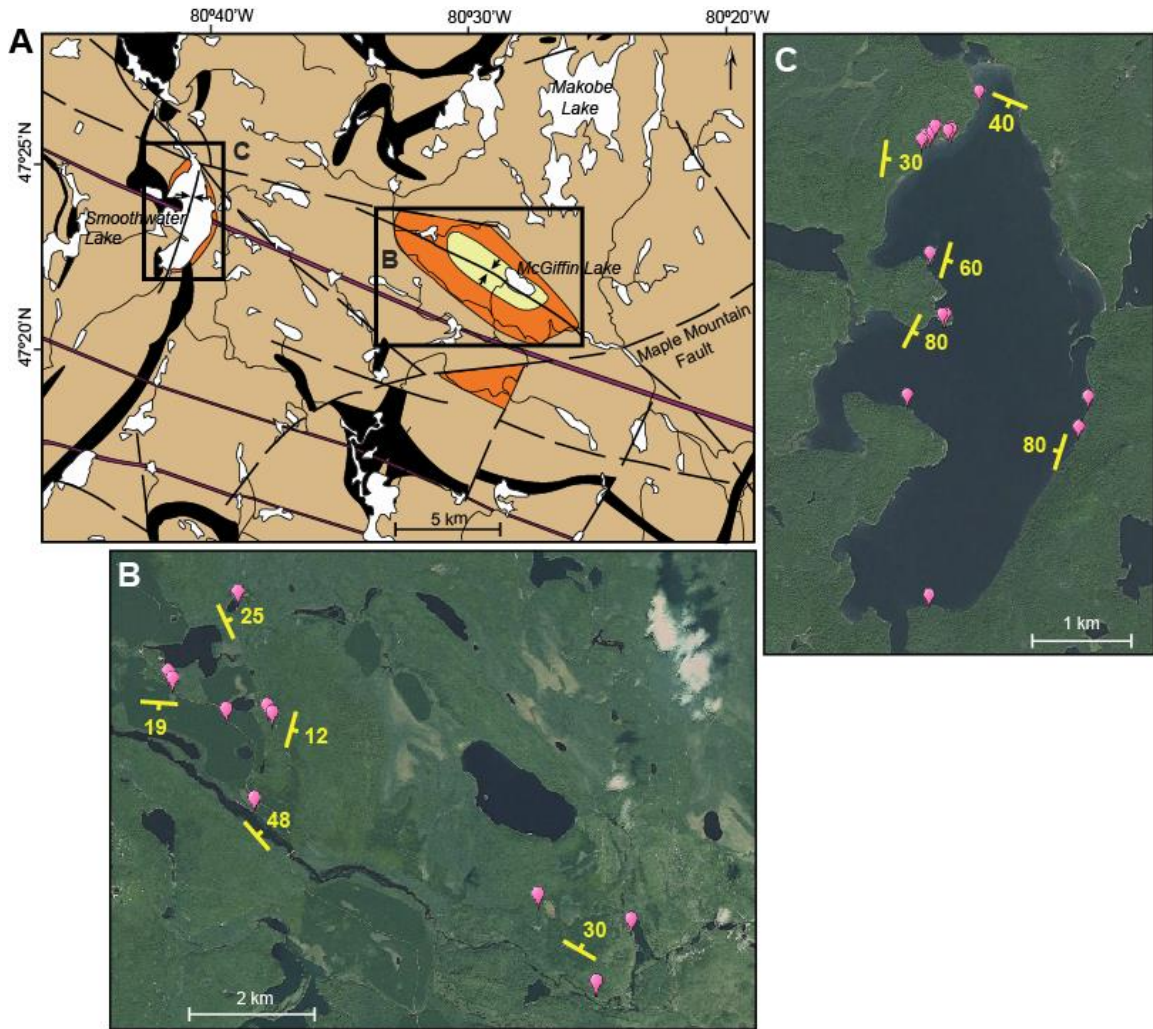


Figure 2.4. Maps of the Lady Evelyn-Smoothwater Provincial Park study area. A) Geological map, modified from Card and Lumbers (1977). Black boxes outline the areas in B and C. Legend as in Figure 2.2. B) Outcrop location map around McGiffin Lake with bedding measurements. C) Outcrop location map on Smoothwater Lake with bedding measurements. Figures B and C modified from Google Earth Pro (2018); map data from Google, CNES/Airbus, DigitalGlobe.

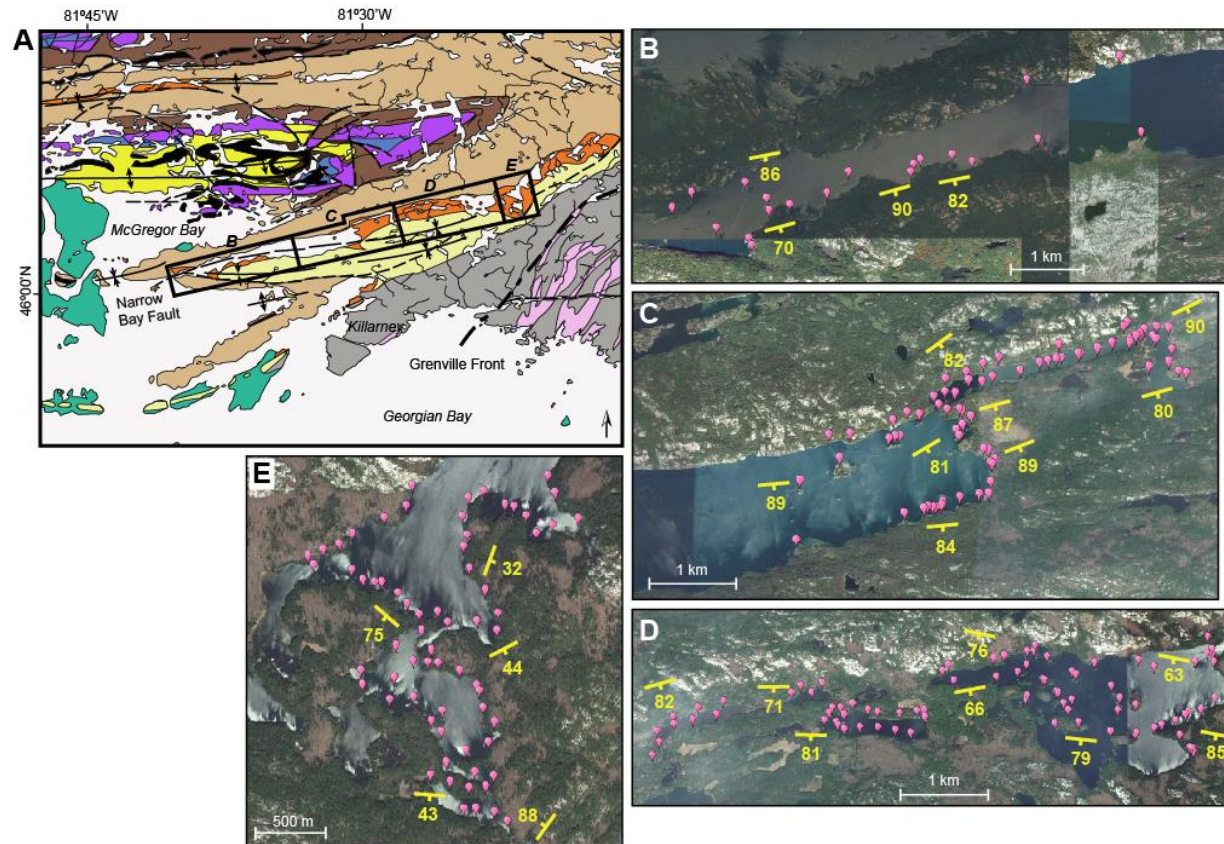


Figure 2.5. Maps of the Baie Fine and Killarney Provincial Park study area. A) Geological map, modified from Card (1978b). Black boxes outline the areas in B-E. Legend as in Figure 2.2. B) Outcrop location map of the western end of Baie Fine, with bedding measurements. C) Outcrop location map of the eastern end of Baie Fine, with bedding measurements. D) Outcrop location map between Artist lake (left) to O.S.A. lake (right), with bedding measurements. E) Outcrop location map of the eastern part of Killarney Lake, with bedding measurements. Figures B-E modified from Google Earth Pro (2018); map data from Google, CNES/Airbus, DigitalGlobe, TerraMetrics.

2.4.1 Very fine- to fine-grained sandstone

Lithofacies 1 consists of green to grey, pink to purple, and beige to white (Munsell colours N4, N5, 5G 4/1, 5YR 6/1, 5Y 6/1, 5R 5/4, 10R 5/4, 5R 5/2, 5Y 7/2, N8), thin to medium bedded, very fine- to fine-grained sandstone (Figures 2.6 and 2.7). Beds are 1-45 cm thick, mainly tabular, and have sharp or scoured basal surfaces, and sharp, rippled or erosional upper surfaces. Bedsets are up to 110 cm thick. Lithofacies 1 is characterized by massive bedded units (Figure 2.6), with lesser planar and trough cross-bedding (Figure 2.7a), and plane-parallel (Figure 2.7b), wavy, and ripple cross-laminae. Rounded to elongate mudstone intra-clasts are present at the base of some beds. Hummocky cross-stratification (HCS), mudstone drapes (Figures 2.7c, d), alignment of mudstone clasts along laminae and foresets, synaeresis cracks, climbing and flat-topped ripples (Figure 2.7e), and iron- and heavy mineral-defined laminae are present locally. Beds are generally laterally continuous, but locally pinch out. Sand-rich clastic dikes and small-scale syn-sedimentary faults were observed in association with LF1 in Baie Fine and Lady Evelyn-Smoothwater Provincial Park (Figure 2.7f). Lithofacies 1 is frequently associated with fine- to medium-grained sandstone (LF2), carbonate (LF3), interlaminated to interbedded mudstone and fine-grained sandstone (LF4), intraformational granular to pebbly sandstone and conglomerate (LF6) and mudstone (LF7).

Four samples were examined from LF1 (CH-14-13, CH-14-30, CH-15-19, GL-16-47). Petrographically, the samples are composed of very fine- to fine-grained quartz arenites, lithic wacke and subarkose. Sandstones of LF1 contain monocrystalline quartz (63-91%), plagioclase (7-13%), potassium feldspar (1-2%), and lithic fragments (1-10%), including chert (>95%) and quartzite (<5%). Detrital zircons are present in trace amounts. Minor micaceous material (<1%), calcite cement (~5%), hematite cement (~5%), quartz overgrowths (~3%), opaque grains (1%) and chlorite (<1%) were observed. Hematite rims or staining frequently coat many grains. Lithofacies 1 samples are moderately to

Table 2.1. Summary, description, and interpretation of lithofacies in the Gordon Lake Formation

Lithofacies and percentage	Lithology, thickness and geometry	Sedimentary structures & other characteristics	Depositional processes	Associated lithofacies	Interpretation
LF1: Very fine- to fine-grained sandstone (26%)	Very fine- to fine-grained sandstone; thin to medium bedded; tabular overall and locally pinch out; beds are up to 45 cm thick	Sharp or scoured basal surface; rippled, planar or erosional top surface; massive bedding; plane-parallel, wavy, and ripple cross-laminae, planar and trough cross-beds, local mudstone rip-up clasts, HCS, mudstone drapes, heavy mineral and iron-stained laminae; local SSDS	Migration of sinuous- and straight-crested subaqueous dunes; plane-bed transport in upper flow regime; uni- or bidirectional ripple migration; bedload transport; influenced by tides and storms	LF2, LF3, LF4, LF6a, LF7	Subtidal, nearshore, possible lower shoreface zone; storm deposits
LF2: Fine- to medium-grained sandstone (8%)	Fine- to medium-grained sandstone; medium to thick bedded; tabular and laterally continuous; beds are up to 90 cm thick	Wavy or scoured base; bidirectional planar and trough cross-beds, massive to planar laminae (predominantly faint), rare mudstone rip-up clasts	Migration of sinuous- and straight-crested subaqueous dunes, influenced by tidal currents, storm currents and waves; plane-bed transport in upper flow regime	LF1, LF7, LF4	Subtidal sand bodies; tidal channel; storm deposits
LF3: Carbonate (6%)	Lenticular and medium to thick bedded fenestral and sandy dolostone; beds are up to 20 cm thick	Irregular to laminoid fenestrae, normal grading of dolomitic rip-up clasts, thin rippled sandstone interbeds and laminae, stratiform and small-scale domal stromatolites	Deposition in relatively shallow water with low clastic influx; minor influence from storms	LF1, LF7	Deposition in inter- to subtidal environment
LF4: Interlaminated to interbedded mudstone and fine-grained sandstone (13%)	Fine-grained sandstone and mudstone; local quartz granules; beds vary laterally and pinch out locally; beds are up to 25 cm thick	Rippled or sharp upper and lower surfaces; sandstone with locally erosive base; lenticular and flaser bedding, wavy to ripple cross-laminae, shrinkage cracks, wave, interference, and combined flow ripples, local normally-graded beds, reactivation surfaces, MISS, mudstone rip-up clasts and drapes	Alternating suspension settling and traction deposition under the influence of tides, waves, and storms; possible episodes of subaerial exposure; frequent fluctuations in depositional conditions	LF1, LF7	Intermittently subaerially exposed mixed intertidal flats that were occasionally influenced by storms; possibly shallow subtidal

LF5: Coarse-grained sandstone (5%)	Coarse-grained sandstone; lenses and thin to medium bedded; contains local pyrite fragments; beds up to 20 cm thick	Mudstone drapes, mudstone rip-up clasts, bidirectional trough cross-beds and local normal grading	Traction deposition from high-energy currents; migration of sinuous-crested subaqueous dunes influenced by tidal currents	LF1, LF7, LF4	Subtidal to shallow shelf deposits by storms or tsunamis; subtidal dunes
LF6a: Intraformational granule to pebbly sandstone and conglomerate (7%)	Intraformational granule to pebbly sandstone and conglomerate; lenses and thin to medium bedded; beds are up to 15 cm thick	Erosive basal surface; well-rounded clasts that align parallel to bedding or along foresets; local nodules, normal grading and gradational transition to overlying beds	Traction deposition in the upper flow regime	LF1, LF4 locally, LF7	Subtidal storm deposits; possible influence from tidal currents
LF6b: Matrix-supported intraformational conglomerate (<1%)	Pebble to cobble size, well-rounded, typically elongate quartzite clasts; sandstone matrix	Structureless	Traction deposition in the upper flow regime by strong currents or oscillatory waves	None observed	Nearshore setting
LF7: Mudstone (35%)	Thin to thick bedded fine- to coarse-grained mudstone; coarse-grained mudstone and very fine-grained sandstone streaks, laminae, and lenses	Local normal grading, shrinkage cracks, large- and small-scale SSDS, minor mudstone rip-up clasts, microbial mat fragments	Primarily suspension settling from standing water; influenced by storms; periodic fluctuations in depositional conditions	LF1, LF3, LF4, LF6a	Subtidal-shallow shelf, storm deposits

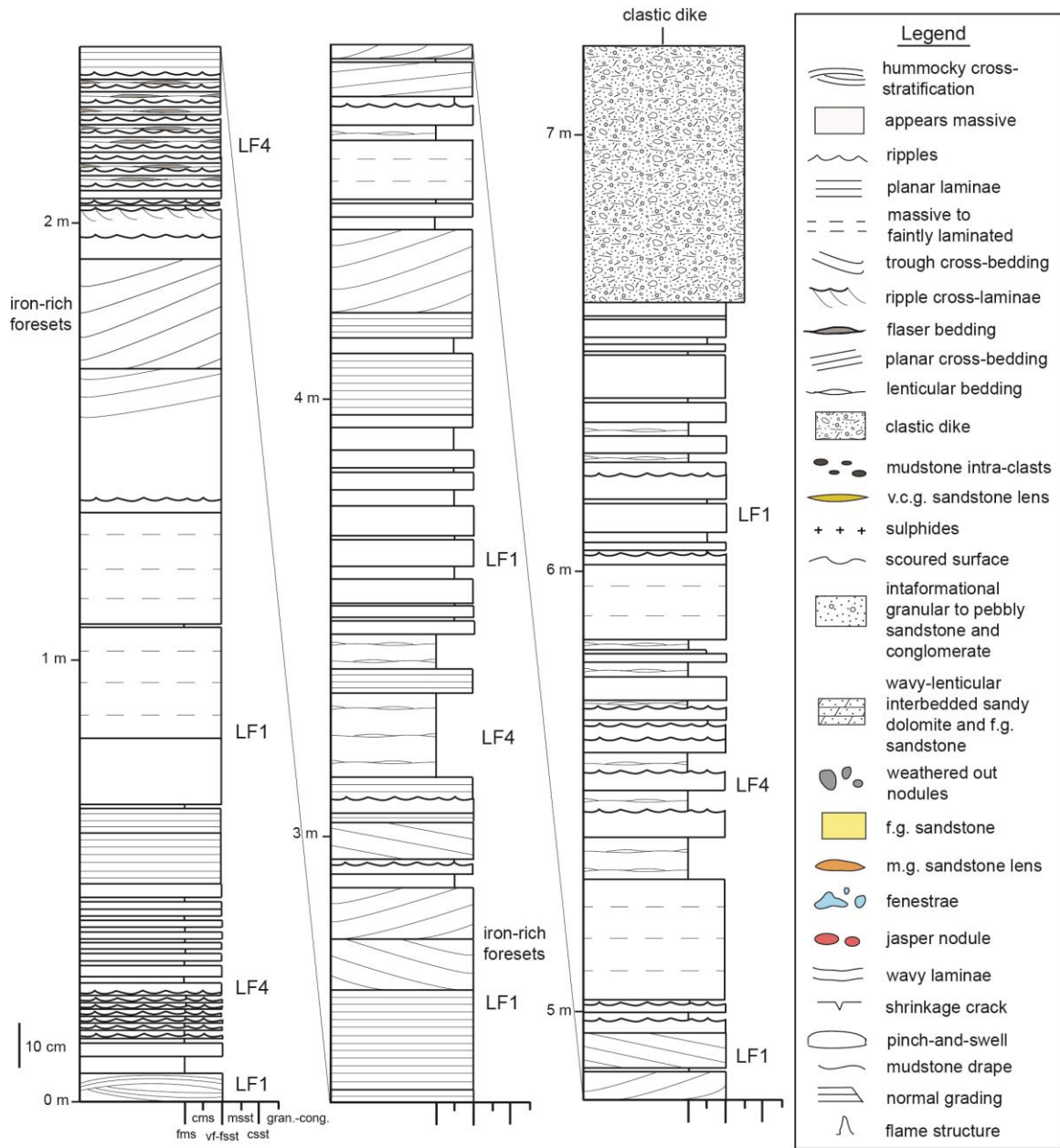


Figure 2.6. Representative stratigraphic section for lithofacies 1 from Smoothwater Lake, Lady Evelyn-Smoothwater Provincial Park. Coordinates for the outcrop are 47°23'39.30"N, 80°41'11.58"W.

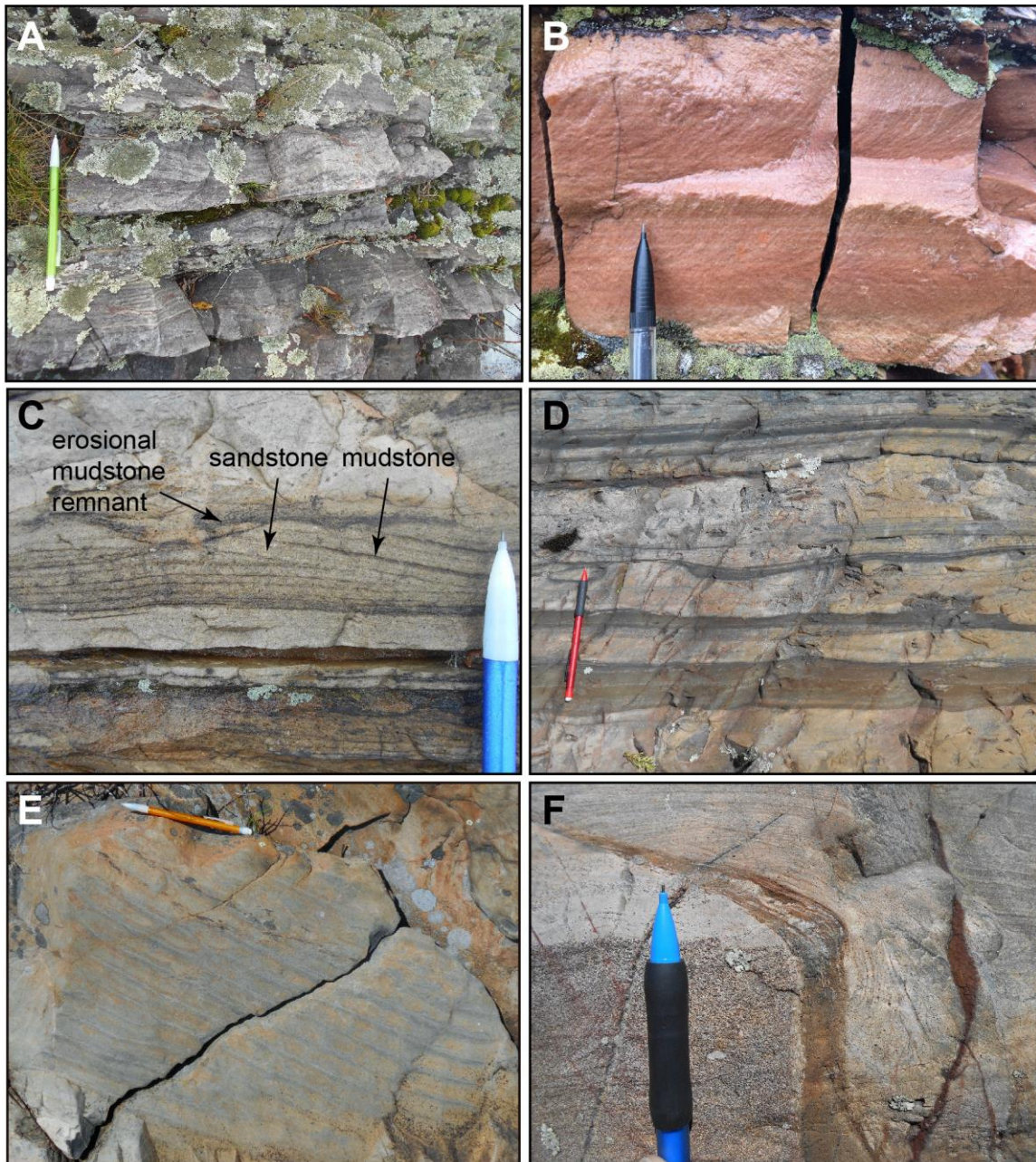


Figure 2.7. Representative photos of lithofacies 1, very fine- to fine-grained sandstone. A) trough cross-bedded and rippled sandstone with iron stained laminae, from Smoothwater Lake. B) Planar laminated sandstone, from Flack Lake area. C) Mudstone drapes between wavy to low angle cross-bedded sandstone, from Baie Fine. D) Sandstone beds with scoured bases, capped by mudstone drapes (interbeds), and local rippled sandstones in Baie Fine. E) Flat-topped ripples with local bifurcations, from Baie Fine. F) Small-scale syndepositional fault, with iron staining, from Baie Fine. Pencils are 14.5 cm long and 8 mm wide.

well sorted, and contain grains that are sub- to well rounded with concavo-convex to sutured contacts. Laminae consist of alternating layers of fine- and very-fine grained sandstone.

Interpretation

Lithofacies 1 is interpreted to have formed by processes including migration of sinuous-crested (trough cross-bedding) and straight-crested (planar cross-bedding) subaqueous dunes, as well as by plane-bed transport under upper flow regime conditions (plane-parallel and wavy laminae). Uni- and bidirectional-opposed currents are indicated by ripple cross-laminae. Local combined flow bedload transport is indicated by the presence of HCS. Scoured bases, wavy and cross stratification, along with mudstone rip-up clasts, indicate deposition typically from strong currents (Ricci Lucchi, 1995; Nichols, 2009). Local flat-topped ripples indicate periods of very shallow water conditions during deposition (Tanner, 1962). Mudstone drapes indicate alternation between high- and low-energy conditions, that allowed mud to settle out of suspension. Plane-parallel laminae are typically associated with the upper flow regime, but are known to form in the lower flow regime. However, the latter typically develop when grains are larger than 0.6 mm (Harms et al., 1982), which excludes this as a possible depositional trigger for these structures. Lateral continuity is typically high, generally exceeding outcrop width, and suggests uniform depositional conditions.

The overall sheet-like nature of the sandstone beds may have developed as a result of storms and tidal influence on a shallow open shelf (Anderton, 1976; Raaf et al., 1977), or by poorly confined drainage on a tidal flat (Donaldson et al., 2002). Beds containing a transition from planar laminae to ripples, or vice versa, indicate a shift between unidirectional and oscillatory flow. Clastic dikes and small-scale syn-sedimentary faults indicate episodes of sediment instability, shortly after initial deposition. Periods of current inactivity were characterized by the oscillatory movement of waves, which produced symmetrical ripples. Minor planar cross-bedding containing mudstone rip-up clasts may have formed by either tidal scour or storm activity (Brenchley, 1989; Shaw et al., 2012). Synaeresis cracks may have formed by dewatering during compaction,

resulting in volume change of mudstone layers, which are subsequently infilled by coarser-grained sediments (McMahon et al., 2017). Heavy mineral accumulations are typical of exposed nearshore or shoreline environments and suggest shallow water conditions where winnowing by marine currents and waves can take place (Levson, 1995). However, the lack of associated aeolian deposits points to a subaqueous environment. This lithofacies is interpreted as having been deposited in a nearshore, subtidal setting.

2.4.2 Fine- to medium-grained sandstone

Lithofacies 2 consists of white to grey and pink (Munsell colours N4, N7, 5YR 7/2, 5YR 8/1, 10R 7/4), medium to thick bedded, fine- to medium-grained sandstone (Figures 2.8, 2.9a-c). Beds are typically tabular and laterally continuous within individual outcrops. They may be planar or trough cross-bedded (Figure 2.9a), or massive to planar laminated (Figure 2.9b), and can have a wavy or scoured base (Figure 2.9c). Planar laminae are often faint (0.1-2 mm), but where visible are generally continuous and parallel. Rippled surfaces are uncommon, and rounded mudstone intra-clasts are subordinate or absent. The paleoflow direction of cross-beds indicate that flow operated locally in both unidirectional and opposing directions. Individual beds are approximately 2 cm to 90 cm thick. Massive mudstone cosets up to 20 cm thick are preserved locally. Lithofacies 2 is frequently found in association with LF1, and is present locally near the base, middle, and top of the Gordon Lake Formation.

Two samples were examined petrographically from LF2 (CH-14-17, GL-16-20). These samples are composed of fine- to medium-grained quartz arenite. The samples contain monocrystalline (>99%) and polycrystalline quartz (<1%) as framework components, and hematite (~5%) and calcite cement (~1%), with minor (accessory) chlorite (~2%). Quartz overgrowths (cement) constitute approximately 2% of the samples. Lithofacies 2 has sub- to well rounded sand grains and is moderately to well sorted. Detrital grains are typically between 150 and 425 μm , with most in the 200-250 μm range. Laminae are characterized by finely alternating layers of fine- and medium-grained sandstone.

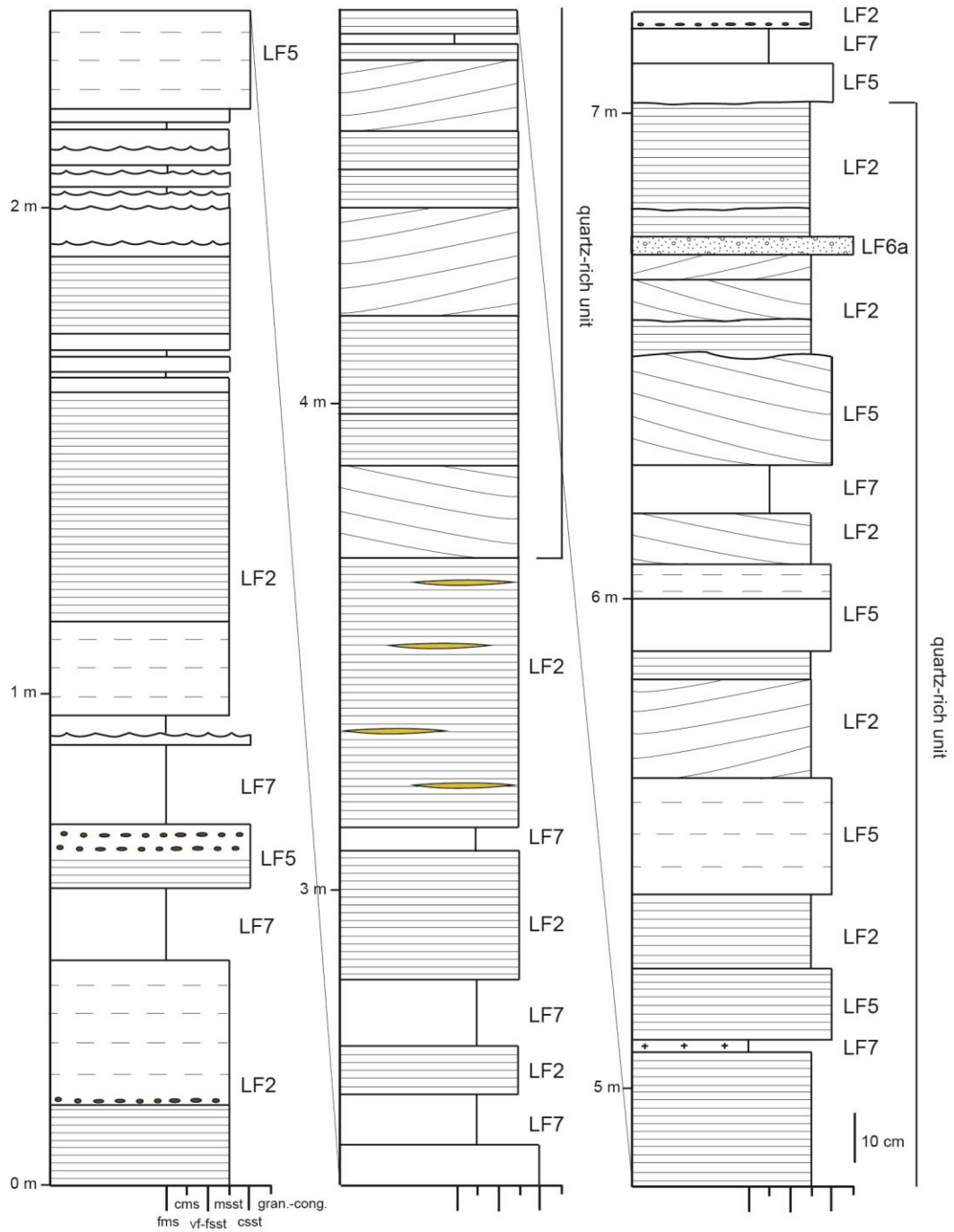


Figure 2.8. Representative stratigraphic section for lithofacies 2 from Baie Fine. Legend as in Figure 2.6. Coordinates for the outcrop are $46^{\circ} 2'8.77''\text{N}$, $81^{\circ}30'22.25''\text{W}$.

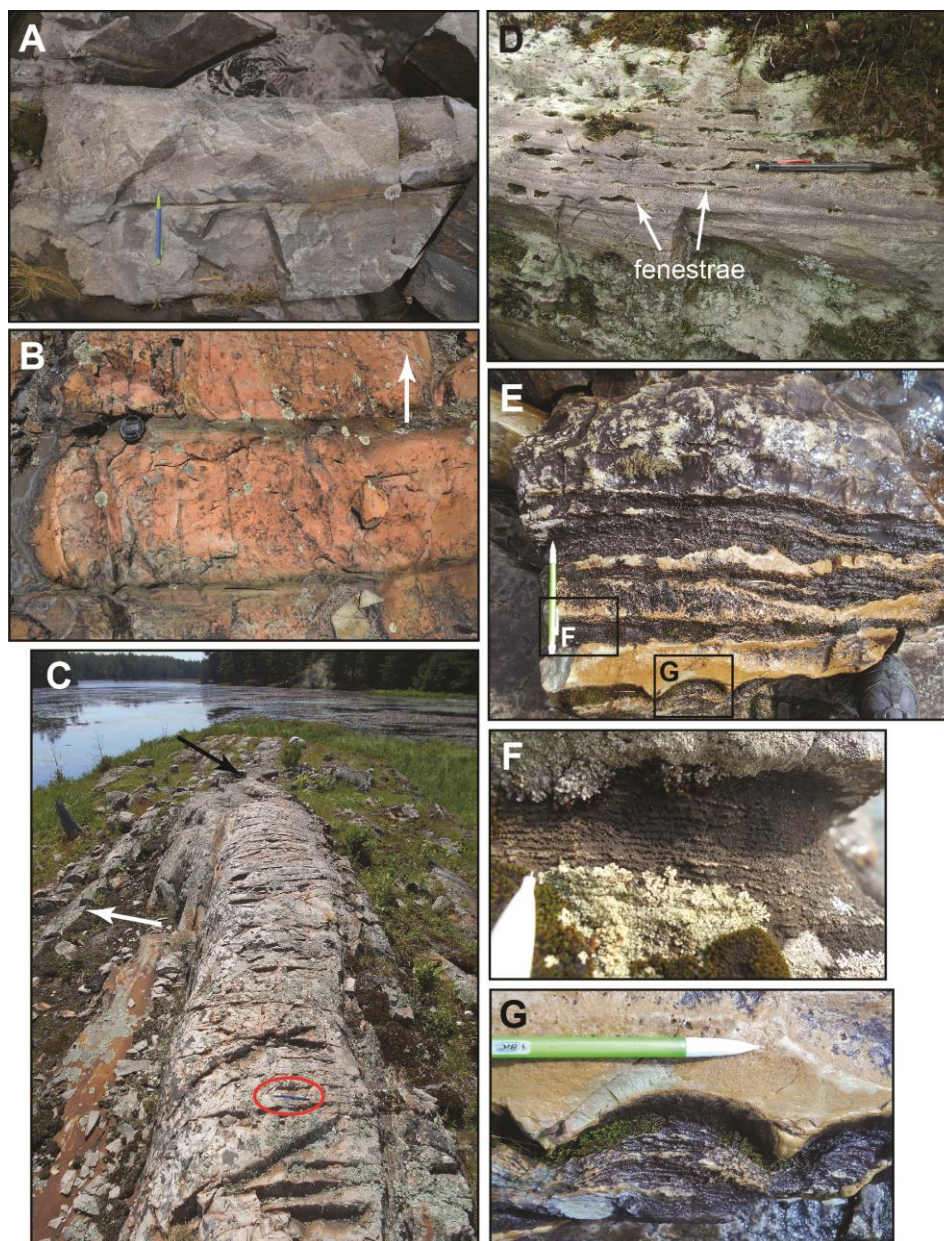


Figure 2.9. Representative photos of lithofacies 2 (A-C) and 3 (D-G). A) trough cross-beds in the quartz-rich middle section in Baie Fine (Figure 2.8). Pencil points to top. B) Massive bedded sandstone with thin mudstone interbeds, in Baie Fine near the upper formational contact. Arrow points to top. C) Massive to faintly laminated sandstone with scoured base that tapers out laterally on Artist Lake in Killarney Provincial Park. Interpreted as a tidal channel deposit. Thin adjacent beds contain mudstone pebbles, minor cross laminae, ripples, and minor SSDS. One nodule bed was observed above the channel. Beds generally thin- up section. Black arrow points to bed termination. White arrow points to top. D) Lenticular bedded fenestral dolostone near Flack Lake. E) Stromatolitic sandy dolostone on Smoothwater Lake. F) Close-up of stratiform stromatolites from E. G) Close-up of laterally-linked, domal stromatolites from E. Pencils are 14.5 cm long and 8 mm wide and camera lens cap is 5.8 cm wide.

Interpretation

Lithofacies 2 is interpreted to have formed by the migration of sinuous-crested (trough cross-bedding) and straight-crested (planar cross-bedding) subaqueous dunes, alternating with plane-bed transport (planar laminae) in the upper flow regime, and deposition of material with a uniform grain size, such that internal structures are not visible (massive bedding). Planar laminae often appear faint, however the thickness of LF2 beds indicates a greater volume of sediment than would be expected of deposition in the lower flow regime (Eriksson et al., 1995). Scoured bases and cross-bedding also indicate deposition under a strong current. This lithofacies is interpreted to primarily represent deposition in the subtidal zone. The most common sedimentary structures are planar laminae and trough cross-beds. Foreset dip directions are bipolar, which indicates tidal current action. Simple and compound dunes created by tides form in littoral and shelf environments (Longhitano et al., 2012); no compound dunes were identified. The horizontally-laminated beds may have been deposited within tidal channels (McKee et al., 1967; Tirsgaard, 1993), as storm beds (Kreisa, 1981), or in the lower shoreface zone (Nichols, 2009).

Fluctuating energy levels are inferred from the presence of horizontal laminae, characteristic of upper flow regime conditions, and trough cross-bedding and ripples indicative of lower flow regime conditions. Convolute laminae were not observed in LF2, which supports sediment deposition in tidal channels, as opposed to a braid-delta where deposition occurs at a higher rate (Eriksson et al. 1995). The lack of sigmoidal foresets, mudstone drapes, and abrupt channel margins in LF2 suggests that inter-tidal channels may not have been present. A thick, laterally pinching, erosive sandstone bed in Baie Fine is interpreted as a tidal channel (Figure 2.9c). In general, it is difficult to differentiate Precambrian tidal channels from that of Precambrian rivers and offshore beds due to their sheet-like nature (Eriksson et al., 1998), although Long (2019) has identified Archean tidal channels based on inclined mudstone laminae. The thick, faintly laminated to massive LF2 beds at the top of the formation may have been deposited as subtidal sand bodies, with the mudstone interbeds representing deposition either between the sand bodies or during slack water conditions.

In Baie Fine, a general fining-upwards shift from interpreted basal nearshore strata, to subtidal storm deposits, to thick bedded subtidal sandstones suggests that a regression may have occurred following transgression, that established shallower water conditions for deposition of LF2 in the middle of the Gordon Lake Formation.

2.4.3 Carbonate

Lithofacies 3 consists of pink, purple and beige (Munsell colours 5YR 7/2, 5R 4/2, 10R 7/4, 10YR 8/2), fenestral and sandy dolostone (Figures 2.9d-g, 2.10). In the Flack Lake area, thin, wavy to lenticular interbeds of fenestral and sandy dolostone, and sandstone were observed. Irregular to laminoid voids, interpreted as fenestrae, are up to 20 cm long and are aligned parallel to bedding (Figure 2.9d). Bedding surfaces are sharp to gradational and the upper surface is locally rippled. In Lady Evelyn-Smoothwater Provincial Park, LF3 is preserved as blocks of interbedded sandy dolostone and sandstone (Figure 2.9e), with calcareous, mm-scale, flat to wavy laminae, and up to 8.5 cm wide and 4.5 cm high laterally linked, laminated domes (Figure 2.9e-g). In the Bruce Mines area, dolostone beds are approximately 8-20 cm thick, and alternate with fine-grained sandstone, mudstone, and intraformational conglomerate. Dolostone beds contain irregular to laminoid fenestrae up to 20 cm long, and local, normally graded, intraformational dolomicrite intra-clasts. Siliciclastic interbeds are planar to wavy laminated, or faintly rippled, and contain minor small-scale SSDS. Calcareous intra-clasts were observed in core. Lithofacies 3 did not outcrop in the Baie Fine-Killarney area.

Three samples were examined petrographically from LF3 (CH-14-19, GL-16-60a, SM-17-9). The fenestral dolostone has a micro- to finely crystalline texture, that can be described as xenotopic (nonplanar). Fenestrae are up to 8 mm high and 7 mm wide, and are filled with a mosaic of hematite-bearing, anhedral, coarse, twinned dolomite spar. Fenestral dolostone beds are well sorted and very fine-grained, with 5-30% siliciclastic grains, including monocrystalline (94%) and polycrystalline (1%) quartz, plagioclase feldspar (2%) and lithic fragments (3%). Rounded intraformational dolomicritic clasts 1-4 mm in diameter were also observed. Hematite staining is principally preserved around the fenestrae and is sparse in the matrix.

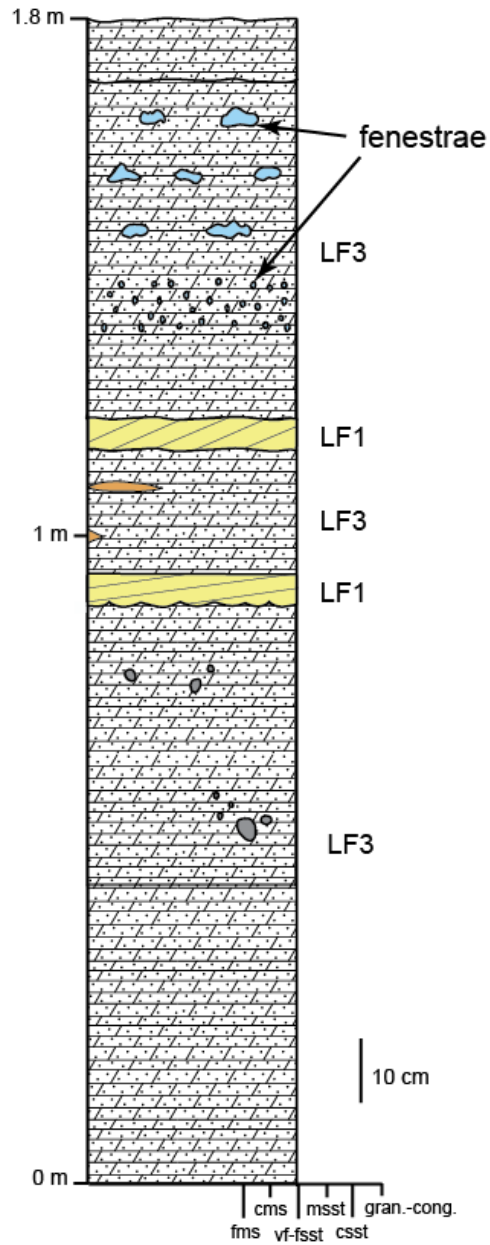


Figure 2.10. Representative stratigraphic section for lithofacies 3 from the Flack Lake area. Legend as in Figure 2.6. Coordinates for the outcrop are 46°37'30.97"N, 82°50'1.90"W.

The sandy dolostone of LF3 consists of approximately 5-30% detrital siliciclastic grains with diameters of ~80-210 μm , with most grains between 80 and 175 μm . The siliciclastic grains consist of sub- to well rounded monocrystalline quartz (90-96%), plagioclase (3-5%) and potassium feldspar (3-5%). Patchy hematite staining and dark (organic?) irregular laminae and lenses were present locally. Sandy dolostone, from the calcareous flat to wavy and domal laminated structures from Smoothwater Lake, was examined in thin section. The laminae consist of alternating, continuous layers of fine-grained sandstone (approximately 0.75-1.5 mm thick), and sandy dolostone (approximately 0.5 mm thick), with a micro- to finely crystalline xenotopic texture. A minor quantity of disrupted calcareous laminae was observed in thin section.

Interpretation

Lithofacies 3 is interpreted to have formed in a shallow marine setting during periods of low clastic influx. The flat to wavy and domal calcareous structures observed at Smoothwater Lake (Figure 2.9e-g) are interpreted as stratiform and domal stromatolites. The presence of dolostone implies that by the end of deposition of the Lorrain Formation there was a return to marine conditions suitable for establishment of microbial communities. Alternating laminae in the sandy dolostone likely formed by fluctuating rates of sediment deposition wherein the sandy laminae represent a higher rate of detrital influx and the dolomitic and stromatolitic laminae represent periods of low detrital influx. The disrupted laminae are here interpreted as primary features, and may have formed by desiccation of the stromatolite surfaces at the time of deposition (Riding, 1991). The overall paucity of ripples suggests low wave activity, however primary sedimentary structures may have been destroyed during dolomitization (Einsele, 2000). Fenestrae are likewise interpreted to have had a microbial origin. These structures have multiple modes of formation, including infill of gas bubbles produced by decaying organic matter (Flügel, 2010), repeat flooding and exposure of carbonate sediments (Shinn, 1968), and desiccation of microbial mats, leading to separation from surrounding sediment (Logan et al., 1974). Fenestrae are often associated with microbially-induced or precipitated sediments that form in carbonate facies on intertidal and supratidal flats (Logan et al., 1974; Mazzullo, 2004), and support carbonate precipitation at least in part influenced by

microbial mats (Grotzinger and Knoll, 1999; Reid et al., 2000; Altermann, 2004; Schopf et al., 2007). Due to the abundance of tidal sedimentary structures and recognition of microbial mat structures in the Flack Lake and Bruce Mines areas, an explanation involving the decay or shrinkage of microbial mats in an inter- to subtidal environment is appropriate for the formation of fenestrae in LF3. Graded beds containing rounded intraformational dolomicritic rip-up clasts likely formed during storm events.

2.4.4 Interlaminated to interbedded mudstone and fine-grained sandstone

Lithofacies 4 consists of interlaminated to interbedded mudstone with fine-grained sandstone (Figures 2.11, 2.13a). The beds are green to grey, pink to purple, and white to grey in colour (Munsell colours 10Y 6/2, 5R 8/2, 5R 4/2, 5RP 2/2, N4, N8). Bedsets can be 10s of centimetres thick and individual beds are 0.5-15 cm thick; on average, mudstone and sandstone beds have equal thickness. Upper and lower contacts are generally sharp and predominantly rippled. The sandstone beds locally have erosive bases. Beds frequently pinch out laterally over 5-10 m. Lenticular and flaser bedding, wavy to ripple-cross laminae, shrinkage cracks, and wave, interference, and combined flow ripples are the dominant sedimentary structures preserved in LF4 (Figure 2.11a, b). Ripples commonly have low, rounded, symmetrical tops, but internally contain different types of laminae, including unidirectional and micro-cross varieties; asymmetrical ripples are rare and where observed had reworked, rounded crests. Reactivation surfaces (Figure 2.11c), single or double mudstone drapes (Figure 2.11d), minor small-scale SSDS, thin normally graded beds, cross-beds (Figure 2.11e), and mudstone clasts are present locally. Microbially induced sedimentary structures (Figure 2.11f) are also preserved in LF4 in the Flack Lake area (see Hill et al., 2016). Identified varieties of MISS include sandcracks, microbial sand and silt chips, large mat chips, remnant gas domes, and iron patches. In Lady Evelyn-Smoothwater Provincial Park, local quartz granules are present in sandstone of LF4. This lithofacies is commonly associated with LF1 and LF7.

Three samples were examined petrographically from LF4 (CH-14-29, CH-14-54, CH-14-78). The samples are composed of fine-grained sandstone, interlaminated and interbedded with fine- to coarse-grained mudstone. The dominant detrital mineral is monocrystalline quartz (99%), followed by plagioclase feldspar (1%). Overall, the grains are subangular

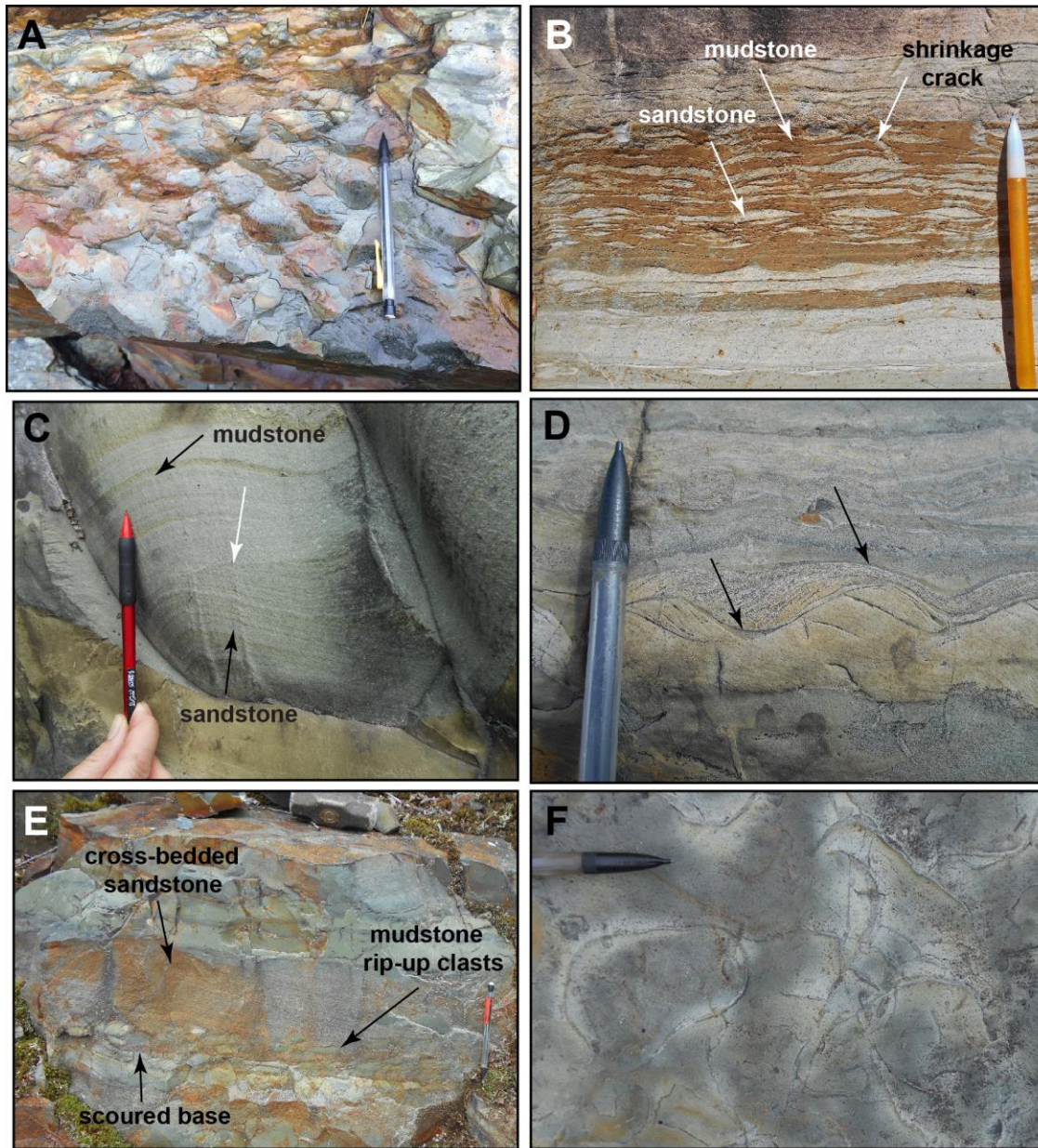


Figure 2.11. Representative photos of lithofacies 4. A) Interference ripples, near Flack Lake. B) Lenticular bedding, desiccation cracks, rippled sandstone and mudstone drapes in Killarney Provincial Park. C) Oblique view of a reactivation surface in Lady Evelyn-Smoothwater Provincial Park. White arrow points to the erosion surface. D) Complete tidal cycle deposit in Baie Fine. Arrows point to mudstone drapes that were deposited in slack water between both ebb and flood current reversals. Ripple cross laminae support bipolar-opposed tidal currents. E) Interpreted small tidal channel deposit, from Flack Lake area. F) Microbially induced curved and sinuous sand cracks near Flack Lake. Pencils are 14.5 cm long and 8 mm wide.

to rounded, however local angular to sub-angular silt grains were observed in thin section. The samples are moderately (sand-size) to well sorted (silt-size). Minor amounts of detrital zircon, lithic (chert) fragments and biotite were also observed. Dark carbonaceous material, pyrite, and hematite staining are preserved locally. Bedding consists of finely alternating layers of fine-grained sandstone (1-23 mm thick) and mudstone (1-10 mm thick). Bimodal ripple cross-stratification, sandstone lenses, truncated micro-cross stratification, desiccation cracks, fine grading, and alternating laminae are common in thin section. Diagenetic chlorite and mudstone drapes predominantly define laminae.

Interpretation

Lithofacies 4 is interpreted to have formed by alternating suspension (mudstone) and traction (sandstone) deposition under the influence of tides and waves (ripples, flaser, and lenticular bedding), with a minor influence from storms. Desiccation cracks and microbially-induced sand cracks formed during periods of subaerial exposure on tidal flats, whereas microbial mat chips formed through erosion of biofilms by wind or waves (Schieber, 2004; Eriksson et al., 2007; Hill et al., 2016). Mudstone drapes formed through suspension settling during slack water periods of tidal cycles (Reineck and Singh, 1981; Dalrymple, 2010). Reactivation surfaces formed when ripples advancing during one tidal phase were eroded by the reversing ebb tidal current (Dalrymple, 2010). Thin, normally graded beds indicate deposition from waning currents, which might be associated with storms, turbidity currents, or fluvial overbank floods (e.g. Kuenen and Menard, 1952; Figueiredo et al., 1982; Nichols, 2009). The frequent association of graded beds with sedimentary structures is possibly indicative of subaerial exposure and deposition by tides and waves points to a shallow marine setting. In addition, the observation that storms were one of the main trigger mechanisms for the formation of SSDS in the Gordon Lake Formation (Hill and Corcoran, 2018), lends support to a waning storm origin for the graded beds. This lithofacies is typical of mixed intertidal flats and shallow marine settings.

2.4.5 Coarse-grained sandstone

Lithofacies 5 consists of white to grey (Munsell colours N7, N8), coarse-grained quartz arenite, that locally contains pyrite grains. In the Bruce Mines area, LF5 was observed as a sandstone lens in one outcrop where it is approximately 4 cm thick at its thickest point and pinches out laterally (Figure 2.12a). It contains generally rounded, circular to elongate pyrite grains (Figure 2.12b), and one load structure. Faint cross-laminae are preserved, however sulphide weathering covers much of the surface, obscuring any structures. In Baie Fine and Lady Evelyn Smoothwater Provincial Park, LF5 is massive to planar laminated and trough cross-bedded with heavy minerals defining laminae locally (Figure 2.12c). Mudstone drapes, rippled bedding planes are preserved locally and mudstone clasts were observed at the bases and tops of some beds.

One sample was examined petrographically from LF5 (PY-17-1). The sample is a coarse-grained quartz arenite that contains pyrite grains (Figure 2.13b). It contains monocrystalline (>94%) and polycrystalline quartz (<1%), plagioclase feldspar (<5%), and is cemented by with microcrystalline and silt-sized quartz. The pyrite grains, which form approximately 45% of the coarse-grained material, display an overlapping relationship with several detrital siliciclastic grains; pyrite appears to have formed as a local cement around smaller quartz grains. Detrital grains in sample PY-17-1 are sub- to well rounded and the sample is moderately sorted with a quartz-rich, silty matrix. Grains are loosely packed, but minor, thin quartz overgrowths were observed.

Interpretation

Lithofacies 5 is interpreted to have formed by traction deposition from high-energy currents. In the Bruce Mines area, LF5 has a scoured base, pinches out laterally, is quartz-rich and distinct from the overall fine-grained over- and underlying strata, suggesting that the sediment originated in a foreshore environment and was transported offshore by storm- or tsunami-generated flows (e.g. Dawson and Stewart, 2007). A number of the rounded and elongate grains are interpreted as pyritized chips representing eroded microbial mats that were mineralized selectively. The pyrite likely formed under favourable anoxic conditions provided by decaying microbial mat chips (e.g. Berner,

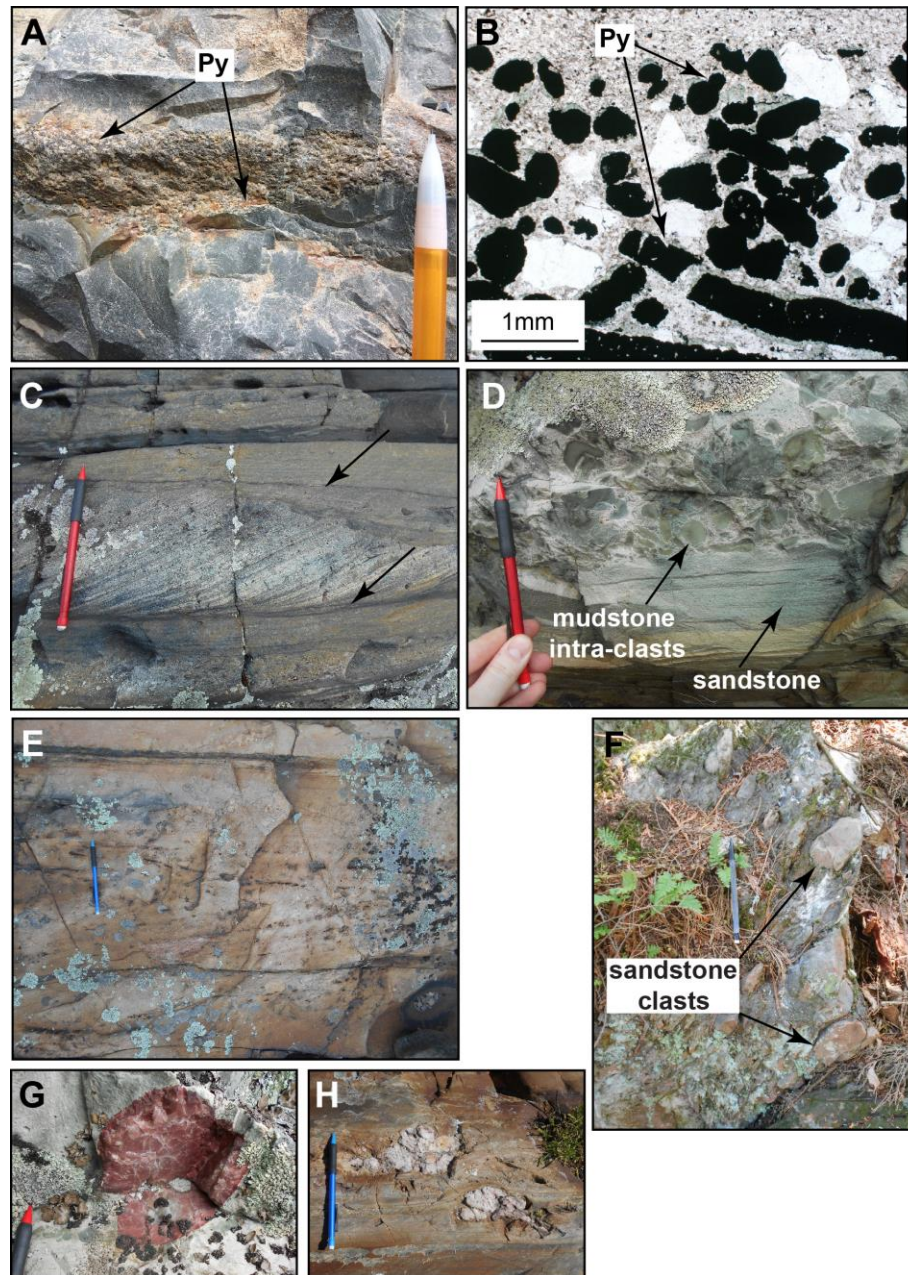


Figure 2.12. Representative photos of lithofacies 5 and 6. A) Lens of LF5 that tapers out laterally, in the Bruce Mines area. Loading is evident at the base of the bed. B) Photomicrograph of pyrite grain morphologies in A. C) Trough cross-bedding outlined by heavy mineral laminae in Baie Fine. Arrows point to over- and underlying mudstone drapes. Bipolar flow directions were observed in this interval. D) Lithofacies 6a in Lady Evelyn-Smoothwater Provincial Park, interpreted as the base of a fining-upwards storm deposit. E) Lithofacies 6a in Baie Fine. Possible herringbone cross stratification. Note pebbles aligned along foresets. F) Lithofacies 6b in Baie Fine. G) Jasper nodules in thin LF5a bed from Lady Evelyn-Smoothwater Provincial Park. H) Sugary quartz nodules from Baie Fine. Note how bedding was displaced by nodule growth after deposition. Pencils are 14.5 cm long and 8 mm wide.

1984; Schieber, 2004). The regular overlapping relationship with adjacent siliciclastic grains and cement indicate a diagenetic origin. In general, LF5 is associated with LF1 and LF7, indicating deposition from strong currents. This lithofacies is interpreted as representing subtidal to shallow shelf deposits. Coarse-grained sediment would have been transported to the coast by fluvial channels or reworked from adjacent coastal areas or older deposits (Sha and De Boer, 1991). Winnowing by storms or tidal currents may have also contributed to the concentration of coarser-grained sediment in some cases (e.g. Nichols, 2009; Reynaud and Dalrymple, 2012).

2.4.6 Intraformational granular to pebbly sandstone and conglomerate

Lithofacies 6 consists of two subfacies: a) green to white-grey (Munsell colours N7, N8, 5GY 5/2), intraformational granular to pebbly sandstone and conglomerate (Figures 2.12d, e; 2.13b), and b) pink (Munsell colour 10R 7/4), matrix-supported intraformational conglomerate (Figure 2.12f). Lithofacies 6a is found in all of the study areas and is composed of mudstone clasts that are <1 mm to 14 cm wide. The clasts are well rounded and appear circular to elongate in two dimensions, with rare irregular forms. The elongate clasts are predominantly aligned parallel to bedding or along foresets. Lithofacies 6a is typically overlain by LF1 or LF7. Association of LF6a with lenticular bedding, shrinkage cracks, and mudstone drapes of LF4 was observed locally. Beds are from approximately 1 to 15 cm thick, and are massive to faintly laminated. Basal surfaces are erosive, and a gradational transition into the overlying LF1 is common. Normal grading was observed locally. Siliceous and sulphate nodules (Chandler, 1988) (Figure 2.12g, h) were found associated with LF6a in the lower portion of the Gordon Lake Formation, however they were not restricted to this lithofacies.

Two samples were examined petrographically from LF6a (CH-14-43a, CH-15-02). The samples are intraformational pebbly sandstone and conglomerate. The intraformational granules, pebbles and cobbles are composed of mudstone. Morphologically, these grains are well rounded, and appear circular, elliptical or irregular in two dimensions; some mudstone clasts contain fine laminae. The detrital component of the sandstone is predominantly composed of very fine- to fine-grained monocrystalline quartz.

Carbonaceous fragments and laminae, and pyrite grains are common features in LF6a.

Alternating 5-6 mm thick laminae of fine- to very-fine grained sandstone lacking mudstone clasts, and 1-13 mm thick intraformational granular to pebbly sandstone and conglomerate were observed in thin section.

Lithofacies 6b is anomalous in the stratigraphy, and was only observed on one small, isolated outcrop exposure in Baie Fine that is highly foliated (Figure 2.12f). In outcrop, it is structureless and contains 1-20 cm wide quartzite clasts that are sub- to well-rounded and typically elongated. One sample from LF6b was examined petrographically (GL-16-9). Clasts were not observed in thin section. The matrix is predominantly composed of fine-grained, monocrystalline quartz (>95%); plagioclase feldspar and detrital zircon grains constitute a minor amount of the matrix. In general, metamorphism has obscured grain contacts. Hematite cement (3%) and chlorite (<1%) are present in the matrix.

Interpretation

Lithofacies 6a is interpreted to have formed by traction deposition in the upper flow regime. Mudstone clasts with preserved undeformed laminae indicate a semi-lithified state of the sediment at the time of erosion. In addition, mudstone beds preserved in the process of being eroded were observed in thin section, which indicates local sourcing of mud (Garzanti, 1991; Schieber et al., 2010). Lithofacies 6a forms the base of fining-upward units that are locally overlain by LF1 and LF7. Lithofacies 4 was found substituting for LF7 in some units. These packages are interpreted as storm deposits (e.g. Kreisa, 1981; Duke et al., 1991a; Cheel and Leckie, 1992). Lithofacies 7 and 4 are not always preserved at the top of storm cycles, but where present are typically overlain by LF1. The mudstone beds may represent fair-weather deposits or the tailings of a waning storm. Consecutive storm deposits likely formed through erosion of mudstone cap layers by ensuing storms and incorporation of the clasts into the basal lag layer (LF6a) of a new storm package (e.g. Kreisa, 1981; Chandler, 1988; Duke et al., 1991a; Cheel and Leckie, 1992). This lithofacies is interpreted to have been deposited in the subtidal to lower shoreface zone. Observation of minor lenticular bedding, possible desiccation cracks, and mudstone drapes indicate deposition within the realm of tidal influence and not in a deep

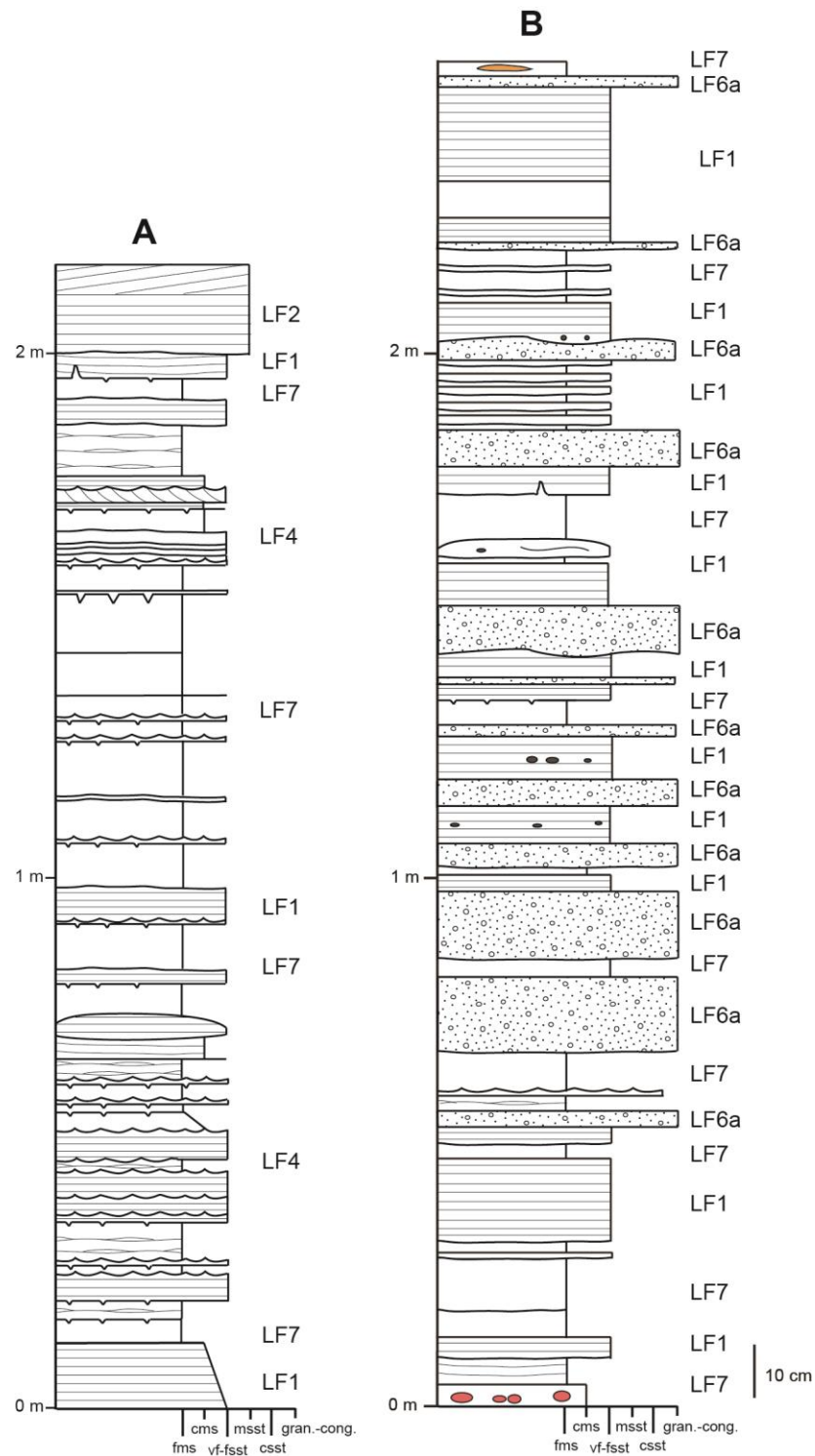


Figure 2.13. A) Representative stratigraphic section for lithofacies 4 and 7 from the Flack Lake area. Coordinates for the outcrop are 46°35'55.00"N, 82°46'27.30"W. B) Representative stratigraphic section for lithofacies 6a from Lady Evelyn-Smoothwater Provincial Park. Coordinates for the outcrop are 47°21'48.78"N, 80°31'2.06"W. Legend as in Figure 2.6.

offshore setting. However, rippled sand and mud can be deposited in offshore settings during weak storms (Plint, 2010; Daidu, 2013), and a number of crack structures are interpreted to be subaqueous syneresis cracks. The association of LF6a with inferred storm beds may therefore be consistent with a shallow shelf environment.

Siliceous nodules are interpreted as replacements of syn-depositional evaporites as indicated by the presence of anhydrite inclusions and calcite, dolomite, and ankerite core fillings in thin section, in addition to local up- and down-warping of the over- and underlying host material (Wood, 1973; Chandler, 1988). The common association of LF6a with nodules suggests that porosity may have played a role in formation of the structures or that some of the nodules have a detrital origin. However, nodules preserved in sandstone or mudstone beds may have formed subaqueously (Chandler, 1988).

Lithofacies 6b is interpreted to have formed by traction in the upper flow regime. Storms may have played a role in deposition and remobilized clasts as a storm lag, however the prevalence of sand in the matrix suggests that little winnowing occurred (c.f. Clifton, 2003). Possible depositional environments and deposits include nearshore/beach, tidal channel, subtidal trough/depression, debris flow, or barrier. All but debris flows are affected by waves, tides, or storm currents, in addition to the potential influence from longshore currents. The small size of the exposure and metamorphic overprinting masking sedimentary structures and lateral associations makes interpretation of LF6b very difficult. A shallow marine setting characterized by strong currents or oscillatory waves, such as the nearshore or a subtidal depression or trough, is tentatively proposed due to the high maturity of the matrix, sub- to well-rounded nature of the clasts, and the stratigraphic association with shallow marine and tidally-influenced deposits. Given that this is an isolated outcrop, with no clear bed limits, LF6b may also represent a post-depositional Sudbury-type breccia (e.g. Rousell et al., 2003; Long, 2004a).

2.4.7 Mudstone

Lithofacies 7 consists of green, grey, pink and purple (Munsell colours 5YR 7/2, 5R 4/2, N4, 10Y 6/2, 5GY 5/2, 5Y 6/1, 10GY 5/2, 5G 4/1), fine- to coarse-grained mudstone (Figures 2.13a, 2.14a, b). Mudstone beds are up to approximately 30 cm thick, and appear

massive, or finely planar and wavy laminated. Coarse-grained mudstone to very-fine-grained sandstone streaks and laminae are common, with local thin, lenticular beds of sandstone and graded beds. Crack structures are also common overall. At Flack Lake, LF7 contains syneresis(?) cracks up to 10 cm long, infilled with fine-grained sandstone, and minor thin lenticular beds of sandstone (Figure 2.14a). Thin, normally graded mudstone beds were also observed in the area. In general, LF7 was observed in association with LF1, LF3, LF4, and LF6a throughout the Gordon Lake Formation.

In the Bruce Mines and Baie Fine areas and in core, LF7 is interbedded with LF1 beds that are massive to planar laminated with flat to undulatory bases and local rippled surfaces. Several intervals hosting a variety of large- and small-scale SSDS (Figure 2.14b), including load casts, pseudonodules and flame structures (see Hill and Corcoran, 2018), normal graded beds and minor intraformational conglomerate are preserved. Lateral variations in thickness are minor. In addition, LF7 in the Bruce Mines area is interbedded with thin to medium bedded, fine- to medium-grained sandstone that is regularly overlain by microbial mats and mat chips. A minor quantity of similar microbial structures was observed in core from the Flack Lake area. Lithofacies 7 also forms a capping mudstone layer on interpreted storm beds across the region. In the Flack Lake area, LF7 can be highly siliceous and resembles chert, however, local sand-sized grains of quartz and muscovite, seen in thin section, indicate a detrital origin for these rocks.

Two samples were examined petrographically from LF7 (CH-15-01, GL-16-78). These samples are composed of fine- to coarse-grained mudstone containing approximately 98% silt-sized monocrystalline quartz, and approximately 2% plagioclase feldspar. The grains are generally sub- to well-rounded and the samples are moderately- to well-sorted. Laminae in LF3 are characterized by alternating 0.2-15 mm thick layers of planar continuous to discontinuous, fine- and coarse-grained mudstone. Small-scale SSDS were observed in thin section.

Interpretation

Lithofacies 7 is interpreted to represent suspension settling from standing water. The presence of coarse-grained mudstone to very fine-grained sandstone streaks and laminae

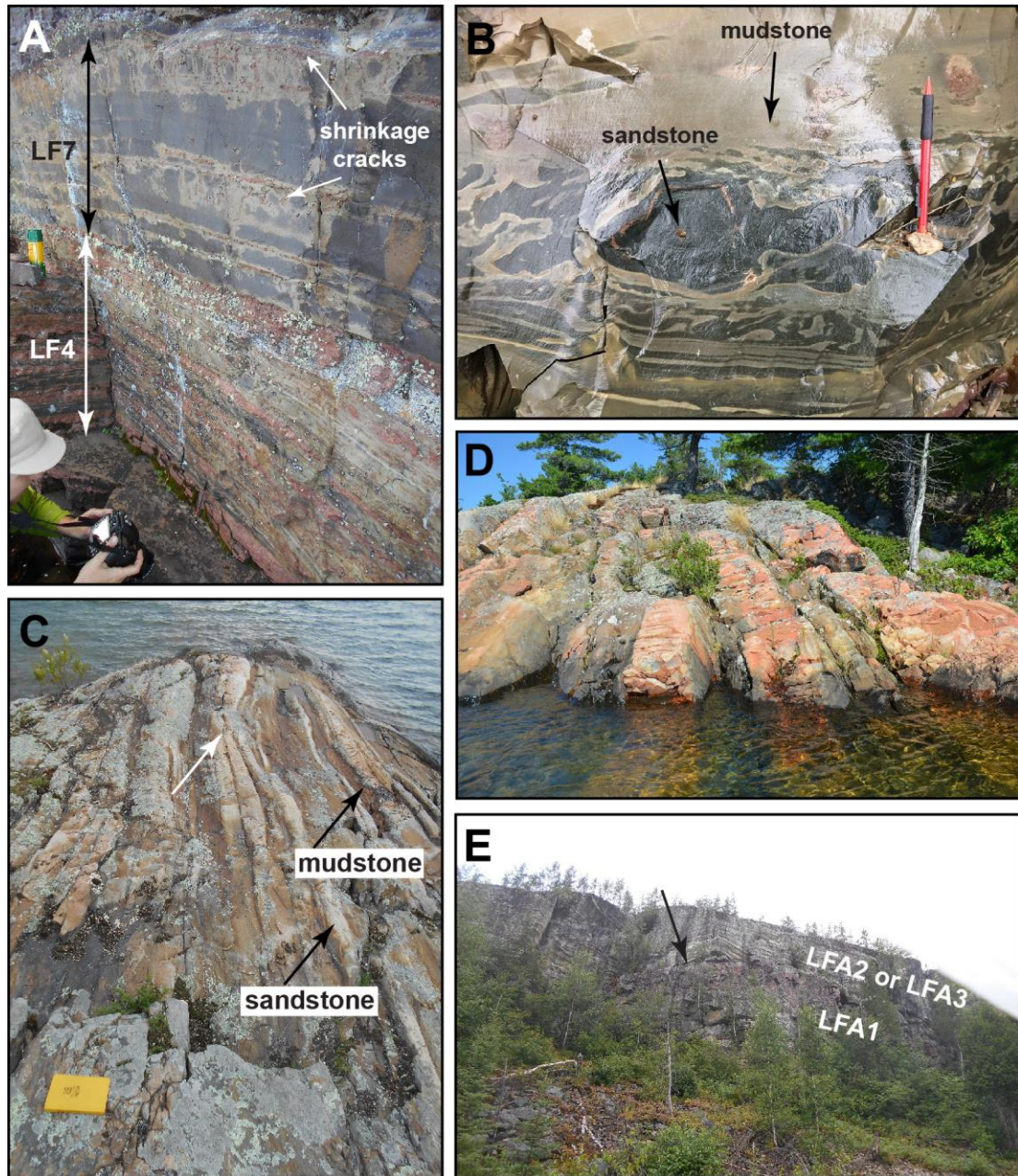


Figure 2.14. Representative photos of lithofacies 7 and bedding types. A) Top of photo shows medium to thick beds of mudstone overlying LF4 in the Flack Lake area. Vertical crack fills and thin lenticular pink sandstone define bedding surfaces. B) Convolute bedding and load structures near Bruce Mines. C) Possible HCS (white arrow) near the top of the formation in Baie Fine. Top to left. D) Thick bedded sandstone (LF2) near the transition with the overlying Bar River Formation in Baie Fine. Top to right. E) Rapid transition from sandy red beds to fine-grained green mudstone beds in a cliff section (marked by arrow) at Lady Evelyn-Smoothwater Provincial Park. Pencil is 14.5 cm long and 8 mm wide and field book is 19 cm long.

and the association of LF7 with LF1 and LF6a point to periodic fluctuations in depositional conditions (Pickett, 2002). This lithofacies is inferred to have been deposited in the subtidal nearshore to shallow shelf zone. Thick mudstone beds require extended periods of quiet water to form, which can be attained during the tidal slack-water flood phase on mud flats or in intertidal ponds, and under fairweather conditions in the subtidal to offshore transition zone (Potter et al., 2005; Dalrymple, 2010). Preservation of long shrinkage cracks near Flack Lake indicates possible extended periods of subaerial exposure, which would have occurred during the ebb tidal phase. Mud is often the topmost constituent of a storm deposit due to the retention of clay and silt sized particles in suspension in high-energy storm currents that get deposited once fairweather conditions are re-established (Duke, 1985; Prave et al., 1996). Interbedded sandstones with erosive bases point to frequent transitions to bedload transport in currents strong enough to erode muddy layers (Schieber, 1999), such as storm and tidal currents. Sandstone with flat or undulatory bedding surfaces may represent episodic storm deposits (Duke, 1985); the graded beds, SSDS, and the infrequent shallow water sedimentary structures support this interpretation.

2.5 Discussion

2.5.1 Paleoenvironmental interpretation and lithofacies associations

This section presents an interpretation of the main sedimentary processes that controlled the deposition and composition of the Gordon Lake Formation, using observations of lithofacies and petrographic analysis. The lithologies and sedimentary structures support deposition in sub-environments developed along an open coast, in mainly siliciclastic, microbial-, tide- and wave-influenced marginal marine to shallow shelf environments.

The seven lithofacies of the Gordon Lake Formation can be arranged into three lithofacies associations: LFA1 (subtidal nearshore), LFA2 (subtidal to shallow shelf), and LFA3 (mixed intertidal flat). Unlike fluvial systems in the Precambrian that experienced episodic discharge and increased rates of runoff due to the absence of vegetation (Long, 2004b), tidal action was constant during deposition and may account for the prevalence of tidal deposits in the geologic record.

2.5.1.1 LFA1: Subtidal nearshore

The association of very fine- to fine-grained sandstone (LF1), fine- to medium-grained sandstone (LF2), and coarse-grained sandstone (LF5) is interpreted to represent deposition in a nearshore setting, such as in subtidal shoals. This association is present in Baie Fine and in Lady Evelyn Smoothwater Provincial Park, near the stratigraphic middle and top of the formation (Figures 2.1, 2.6 and 2.8). Medium to thick bedded, quartz-rich sandstone interbedded with thin to medium bedded mudstone characterize this lithofacies association. Recurring sedimentary structures include planar laminae, massive bedding, and planar and trough cross-bedding with minor ripples. Mudstone in LFA1 is preserved in a relatively small abundance compared to the other lithofacies associations. Minor clastic dikes and small-scale syn-sedimentary faults were locally observed in association with this lithofacies association.

Planar-laminated and bipolar-opposed trough cross-bedded sandstone stratigraphically overlies interpreted sandy storm beds in Baie Fine (see LFA2), and appears to record a transition in depositional processes from primarily storm-induced oscillatory flows to an increased influence of tidal currents. The absence of rippled bedding planes in the upper portion of the middle LFA3 section in Baie Fine is a result of deposition under higher-energy water conditions (Harris and Eriksson, 1990). The upward decrease in mudstone may indicate an increase in the frequency of storm events, which remove fine-grained, fair-weather deposits. The trough cross-bedded sandstone of LFA1 has a high maturity, but does not contain truncating sets of cross-bedding, banded sigmoidal foresets, reactivation surfaces, mudstone drapes, lag deposits, or associated inclined heterolithic bedding, which suggests that LFA1 is unlikely to represent deposition in tidal channels (Hamberg, 1991; Ehlers and Chan, 1999; Dalrymple and Choi, 2007). However, at least one bed of fine- to medium-grained sandstone in Baie Fine resembles a channel (Figure 2.9c). No clear relationship between grain size and cross-bed set thickness was observed, however a number of the sandstone beds exhibit marked lateral variability in thickness. Beds have flat to undulatory surfaces and generally exhibit a tabular form, suggesting a possible broadly-alternating sequence of storm sheet beds and tidal sand shoals (Goldring and Bridges, 1973; Johnson, 1977). The lack of wedge-shaped elements containing cross-

bedding points to a non-barrier subenvironment (Kumar and Sanders, 1974; Murakoshi and Masuda, 1992).

A tidal shelf ridge interpretation may be appropriate for the middle quartz-rich sequence in Baie Fine due to the interpreted under- and overlying offshore storm deposits. In addition, tidal shelf sand ridges are characteristic features of tide-dominated, transgressive shelves and can form in water as shallow as 30 m (Liu et al., 2007). Approximately 6 km northeast of the middle quartz-rich sequence in Baie Fine (46°2'8.41"N, 81°30'19.69"W) lies a 26 m thick planar-laminated and trough cross-bedded quartz arenite succession interbedded with minor mudstone (located at 46°3'4.46"N, 81°25'48.47"W), and is proposed to be stratigraphically equivalent. The apparent lateral continuity of LFA1 points to a continuous zone of deposition, typified by subtidal deposits and offshore tidal shelf ridges, which can be spaced 1 to 30 km apart and reach lengths of over 20 km (Posamentier, 2002). Overall, LFA1 is thought to represent deposition in the subtidal zone on a storm-influenced continental shelf.

In general, the formational contacts of the Gordon Lake Formation are associated with LFA1. Sandstone of LF1 and LF2, with mudstone interbeds, are characteristic of this interval. A transition from planar to ripple cross-laminae, or vice versa, was observed locally at the tops of convex-up and planar surfaced sandstone beds suggesting shallowing water conditions during deposition or a shift from oscillatory to unidirectional flow (c.f. Ainger and Reineck, 1982). The basal contacts of beds are often erosive in these units and many appear hummocky (Figure 2.14c). Regular intercalation of mudstone beds with sandstone indicates that flow was intermittent, but the absence of mudstone rip-up clasts indicates that the flows were not significantly erosive (Duke and Prave, 1991), or the muds remained fluid. Variations in stratification also points to fluctuations in flow velocity, from rapid deposition of sand, to slack water deposition of mud. The overall lack of simple wave-influenced structures and high-angle cross-beds suggests deposition in a subtidal shelf environment. Hummocky lower surfaces and ripple cross lamination may be a result of emplacement by storms.

2.5.1.2 LFA2: Subtidal to shallow shelf

Multiple examples of storm-generated deposits are preserved in the Gordon Lake Formation, and specifically in fining-upward intervals of LF6a, LF1, and LF7 or LF4 that are interpreted as representing subtidal to shallow shelf deposits (Figure 2.13b). The mudstone caps suggest waning current or fair-weather deposits. These units are best observed in Lady Evelyn-Smoothwater Provincial Park, Baie Fine, and in core from the Flack Lake area. Tide-related sedimentary structures in these intervals are minor.

Overall tabular, thin to medium bedded sandstone and mudstone beds that contain normal grading, planar to wavy laminae, syneresis cracks, and minor HCS are interpreted as a type of storm deposit. These deposits are best observed in strata at Baie Fine where they are underlain by thin beds and lenses of LF6a, and minor tide-generated deposits. The overlying strata consist of tabular, laminated sandstone with minor mudstone clasts. Small-scale SSDS, including load casts, pseudonodules, and flame structures, were observed throughout the storm beds and indicate local sediment instability.

A second type of storm-influenced, subtidal to shallow shelf deposit consists of stacked interlaminated and interbedded mudstone (LF7) and sandstone (LF1, with minor LF4). Mudstone-rich intervals are characterized by thin to thick bedded mudstone with less common very fine-grained sandstone beds. Normal grading and an abundance of SSDS of varying size and type were observed in LFA2. These deposits are best observed in the Bruce Mines and Baie Fine areas and in core from the Flack Lake area. A few medium-grained sandstone beds containing mudstone pebbles, planar laminae, and low angle cross-bedding were observed adjacent to interpreted storm deposits in Baie Fine. These sands may have been transported offshore during large storm events, or were reworked from older deposits (Sha and De Boer, 1991). Episodes of high-energy reworking can occur when tidal currents, which are strongest in the intertidal and subtidal-offshore zones (Hayes, 2005), are enhanced by storm waves (Johnson, 1977; Aigner and Reineck, 1982). In general, changing water depth produces considerable variability in storm-generated sequences (Kreisa, 1981).

The abundance and variety of SSDS in LFA2 led Hill and Corcoran (2018) to propose a primary storm or tsunami trigger mechanism for their formation. Thin sandy event beds observed in the Bruce Mines area are interpreted to represent tsunami deposits that were frequently colonized by microbial mats. Density inversions, overpressuring by microbial mats, and seismic events were interpreted as possible secondary trigger mechanisms. Based on available outcrop exposure and core, the SSDS-rich middle interval is preserved across at least half of the Huronian basin, pointing to large-scale, possibly basin-wide trigger mechanisms, such as storms, tsunamis, or earthquakes.

2.5.1.3 LFA3: Mixed intertidal flat

This association includes interlaminated to interbedded mudstone and fine-grained sandstone (LF4), alternating with fine-grained sandstone (LF1) and mudstone (LF7), and is interpreted to represent deposition on mixed intertidal flats. Characteristic sedimentary structures of this sub-environment include flaser and lenticular bedding, wave and interference ripples, ripple cross- and planar laminae, bi-directional-opposed ripples separated by mudstone drapes, desiccation cracks, and MISS. Minor small-scale SSDS are developed locally. Tabular, sheet sandstones of this type may have formed as a result of poorly confined drainage on a tidal flat (Donaldson et al., 2002), and small tidal channels have been recognized locally (Figure 2.11e). This lithofacies association was observed mainly in the Flack Lake and Lady-Evelyn Smoothwater Provincial Park study areas, which suggests that overall, tides played an important role in sediment deposition, in addition to waves. Sporadic storm events are indicated by graded bedding.

The alternating association of carbonate (LF3) with very fine- to fine-grained sandstone (LF1) and mudstone (LF7) in the Bruce Mines and Flack Lake areas and in Lady Evelyn-Smoothwater Provincial Park is interpreted to represent deposition on intertidal to subtidal flats. Stratiform stromatolites are known to form in low-energy to intertidal settings and small domal stromatolites in subtidal regions of modern tidal flats (e.g. Eriksson, 1977; Jahnert and Collins, 2012). In the Precambrian, stromatolites may also be expected in subtidal settings (Gebelein, 1976; Pratt, 1982; Grotzinger and Knoll, 1999), as there were no predators to provide grazing pressure. Dongjie et al. (2013) interpreted stratiform and domal stromatolites in the Mesoproterozoic Wumishan Formation, China,

to have formed in upper intertidal and lower intertidal areas, respectively. Similarly, Melezhik et al. (1999) interpreted stratiform stromatolites from the Paleoproterozoic Tulomozerskaya Formation, Russian Karelia, to have formed in the upper tidal zone, ponded tidal flat, lagoon, or playa lake. Laterally-linked stromatolites become isolated with increasing water turbulence (McIntyre and Fralick, 2017), suggesting that the domal stromatolites in LF3 at Smoothwater Lake formed under relatively low energy conditions, a theory that is supported by the presence of wave ripples and lack of cross-bedding.

Thin interbeds and interlaminae of sandstone and mudstone in LFA3 represent vertical accretion and shifts in sand and mud placement on mixed intertidal flats (e.g. Dalrymple, 2010; Daidu, 2013.). The abundance of tidal signatures in the Gordon Lake Formation supports the action of tidal currents throughout the majority of deposition. Although the absence of land plants would have led to increased rates of runoff, the colonization of microbial mats would have enhanced sediment stabilization and led to increased preservation of tidal flat deposits and mud (Eriksson and Simpson, 2012). Recognition of MISS and stromatolites in the Gordon Lake Formation support the contribution of biofilms to preservation of the succession.

Although the paleoenvironment represented by the upper Lorrain Formation has been much disputed it is generally agreed that a transgression took place (Chandler, 1986), which would have resulted in increased accommodation for deposition of the Gordon Lake Formation. Upon initiation, the sedimentary processes forming the sandy alluvial and nearshore deposits of the upper Lorrain Formation appear to have changed to tide-dominated processes (Figure 2.15). Bimodal-opposed cross stratification is present in both the upper few metres of the underlying Lorrain Formation at Welcome Lake (Long, 2004a), and overlying Bar River Formation (Rust and Shields, 1987; Aranha, 2015). The Kona Dolomite of the Marquette Range Supergroup, Michigan, is interpreted to be correlative with the lower Gordon Lake Formation (Young, 1983; Bekker et al., 2006; Bennett, 2006), suggesting that a period of overall low sediment influx associated with the onset of transgression may have facilitated carbonate production.

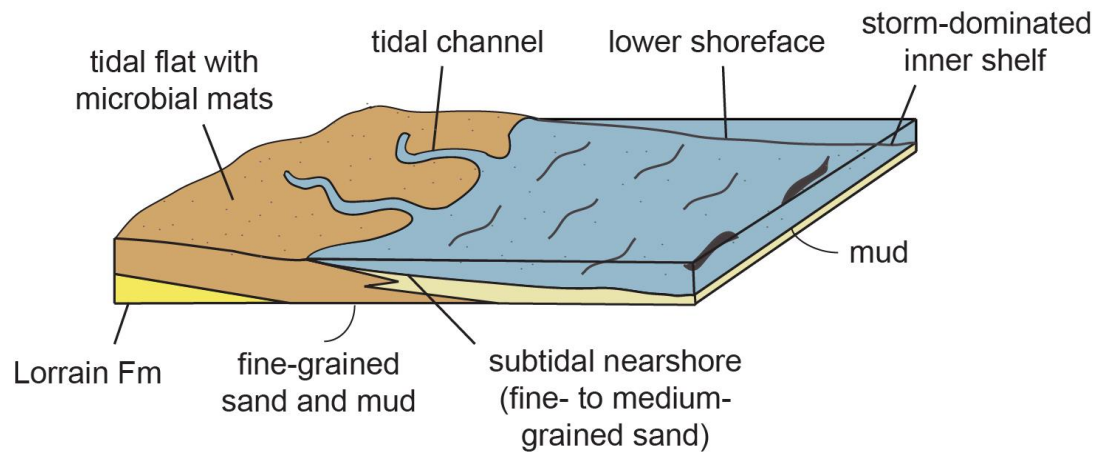


Figure 2.15. Depositional model for the Gordon Lake Formation. Deposition of the lower part of the formation is interpreted to have occurred in the subtidal nearshore to shallow shelf zones along a passive margin. Deposition of the upper part of the formation is interpreted to have occurred in the subtidal nearshore to mixed intertidal flat zones along a passive margin.

2.5.2 Basin dynamics

The upper Huronian Supergroup is interpreted to have been deposited along a passive margin (Young and Nesbitt, 1985; Young et al., 2001; Long, 2004a, 2009). The characteristics of the Gordon Lake Formation support this interpretation, in that it thickens southward towards the proposed paleomargin, does not noticeably change thickness across faults, and contains sedimentary structures indicative of a marginal marine origin (Wood, 1973; Chandler, 1986; 1988; Hill et al., 2016; 2018). Rifting took place during deposition of the lower Huronian Supergroup (Card et al., 1977; Young, 1983; Young et al., 2001; Long, 2004a), and extensional faults would have still been active during deposition of the Gordon Lake Formation. Potential evidence of fault movement at the time of deposition includes SSDS, syn-sedimentary faults, and brecciated beds. A primary trigger mechanism of storm or tsunami waves was interpreted for the SSDS due in part to a lack of firm evidence for seismic activity in the associated intervals (Hill and Corcoran, 2018). Seismic events, however, cannot be excluded. Clastic dikes and small-scale syn-sedimentary faults may have formed due to local instabilities, or slope failure.

The basal, overall fining- and thinning-upward trend in the Gordon Lake Formation (Figure. 2.14e) may signify transgression brought on by regional subsidence of the newly formed Huronian passive margin. In general, it is difficult to evaluate the cause of Paleoproterozoic transgressions, and to conclude the relative importance of eustatic over tectonic influence (Eriksson et al., 1998). The top of the formation is characterized by a coarsening- and thickening-upward succession, which may be a result of regression or an increase in sediment supply. A combination of sea-level rise, subsidence, and microbial mat development may have led to enhanced preservation of strata in the Gordon Lake Formation. Bradley et al. (2018) compiled a list of reported pre-vegetation tidal successions, and determined that out of 40, 21 contain <2% mudstone and are dominated by quartz-rich sandstone. The muddy nature of the Gordon Lake Formation and preservation of lenticular bedding, mudstone drapes, and shrinkage cracks sets it apart from many other Precambrian tide-influenced successions.

2.5.3 Summary of the depositional history of the Gordon Lake Formation

The paleoenvironmental model proposed herein is in general agreement with several findings of previous workers, however the regional approach taken in this study allowed an integrated model to be developed. The vertical association of lithofacies in the Gordon Lake Formation supports deposition from the intertidal zone to shallow shelf. Overall, the formation is characterized by tabular bedding, however many basal surfaces are erosive or undulatory in nature, supporting deposition above storm wave base. Both tide and storm processes played a major role in sedimentation during deposition, as indicated by tide- and storm-generated structures throughout much of the formation. An open coast tidal flat environment is envisioned in part due to the relative abundance of sedimentary structures formed by waves or combined-flows as opposed to channel-fill deposits, which would be expected in a sheltered tidal flat environment (Dalrymple, 2010; Daidu, 2013). Coastal barriers are not considered to have been present during deposition of the formation because dominant tidal currents would have disseminated sand offshore (Hayes, 2005), and tidal inlet deposits are lacking. The tidal range is estimated to be macrotidal (>4m) based on: 1) the presence of wave-reworked strata in the interpreted mixed intertidal and subtidal zones, indicating exposure to open ocean waves at the time of deposition (Hiscott, 1982), 2) the lack of barrier deposits, which are commonly found in micro- and meso-tidal ranges (Nichols, 1989; Shaw et al., 2010), and 3) the closer proximity of the Moon to Earth during the Precambrian, which would have resulted in a larger tidal range (Williams, 2000). Similar tidal deposits and associations have been described from the Paleoproterozoic Palms and Pokegama formations, Canada (Ojakangas, 1983), Ordovician Graafwater Formation, South Africa (Rust, 1977), and early Precambrian Pongola Supergroup, South Africa (Von Brunn and Hobday, 1976).

Deposition of the Gordon Lake Formation is interpreted to have been initiated in response to rising sea levels. This is supported by the gradual shift from an alluvial or nearshore environment of the upper Lorrain Formation to an inferred open coast tidal flat setting of the Gordon Lake Formation, where carbonate deposition took place locally, nodular evaporites formed, and alternations of mud and sand were deposited. Increasing

sea level and storm activity would have led to the accumulation of stacked fining-upward storm units, characterized by a basal layer of intraformational granular to pebbly sandstone or conglomerate, overlain by fine-grained sandstone, and locally capped by mudstone. Fluctuations in sea level would have resulted in deposition of sandy inter- to subtidal deposits overlain by sandy storm beds. A quartz-rich sandstone interval preserved in Baie Fine and Killarney Provincial Park indicates that accommodation fluctuated and experienced at least one reversal, which is considered normal for a transgressive coast (Kraft, 1978). Thin, tabular, scoured mudstone and sandstone beds interpreted as subtidal to shallow shelf deposits overlie the quartz-rich unit and indicate a return to deeper marine conditions. A regression, that decreased the available accommodation space, or an increase in sediment supply (coastal progradation) is indicated by an upward-coarsening and -thickening trend, that extends to the top of the formation. On a small scale, it is possible that some variations in bed thickness may be due to spring and neap tides, or storm influence on sedimentation (Allen, 1985; Li et al., 2000). Waning tidal currents can also cause a significant amount of fine-grained material to be deposited from suspension (Dalrymple et al., 1991).

2.6 Conclusion

Sedimentary structures formed by tides and storms are common in the Gordon Lake Formation. The combination and distribution of lithologies and suites of physical and biogenic sedimentary structures preserved in the formation suggests deposition on a tide- and storm-influenced continental shelf. Seven lithofacies were recognized that comprise three lithofacies associations: subtidal nearshore (LFA1), subtidal to shallow shelf (LFA2), and mixed intertidal flat (LFA3). The overlying Bar River Formation may represent uninterrupted deposition and form the top of a shoaling cycle. The contacts between the Gordon Lake Formation and the underlying Lorrain and overlying Bar River formations are typically obscured by gabbro sills. Further work is needed to elucidate the depositional histories of the under- and overlying formations.

2.7 References

- Aigner, T., Reineck, H.-E., 1982. Proximality trends in modern sands from the Heligoland Bight (North Sea) and their implications for basin analysis. *Senck. Marit.* 14, 5: 183-215.
- Al-Hashim, M.H., 2016. Sedimentology and geochemistry of the mixed carbonate-siliciclastic Espanola Formation, Paleoproterozoic Huronian Supergroup, Bruce Mines-Elliot Lake Area, Ontario, Canada (PhD Thesis), The University of Western Ontario. Electronic Thesis and Dissertation Repository, 4350.
- Allen, J.R.L., 1985. Principles of physical sedimentology. Springer Netherlands, 272p.
- Altermann, W., 2004. Evolving life and its effect on Precambrian sedimentation. In: Eriksson, P.G., Altermann, W., Nelson, D.R., Mueller, W.U., Catuneanu, O. (Eds.), *The Precambrian Earth: Tempos and Events, Developments in Precambrian Geology*, vol. 12. Elsevier, pp. 539–545.
- Anderton, R.A., 1976. Tidal-shelf sedimentation: an example from the Scottish Dalradian. *Sedimentology* 23, 429-458.
- Aspler, L.B., Chiarenzelli, J.R., 1998. Two Neoproterozoic supercontinents? Evidence from the Paleoproterozoic. *Sediment. Geol.* 120, 75-104.
- Bekker, A., Karhu, J.A., Kaufman, A.J., 2006. Carbon isotope record for the onset of the Lomagundi carbon isotope excursion in the Great Lakes area, North America. *Precambrian Res.* 148, 145–180.
- Bennett, G., 2006. Geological features and correlation of a dolostone unit in Fenwick Township, northeast of Sault Ste Marie, Ontario. In: *The Huronian Supergroup between Sault Ste Marie and Elliot Lake. Field Trip Guidebook*, 49–50 Part 4.
- Bennett, G., Born, P., Hatfield, K., 1989. A report on a recently identified dolostone unit in Fenwick Township, Goulais Bay area, District of Algoma. In: Fenwick, K.G., Gibling, P.E., Pitts, A.E. (Eds.), *Report of activities 1988, Ontario Geological Survey Miscellaneous Paper 142*, 211–215.
- Berner, R.A., 1984. Sedimentary pyrite formation; an update. *Geochim. Cosmochim. Acta* 48, 605–615.
- Bleeker, W., Kamo, S., Ames, D., 2013. New field observations and U-Pb age data for footwall (target) rocks at Sudbury: towards a detailed cross-section through the Sudbury Structure. *Large Meteorite Impacts and Planetary Evolution V. Geol. Soc. Am. Special Papers* 3112.
- Bleeker, W., Kamo, S.L., Ames, D.E., Davis, D., 2015. New field observations and U-Pb ages in the Sudbury area: toward a detailed cross-section through the deformed Sudbury Structure. In: Aimes, D.E., Houllé, M.G. (Eds.), *Targeted Geoscience Initiative 4: Canadian Nickel-Copper Platinum Group Elements-Chromium Ore Systems – Fertility. New and Revised Models*, Geological Survey of Canada Open File 7856, 153–166.

- Bradley, G.-M., Redfern, J., Hodgetts, D., George, A.D., Wach, G.D., 2018. The applicability of modern tidal analogues to pre-vegetation paralic depositional models. *Sedimentology* 65, 2171-2201.
- Brenchley, P., 1989. Storm sedimentation. *Geol. Today* 5, 4: 133-137.
- Card, K.D., 1976. Geology of the McGregor Bay-Bay of Islands area, Districts of Sudbury and Manitoulin. Ontario Division of Mines Geoscience, Report 138, 63p.
- Card, K.D., 1978a. Geology of the Sudbury-Manitoulin area, districts of Sudbury and Manitoulin. Ontario Geological Survey, Geoscience Report 166, 238p.
- Card, K.D., 1978b. Sudbury-Manitoulin, Sudbury and Manitoulin districts. Ontario Geological Survey, Map 2360, scale 1:126 720 or 1 inch to 2 miles.
- Card, K.D., Innes, D.G., Debicki, R.L., 1977. Stratigraphy, Sedimentology, and Petrology of the Huronian Supergroup of the Sudbury-Espanola Area. Ontario Division of Mines, Geoscience Study 16, 99p.
- Card, K.D., Lumbers, S.B., 1977. Sudbury-Cobalt, geological compilation series, Algoma, Manitoulin, Nipissing, Parry Sound, Sudbury and Timiskaming districts. Ontario Geological Survey, Map 2361, scale 1:253 440 or 1 inch to 4 miles.
- Casshyap, S.M., 1966. Sedimentary petrology and stratigraphy of the Huronian rocks south of Espanola, Ontario. The University of Western Ontario, unpublished PhD thesis, 232p.
- Chandler, F.W., 1984. Sedimentary setting of an early Proterozoic copper occurrence in the Cobalt Group, Ontario: a preliminary assessment. In: *Current Research, Part A. Geological Survey of Canada Paper 84-1A*, pp. 185–192.
- Chandler, F.W., 1986. Sedimentology and paleoclimatology of the Huronian (Early Aphebian) Lorrain and Gordon Lake Formations and their bearing on models for sedimentary copper mineralization. In: *Geological Survey of Canada Paper 86-1A*, pp. 121–132.
- Chandler, F.W., 1988. Diagenesis of sabkha-related, sulphate nodules in the early Proterozoic Gordon Lake Formation, Ontario, Canada. *Carbonates Evaporites* 3, 75–94.
- Cheel, R.J., Leckie, D.A., 1992. Coarse-grained storm beds of the upper Cretaceous Chungo Member (Wapiabi Formation), southern Alberta, Canada. *J. Sed. Petrol.* 62, 6: 933-945.
- Clifton, H.E., 2003. Supply, segregation, successions, and significance of shallow marine conglomeratic deposits. *B. Can. Petrol. Geol.* 51, 4:370-388.
- Clifton, H.E., 2005. Coastal sedimentary facies. In: Schwartz, M.L. (Ed.) *Encyclopedia of Coastal Science*, Springer, pp. 270-278.
- Collins, W.H., 1925. North Shore of Lake Huron. Geological Survey of Canada, Memoir 143, 160p. Accompanied by Maps 1969, 1970, 1971, scale 1:126 720 or 1 inch to 2 miles.

- Condie, K.C., 1998. Episodic continental growth and supercontinents: a mantle avalanche connection? *Earth Planet Sc. Lett.* 163, 97–108.
- Corfu, F., Andrews, A.J., 1986. A U-Pb age for mineralized Nipissing diabase, Gowganda, Ontario. *Can. J. Earth Sci.* 23 (1), 107–109.
- Daidu, F., 2013. Classifications, sedimentary features and facies associations of tidal flats. *J. Paleogeog.* 2, 1: 66-80.
- Dalrymple, R.W., 2010. Tidal depositional systems. In: James, N.P., Dalrymple, R.W., (Eds), *Facies Models 4*. Geological Association of Canada, *GEOtext* 6, 201-232.
- Dalrymple, R.W., Choi, K.S., 2007. Morphologic and facies trends through the fluvial-marine transition in tide-dominated depositional systems: a systematic framework for environmental and sequence-stratigraphic interpretation. *Earth Sci Rev.* 81:135–174.
- Dalrymple, R.W., Makino, Y., Zaitlin, B.A., 1991. Temporal and spatial patterns of rhythmite deposition on mud flats in the macrotidal Cobequid Bay-Salmon River estuary, Bay of Fundy, Canada. In: Smith, D.G., Reinson, G.E., Zaitlin, A., and Rahmani, R.A. (Eds.), *Clastic tidal sedimentology*. *Can. Soc. Pet. Geol. Memoir* 16, 137-160.
- Dawson, A.G., Stewart, I. 2007. Tsunami deposits in the geological record. *Sed. Geol.* 200, 166-183.
- Donaldson, J.A., Eriksson, P.G., Altermann, W., 2002. Actualistic versus non-actualistic conditions in the Precambrian sedimentary record: reappraisal of an enduring discussion. *Spec. Publs. int. Ass. Sediment.* 33, 3-13.
- Dongjie, T., Xiaoying, S., Ganqing, J., Yunpeng, P., Wenhao, Z., 2013. Environment controls on Mesoproterozoic thrombolite morphogenesis: a case study from the North China Platform. *J. Palaeogeogr.* 2, 275-296.
- Duke, W.L., 1985. Hummocky cross-stratification, tropical hurricanes, and intense winter storms. *Sedimentology* 32, 167-194.
- Duke, W.L., Arnott, R.W.C., Cheel, R.J. 1991a. Shelf sandstones and hummocky cross-stratification: new insights on a stormy debate. *Geology* 19, 625-628.
- Duke, W.L., Prave, A.R., 1991b. Storm- and tide-influenced prograding shoreline sequences in the Middle Devonian Mahantango Formation, Pennsylvania. In: Smith, D.G., Reinson, G.E., Zaitlin, A., and Rahmani, R.A. (Eds.), *Clastic tidal sedimentology*. *Can. Soc. Pet. Geol. Memoir* 16, 349-370.
- Ehlers, T.A., Chan, M.A., 1999. Tidal sedimentology and estuarine deposition of the Proterozoic Big Cottonwood Formation, Utah. *J. Sed. Res.* 69, 6: 1169-1180.
- Einsele, G., 2000. Coastal and Shallow Sea Sediments (including carbonates). In: Einsele, G. (Ed.), *Sedimentary Basins: Evolution, Facies, and Sediment Budget*. Springer-Verlag, Berlin, 94-153.
- Eisbacher, G.H., Bielenstein, H.U., 1969. The Flack Lake depression, Elliot Lake area, Ontario (41 J/10). *Geological Survey of Canada Paper* 69-1B, pp. 58–60.

- Eriksson, K.A., 1977. Tidal flat and subtidal sedimentation in the 2250 m.y. Malmani Dolomite, Transvaal, South Africa. *Sed. Geol.* 18, 223-244.
- Eriksson, K.A., Simpson, E., 2012. Precambrian Tidal Facies. In: Davis, R.A. Jr., Dalrymple, R.W. (Eds.), *Principles of Tidal Sedimentology*. Springer, pp. 397-420.
- Eriksson, P.G., Bumby, A.J., Popa, M., 2004. Sedimentation through time. In: Eriksson, P.G., Altermann, W., Nelson, D.R., Mueller, W.U., Catuneanu, O. (Eds.), *The Precambrian Earth: Tempos and Events, Developments in Precambrian Geology*, vol. 12. Elsevier, pp. 593-602.
- Eriksson, P.G., Condie, K.C., Tirsgaard, H., Mueller, W.U., Altermann, W., Miall, A.D., Aspler, L.B., Catuneanu, O., Chiarenzelli, J.R., 1998. Precambrian clastic sedimentation systems. *Sediment. Geol.* 120, 5-53.
- Eriksson, P.G., Reczko, B.F.F., Boshoff, A.J., Schreiber, U.M., Van der Neut, M., Snyman, C.P., 1995. Architectural elements from Lower Proterozoic braid-delta and high-energy tidal flat deposits in the Magaliesberg Formation, Transvaal Supergroup, South Africa. *Sediment. Geol.* 97, 99-117.
- Eriksson, P.G., Catuneanu, O., Aspler, L.B., Chiarenzelli, J.R., Martins-Neto, M.A., 2001. Preface, special issue: the influence of magmatism, tectonics, sea level change and palaeo-climate on Precambrian basin evolution: change over time. *Sediment. Geol.* 141/142, vii-xi.
- Eriksson, P.G., Porada, H., Banerjee, S., Bouougri, E., Sarkar, S., Bumby, A.J., 2007a. Mat-destruction features. In: Schieber, J., Bose, P.K., Eriksson, P.G., Banerjee, S., Sarkar, S., Altermann, W., Catuneanu, O. (Eds.), *Atlas of Microbial Mat Features Preserved within the Siliciclastic Rock Record, Atlases in Geoscience 2*. Elsevier, pp. 76-105.
- Flannery, D.T., Summons, R.E., Walter, M.R., 2018. Archean lakes as analogues for habitable Martian paleoenvironments. In: Cabrol, N.A., and Grin, E.A. (Eds.) *From Habitability to Life on Mars*. Elsevier, p.127-152.
- Flügel, E., 2010. Microfacies data: Fabrics. In: *Microfacies of carbonate rocks: analysis, interpretation and application*, 2nd ed. Springer, pp. 177-242.
- Frarey, M.J., 1967. Three new Huronian formational names. *Geological Survey of Canada Paper 67-6*, 3p.
- Frarey, M.J., 1977: *Geology of the Huronian Belt Between Sault Ste. Marie and Blind River, Ontario*. Geological Survey of Canada, Memoir 383, 87p.
- Figueiredo, A.G.Jr., Sanders, J.E., Swift, D.J.P., 1982. Storm-graded layers on inner continental shelves: Examples from Brazil and the Atlantic coast of the central United States. *Sed. Geol.* 31, 3-4: 171-190.
- Garzanti, E., 1991. Non-carbonate intrabasinal grains in arenites: their recognition, significance, and relationship to eustatic cycles and tectonic setting. *J. Sed. Petrol.* 61, 6: 959-975.

- Gebelein, C.D., 1976. The effects of the physical, chemical and biological evolution of the earth. In: Walker, E.D. (Ed.) *Stromatolites, Developments in Sedimentology* 20. Elsevier, Amsterdam, pp. 499-517.
- Giblin, P.E., Leahy, E.J., Robertson, J.A. 1979. Sault Ste. Marie-Elliot Lake, geological compilation series, Algoma, Manitoulin and Sudbury districts. Ontario Geological Survey, Map 2419, scale 1:253 440 or 1 inch to 4 miles.
- Goldring, R., Bridges, P., 1973. Sublittoral sheet sandstones. *J. Sed. Pet.* 43, 3: 736-747.
- Google Earth Pro 7.3.2 (2018). Retrieved January 14, 2019 from <https://www.google.com/earth/versions/#earth-pro>.
- Grotzinger, J.P., Knoll, A.H., 1999. Stromatolites in Precambrian carbonates: evolutionary mileposts or environmental dipsticks? *Annu. Rev. Earth Planet. Sci.* 27, 313-358
- Hamberg, L., 1991. Tidal and seasonal cycles in a Lower Cambrian shallow marine sandstone (Hardeberga Fm.) Scania, Southern Sweden. In: Smith, D.G., Reinson, G.E., Zaitlin, A., and Rahmani, R.A. (Eds.), *Clastic tidal sedimentology*. Can. Soc. Pet. Geol. Memoir 16, 255-274.
- Harms, J.C., Southard, J.B. and Walker, R.G., 1982. Structures and sequences in clastic rocks. *Soc. Econ. Paleontol. Mineral., Short Course*, 9.
- Harris, C.W., Eriksson, K.A., 1990. Allogenic controls on the evolution of storm to tidal shelf sequences in the Early Proterozoic Uncompahgre Group, southwest Colorado, USA. *Sedimentology* 37, 189-213.
- Hayes, M.O., 2005. Tide-Dominated Coasts. In: Schwartz, M.L. (Ed.) *Encyclopedia of Coastal Science*, Springer, pp. 982-983.
- Hill, C., Corcoran, P.L., Aranha, R., Longstaffe, F.J., 2016. Microbially induced sedimentary structures in the Paleoproterozoic, upper Huronian Supergroup, Canada. *Precambrian Res.* 281, 155–165.
- Hill, C.M., Corcoran, P.L., 2018. Processes responsible for the development of soft-sediment deformation structures (SSDS) in the Paleoproterozoic Gordon Lake Formation, Huronian Supergroup, Canada. *Precambrian Res.* 310, 63–75.
- Hill, C.M, Davis, D.W., Corcoran, P.L., 2018. New U-Pb geochronology evidence for 2.3 Ga detrital zircon grains in the youngest Huronian Supergroup formations, Canada. *Precambrian Res.* 314, 428-433.
- Hiscott, R.N., 1982. Tidal deposits of the Lower Cambrian Random Formation, eastern Newfoundland: facies and paleoenvironments. *Can. J. Earth Sci.* 19, 10: 2028-2042.
- Hofmann, H.J., Pearson, D.A.B., Wilson, B.H., 1980. Stromatolites and fenestral fabric in early Proterozoic Huronian Supergroup, Ontario. *Can. J. Earth Sci.* 17 (10), 1351–1357.
- Hoyt, J.H., Vernon, J.H. Jr., 1967. Influence of island migration on barrier-island sedimentation. *Geol. Soc. Am. Bull.* 78, 1:77-86.

- Ingersoll, R.V., Bullard, T.F., Ford, R.L., Grimm, J.P., Pickle, J.D., Sares, S.W., 1984. The effect of grain size on detrital modes: a test of the Gazzi-Dickinson point-counting method. *J. Sed. Petrol.* 54, 1: 103-116.
- Jahnert, R.J., Collins, L.B., 2012. Characteristics, distribution and morphogenesis of subtidal microbial systems in Shark Bay, Australia. *Mar. Geol.* 303-306, 115-136.
- Johnson, H.D., 1977. Shallow marine sand bar sequences: an example from the late Precambrian of North Norway. *Sedimentology* 24, 245-270.
- Ketchum, K.Y., Heaman, L.M., Bennett, G., Hughes, D.J., 2013. Age, petrogenesis and tectonic setting of the Thessalon volcanic rocks, Huronian Supergroup, Canada. *Precambrian Res.* 233, 144-172.
- Kraft, J.C., 1978. Coastal Stratigraphic Sequences. In: Jr. Davis, R.A. (Ed.) *Coastal Sedimentary Environments*. Springer-Verlag, 361-381.
- Kreisa, R.D., 1981. Storm-generated sedimentary structures in subtidal marine facies with examples from the middle and upper Ordovician of southwestern Virginia. *J. Sed. Res.* 51, 3: 823-848.
- Krogh, T.E., Davis, D.W., Corfu, F., 1984. Precise U-Pb zircon and baddeleyite ages for the Sudbury Structure. In: Pye, E.G., Naldrett, A.J., Giblin, P.E. (Eds.), *Geology and Ore Deposits of the Sudbury Structure*. Ontario Geological Survey, pp. 431-446.
- Kuenen, P.H.H., Menard, H.W., 1952. Turbidity currents, graded and non-graded deposits. *J. Sed. Petrol.* 22, 2:83-96.
- Kumar, N., Sanders, J.E., 1974. Inlet sequence: a vertical succession of sedimentary structures and textures created by the lateral migration of tidal inlets. *Sedimentology* 21, 491-532.
- Levson, V. M., 1995. Marine Placers. In: Lefebvre, D.V., Ray, G.E., (Eds) *Selected British Columbia Mineral Deposit Profiles, Volume 1 - Metallics and Coal*. British Columbia Ministry of Energy of Employment and Investment, Open File 1995-20, 29-31.
- Liu, Z., Berné, S., Saito, Y., Yu, H., Trentesaux, A., Uehara, K., Yin, P., Liu, J.P., Li, Chaoxing, Hu, Guanghai, Wang, Xiangqin, 2007. Internal architecture and mobility of tidal sand ridges in the East China Sea. *Cont. Shelf Res.* 27, 13: 1820-1834.
- Logan, B.W., Hoffman, P., Gebelein, C.D., 1974. Algal mats, cryptalgal fabrics and structures, Hamelin Pool, Western Australia. In: Logan, B.W. (Ed.), *Evolution and Diagenesis of Quaternary Carbonate sequences, Shark Bay, Western Australia*. Am. Assoc. Petrol. Geologists, *Memoir* 22, pp. 140-194.
- Long, D.G.F., 2004a. The tectonostratigraphic evolution of the Huronian basement and subsequent basin fill: geological constraints on impact models of the Sudbury event. *Precambrian Res.* 129, 203-223.

- Long, D.G.F., 2004b. Precambrian Rivers. In: Eriksson, P.G., Altermann, W., Nelson, D.R., Mueller, W.U., Catuneanu, O. (Eds.), *The Precambrian Earth: tempos and events*. *Developments in Precambrian Geology* 12, Elsevier, 660-662.
- Long, D.G.F., 2009. The Huronian Supergroup. In: Rousell, D.H., Brown, G.H. (Eds.), *A Field Guide to the Geology of Sudbury, Ontario*. Ontario Geological Survey, Open File Report 6243, pp. 14–30.
- Long, D.G.F., 2019. Archean fluvial deposits: a review. In: Mazumder, R., Eriksson, P. (Eds.), *Archean Earth Processes*. *Earth Sci. Rev.* 188, 148-175.
- Longhitano, S.G., Mellere, D., Steel, R.J., Ainsworth, R.B., 2012. Tidal depositional systems in the rock record: a review and new insights. *Sed. Geol.* 279, 2-22.
- Mazzullo, S.J., 2004. Overview of porosity evolution in carbonate reservoirs. *Kansas Geological Society Bulletin* 79, 1: 22-28.
- McIntyre, T., Fralick, P., 2017. Sedimentology and Geochemistry of the 2930 Ma Red Lake-Wallace Lake Carbonate Platform, Western Superior Province, Canada. *Dep. Rec.* 3, 2: 258-287.
- McKee, E.D., Crosby, E.J., Berryhill, H.L., Jr., 1967. Flood deposits, Bijou Creek, Colorado, June 1965. *J. Sediment. Petrol.* 37, 3: 829-851.
- McMahon, S., van Smeerdijk Hood, A., McIlroy, D., 2017. The origin and occurrence of subaqueous sedimentary cracks. In: Brasier, A.T., McIlroy, D., McLoughlin, N. (Eds.), *Earth Systems Evolution and Early Life: a celebration of the work of Martin Brasier*. Geological Society, London, Special Publications, 448, 285-309.
- Melezhik, V.A., Fallick, A.E., Medvedev, P.V., Makarikhin, V.V., 1999. Paleoproterozoic magnesite-stromatolite-dolomite-‘red beds’ association, Russian Karelia: paleoenvironmental constraints on the 2.0 Ga positive carbon isotope shift. *Geological Survey of Norway, Report* 99.052, 39 p.
- Murakoshi, N., Masuda, F., 1992. Estuarine, barrier-island to strand-plain sequence and related ravinement surface developed during the last interglacial in the Paleo-Tokyo Bay, Japan. *Sed. Geol.* 80, 167-184.
- Murray, A., 1858. On the topography and geology of the coast of Georgian Bay at the mouth of the French River; on Echo Lake and its environs; and on the Huronian limestone near Bruce Mine. *Geological Survey of Canada, Report of Progress for the year 1857*, p. 13-27, p. 18-26.
- Nichols, G., 2009. *Sedimentology and Stratigraphy*, 2nd ed. Wiley-Blackwell, UK, 419p.
- Nichols, M.M., 1989. Sediment accumulation rates and relative sea-level rise in lagoons. *Mar. Geol.* 88, 201–219.
- Ojakangas, R.W., 1983. Tidal deposits in the early Proterozoic basin of the Lake Superior region – the Palms and the Pokegama formations: evidence for subtidal-shelf deposition of Superior-type banded iron-formation. In: Medaris, L.D., Jr. (Ed.), *Early Proterozoic Geology of the Great Lakes Region*: Geological Society of America Memoir 160, 49-66.

- Pickett, C., 2002. A sedimentary facies analysis of the >2.8 Ga Beniah and Bell Lake Formations, Slave Province, Northwest Territories. MSc. Thesis, l'Université du Québec à Chicoutimi, Chicoutimi, 136 p.
- Plint, A.G., 2010. Wave- and storm-dominated shoreline and shallow-marine systems. In: James, N.P., Dalrymple, R.W., (Eds), *Facies Models 4*. Geological Association of Canada, *GEOtext* 6, 201-232.
- Posamentier, H.W., 2002. Ancient shelf ridges – a potentially significant component of the transgressive systems tract: case study from offshore northwest Java. *AAPG Bull.* 86, 1:75-106.
- Potter, P.E., Maynard, J.B., Depetris, P.J., 2005. *Mud and mudstones: introduction and overview*. Springer-Verlag, 296pp.
- Pratt, B.R., 1982. Stromatolite decline – a reconsideration. *Geology* 10, 512-515.
- Prave, A.R., Duke, W.L., Slattery, W., 1996. A depositional model for storm- and tide-influenced prograding siliciclastic shorelines from the Middle Devonian of the central Appalachian foreland basin, USA. *Sedimentology* 43, 611-629.
- Raaf, J.F.M., Boersma, J.R., Gelder, A., 1977. Wave-generated structures and sequences from a shallow marine succession, Lower Carboniferous, County Cork, Ireland. *Sedimentology* 24, 451-483.
- Rasmussen, B., Bekker, A., Fletcher, I.R., 2013. Correlation of paleoproterozoic glaciations based on U-Pb zircon ages for tuff beds in the Transvaal and Huronian Supergroups. *Earth Planet. Sc. Lett.* 382, 173–180.
- Reid, R.P., Visscher, P.T., Decho, A.W., Stolz, J.K., Bebout, B.M., Dupraz, C., Mactintyre, I.G., Paerl, H.W., Pinckney, J.L., Prufert-Bebout, L., Steppe, T.F., Des Marais, D.J., 2000. The role of microbes in accretion, lamination and early lithification of modern marine stromatolites. *Nature* 406, 989–992.
- Reineck, H.E., Singh, I.B., 1980. *Depositional sedimentary environments with reference to terrigenous clastics*, 2nd ed. Springer-Verlag, 549p.
- Reynaud, J.-Y., Dalrymple, R.W., 2012. Shallow-marine tidal deposits. In: Davis, R.A. Jr., Dalrymple, R.W. (Eds.), *Principles of Tidal Sedimentology*. Springer, pp. 335-369.
- Ricci Lucchi, F., 1995. *Sedimentographica: photographic atlas of sedimentary structures*, 2nd ed. Columbia University Press, New York, 255p.
- Rice, R.J., 1986. Regional sedimentation in the Lorrain Formation (Aphebian), central Cobalt Embayment. *Summary of Field Work and Other Activities: Ontario Geological Survey Miscellaneous Paper* 137, 210–216.
- Riding, R., 1991. Classification of microbial carbonates. In: Riding, R. (Ed.) *Calcareous Algae and Stromatolites*. Springer-Verlag, pp. 21-51.
- Riggs, S.R., 2010. North Carolina. In: Bird, E.C.F. (Ed.) *Encyclopedia of the world's coastal landforms*, vol. 1. Springer, Dordrecht, p.99-106.

- Robertson, J.A., Card, K.D., 1988. Geology and Scenery: North shore of Lake Huron Region. Ontario Geological Survey, Geological Guidebook, 224p.
- Rousell, D.H., Fedorowich, J.S., Dressler, B.O., 2003. Sudbury Breccia (Canada): a product of the 1850 Ma Sudbury Event and host to footwall Cu-Ni-PGE deposits. *Earth. Sci. Rev.* 60, 147-174.
- Rust, B.R., Shields, M.J., 1987. The sedimentology and depositional environments of the Huronian Bar River Formation, Ontario. Grant 189, Ontario Geological Survey Open File Report 5672, pp. 37.
- Rust, I.C., 1977. Evidence of shallow marine and tidal sedimentation in the Ordovician Graafwater Formation, Cape Province, South Africa. *Sed. Geol* 18, 123-133.
- Schieber, J., 1999, Distribution and deposition of mudstone facies in the Upper Devonian Soneya Group of New York. *J. Sed. Res.* 69, 909-925.
- Schieber, J., 2004. Microbial mats in the siliciclastic rock record: a summary of diagnostic features. In: Eriksson, P.G., Altermann, W., Nelson, D.R., Mueller, W.U., Catuneanu, O. (Eds.), *The Precambrian Earth: Tempos and Events, Developments in Precambrian Geology*, vol. 12. Elsevier, pp. 663-673.
- Schieber, J., Southard, J.B., Schimmelmann, A., 2010. Lenticular shale fabrics resulting from intermittent erosion of water-rich muds – interpreting the rock record in the light of recent flume experiments. *J. Sed. Res.* 80, 119-128.
- Schopf, J.W., 1975. Precambrian paleobiology: problems and perspectives. *Annu. Rev. Earth. Pl. Sc.* 3, 213-249.
- Schopf, J.W., Kudryavtsev, A.B., Czaja, A.D., Tripathi, A.B., 2007. Evidence of Archean life; stromatolites and microfossils. *Precambrian Res.* 158, 141-155.
- Schulz, K.J., Cannon, W.F., 2007. The Penokean orogeny in the Lake Superior region. *Precambrian Res.* 157, 4-25.
- Sha, L.P., De Boer, P.L., 1991. Ebb-tidal deposits along the west Frisian Islands (The Netherlands): processes, facies architectures and preservation. In: Smith, D.G., Reinson, G.E., Zaitlin, A., and Rahmani, R.A. (Eds.), *Clastic tidal sedimentology*. *Can. Soc. Pet. Geol. Memoir* 16, 199-218.
- Shaw, J., Amos, C.L., Greenberg, D.A., O'Reilly, C.T., Parrot, D.R., Patton, E., 2010. Catastrophic tidal expansion in the Bay of Fundy, Canada. *Can. J. Earth Sci.*, 47:1079–1091.
- Shaw, J., Todd, B.J., Li, M.Z., Wu, Y., 2012. Anatomy of the tidal scour system at Minas Passage, Bay of Fundy, Canada. *Mar. Geol.* 323-325, 123-134.
- Shinn, E.A., 1968. Practical significance of birdseye structures in carbonate rocks. *J. Sediment. Petrol.* 38, 1: 215-223.
- Siemiatkowska, K.M., 1978. Geology of the Endikai Lake Area, District of Algoma. Ontario Geological Survey, Report 178, 79p.
- Tanner, W.F., 1962. Falling water level ripple marks. *Gulf Coast Ass. Geol. Soc. Transac.* 12, 295-301.

- Tirsgaard, H., 1993. The architecture of Precambrian high energy tidal channel deposits: an example from the Lyell Land Group (Eleonore Bay Supergroup), northeast Greenland. *Sed. Geol.* 88, 137-152.
- Van Schmus, W.R., 1976. Early and middle Proterozoic history of the Great Lakes area, North America. *Philos. Trans. R. Soc. Lond., Ser. A* 280 (1298), 605–628.
- Von Brunn, V., Hobday, D.K., 1976. Early Precambrian tidal sedimentation in the Pongola Supergroup of South Africa. *J. Sed. Pet.* 46, 3: 670-679.
- Williams, G.E., 2000. Geological constraints on the Precambrian history of Earth's rotation and the Moon's orbit. *Rev. Geophys.* 38, 1: 37-59.
- Wood, J., 1973. Stratigraphy and depositional environments of Upper Huronian rocks of the Rawhide Lake-Flack Lake area, Ontario. *The Geological Association of Canada Special Paper* 12, 73-95.
- Young, G.M., 1983. Tectono-sedimentary history of early Proterozoic rocks of the northern Great Lakes Region. *Geol. Soc. Am. Mem.* 160, 15–32.
- Young, G.M., Nesbitt, H.W., 1985. The lower Gowganda Formation in the southern part of the Huronian outcrop belt, Ontario, Canada: stratigraphy, depositional environments and tectonic setting. *Precambrian Res.* 29, 265–301.
- Young, G.M., Long, D.G.F., Fedo, C.M., Nesbitt, H.W., 2001. Proterozoic Huronian basin: product of a Wilson cycle punctuated by glaciations and a meteorite impact. *Sediment. Geol.* 141–142, 233–254.
- Zhou, L., McKenna, C.A., Long, D.G.F., Kamber, B.S., 2017. LA-ICP-MS elemental mapping of pyrite: an application to the Palaeoproterozoic atmosphere. *Precambrian Res.* 297, 33–55.

Chapter 3

3 Microbially induced sedimentary structures in the Paleoproterozoic, upper Huronian Supergroup, Canada

3.1 Introduction

Microbially induced sedimentary structures (MISS; Noffke et al., 1996) develop during growth, metabolism, destruction and decay of microbial mats in siliciclastic-dominated environments (Schieber, 2004; Noffke, 2010). These microbial mats, or biofilms, encrust siliciclastic substrates in diverse natural environments (Gerdes, 2007; Noffke and Chafetz, 2012 and references therein). Although biofilms have existed for billions of years, their preservation in the rock record is highly dependent on the presence of more complex life forms. The majority of Earth's Proterozoic eon was devoid of eukaryotic organisms. This would have enabled microbial mats to readily colonize clastic sedimentary deposits without the interference of grazers, thereby improving the cohesiveness of sand grains and decreasing erodibility of the sediment (Schieber et al., 2007a; Sarkar et al., 2008; Eriksson et al., 2012). Microbially induced sedimentary structures are therefore an invaluable trace fossil when working with Precambrian sedimentary rocks. Numerous structures interpreted as having been related to microbial activity have been described in the literature (e.g. Hagadorn and Bottjer, 1997; Gehling, 1999; Schieber et al., 2007b, and references therein; Noffke, 2010 and references therein), with several examples of Paleoproterozoic MISS (e.g. Parizot et al., 2005; Banerjee and Jeevankumar, 2005; Chakrabarti and Shome, 2010; Eriksson et al., 2012; Simpson et al., 2013). However, we are unaware of any scientific publications reporting the preservation of MISS in rocks of the Paleoproterozoic Huronian Supergroup.

Here we describe possible microbially induced sedimentary structures from the Gordon Lake and Bar River formations, Huronian Supergroup. Identification of these structures is based on comparisons with modern and other ancient analogues, as well as the six criteria for MISS biogenicity as outlined in Noffke (2009). Recognizing different types of MISS in these rocks can provide critical information regarding sedimentary processes,

hydraulic energy, and paleoenvironmental settings (Noffke, 2010; Bose and Chafetz, 2012).

3.2 Geological Setting

The Paleoproterozoic Huronian Supergroup forms part of the Southern Geological Province, and is well exposed along the north shore of Lake Huron, Canada (Figure 3.1). The siliciclastic-dominated, up to 12 km thick succession contains volcanic formations at the base of the stratigraphy (Figure 3.2). Zircon from a lower rhyolite unit yielded a U-Pb date of ca. 2.45 Ga (Krogh et al., 1984; Ketchum et al., 2013), whereas an upper age limit of ca. 2.22 Ga was determined from primary baddeleyite in gabbro intrusions that cut the stratigraphy (Corfu and Andrews, 1986). An alternative upper age limit of ca. 2.31 Ga was proposed by Rasmussen et al. (2013), as determined from zircon in purported tuff beds in the Gordon Lake Formation. However, Young (2014) argues that these zircons may be of detrital origin.

The Huronian Supergroup unconformably overlies Archean rocks of the Superior Province to the northwest (Card et al., 1977; Card, 1978; Young et al., 2001; Rousell and Card, 2009) and is overlain in the south by a Paleozoic succession with a depositional hiatus of 1.7 b.y. (Corcoran, 2008). The Grenville Front Tectonic Zone separates the Southern and Grenville provinces to the southeast (Card, 1978; Rousell and Card, 2009). Rocks of the Huronian Supergroup in the study area have undergone subgreenschist to greenschist grade metamorphism, but the prefix “meta” is herein omitted for simplicity.

Young and Nesbitt (1985) suggested that the Huronian Supergroup formed in a tectonic setting that evolved from rift basin to passive margin. Long (2004) later interpreted the succession as lower pull-apart basin to upper passive margin deposits. In contrast, Hoffman (2013) suggested that the entire Huronian succession was deposited along a passive margin. However, Young (2014) argued that the lower units have limited areal extent, show minor marine influence, display thickness changes across major faults, and contain seismic-related deposits, all of which suggest deposition in restricted fault-bound basins.

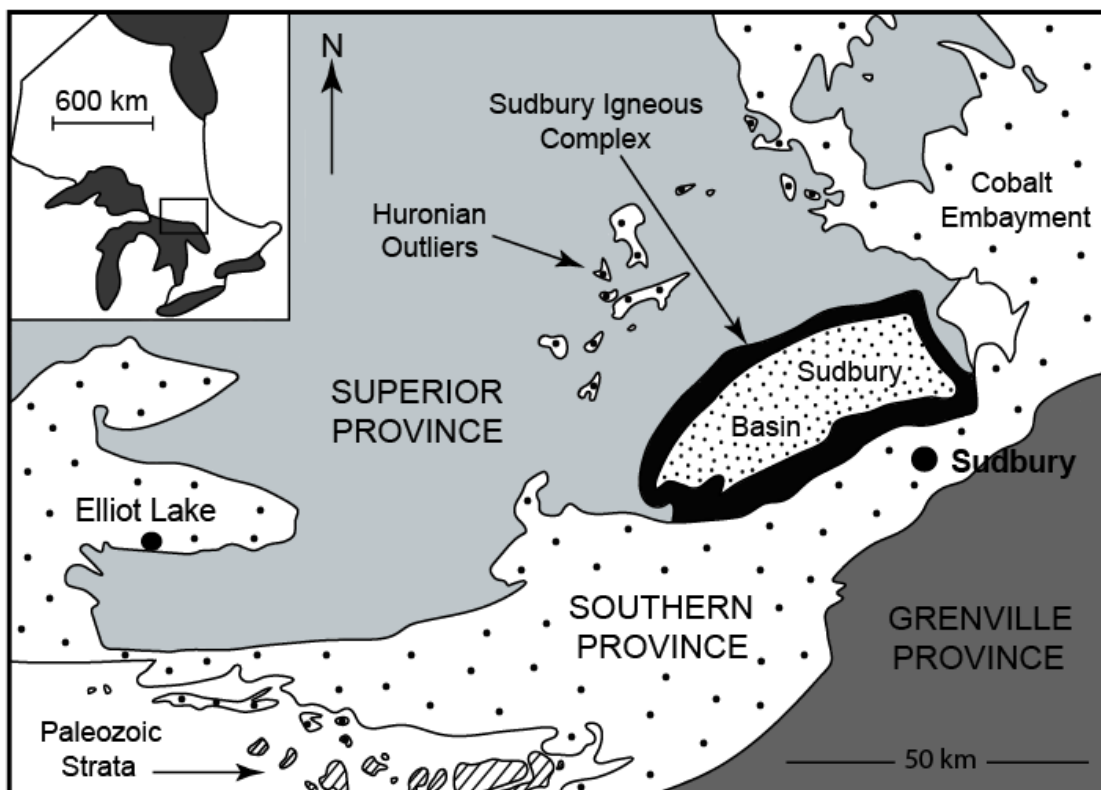


Figure 3.1. Simplified geologic map of the distribution of the Huronian Supergroup north of Lake Huron. The study area is located 29 km north of Elliot Lake. Modified from Young et al. (2001) and Long (2009).

The Huronian Supergroup is composed of five groups, which include in ascending order, the Elliot Lake, Hough Lake, Quirke Lake, Cobalt and Flack Lake groups (Figure 3.2). The cyclical nature of the Hough Lake, Quirke Lake and Cobalt groups form the basis for tripartite divisions consisting of lower diamictite, overlain by siltstone-mudstone-carbonate, and capped by sandstone (Roscoe, 1957; Wood, 1973; Card et al., 1977; Young et al., 2001; Long, 2004). The diamictite units are of glacial origin, whereas the overlying fine-grained formations are interpreted as deeper water deltaic deposits that formed following post-glacial sea level rise (Card et al., 1977; Robertson and Card, 1988; Long, 2009). The sandstone units in each division are mainly interpreted as fluvial deposits (McDowell, 1957; Long, 1978; Chandler, 1988a), although Rice (1986) suggested that the top of the Lorrain Formation (Cobalt Group) may be marine in origin. Young et al. (1991) suggested that the initiation of the Huronian glaciations was related to the formation of the supercontinent Kenorland. Increased exposure of the buoyant

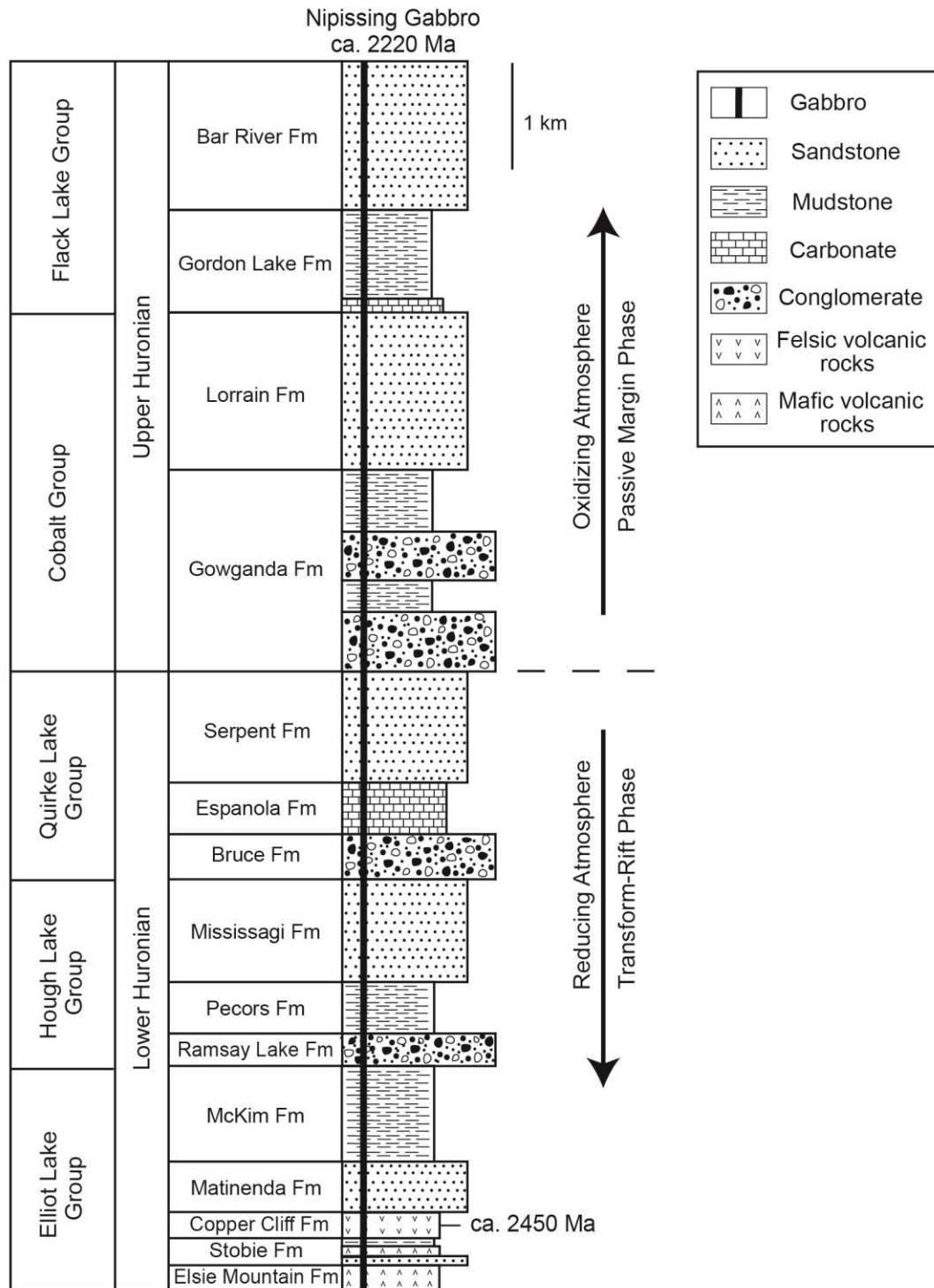


Figure 3.2. General stratigraphy of the Huronian Supergroup. Modified from Long (2004) and Young (2013). Date for Nipissing Gabbro from Corfu and Andrews (1986). Date for Copper Cliff Formation from Krogh et al. (1984) and Ketchum et al. (2013).

supercontinent enabled enhanced rates of continental weathering to occur, drawing down significant amounts of atmospheric CO₂. The resultant drop in temperature would have initiated the process of glaciation. Alternatively, a decrease in the greenhouse effect during each cycle may have occurred through elimination of atmospheric CH₄ during the rise of O₂ (Pavlov et al., 2000; Tang and Chen, 2013). It has also been suggested that the two lower glaciogenic formations, the Ramsay Lake and Bruce, represent early deposition of detritus at the front edge of a mountain ice sheet, which later grew into a continental ice sheet that deposited the thick and laterally extensive Gowganda Formation (Eyles, 1993; Eyles and Januszczak, 2004; Young, 2014).

The Huronian Supergroup contains a record of the transition from an oxygen-deficient to oxygen-rich Earth atmosphere, as recorded in the presence of detrital uranium-bearing minerals in the Matinenda Formation (Elliot Lake Group), followed up-section by the first appearance of red beds in the Gowganda Formation (Cobalt Group), red beds in the Lorrain Formation (Cobalt Group), and red beds and evaporite minerals in the Gordon Lake Formation (Flack Lake Group) (Wood, 1973). The MISS described in this study are preserved in the formations of the Flack Lake Group.

3.2.1 Flack Lake Group

The Flack Lake Group consists of the Gordon Lake and Bar River formations (Figure 3.2). The 300-760 m thick Gordon Lake Formation is composed of varicoloured siltstone, argillite, chert, minor sandstone, and anhydrite and gypsum nodules (Card et al., 1977; Card, 1978, 1984; Robertson, 1986; Chandler, 1986, 1988b). The presence of extensive red beds, evaporites and hematite oolites suggests that a significant amount of oxygen was present in the atmosphere during deposition of these units (Wood, 1973; Chandler, 1988b; Baumann et al., 2011). Reported sedimentary structures within siltstone and argillite units include planar laminae, graded beds, convolute bedding, ball and pillow structures, desiccation cracks and syneresis cracks, whereas cross laminae and graded beds are common in the sandstone units (Wood, 1973; Robertson, 1976; Card et al., 1977; Card, 1978, 1984; Chandler, 1986; Rust and Shields, 1987; Bennett et al., 1991). Local dolostone containing fenestral cavities was identified near the base of the formation

(Hofmann et al., 1980). The sedimentary structures, combined with evaporite minerals and fenestral fabrics, indicate deposition in a low-energy, tidal-flat, lagoonal or sabkha environment (Wood, 1973; Card et al., 1977; Card, 1978, 1984; Chandler, 1986; Rust and Shields, 1987).

The conformably overlying, 100-900 m thick Bar River Formation is predominantly a quartz arenite succession with minor siltstone interbeds (Wood, 1973; Card et al., 1977, Card, 1978; Chandler, 1984; Rust and Shields, 1987; Bennett et al., 1991). Sandstone units contain massive beds, trough, tangential and planar cross-beds, ripple marks, herringbone cross-stratification, and granule-pebble lags, whereas desiccation cracks and sphaeresis cracks are common in the siltstone units (Wright and Rust, 1985; Rust and Shields, 1987; Bennett et al., 1991). Roscoe and Fraey (1970) suggested that the Bar River Formation was deposited in a fluvial environment with mature quartz grains being derived from a regolith source. In contrast, Wood (1973) proposed that the Bar River Formation represents a beach deposit that was subjected to aeolian influence. However, the sedimentary structures, polymodal and bimodal paleocurrent patterns, and textural and compositional maturity are more consistent with deposition in a near-shore, shallow marine environment (Pettijohn, 1970; Robertson, 1976; Card, 1978; Chandler, 1984; Rust and Shields, 1987; Bynoe, 2011). More specifically, Rust and Shields (1987) suggested that the Bar River Formation in the Flack Lake area may have been deposited in a tidal channel environment.

To date, there is no consensus on the depositional settings represented by the Gordon Lake and Bar River formations, although most authors agree that the succession reflects deposition along a continental shelf. We postulate that the predominance of certain types of MISS may help in recognizing the physical sedimentary dynamics and associated depositional setting(s) of the top-most formations of the Huronian Supergroup.

We studied the deposits of the Gordon Lake and Bar River formations in the Flack Lake area, near Elliot Lake, Ontario (Figure 3.1). The rocks were mapped in detail along Highway 639 and along the shoreline of Flack Lake. In this area, the contact between the

Bar River Formation and the underlying Gordon Lake Formation is obscured by a diabase sill. Exposed sections are predominantly flat-lying to gently dipping.

3.3 Upper Huronian Supergroup MISS

Young (1967) proposed that the Gordon Lake and Bar River formations near Flack Lake contained organic vermiform casts, but he later discounted that finding by attributing the elliptical, spindle-shaped and overlapping structures to infilling of shrinkage cracks both from above and below (Young, 1969). Donaldson (1967) suggested that the spindle-shaped structures described from the Flack Lake area in addition to similar structures described from Michigan (e.g. Faul, 1949; Frarey and McLaren, 1963; Hofmann, 1967; Young, 1967) may have formed from desiccation of algal mats. Since that time, the sedimentology of the Gordon Lake and Bar River formations in the Flack Lake area has been investigated by several workers (e.g. Wood, 1973; Card et al., 1977; Wright and Rust, 1985; Chandler, 1986, 1988a, 1988b; Rust and Shields, 1987; Robertson and Card, 1988). However, these authors indicated that the abundant polygonal, linear and elliptical structures in the rocks were desiccation or syneresis cracks. Although our present detailed investigation affirms that the polygonal structures are desiccation cracks, the spindle-shaped, overlapping linear structures are consistent with microbially induced sedimentation. These structures are herein described according to Schieber's (2004) process-related classification scheme, which includes development during mat growth, metabolism, physical destruction, and decay. Only the latter two categories of structures were identified in the Flack Lake area.

3.3.1 Mat-Destruction Structures

In the study area, the physical destruction of microbial mats is indicated by various types of sand cracks, microbial mat chips, microbial sand and silt chips, and torn mat chips (Table 3.1). Sand cracks result from rupturing of an overlying microbial mat that has been placed under stress from wind or water, or desiccation (Gerdes, 2007; Eriksson et al., 2007b). Impressions of the tears in the mat may be preserved in the underlying sand or silt. Cracks representing single incipient tears were identified in quartz arenite of the

Bar River Formation and siltstone of the Gordon Lake Formation, and range from 0.5-1.5 cm in size (Figure 3.3a). Sand-filled, 0.5-9.5 cm triradiate cracks are common in sandstones of both formations, and are inferred to have formed when sand was transported to the mat

Table 3.1. Summary of the microbially induced sedimentary structures (MISS) identified in the Gordon Lake and Bar River formations in the Flack Lake area.

Mat-related Feature	Gordon Lake Formation	Bar River Formation
Sandcracks		
single incipient tears	=====	=====
triradiate	=====	=====
curved	=====	=====
lenticular	=====	
spindle	=====	
sinuous	=====	
Microbial sand and silt chips	=====	
Torn mat fragments	=====	
Mat chips		=====
Gas domes	=====	
Iron patches		=====
Iron laminae		=====

surface and filled the open ruptures from above (Figure 3.3b). Fine-grained sandstones and siltstones of the Gordon Lake Formation preserve abundant, up to 30 cm long, lenticular, curved, sinuous, and spindle-shaped cracks (Figure 3.3c and d). These irregular structures, unlike polygonal mud cracks that form through desiccation, reflect the elasticity of microbial mats, in which tearing results in curved or upturned margins (Gerdes, 2007). Although less common in the Bar River Formation, curved cracks at one locality were clearly infilled with sand from above (Figure 3.3e). Locally, cm-size cracks characterize the crests of interference ripples (Figure 3.3f). These cracks are interpreted to have formed when fluid was expelled from microbial mats that colonized the ripple crests. Desiccation of the mat may have also led to the formation of these cracks.

Microbial mat chips develop from high-energy erosion of desiccated, mat-adhered sand, forming curved, irregular fragments (Schieber, 2004; Erikssen et al., 2007a). Mat chips, 2-3.5 cm long, were identified in iron-stained Bar River quartz arenite at one locality (Figure 3.4a). Microbial sand and silt chips are 0.25-9 cm long, and were identified

mainly in the Gordon Lake Formation (Figure 3.4b-d). These structures develop from abrasion of flipped-over mat margins by water or wind, and are normally preserved as rounded or elongated fragments (Erikssen et al., 2007a). Torn mat chips were identified only in the siltstone and fine-grained sandstone of the Gordon Lake Formation, and range from 7-150 cm long and 3-30 cm wide (Figure 3.4d-f). The edges of the mat chips are sharp, frayed or irregular. Small chips appear to have been curled (Figure 3.4e), which is consistent with erosion of a dried out mat in an environment that is proximal to the site of deposition (Schieber, 2007). Larger, uncurled mat chips contain biolamination and smaller microbial mat chips (Figure 3.4d), which suggest that the mat was wet during erosion (Schieber, 2007). One mat chip appears to have a mottled texture (Figure 3.4f), which probably reflects mat growth prior to erosion.

3.3.2 Mat-Decay Structures

Microbial mat decay in the Flack Lake area is indicated by gas domes, pyrite patches, and iron laminae. Gas domes were identified in fine-grained sandstone of the Gordon Lake Formation, where they are characteristically associated with iron staining (Figure 3.5a). The domes are 1-2 cm across and are surrounded by curved sand cracks. The domes appear to be ruptured locally, resembling radial gas escape structures (c.f. Dornbos et al., 2007; Figure 3.5b), but these characteristics may also be the results of dome erosion during Pleistocene glaciation.

Pyrite patches were identified in the troughs of interference ripples in Bar River quartz arenite at one locality (Figure 3.5c). The pyrite patches are inferred to represent the locations of former microbial mats. The lower portions of a microbial mat are typically anoxic due to the decay of organic matter; this environment is conducive to the formation of reduced minerals, such as pyrite (Berner, 1984; Gerdes et al., 1985). Microbial mats were presumably the dominant source of organic matter during the Paleoproterozoic and would have provided the necessary organic debris within sand of the Bar River Formation at the time of deposition. Iron laminae were identified in quartz arenite of the Bar River Formation at two localities, where they are wavy (Figure 3.5d) and cross-laminated. In general, purple, iron-rich laminae are thinner than pink, quartz-rich

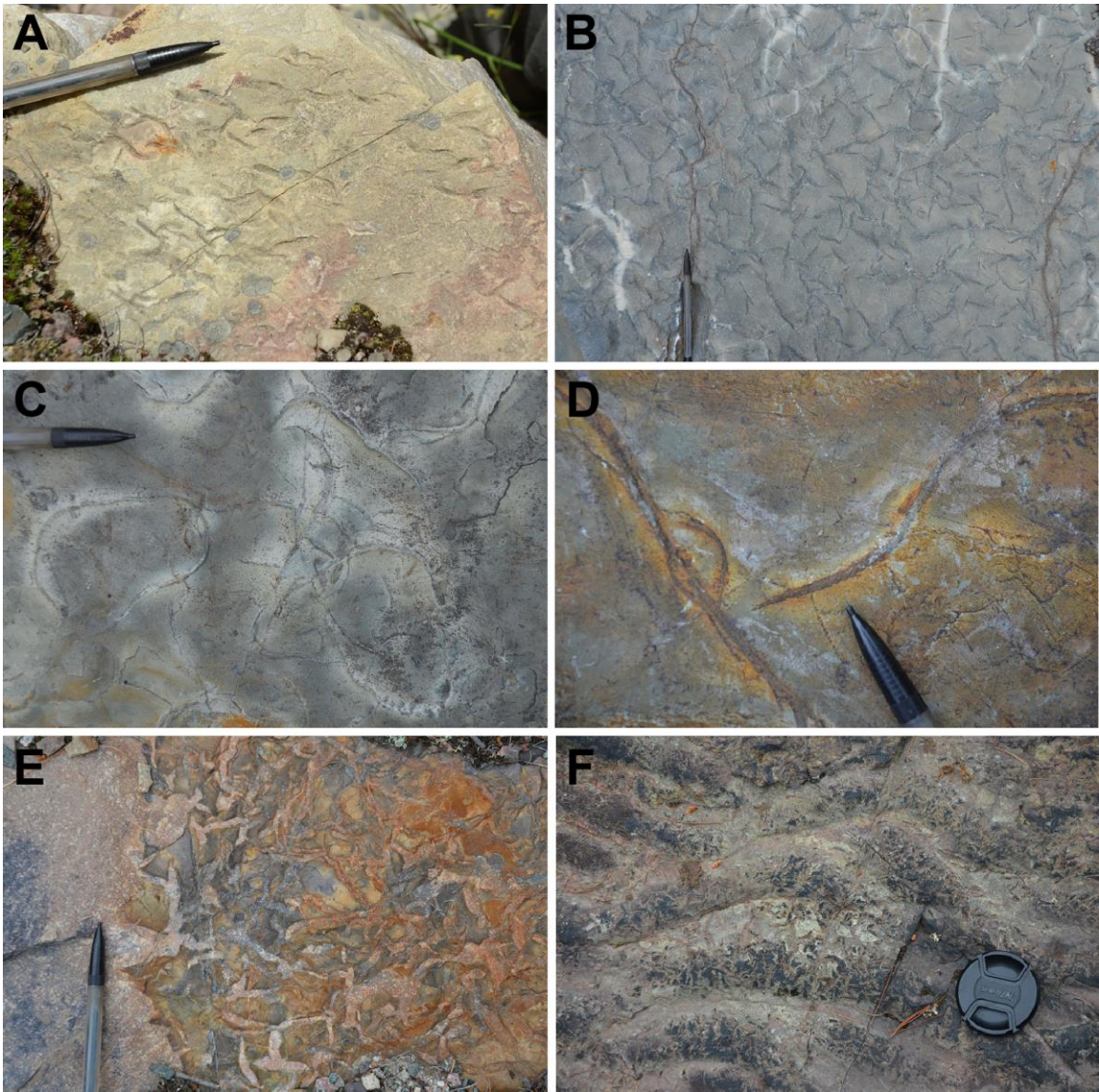


Figure 3.3. Mat-destruction structures identified in the Flack Lake area. Scales include pencil (14.5 cm) and camera lens cap (5.8 cm). (A) Single incipient tears preserved in fine-grained sandstone of the Bar River Formation. (B) Triradiate cracks preserved in fine-grained sandstone of the Gordon Lake Formation. (C) Curved, sinuous sand cracks preserved in siltstone of the Gordon Lake Formation. (D) Curved, corrugated sand cracks preserved in siltstone of the Gordon Lake Formation. (E) Curved sand cracks filled from above preserved in fine-grained sandstone of the Bar River Formation. (F) Curved cracks confined to the crests of interference ripples preserved in fine-grained sandstone of the Bar River Formation.

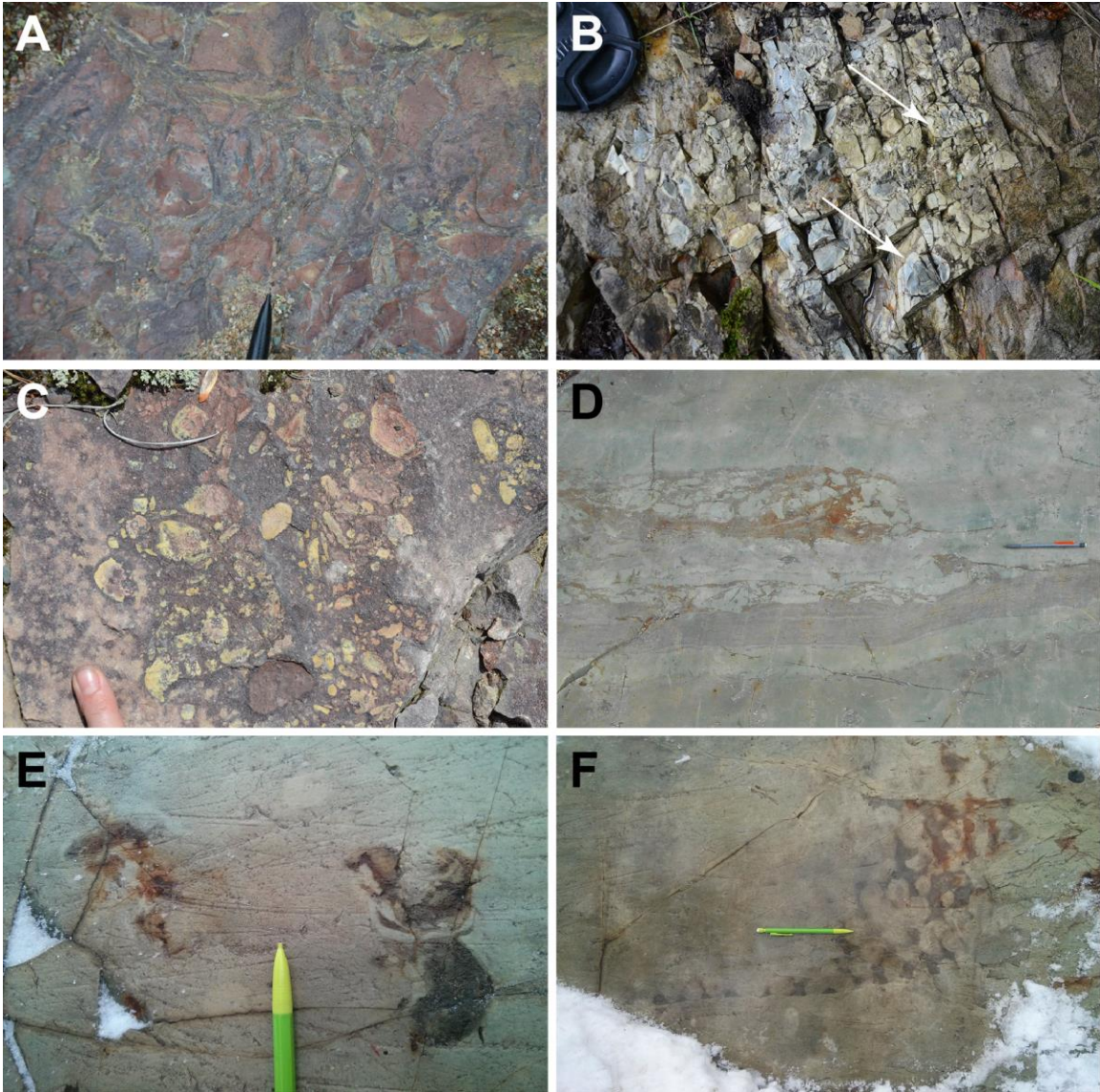


Figure 3.4. Mat-destruction structures identified in the Flack Lake area. Scales include pencil (14.5 cm) and camera lens cap (5.8 cm). (A) Microbial mat chips preserved in iron stained, fine-grained sandstone of the Bar River Formation. (B) Microbial sand and silt chips preserved in fine-grained sandstone of the Gordon Lake Formation. (C) Microbial sand and silt chips preserved in fine-grained sandstone of the Bar River Formation. (D) Microbial sand and silt chips preserved in fine-grained sandstone of the Gordon Lake Formation. Note the frayed margins of the large mat chip and the biolaminations below the pencil. (E) Microbial mat chips preserved in fine-grained sandstone of the Gordon Lake Formation. Note the curled appearance of these chips. (F) Torn mat chip preserved in the same fine-grained sandstone bed as Figure 4-E. Note the mottled appearance of the mat and distinct torn margins.

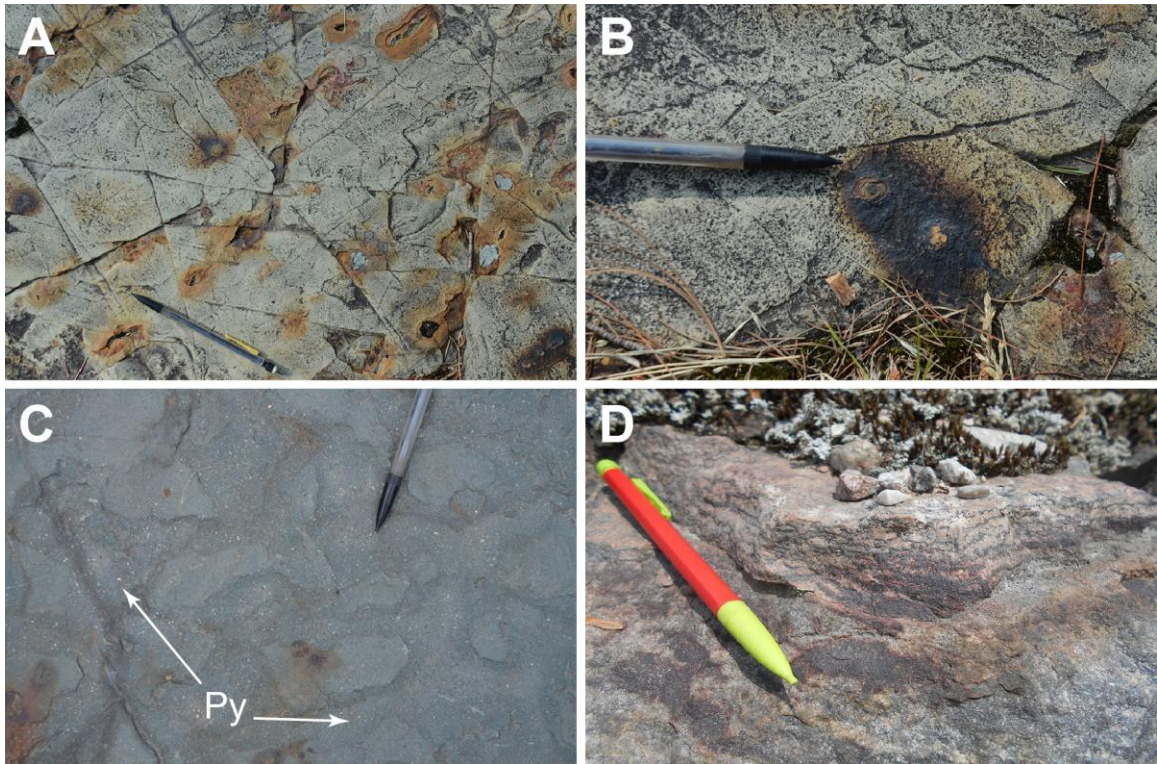


Figure 3.5. Mat-decay structures identified in the Flack Lake area. Pencil for scale (14.5 cm). (A) Gas domes preserved in fine-grained sandstone of the Gordon Lake Formation. Note the iron staining concentrated around the domes and the shrinkage cracks in the upper left portion of the figure. (B) Close-up of ruptured gas dome preserved in fine-grained sandstone of the Gordon Lake Formation. Note the radial nature of the dome center. (C) Pyrite patches preserved in the troughs of interference ripples in fine- to medium-grained sandstone of the Bar River Formation. (D) Wavy iron laminae preserved in fine- to medium-grained sandstone of the Bar River Formation.

laminae. The darker laminae may represent periods of calm hydrological conditions during which microbial mats were able to grow, whereas the pink laminae may represent periods of higher energy conditions during which growth of microbial mats was limited (Noffke et al., 2002; Druschke et al., 2009). The permeability of sandstones causes organic matter to be removed fairly early in burial history, therefore the stratiform iron laminae represent residual layers of mat-decay minerals (Schieber et al., 2007b).

3.4 Criteria for the biogenicity of MISS in the upper Huronian Supergroup

Fossil sedimentary structures of the Gordon Lake and Bar River formations in the Flack Lake area fulfill the six criteria for biogenicity, as outlined by Noffke (2009), and are therefore defined as MISS. The first criterion is that the sedimentary rocks must not have been subjected to metamorphism greater than greenschist grade. The studied rocks in the Flack Lake area are of subgreenschist metamorphic grade (Card, 1978). The second criterion states that the sedimentary structures are found at stratigraphic transgression-regression points. Deposition of the Flack Lake Group has been interpreted to have occurred along a continental shelf. Detailed geological mapping of the Gordon Lake Formation in the Flack Lake area supports deposition on a tidal flat, whereas the overlying Bar River Formation in the study area contains structures consistent with a tidal channel or estuarine sand shoal environment. The stratigraphic relationship is therefore consistent with a transgression. However, the occurrence of a regression is not preserved unless the transition from the Lorrain Formation to the overlying Gordon Lake Formation supports a falling water level. The majority of the Lorrain Formation is inferred to have been deposited in a fluvial environment, which does not fit a regressive sequence. However, a regression may have taken place following deposition of the Bar River Formation, although any overlying units have been eroded away.

The third criterion of Noffke (2009) is that the structures are part of the “microbial mat facies”, which involves preferential microbial mat development on quartz-rich, fine-grained sand that is frequently associated with small-scale ripples. The ideal environment for establishment of a microbial colony is one of moderate energy in which currents and

waves are not strong enough to damage or destroy the microbial mat. However, depositional energy must be strong enough that mud and other fine grains remain in suspension, thereby reducing the likelihood of sunlight obstruction (Noffke, 2009). In the Flack Lake area, MISS of the upper Huronian Supergroup are preserved on quartz-rich, fine-grained sandstone and siltstone beds, repeatedly on and in the stratigraphic vicinity of rippled bedding planes.

Criterion 4 states that the distribution of the structures reflects the hydrodynamic conditions of the depositional environment. The types of MISS identified in the Gordon Lake Formation are consistent with distribution in an intertidal to supratidal setting. These environments experience a complex array of hydrodynamic conditions and are therefore generally colonized by more robust organisms, such as microbial mats. These mats influence the erosion and deposition of sediment, thereby resulting in MISS (Noffke and Krumbein, 1999). Models of both ancient and modern MISS distribution in siliciclastic tidal environments illustrate that mat chips are found in the lower intertidal zone, sand cracks in the upper intertidal to lower supratidal zones, and gas domes in the upper and lower supratidal zones (Noffke et al., 2001; Bose and Chafetz, 2009; Noffke, 2009; Tang et al., 2012). Torn mat chips may also be found in the intertidal zone (Noffke et al., 2013). The sedimentary structures of both formations reflect deposition in a shallow marine, tidally-influenced environment, and the identified MISS (Table 3.1) are consistent with this interpretation. Criterion 5 of Noffke (2009) states that the structures resemble and compare geometrically to modern MISS. Microbially induced sedimentary structures appear to have remained largely unchanged throughout Earth's history, thus the comparison of ancient MISS to modern analogues is not only appropriate, but is integral for determination of a biogenic origin (Noffke, 2009). Examples of modern and ancient MISS (e.g. Dornbos et al., 2007; Eriksson et al., 2007b; Bose and Chafetz, 2012; Tang et al., 2012; Lan et al., 2013; Noffke et al., 2013; Cuadrado et al., 2014) are comparable to the various forms of MISS identified in the Gordon Lake and Bar River formations presented herein.

The final criterion for biogenicity of MISS requires that microtextures identified in thin section denote a relationship to biofilms or microbial mats. In addition to the mesoscopic

structures identified in the Flack Lake outcrops, thin sections from the Gordon Lake Formation reveal a variety of microtextures that are characteristic of microbial mat activities, such as growth and trapping. Wavy crinkled laminae, 0.55-3.25 mm torn mat chips and 0.2-1.8 mm mat chips are interpreted as portions of ancient microbial mat layers (Figure 3.6a-e). Mat chips formed during erosion and transportation of microbial mats. Locally, the mat chips are layered, which reflects successive periods of mat growth prior to erosion (Figure 3.6d), whereas folded mat chips are consistent with transport of eroded material (Figure. 3.6d). Bands of concentrated heavy minerals may represent the edge of a once-present mat layer (Noffke, 2009). Heavy minerals accumulate on mat surfaces where they are trapped and bound to the sticky mat exterior (Gerdes, 2007; Noffke, 2009). Oriented grains, 0.1-0.2 mm in size, are also identified in thin section (Figure. 3.6f). These structures develop when gas production in submerged microbial mats, or desiccation of a subaerial mat causes the mat to break into fragments, which then float and are deposited on muddy sediment (Eriksson et al., 2007b; Schieber, 2007). The positive identification of microbial mat chips on a microscopic scale, as illustrated in Figure 3.6 (a-f), meets the final criterion for biogenicity of MISS in the sedimentary deposits of the Flack Lake Group.

3.5 Discussion

Previous reports of biosignatures in the Paleoproterozoic Huronian Supergroup include stromatolites in the carbonate-rich Espanola Formation (Hofmann et al., 1980; Bekker et al., 2005; Long, 2009; Al-Hashim, 2015) and laminated fenestral dolostone in the Gordon Lake Formation at one locality (Hofmann et al., 1980). The identification of MISS in this study has significantly increased the quantity of biosignatures reported from the Huronian Supergroup, and contributes to the relatively small group of reported Paleoproterozoic examples.

Sand cracks in the study area have previously been interpreted as shrinkage or syneresis cracks (e.g. Young, 1969; Card, 1978; Chandler, 1984, 1986; Wright and Rust, 1985; Rust and Shields, 1987). Syneresis cracks are narrow, curved to linear, tapering structures that have a non-polygonal pattern in plan view and contorted sides in cross-

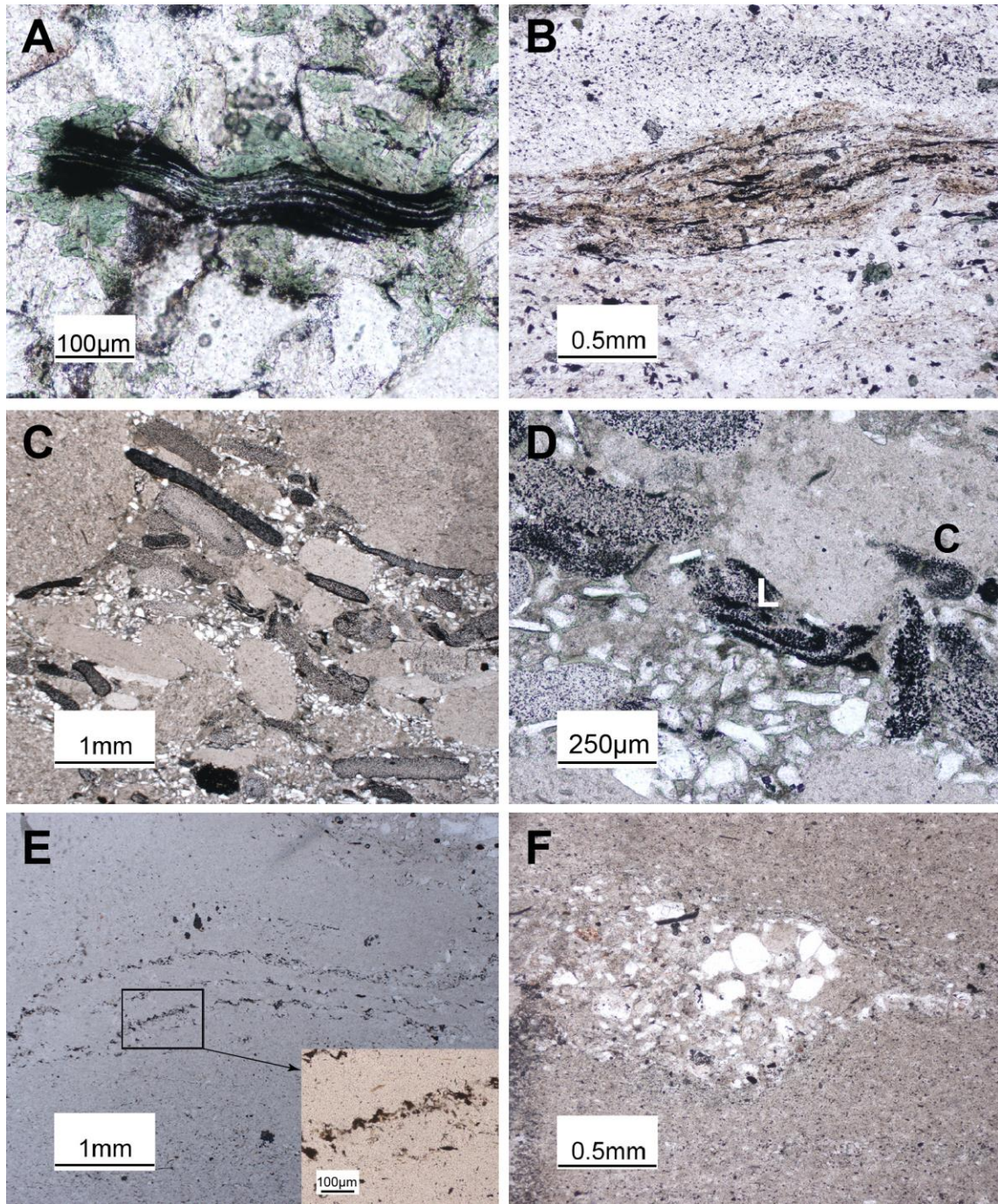


Figure 3.6. Mat microtextures identified in thin sections from the Gordon Lake Formation. (A) Frayed mat chip preserved in fine-grained sandstone. Note the internal layering and torn margin on the right side of the mat chip. (B) Mat chip preserved in siltstone. Note the iron cement concentrated around the wavy carbonaceous laminae. (C) Mat chips preserved in a granule- to pebble-conglomerate with a siltstone to fine-grained sandstone matrix. (D) Close-up of the center of Figure 6-C showing a layered mat chip (L) and curled mat chip (C). (E) Carbonaceous laminae preserved in siltstone. (F) Oriented quartz grains preserved in mudstone.

section (Pratt, 1998; Harazim et al., 2013; Davies et al., 2016). Although there is much debate on the mechanism of formation of synaeresis cracks, many authors agree that the structures form in muddy sediment through the rapid shrinkage of clay under changing salinity conditions in a shallow submarine environment (Jüngst 1934; White, 1961). Other proposed methods of formation include: desiccation (Allen, 1982), desiccation and infilling of evaporite molds (Astin and Rogers, 1991), seismic deformation (Pratt, 1998), and microbial facilitation (Pflüger, 1999; Harazim et al., 2013). Harazim et al. (2013) determined that cracked mudstones of the Ordovician Beach Formation in Newfoundland, Canada, were colonized by microbial mats, whereas non-cracked mudstones show no indication of microbial mat development. The authors suggest that microbial mats may be a pre-requisite for intra-stratal shrinkage crack formation, however Davies et al. (2016) suggest that synaeresis cracks may be polygenetic in nature and that there is no universal mode of formation. The curved, spindle and lenticular structures in the study area occur primarily on fine-sand to siltstone beds in the stratigraphic vicinity of other varieties of MISS, thus favouring a mat-induced origin. Associated sedimentary structures, such as desiccation cracks and flaser and lenticular bedding, support deposition in an environment that experienced periods of subaerial exposure, which is contradictory to synaeresis crack formation, which occurs in a submerged environment. Many of the cracks occur on rippled bedding planes, indicating that the sediment was stabilized, presumably by biofilms. Pyrite grains, horizons and patches are also found in many of the outcrops with sand cracks and may have formed under reducing conditions created by the decay of microbial mats.

A greater diversity and quantity of MISS is preserved in the Gordon Lake Formation compared to the Bar River Formation (Table 3.1). This discrepancy can be attributed to the different depositional environments of the formations within a tidally-influenced setting. The recurrence of desiccation structures in the Gordon Lake Formation documents numerous periods of subaerial exposure. Desiccation cracks were also identified in the Bar River Formation, but in a comparably minor amount. The main rock types in which MISS of the Gordon Lake Formation are found include thin siltstone and fine-grained sandstone beds. These beds are mainly planar to wavy laminated and bedding planes display oscillation ripples, local interference ripples and abundant

desiccation cracks. Our interpretation is that the Gordon Lake Formation was deposited on a tidal flat where microbial mats flourished during relatively calm water conditions (Figure 3.7). Large mat chips and microbial sand and silt chips would have developed during periods of strong wind or wave action, which detached and transported mat chips to an adjacent location. Microbial mat tears and chips are common in wet microbial mats in protected inter- and supra-tidal environments due to the effects of wind shear on very shallow tidal ponds or directly on exposed mats (Bouougri and Porada, 2012). Microbial shrinkage and sand cracks analogous to the types observed in the Flack Lake area occur in the intertidal and lower supratidal zones and often display a range of shapes that are linked to the maturity, cohesiveness, and the extent of desiccation of the microbial mat (Eriksson et al., 2007a). In addition, gas domes generally occur only in the intertidal zone (Dornbos et al., 2007). Similar MISS to those herein described are reported from the tidally influenced Proterozoic succession of the southern North China Platform (Tang et al., 2012), the Neoproterozoic peritidal deposits of the West African Craton (Bouougri and Porada, 2002), and the Mediterranean coast of modern southern Tunisia (Eriksson et al., 2007a).

The quartz arenite nature of the Bar River Formation and internal sedimentary structures, such as tangential and planar cross-beds and granule-pebble lags suggest relatively higher energy conditions at the time of deposition compared with those during deposition of the Gordon Lake Formation. Sand cracks identified in fine- to medium-grained sandstone beds are a reflection of microbial influence, as microbial filaments increase the cohesiveness between sand- and silt-sized sediment grains that would otherwise remain unaltered during desiccation (Gerdes et al., 2000). Microbial mats cannot form in a high-energy environment as they will be eroded before they have sufficient time to establish. However, once established, a microbial mat is robust enough to tolerate high-energy conditions (Noffke, 2010). This may account in part for the lower diversity and the reduced number of MISS in the Bar River Formation relative to the Gordon Lake Formation. The coarser grained, more porous and permeable nature of the Bar River Formation may have also contributed to poorer preservation of microbial mats.

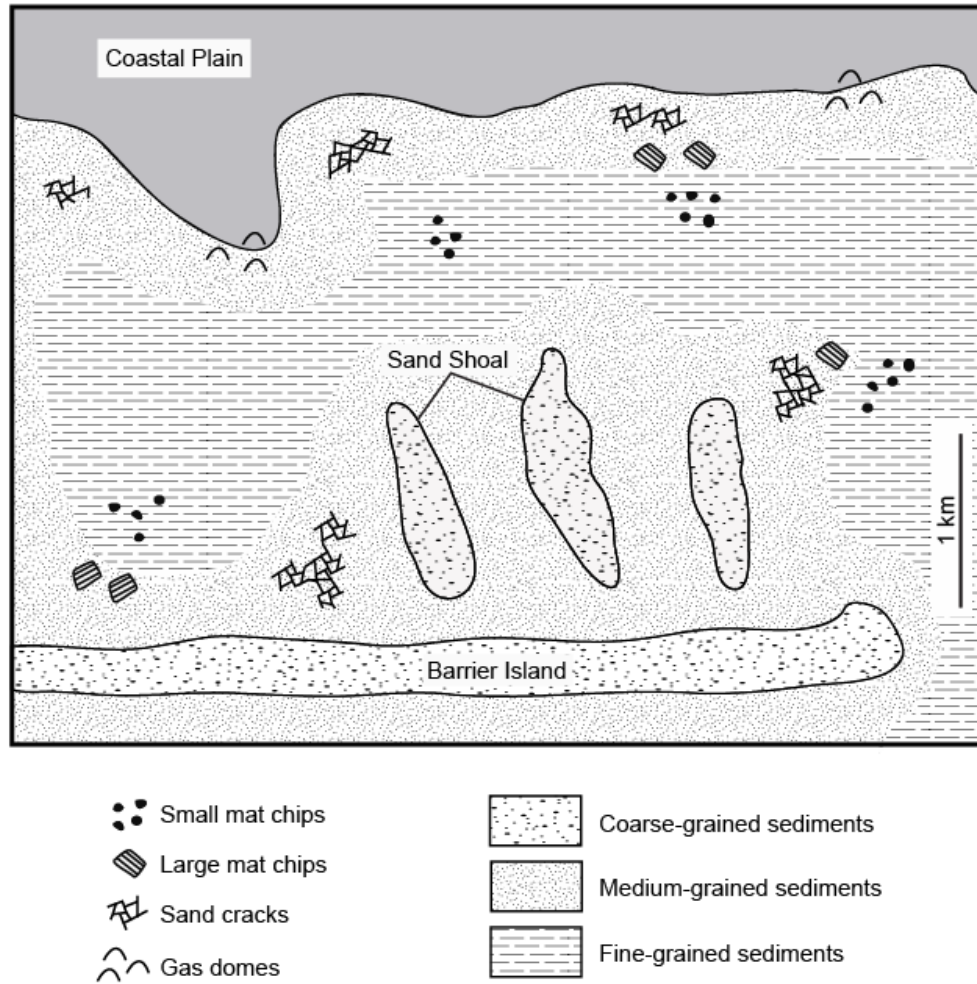


Figure 3.7. Paleoenvironmental setting of upper Huronian Supergroup MISS. Note that the distribution of MISS is related to, but not restricted by, the tidal zones.

Many examples of ancient MISS are found in coastal, passive margin settings (Schieber et al., 2007a), thus the inferred deposition of the upper Huronian Supergroup along a continental margin would be conducive to the development of MISS. The types of MISS identified in the Gordon Lake and Bar River formations are valuable indicators of depositional environment and support the interpretation of deposition in a transgressive, tide-influenced setting.

3.6 Conclusions

Paleoproterozoic microbial mats developed, decayed and were destroyed in shallow marine environments where they influenced sedimentation patterns. The structures described from the Gordon Lake and Bar River formations contribute substantial evidence for microbial colonization during deposition of the upper Huronian Supergroup. The varieties of sand cracks, mat chips, pyrite patches, iron laminae, microbial sand and silt chips, torn mat chips and gas domes identified in the Flack Lake area satisfy the criteria for biogenicity as outlined by Noffke (2009). The differences between the MISS identified in the two formations are a function of varying composition and grain size, which are the direct results of water energy and depth in each depositional environment.

3.7 References

- Al-Hashim, M.H.M., 2015. Sedimentology and facies analysis of the Paleoproterozoic mixed carbonate-siliciclastic Espanola Formation, Huronian Supergroup, Canada: Reassessment of depositional environments. Presented at AESRC 2015, Kingston, ON.
- Allen, J.R.L., 1982. Sedimentary structures, their character and physical basis Volume II. Developments in Sedimentology 30B, Elsevier, Amsterdam, 663pp.
- Astin, T.R., and Rogers, D.A., 1991. "Subaqueous shrinkage cracks" in the Devonian of Scotland reinterpreted. *Journal of Sedimentary Petrology* 61, 850-859.
- Banerjee, S., and Jeevankumar, S., 2005. Microbially originated wrinkle structures on sandstone and their stratigraphic context: Paleoproterozoic Koldaha Shale, central India. *Sedimentary Geology* 176, 211-224.
- Baumann, S.D.J., Arrospide, T. and Wolosyzn, A.E., 2011. Preliminary redefinition of the Cobalt Group (Huronian Supergroup), in the Southern Geologic Province, Ontario, Canada. MIGE Report G-012011-2A.

- Bekker, A., Kaufman, A. J., Karhu, J. A., Eriksson, K. A., 2005. Evidence for Paleoproterozoic cap carbonates in North America. *Precambrian Research* 137, 3, 167-206.
- Bennett, G., Dressler, B.O., and Robertson, J.A., 1991. The Huronian Supergroup and associated intrusive rocks. In: Thurston, P.C., Williams, H.R., Sutcliffe, R.H., Scott, G.M. (Eds.), *Geology of Ontario, Part 1: Ontario Geological Survey*, Toronto, pp. 549-591.
- Berner, R.A., 1984. Sedimentary pyrite formation; an update. *Geochimica et Cosmochimica Acta* 48, 605-615.
- Bose, S., and Chafetz, H.S., 2009. Topographic control on distribution of modern microbially induced sedimentary structures (MISS): a case study from Texas coast. *Sedimentary Geology* 213, 136-149.
- Bose, S., and Chafetz, H., 2012. Morphology and distribution of MISS: a comparison between modern siliciclastic and carbonate settings. In: Noffke, N., and Chafetz, H., (Eds) *Microbial Mats in Siliciclastic Systems Through Time*, SEPM Special Publication No. 101, Elsevier, pp. 3-14.
- Bose, P.K., Sarkar, S., Banerjee, S., and Chakraborty, S., 2007. Mat-related features from sandstones of the Vindhyan Supergroup in Central India. In: Schieber, J., Bose, P.K., Eriksson, P.G., Banerjee, S., Sarkar, S., Altermann, W., and Catuneanu, O. (Eds) *Atlas of Microbial Mat Features Preserved within the Siliciclastic Rock Record*, *Atlases in Geoscience* 2, Elsevier, pp. 181-188.
- Bouougri, E., and Porada, H., 2002. Mat-related sedimentary structures in Neoproterozoic peritidal passive margin deposits of the West African Craton (Anti-Atlas, Morocco). *Sedimentary Geology* 153, 85-105.
- Bouougri, E., and Porada, H., 2012. Wind induced mat deformation structures in recent tidal flats and sabkhas of SE-Tunisia and their significance for environmental interpretation of fossil structures. *Sedimentary Geology* 263-264, 56-66.
- Bynoe, L., 2011. The role of provenance, chemical weathering and mechanical erosion on the formation of 2.2 Ga quartz arenites. Unpublished undergraduate thesis, University of Western Ontario, London, Ontario, 38p.
- Card, K.D., 1978. *Geology of the Sudbury-Manitoulin Area, Districts of Sudbury and Manitoulin*. Ontario Geological Survey Report 166, 238p.
- Card, K. D., 1984. *Geology of the Espanola-Whitefish Falls Area, District of Sudbury, Ontario*. Ontario Geological Survey, Report 131, 70p. Accompanied by Maps 2311, 2312, scale 1:31 680 or 1 inch to 1/2 mile, and 2 charts.

- Card, K. D., Innes, D. G., and Debicki, R. L., 1977. Stratigraphy, Sedimentology, and Petrology of the Huronian Supergroup of the Sudbury-Espanola Area. Ontario Division of Mines, OFR5107, 307 p. Accompanied by 4 charts and one figure.
- Chakrabarti, G., and Shome, D., 2010. Interaction of microbial communities with clastic sedimentation during Palaeoproterozoic time – an example from basal Gulcheru Formation, Cuddapah basin, India. *Sedimentary Geology* 226, 22-28.
- Chandler, F.W., 1984, Sedimentary Setting of an Early Proterozoic Copper Occurrence in the Cobalt Group, Ontario; A Preliminary Assessment, In: Current Research, Part A, Geological Survey of Canada Paper 84-1A, 185-192.
- Chandler, F.W., 1986. Sedimentology and paleoclimatology of the Huronian (Early Aphebian) Lorrain and Gordon Lake Formations and their bearing on models for sedimentary copper mineralization. Geological Survey of Canada Paper 86-1A, 121-132.
- Chandler, F.W., 1988a. Quartz arenites: review and interpretation. *Sedimentary Geology* 58, 105-126.
- Chandler, F.W., 1988b. Diagenesis of sabkha-related, sulphate nodules in the early Proterozoic Gordon Lake Formation, Ontario, Canada. *Carbonates and Evaporites* 3, 75-94.
- Corcoran, P.L., 2008. Ordovician paleotopography as evidenced from original dips and differential compaction of dolostone and shale unconformably overlying Precambrian basement on Manitoulin Island, Canada. *Sedimentary Geology* 207, 22-33.
- Corfu, F. and Andrews, A.J., 1986. A U-Pb age for mineralized Nipissing diabase, Gowganda, Ontario. *Canadian Journal of Earth Sciences* 23, 107-109.
- Cuadrado, D.G., Perillo, G.M.E., and Vitale, A.J., 2014. Modern microbial mats in siliciclastic tidal flats: Evolution, structures and the role of hydrodynamics. *Marine Geology* 352, 367-380.
- Davies, N.S., Liu, A.G., Gibling, M.R., and Miller, R.F., 2016. Resolving MISS conceptions and misconceptions: a geological approach to sedimentary surface textures generated by microbial and abiotic processes. *Earth-Science Reviews* 154, 210-246.
- Donaldson, J.A., 1967. Precambrian vermiform structures: a new perspective. *Canadian Journal of Earth Sciences* 4, 1273-1276.
- Dornbos, S.Q., Noffke, N., and Hagadorn, J.W., 2007. Mat-decay Features. In: Schieber, J., Bose, P.K., Eriksson, P.G., Banerjee, S., Sarkar, S., Altermann, W., and Catuneanu, O. (Eds) *Atlas of Microbial Mat Features Preserved within the Siliciclastic Rock Record, Atlases in Geoscience* 2, Elsevier, pp. 106-110.

- Druschke, P.A., Jiang, G., Anderson, T.B., and Hanson, A.D., 2009. Stromatolites in the Late Ordovician Eureka Quartzite: implications for microbial growth and preservation in siliciclastic settings. *Sedimentology* 56, 1275-1291.
- Eriksson, P.G., Bartman, R., Catuneanu, O., Mazumder, R., and Lenhardt, N., 2012. A case study of microbial mat-related features in coastal epeiric sandstones from the Paleoproterozoic Pretoria Group (Transvaal Supergroup, Kaapvaal craton, South Africa); The effect of preservation (reflecting sequence stratigraphic models) on the relationship between mat features and inferred paleoenvironment. *Sedimentary Geology* 263-264, 67-75.
- Eriksson, P.G., Porada, H., Banerjee, S., Bouougri, E., Sarkar, S., and Bumby, A.J., 2007a. Mat-destruction features. In: Schieber, J., Bose, P.K., Eriksson, P.G., Banerjee, S., Sarkar, S., Altermann, W., and Catuneanu, O. (Eds) *Atlas of Microbial Mat Features Preserved within the Siliciclastic Rock Record, Atlases in Geoscience 2*, Elsevier, pp. 76-105.
- Eriksson, P.G., Schieber, J., Bouougri, E., Gerdes, G., Porada, H., Banerjee, S., Bose, P.K., and Sarkar, S., 2007b. Classification of structures left by microbial mats in their host sediments. In: Schieber, J., Bose, P.K., Eriksson, P.G., Banerjee, S., Sarkar, S., Altermann, W., and Catuneanu, O. (Eds) *Atlas of Microbial Mat Features Preserved within the Siliciclastic Rock Record, Atlases in Geoscience 2*, Elsevier, pp. 39-52.
- Eriksson, P.G., Simpson, E.L., Eriksson, K.A., Bumby, A.J., Steyn, G.L., and Sarkar, S., 2000. Muddy roll-up structures in siliciclastic interdune beds of the c. 1.8 Ga Waterberg Group, South Africa. *Palaios* 15, 177-183.
- Eyles, N., 1993. Earth's glacial record and its tectonic setting. *Earth Science Reviews* 35, 1-248.
- Eyles, N. and Januszczak, N., 2004. 'Zipper-rift': a tectonic model for Neoproterozoic glaciations during the breakup of Rodinia after 750 Ma. *Earth Science Reviews* 65, 1-73.
- Faul, H., 1949. Fossil burrows from the Pre-Cambrian Aibik Quartzites of Michigan. *Nature* 164, 32.
- Frarey, M.J. and McLaren, D.J., 1963. Possible metazoans from the Early Proterozoic of the Canadian Shield. *Nature* 200, 461-462.
- Gehling, J.G., 1999. Microbial mats in terminal Proterozoic siliciclastics: Ediacaran death masks. *Palaios* 14, 40-57.
- Gerdes, G., 2007. Structures left by modern microbial mats in their host sediments. In: Schieber, J., Bose, P.K., Eriksson, P.G., Banerjee, S., Sarkar, S., Altermann, W., and Catuneanu, O. (Eds) *Atlas of Microbial Mat Features Preserved within the Siliciclastic Rock Record, Atlases in Geoscience 2*, Elsevier, pp. 5-38.

- Gerdes, G., Klenke, Th., and Noffke, N., 2000. Microbial signatures in peritidal siliciclastic sediments: a catalogue. *Sedimentology* 47, 279-308.
- Gerdes, G., Krumbein, W.E., and Reineck, H.-E., 1985. The depositional record of sandy, versicolored tidal flats (Mellum Island, southern North Sea). *Journal of Sedimentary Petrology* 55, 265-278.
- Hagadorn, J.W., and Bottjer, D.J., 1997. Wrinkle structures: microbially mediated sedimentary structures common in subtidal siliciclastic settings at the Proterozoic–Phanerozoic transition. *Geology* 25, 1047-1050.
- Harazim, D., Callow, R.H.T., and McIlroy, D., 2013. Microbial mats implicated in the generation of intrastratal shrinkage ('synaeresis') cracks. *Sedimentology* 60, 1621-1638.
- Hoffman, P.F., 2013. The Great Oxidation and a Siderian snowball Earth: MIF-S based correlation of Paleoproterozoic glacial epochs. *Chemical Geology* 362, 143-156.
- Hofmann, H.J., 1967. Precambrian fossils (?) near Elliot Lake, Ontario. *Science* 156, 500-504.
- Hofmann, H.J., Pearson, D.A.B., and Wilson, B.H., 1980. Stromatolites and fenestral fabric in early Proterozoic Huronian Supergroup, Ontario. *Canadian Journal of Earth Sciences* 17, 10, 1351-1357.
- Jüngst, H., 1934. Zur geologischen bedeutung der synärese. *Geologische Rundschau* 15, 312–325.
- Ketchum, K.Y., Heaman, L.M., Bennett, G. and Hughes, D.J., 2013. Age, petrogenesis and tectonic setting of the Thessalon volcanic rocks, Huronian Supergroup, Canada. *Precambrian Research* 233, 144-172.
- Krogh, T.E., Davis, D. W., and Corfu, F., 1984. Precise U-Pb zircon and baddeleyite ages for the Sudbury Structure. In: Pye, E. G., Naldrett, A.J., Giblin, P.E. (Eds.), *Geology and Ore Deposits of the Sudbury Structure*, Ontario Geological Survey, v. 1, pp. 431-446.
- Lan, Z.-W., and Chen, Z.-Q., 2012. Proliferation of MISS-forming microbial mats after the late Neoproterozoic glaciations: evidence from the Kimberley region, NW Australia. *Precambrian Research* 224, 529-550.
- Lan, Z.-W., Chen, Z.-Q., Li, X.-H., and Kaiho, K., 2013. Microbially induced sedimentary structures from the Mesoproterozoic Huangqikou Formation, Helan Mountain region, northern China. *Precambrian Research* 233, 73-92.
- Long, D.G.F., 1978. Depositional environments of a thick Proterozoic sandstone, the (Huronian) Mississagi Formation of Ontario, Canada. *Canadian Journal of Earth Sciences* 15, 190-206.

- Long, D.G.F., 2004. The tectonostratigraphic evolution of the Huronian basement and subsequent basin fill: geological constraints on impact models of the Sudbury event. *Precambrian Research* 129, 203-223.
- Long, D.G.F., 2009. The Huronian Supergroup. In: Rousell, D.H., and Brown, G.H. (Eds.), *A Field Guide to the Geology of Sudbury, Ontario: Ontario Geological Survey Open File Report 6243*, pp. 14-30.
- McDowell, J.P., 1957. The sedimentary petrology of the Mississagi quartzite in the Blind River area. *Ontario Department of Mines, Geological Circular* 6, 31p.
- Noffke, N., 2009. The criteria for the biogenicity of microbially induced sedimentary structures (MISS) in Archean and younger, sandy deposits. *Earth-Science Reviews* 96, 173-180.
- Noffke, N., 2010. *Geobiology: Microbial Mats in Sandy Deposits from the Archean Era to Today*, Springer-Verlag, Berlin, 194p.
- Noffke, N., Beukes, N., Gutzmer, J., and Hazen, R., 2006. Spatial and temporal distribution of microbially induced sedimentary structures: a case study from siliciclastic storm deposits of the 2.9 Ga Witwatersrand Supergroup, South Africa. *Precambrian Research* 146, 35-44.
- Noffke, N., and Chafetz, H., 2012. Introduction. In: Noffke, N., and Chafetz, H., (Eds) *Microbial Mats in Siliciclastic Systems Through Time*, SEPM Special Publication No. 101, Elsevier, pp. 1.
- Noffke, N., Christian, D., Wacey, D., and Hazen, R.M., 2013. Microbially induced sedimentary structures recording an ancient ecosystem in the ca. 3.48 Billion-year-old Dresser Formation, Pilbara, Western Australia. *Astrobiology* 13, 12, 1103-1124.
- Noffke, N., Gerdes, G., Klenke, T., and Krumbein, W.E., 1996. Microbially induced sedimentary structures – examples from modern sediments of siliciclastic tidal flats. *Zentralblatt für Geologie und Paläontologie, Teil I*, H. 1/2, 307-316.
- Noffke, N., Gerdes, G., Klenke, T., and Krumbein, W.E., 2001. Microbially induced sedimentary structures indicating climatological, hydrological and depositional conditions within recent and Pleistocene coastal facies zones (Southern Tunisia). *Facies* 44, 23-30.
- Noffke, N., Knoll, A.H., and Grotzinger, J.P., 2002. Sedimentary controls on the formation and preservation of microbial mats in siliciclastic deposits: a case study from the Upper Neoproterozoic Nama Group, Namibia. *Palaios* 17, 533-544.
- Noffke, N., and Krumbein, W.E., 1999. A quantitative approach to sedimentary surface structures contoured by the interplay of microbial colonization and physical dynamics. *Sedimentology* 46, 417-426.

- Parizot, M., Eriksson, P.G., Aifa, T., Sarkar, S., Banerjee, S., Catuneanu, O., Altermann, W., Bumby, A.J., Bordy, E.M., Rooy, J.L.V., and Boshoff, A.J., 2005. Suspected microbial mat-related crack-like sedimentary structures in the Palaeoproterozoic Magaliesberg Formation sandstones, South Africa. *Precambrian Research* 138, 274-296.
- Pavlov, A.A., Kasting, J.F., and Brown, L.L., 2000. Greenhouse warming by CH₄ in the atmosphere of early Earth. *Journal of Geophysical Research* 105, 11981-11990.
- Pettijohn, F. J., 1970. The Canadian Shield-A Status Report, 1970. In: A. J. Baer, (Ed.), *Symposium on Basins and Geosynclines of the Canadian Shield: Geological Survey of Canada Paper 70-40*, 239-255.
- Plüger, F., 1999, Matground structures and redox facies. *Palaios* 14, 25-39.
- Pratt, B.R., 1998. Syneresis cracks: subaqueous shrinkage in argillaceous sediments caused by earthquake-induced dewatering. *Sedimentary Geology* 117, 1-10.
- Rasmussen, B., Bekker, A., and Fletcher, I.R., 2013. Correlation of Paleoproterozoic glaciations based on U-Pb zircon ages for tuff beds in the Transvaal and Huronian Supergroups. *Earth and Planetary Science Letters* 382, 173-180.
- Rice, R.J., 1986. Regional sedimentation in the Lorrain Formation (Aphebian), central Cobalt Embayment. In: *Summary of Field Work and Other Activities: Ontario Geological Survey Miscellaneous Paper 137*, 210-216.
- Robertson, J.A., 1976. The Blind River uranium deposits: the ores and their setting. *Ontario Division of Mines Miscellaneous Paper 65*, 1-54.
- Robertson, J.A., 1986. Huronian Geology and the Blind River (Elliot Lake) uranium deposits, the Pronto Mine. In: *Uranium Deposits of Canada*, Canadian Institute of Mining and Metallurgy, Special Paper 33, 46-43.
- Robertson, J.A. and Card, K.D., 1988. *Geology and Scenery: North shore of Lake Huron Region*. Ontario Geological Survey, Geological Guidebook 4.
- Roscoe, S.M., 1957. Stratigraphy, Quirke Lake-Elliot Lake Senior, Blind River area, Ontario. *Royal Society of Canada Special Publication Number 6*, 54-58.
- Roscoe, S.M., and Frarey, M.J., 1970. Comments on: The Canadian Shield - A status report, 1970, by F.J. Pettijohn. In: A. J. Baer, (Ed.), *Symposium on Basins and Geosynclines of the Canadian Shield*, Geological Survey of Canada Paper 70-40, 255-262.
- Rousell, D.H., and Card, K.D., 2009. Sudbury area geology and mineral deposits. In: Rousell, D.H., and Brown, G.H. (Eds.) *A Field Guide to the Geology of Sudbury, Ontario*, Ontario Geological Survey Open File Report 6243, 1-6.

- Rust B.R., and Shields M.J., 1987. The Sedimentology and Depositional Environments of the Huronian Bar River Formation, Ontario, Grant 189, Geoscience Research Grant Program. Ontario Geological Survey Open File Report, 1-37.
- Sarkar, S., Bose, P.K., Samanta, P., Sengupta, P., and Eriksson, P.G., 2008. Microbial mat mediated structures in the Ediacaran Sonia Sandstone, Rajasthan, India, and their implications for Proterozoic sedimentation. *Precambrian Research* 162, 248-263.
- Schieber, J., 2004. Microbial mats in the siliciclastic rock record: a summary of diagnostic features. In: Eriksson, P.G., Altermann, W., Nelson, D.R., Mueller, W.U., and Catuneanu, O. (Eds) *The Precambrian Earth: Tempos and Events, Developments in Precambrian Geology*, Elsevier 12, pp. 663-673.
- Schieber, J., 2007. Microbial mats on muddy substrates – examples of possible sedimentary features and underlying processes. In: Schieber, J., Bose, P.K., Eriksson, P.G., Banerjee, S., Sarkar, S., Altermann, W., and Catuneanu, O. (Eds) *Atlas of Microbial Mat Features Preserved within the Siliciclastic Rock Record, Atlases in Geoscience 2*, Elsevier, pp. 117-134.
- Schieber, J., Bose, P.K., Eriksson, P.G., and Sarkar, S., 2007a. Palaeoenvironmental and chronological relationships of mat-related features, and sequence stratigraphic implications of microbial mats. In: Schieber, J., Bose, P.K., Eriksson, P.G., Banerjee, S., Sarkar, S., Altermann, W., and Catuneanu, O. (Eds) *Atlas of Microbial Mat Features Preserved within the Siliciclastic Rock Record, Atlases in Geoscience 2*, Elsevier, 267-275.
- Schieber, J., Bose, P.K., Eriksson, P.G., Banerjee, S., Sarkar, S., Altermann, W., and Catuneanu, O. (Eds), 2007b. *Atlas of Microbial Mat Features Preserved within the Siliciclastic Rock Record, Atlases in Geoscience 2*, Elsevier, 311 p.
- Simpson, E.L., Heness, E., Bumby, A., Eriksson, P.G., Eriksson, K.A., Hilbert-Wolf, H.L., Linnevelt, S., Fitzgerald, M., Modungwa, T., and Okafor, O.J., 2013. Evidence for 2.0 Ga continental microbial mats in paleodesert setting. *Precambrian Research* 237, 36-50.
- Tang, D-J., Shi, X-Y., Jiang, G., and Wang, X-Q., 2012. Morphological association of microbially induced sedimentary structures (MISS) as a paleoenvironmental indicator: an example from the Proterozoic succession of the Southern North China Platform. In: Noffke, N., and Chafetz, H., (Eds) *Microbial Mats in Siliciclastic Systems Through Time*, SEPM Special Publication No. 101, Elsevier, pp. 163-175.
- Tang, H., and Chen, Y., 2013. Global glaciations and atmospheric change at ca. 2.3 Ga. *Geoscience Frontiers* 4, 583-596.
- White, W.A., 1961. Colloid phenomena in sedimentation of argillaceous rocks. *Journal of Sedimentary Research* 31, 560–570.

- Wood, J., 1973. Stratigraphy and depositional environments of upper Huronian rocks of the Rawhide Lake-Flack Lake area, Ontario. The Geological Association of Canada Special Paper Number 12, 73-95.
- Wright, D.J., and Rust, B.R., 1985. Preliminary report on the stratigraphy and sedimentology of the Bar River Formation. In: Milne, V.G. (Ed.), Grant 189, Geoscience Research Grant Program, Summary of Research, 1984-1985, Ontario Geological Survey Miscellaneous Paper 127, pp. 119-123.
- Young, G.M., 1967. Possible organic structures in early Proterozoic (Huronian) rocks of Ontario. Canadian Journal of Earth Sciences 4, 565-568.
- Young, G.M., 1969. Inorganic origin of corrugated vermiform structures in the Huronian Gordon Lake Formation near Flack Lake, Ontario. Canadian Journal of Earth Sciences 6, 795-799.
- Young, G.M., 2013. Precambrian supercontinents, glaciations, atmospheric oxygenation, metazoan evolution and an impact that may have changed the second half of Earth history. Geoscience Frontiers 4, 247-261.
- Young, G.M., 2014. Contradictory correlations of Paleoproterozoic glacial deposits: Local, regional or global controls? Precambrian Research 247, 33-44.
- Young, G.M., Long, D.G.F., Fedo, C.M., and Nesbitt, H.W., 2001. Proterozoic Huronian Basin: Product of a Wilson cycle punctuated by glaciations and a meteorite impact. Sedimentary Geology 141-142, 233-254.
- Young, G.M., and Nesbitt, H.W., 1985. The lower Gowganda Formation in the southern part of the Huronian outcrop belt, Ontario, Canada: Stratigraphy, depositional environments and tectonic setting. Precambrian Research 29, 265-301.

Chapter 4

4 Processes responsible for the development of soft-sediment deformation structures (SSDS) in the Paleoproterozoic Gordon Lake Formation, Huronian Supergroup, Canada

4.1 Introduction

Soft-sediment deformation structures form when unconsolidated sediment is destabilized by any mechanism that reduces sediment strength, followed by a force that induces deformation (Owen, 1987; van Loon, 2009). These structures have been reported from a variety of modern and ancient sedimentary deposits (e.g. Davenport and Ringrose, 1987; Molina et al., 1998; Chen and Lee, 2013; Sarkar et al., 2014; Stárková et al., 2015; Roy and Banerjee, 2016). Liquefaction and fluidization are common mechanisms that reduce sediment strength and are the results of pore-fluid overpressuring. Fluidization requires a continuous flow of fluid in order to support and transport particles in suspension, whereas during liquefaction, the internal friction of sediment is reduced to nearly zero, causing the material to temporarily act as a fluid (Owen, 1987; Maltman 1994; Owen and Moretti, 2011). Liquefaction and fluidization of near surface sediment may be triggered by a number of processes, such as rapid sedimentation, seismic waves, groundwater movement, breaking waves, and storm action (Maltman, 1994; van Loon, 2009). In general, identification of the trigger mechanism(s) of SSDS is important in understanding conditions at the time of, and shortly following deposition, in addition to evaluating their use as possible indicators of basin tectonism. Combinations of multiple processes and mechanisms are often responsible for the formation of SSDS, resulting in a range of complex bedforms (van Loon, 2009).

This paper describes a variety of SSDS and associated biogenic structures that are exposed in a large outcrop of the Paleoproterozoic Gordon Lake Formation of the Huronian Supergroup in the vicinity of Bruce Mines, Ontario, Canada. The objective of this project was to evaluate the origin and possible trigger mechanisms that produced the SSDS and to determine the role of microbial mats in their formation. The abundance and

variety of SSDS in the study area provides further clues regarding the paleodepositional environment and local basin conditions during and shortly after deposition.

4.2 Geological Setting

The SSDS described here are found in the Gordon Lake Formation of the Huronian Supergroup. The Huronian Supergroup is a Paleoproterozoic succession of primarily siliciclastic rocks that forms part of the Southern Geological Province of Ontario, Canada (Figure 4.1). It is well exposed along the north shore of Lake Huron, and extends northeast into the Cobalt Embayment. Maximum U-Pb ages of $2450 \pm 25/-10$ Ma (Krogh et al., 1984) and 2452.5 ± 6.2 Ma (Ketchum et al., 2013) were determined from zircon in a rhyolite unit near the base of the supergroup, whereas primary baddeleyite from gabbro intrusions that cut the stratigraphy provide a minimum age limit of 2219.4 ± 3.5 Ma (Corfu and Andrews, 1986). Rasmussen et al. (2013) proposed an alternative upper age limit of ca. 2.31 Ga, which was determined from zircon in purported tuff beds of the Gordon Lake Formation. These zircons, however, have been interpreted as having a detrital rather than volcanic origin (Young, 2014).

Young and Nesbitt (1985) proposed that the Huronian Supergroup was deposited in a tectonic setting that evolved from rift basin to passive margin. Similarly, Long (2004; 2009) suggested that the succession formed in a pull-apart basin that later transitioned into a passive margin. The Huronian Supergroup is composed of five groups: the Elliot Lake, Hough Lake, Quirke Lake, and Cobalt groups, as well as the informal Flack Lake group. The Hough Lake, Quirke Lake and Cobalt groups contain tripartite divisions (Roscoe, 1957; Wood, 1973; Card et al., 1977; Young et al., 2001; Long, 2004) that are interpreted as having been sequentially deposited by glaciers, deltas and fluvial systems (McDowell, 1957; Card et al., 1977; Long, 1978; Chandler, 1988a; Robertson and Card, 1988; Long, 2009). Soft-sediment deformation structures have been reported throughout the Huronian Supergroup, a stratigraphic summary of which is found in Table 4.1.

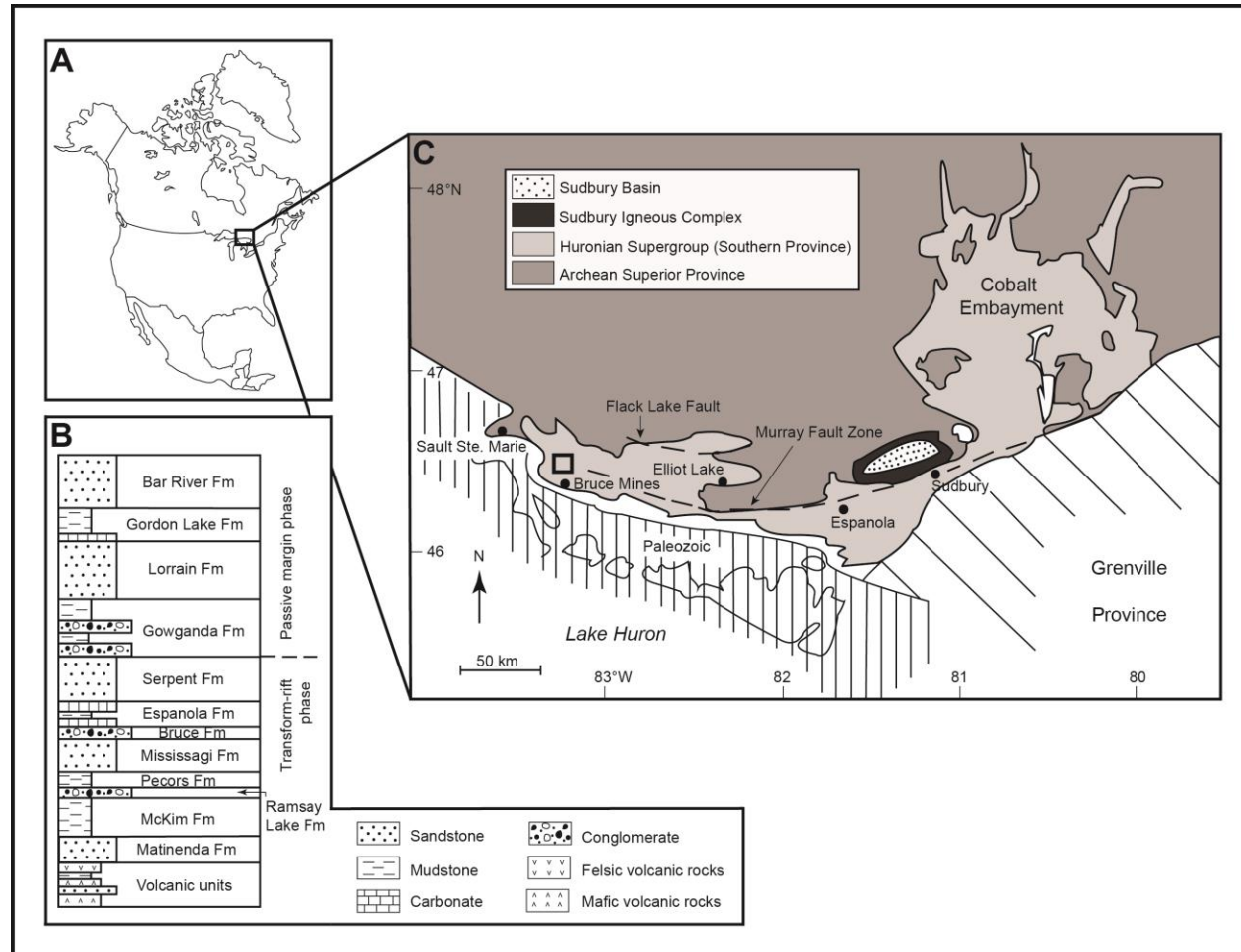


Figure 4.1. Simplified geologic map of the distribution of the Huronian Supergroup north of Lake Huron with major fault zones. The study area is located approximately 11.5 km north-northwest of Bruce Mines (small black box). Modified from Young et al. (2001).

Table 4.1. Summary of soft-sediment deformation structures described in the Huronian Supergroup.

Group	Formation	Type of SSDS	Reference
Flack Lake (unofficial)	Bar River	overturned cross-beds	Aranha, 2015
	Gordon Lake	ball-and-pillow structures, load casts, flame structures, pseudonodules, de-watering pipe, convolute bedding, clastic dikes, syn-sedimentary faults	Young, 1968; Card, 1976; Card, 1978; Chandler, 1986; This paper and the authors' personal observations
Cobalt	Lorrain	ball-and-pillow structures	Young, 1968
	Gowganda	clastic dikes, ball-and-pillow structures	Young, 1968; Chandler, 1973; Card, 1984
Quirke Lake	Serpent	clastic dikes	Young, 1968; Card, 1976
	Espanola	clastic dikes, ball-and-pillow structures	Young, 1968; Eisbacher, 1970; Chandler, 1973; Card, 1984; Peredery, 1991; Al-Hashim, 2016
	Bruce	clastic dikes	Card, 1984
Hough Lake	Mississagi	clastic dikes	Card, 1976
	Pecors	clastic dikes, ball-and-pillow structures	Peredery, 1991
	Ramsay Lake	-	-
Elliot Lake	McKim	clastic dikes, ball-and-pillow structures	Peredery, 1991
	Matinenda	-	-
	Volcanic units	-	-
Multiple formational contacts proximal to fault structures		slumps	Young, 1983; Al-Hashim, 2016

The Huronian Supergroup contains a record of Earth's transition from a reducing to oxygenated atmosphere. Evidence supporting low atmospheric oxygen is provided by sulphur isotopes in pyrite (Zhou et al., 2017), and the presence of detrital uranium-bearing minerals in the Matinenda Formation (Elliot Lake Group). Red beds in the Gowganda and Lorrain formations (Cobalt Group), and in the Gordon Lake and Bar River formations (Flack Lake group) indicate that the atmosphere was oxygenated at the time the upper half of the stratigraphic succession was deposited.

4.2.1 Gordon Lake Formation

The Gordon Lake Formation is the second youngest formation in the Huronian Supergroup and is part of the Flack Lake group. It is 300-1100 m thick and generally agreed to have been deposited along a continental shelf; a transgressive relationship has been interpreted between the Gordon Lake Formation and overlying Bar River Formation (Hill et al., 2016). Red beds, evaporites, hematite oolites, and microbially induced sedimentary structures (MISS) have been reported from the formation, suggesting that the atmosphere at the time of deposition contained a significant amount of oxygen (Wood, 1973; Chandler, 1988b; Baumann et al., 2011; Hill et al., 2016). Existing evidence for microbial colonization at the time of deposition includes MISS in the Flack Lake area (Hill et al., 2016) and fenestral fabrics in dolostone in the Bruce Mines area near the base of the formation (Hofmann et al., 1980).

The Gordon Lake Formation is fine-grained overall and is composed of siltstone and mudstone, with minor sandstone, chert and intra-formational conglomerate (Card et al., 1977; Card, 1978, 1984; Robertson, 1986; Chandler, 1986, 1988b). Reported sedimentary structures include ripples, planar laminated siltstone and mudstone beds, graded siltstone and sandstone beds, ball-and-pillow structures, desiccation cracks, MISS, and cross-laminated sandstone beds (Wood, 1973; Robertson, 1976; Card et al., 1977; Card, 1978, 1984; Chandler, 1986; Rust and Shields, 1987; Bennett et al., 1991; Hill et al., 2016). The sedimentary structures, combined with evaporites and fenestral fabrics, indicate deposition under alternating flow energy and multi-directional flow conditions in a tidally

influenced environment (Wood, 1973; Card, 1976, 1984; Frarey, 1977; Chandler, 1988b; Hill et al., 2016).

The Gordon Lake Formation has been interpreted to be correlative with the Kona Dolomite in the Marquette Range Supergroup, Michigan, USA, (Young, 1983; Bekker et al., 2006; Bennett, 2006). Algal structures are abundant in the Kona Dolomite and ooids are also preserved. Overall, the two formations share similarities in appearance and lithology, suggesting that the lowermost beds of the Gordon Lake Formation may represent an eastern extension of the algal-rich, shallow-marine environment. In addition, Bennett (2006) and Ramsay and Fralick (2017) observed hummocky cross-stratification (HCS) in some outcrops in Fenwick Township, approximately 60 km northwest of the Old Soo Road outcrop. The difference between the two formations can be explained by the area occupied by the Gordon Lake Formation receiving a greater influx of clastic material during deposition.

The main outcrop in the study area is located along Old Soo Rd., approximately 630 m south of Gordon Lake and 11.4 km north-northwest of Bruce Mines, Ontario (Figure 4.2). One of the most important structural elements in the study area is the Murray Fault system, a generally east-west trending fault zone that extends over 200 km east to the Grenville front (Card et al., 1975; Young et al., 2001). Many formations within the Huronian Supergroup display a significant increase in thickness and metamorphic grade south of the Murray Fault, however metamorphic grade does not change across the fault in the Bruce Mines area (Jackson, 1994). The Murray Fault has been interpreted as an early normal growth fault that was active during deposition of the Huronian Supergroup and later converted into a reverse or thrust fault during the Penokean orogeny (Roscoe, 1969; Card, 1978; Zolnai et al., 1984). Long (2004; 2009) suggested that the high angle of the Murray Fault, in addition to a kinked Archean/Proterozoic contact southwest of the Sudbury structure, indicate that the fault has a strike-slip origin. Conversely, Jackson (2001) argued that the Murray Fault may not have been active during deposition of the Huronian Supergroup and that compressional deformation resulted in the formation of thrust faults, which may account for the juxtaposition of units. This argument, however,

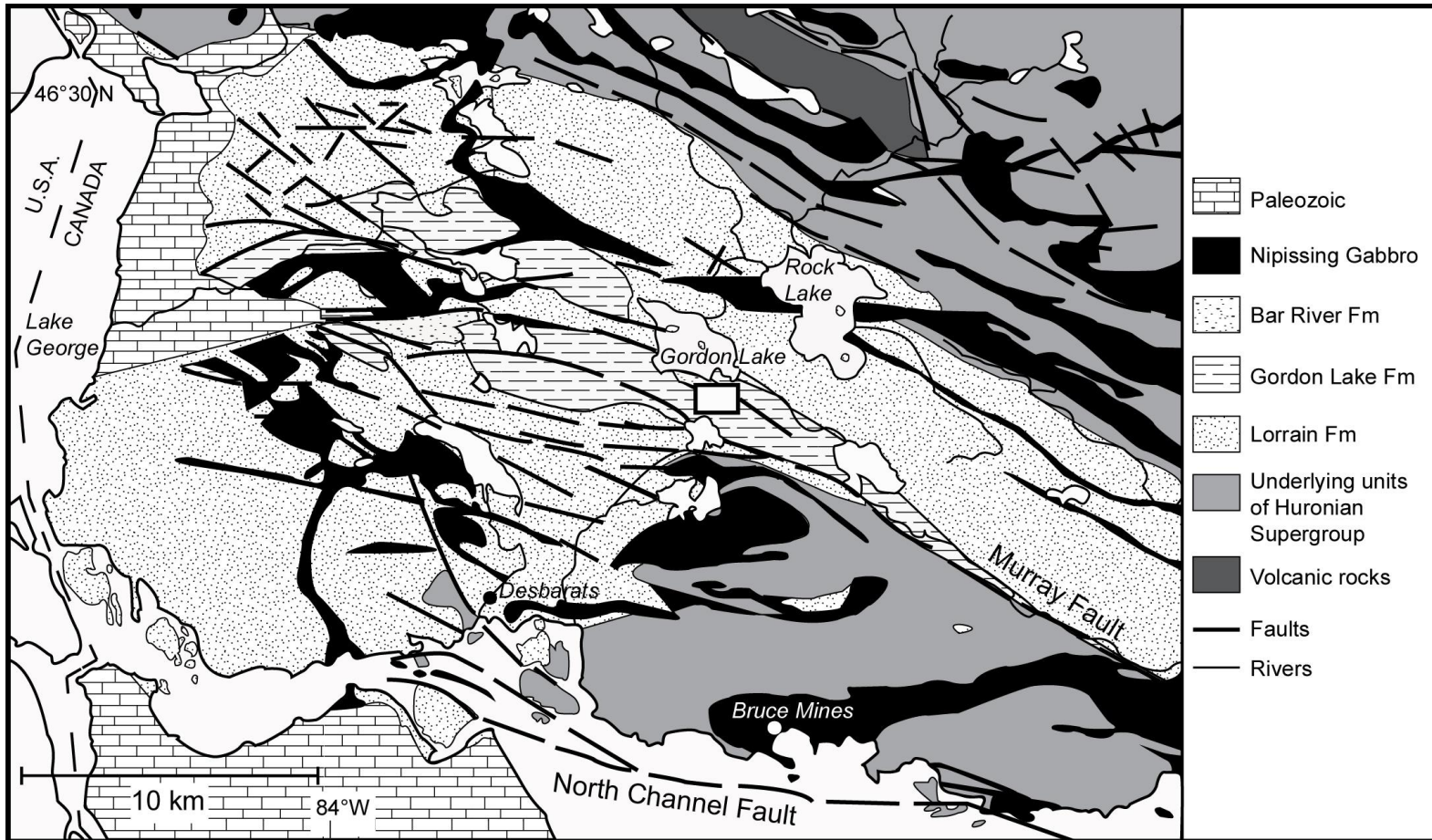


Figure 4.2. Geological map of the Bruce Mines area. The study area is indicated by the white rectangle. Roads not shown for the purpose of clarity. Coordinates for the outcrop are 46°24'08.6"N, 83°49'22.4"W. Modified from Giblin et al. (1979).

does not explain the increased thickness distribution in the Huronian Supergroup south of the Murray Fault.

4.3 Bruce Mines area exposure

The exposure of the Gordon Lake Formation along Old Soo Road consists primarily of medium to thinly bedded, light grey and purple mudstone, dark grey and pink siltstone and fine-grained sandstone, and chert, with minor medium-grained sandstone (Figures 4.3 and 4.4). Grain size increases slightly toward the top of the section and off-white, fine- to medium-grained sandstone and green mudstone characterize the top 3 m of the outcrop. The exposure is approximately 136 m thick with 47 m of intervening cover. The beds strike at 291° and dip at 19° . Structures consistent with a shallow marine environment, such as ripples, low angle cross-bedding and desiccation cracks, are well preserved in the top few metres of the section. Lenticular bedding, planar to wavy lamination, graded beds, minor intraformational conglomerate (Figure 4.3b), and rippled sandstone beds are visible in the lower parts of the section. Undeformed beds are massive, planar to wavy laminated, or normally graded. In general, SSDS are the most common features in the outcrop (Figures 4.3a-c; 4.4a-e; 4.5). Based on the three general subdivisions of the Gordon Lake Formation proposed by Eisbacher and Bielenstein (1969), the outcrop is considered to represent part of the middle and upper units of the formation.

4.3.1 Soft-sediment deformation structures

The SSDS are well developed in siltstone to fine-grained sandstone beds. The SSDS include: 1) load casts, 2) convolute bedding, 3) pseudonodules, 4) ball-and-pillow structures, 5) flame structures and 6) one observed dewatering pipe.

Load casts and convolute bedding are the most abundant SSDS throughout the outcrop. Load casts are from 6 to 106 cm wide, and 3 to 36 cm high, and are most visible where siltstone or fine-grained sandstone has descended into underlying mudstone. These load structures include a variety of shapes, but most have a simple form (c.f. Owen, 2003).

These structures are commonly symmetric, but rare intervals of asymmetric forms are present. Internal lamination is often preserved. Beds containing load casts are laterally continuous (Figure 4.4e). Two beds approximately 5.5 m from the base of the outcrop contain extremely well-preserved load casts (Figure 4.4d); load casts within the lower bed contain laminations that pass laterally into undeformed strata.

Convolute bedding is most common in the interbedded siltstone and fine-grained sandstone intervals in the lower and middle parts of the stratigraphy. These beds display complex syn-sedimentary folding, are mainly highly deformed and disrupted, and the intensity of convolution declines upwards in some beds.

Pseudonodules are approximately 1 to 15 cm wide and appear throughout the exposure, but are most common in the middle section. They are present in both detached and partially-detached configurations. Texturally, these structures consist of siltstone to medium-grained sandstone, with mudstone rip-up clasts and heavy minerals. They are typically coarser grained than the surrounding strata (Figures 4.6a-f). The detrital grains are predominantly composed of quartz, mudstone and chert, however, minor feldspar grains are also present. The pseudonodules are poorly sorted, and most grains are subangular to subrounded. Morphologically, these structures are well rounded (Figure 4.6a and b) and many are circular (Figures 4.6b, 7c), but are not folded around themselves. Many pseudonodules appear to have formed beneath a stabilized surface (Figures 4.6b and e; 7c). Where they appear undeformed, the beds that acted as the source of the pseudonodules are approximately 0.5 to 2 cm thick.

Ball-and-pillow structures are 15 to 120 cm wide and 10 to 78 cm thick. They occur where siltstone to fine-grained sandstone sinks into mudstone and siltstone beds. Morphologically, these structures are highly rounded, circular to irregular, and elliptical. The ball structures predominantly contain thin internal laminae, which is often connected circularly (Figure 4.4b), however, chaotic internal laminae were also identified. Several of the largest ball-and-pillow structures exhibit internal water-escape structures. The largest ball-and-pillow structures are found in the lowest part of the outcrop (Figure 4.3c).

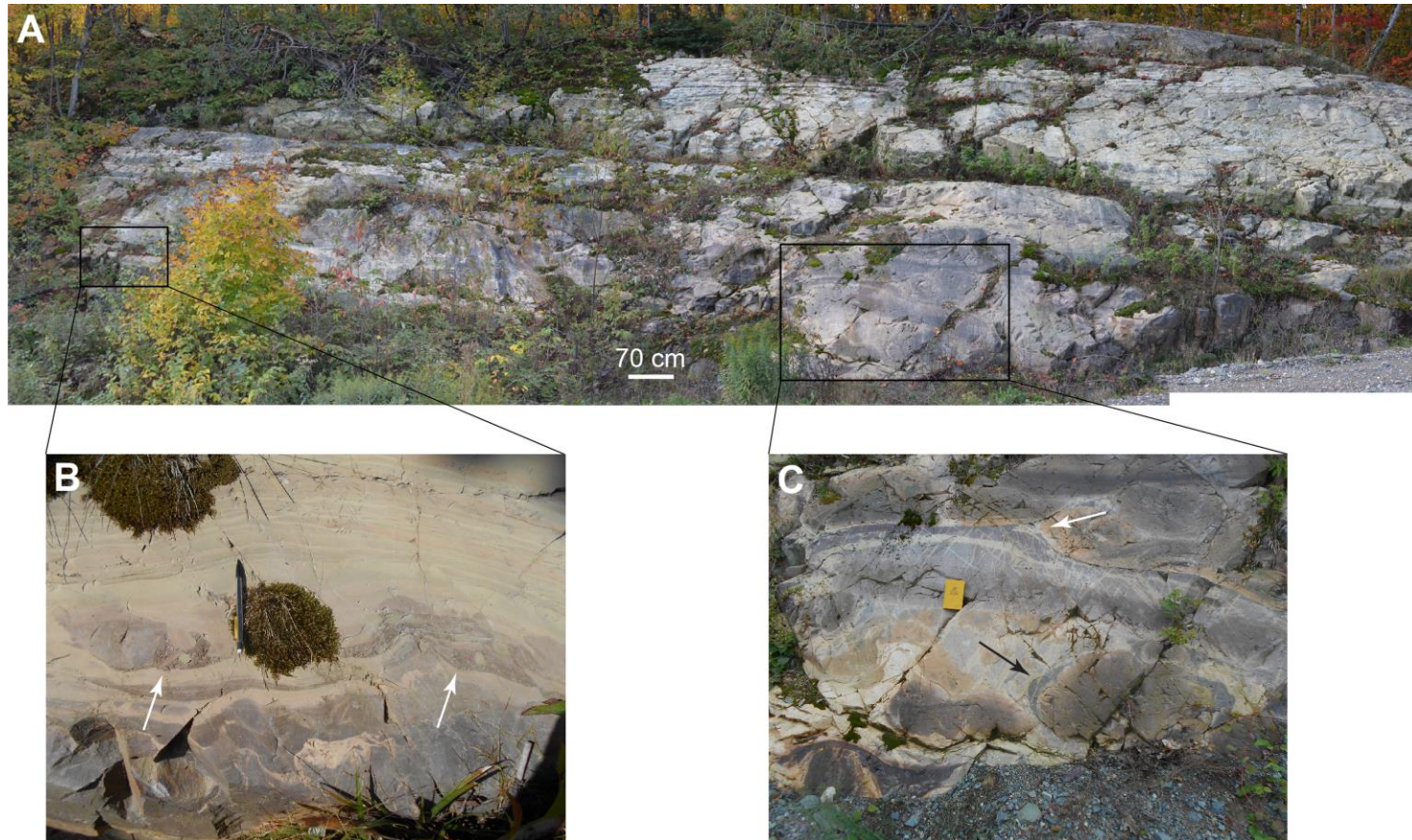


Figure 4.3. Exposure of the Gordon Lake Formation in the study area. A) Lowest stratigraphic interval exposed along Old Soo Road, composed of mudstone, siltstone, chert, fine-grained sandstone and minor medium-grained sandstone. B) Discontinuous intraformational conglomerate with small-scale load structures indicated by white arrows. C) Large flame (white arrow) and ball-and-pillow structures (black arrow). Note the chaotic nature of the base of this outcrop. Pencil is 14.5 cm long and field book is 19 cm long.

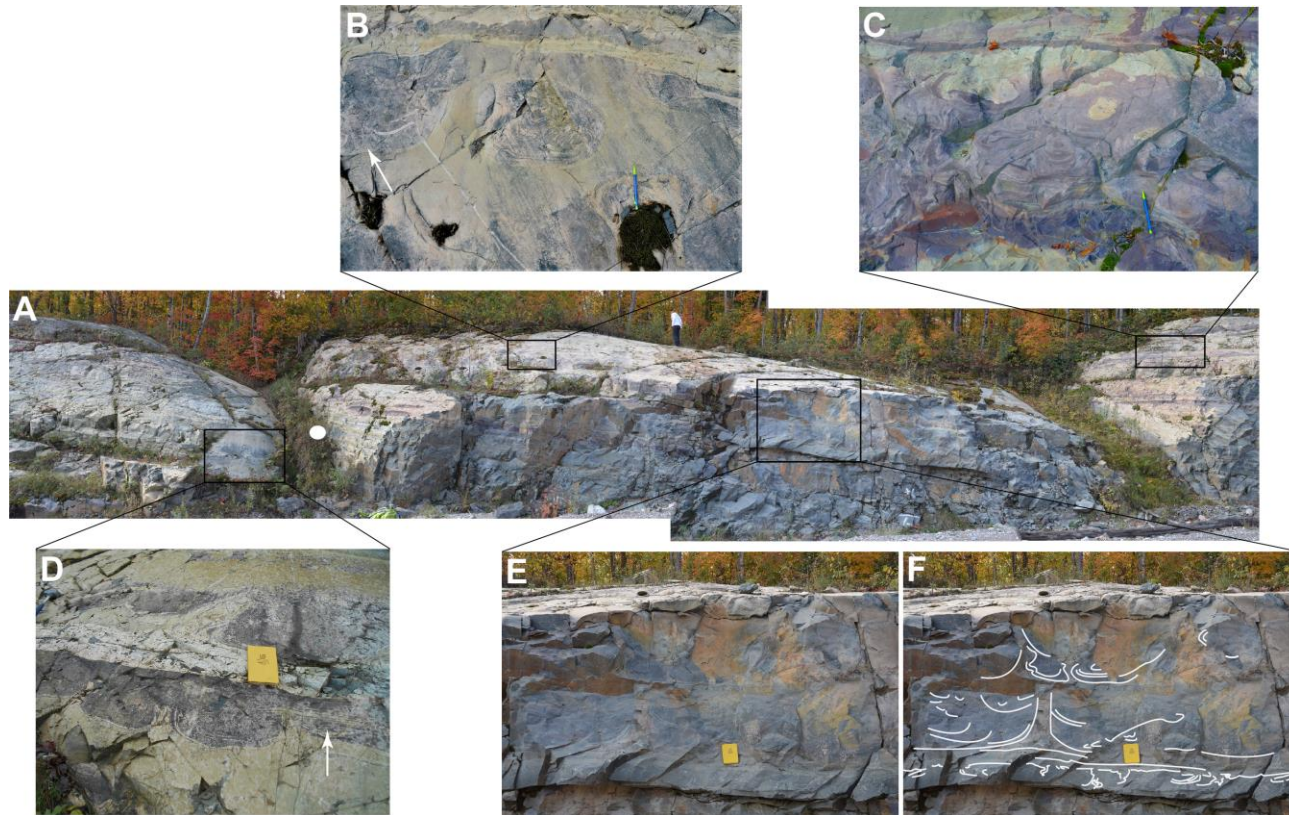


Figure 4.4. Continuation of the Gordon Lake Formation exposure in the study area. A) Stratigraphic continuation of the outcrop in Figure 4.3a. This section contains thin beds of mudstone, siltstone, fine-grained sandstone and minor medium-grained sandstone. The white circle indicates the start of the stratigraphic section in Figure 5. B) Large ball structures and load casts. Note the thin internal laminations. White arrow indicates an internal water-escape structure. Photo colour saturation increased to enhance structures. C) Convolute bedding and load casts. Note the dark microbial mat capping a bedding surface. D) Simple load casts with flame structures. White arrow indicates relatively undeformed laminae. E) Load casts and flame structures. F) Line markings highlighting the main deformation styles in Figure 4e. Person for scale is 178 cm tall, pencil is 14.5 cm long and field book is 19 cm long.

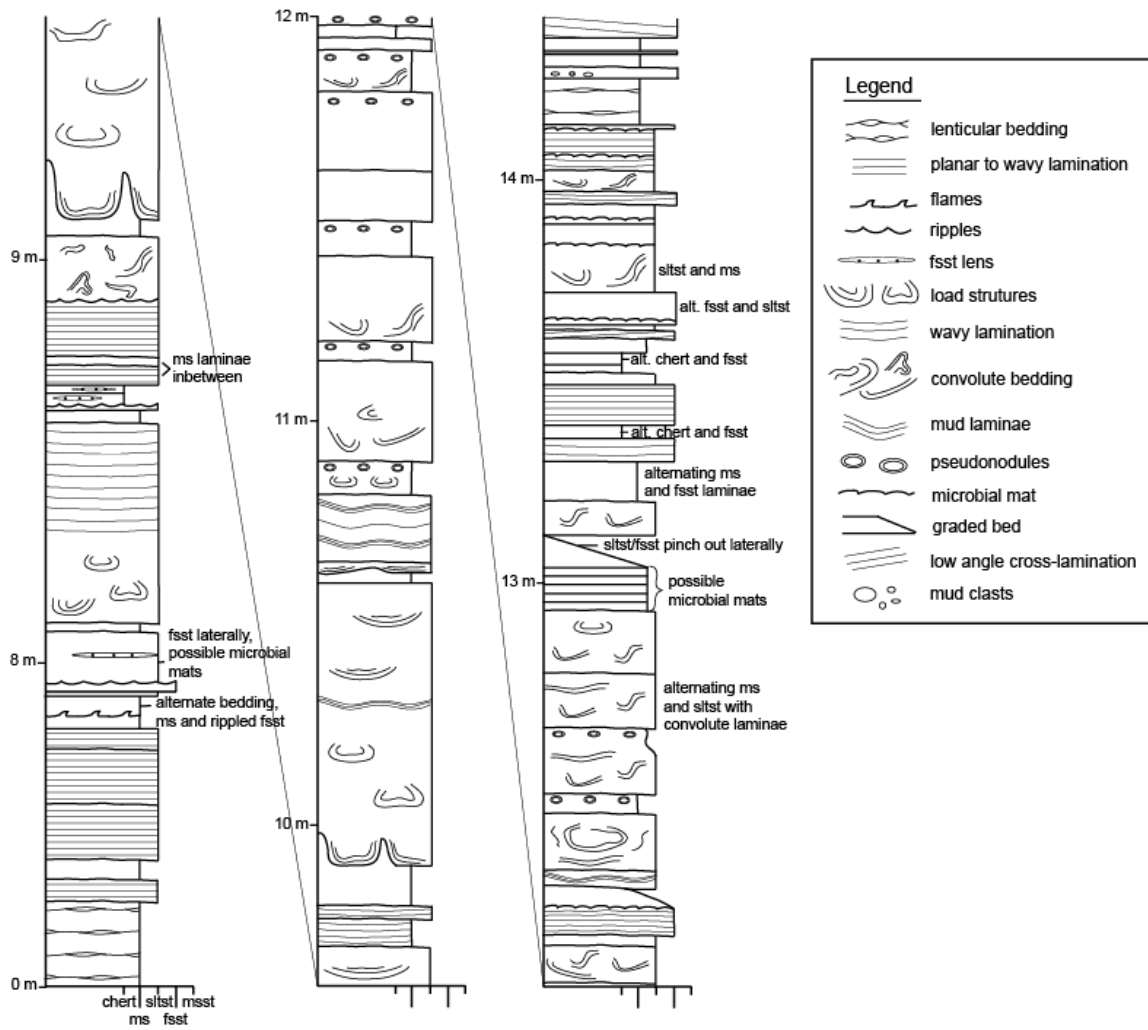


Figure 4.5. Stratigraphic section illustrating the lower to middle portion of the Gordon Lake Formation exposure on Old Soo Road. Starting interval indicated in Figure 4.4a. Abbreviations: alt., alternating; ms, mudstone; siltst, siltstone; fsst, fine-grained sandstone; msst, medium-grained sandstone.

Flame structures are most common in the lower half of the exposure and are up to 51 cm high. They occur where mud was pushed up into overlying siltstone to fine-grained sandstone beds. Local flame structures have truncated tops.

One structure interpreted as a dewatering pipe is present within a bed containing pseudonodules. The sediment-infilled portion of the pipe is approximately 20 cm long and contains fine- to medium grained sandstone and a light grey chert pebble at its base (Figure 4.6f). The bed containing the dewatering pipe may be laminated, but any laminations are largely obscured due to weathering on the bed's surface.

4.3.2 Microbial mats

Many SSDS in the interval 10-20 m from the base of the outcrop formed above and below purple iron-stained beds that contain wavy, wrinkled laminae (Figures 4.4c; 4.7a and d; 4.8a, b, e, f), botryoidal texture (Figures 4.7b and e), and ovoid patches with irregular relief (Figures 4.8c and d). Laterally continuous, flat to wavy, light and dark laminae were observed in multiple fine-grained, purple beds and during petrographic analysis. A number of small cavities parallel to wavy laminae (Figure 4.7d) were also observed in several beds. An *in situ* microbial mat origin is inferred for these structures, as their morphology and size resemble documented examples of both modern (e.g. Gerdes, 2007; Bouougri and Porada, 2011) and ancient microbial mats (e.g. Allwood et al., 2006; Noffke et al., 2008), and mat microtextures are present in thin sections. Microbial microtextures include: concave-upward (Figure 4.8e), wavy, and crinkled carbonaceous laminae (Figure 4.8f), fine sand to medium silt quartz grains aligned along faint laminae (Figure 4.8e), and silt-sized grains preserved within carbonaceous laminae (Figure 4.8e, f). These microtextures reflect the baffling, trapping and binding of microbial mats (Noffke, 2010). The small cavities resemble fenestrae.

Irregular, laminated fragments, 5 to 11 cm long, were identified at the same stratigraphic interval as the *in situ* mats (Figure 4.7f). Some of these structures display ragged edges. Purple, 15 to 100 cm long elongated patches, with irregular negative relief and a spongy texture were also observed in the study area (Figures 4.8c and d). The edges of these structures are generally sub-rounded, but appear torn or eroded. We interpret both of

these types of structures as microbial mat chips, the former containing biolamination. The ragged edges of the small mat chips may have formed during erosion of a wet mat. The mottled surface of the large mat chips may indicate mat growth prior to erosion or soft-sediment deformation. Intervals containing microbial mats and mat chips typically display weathering of sulphide minerals (Figure 4.6a, b, f; 4.7a, c) and are stained with iron oxides (Figures 4.4c; 4.7a-e; 4.8a-d). The lower sections of microbial mats are conducive to the formation of reduced minerals, such as pyrite, as they are naturally anoxic due to the presence of decaying organic matter (Berner, 1984; Gerdes et al., 1985).

Several thin, fine-grained, pink, undulating beds with an irregular surface are present throughout the outcrop, and are most common within the microbial mat-mat chip interval above small pseudonodules (Figures 4.6a, b, f; 4.7c). The speckled nature of the beds, presence of sulphide minerals, and evidence that they were cohesive suggests that the sediment was stabilized and bound by microbial mats.

4.4 Discussion

In the pursuit of accuracy, we have endeavored to take a context-based approach to demonstrate how the SSDS in Gordon Lake Formation in the Bruce Mines area formed. All aspects of sedimentology and paleoenvironment have been used to assess possible autogenic and allogenic trigger mechanisms.

4.4.1 Significance of the assemblage of SSDS in the study area

The varied assemblage of SSDS in the Bruce Mines area points to variations relating to starting conditions, lithologies, paleoenvironment, and triggers. The SSDS observed in the study area formed in fine-grained, unconsolidated, water-saturated sediment that was at or near the surface at the time of deformation. Silts and fine-grained sands are easily liquefied and plastically deformed because the cohesion between grains is not high and they are light enough to be supported by pore fluid (Moretti et al., 1999; Owen and Moretti, 2011). The rock types and sedimentary structures support deposition under

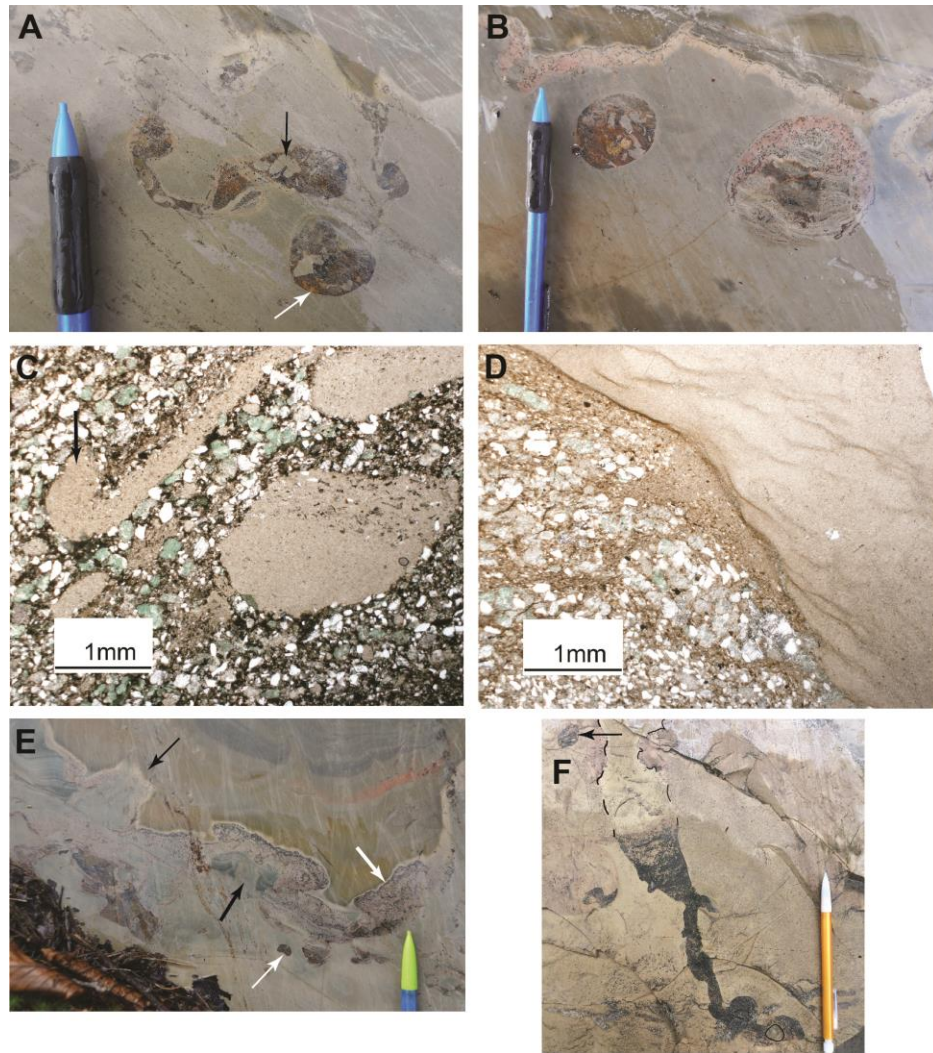


Figure 4.6. Pseudonodules and dewatering pipe. A) Small, elongate to circular pseudonodules containing sulphide minerals (white-arrow) and mud rip-up clasts (black arrow). B) Two pseudonodules below a biofilm-bound surface (pencil top). The left structure contains abundant sulphides and mud rip-up clasts, whereas the right structure contains internal laminations and minor sulphides. C) Thin section photomicrograph illustrating the general grain size, sorting, roundness and mineralogy of a pseudonodule. Note the curled, plastic nature of the leftmost mud clast (black arrow). D) Photomicrograph illustrating the general grain size, sorting, roundness and mineralogy of a pseudonodule, and the contact with the surrounding sediment. Note the wispy, soft-sediment deformation patterns that formed in the surrounding sediment during pseudonodule development. E) Small pseudonodules (white arrow) detached from an event layer (oblique section). Note the path of water-escape that successfully pierced through the stabilized layer (thin black arrow) and one that did not (thick black arrow). The bright, undulating bed is interpreted to be biofilm-bound (thick white arrow). F) Cylindrical structure interpreted as a dewatering-pipe. The dashed lines outline the neck of the pipe. Note the chert pebble outlined in black at the base of the pipe and the pseudonodule to the left of the pipe (black arrow). Pencil is 14.5 cm long and 8 mm wide.

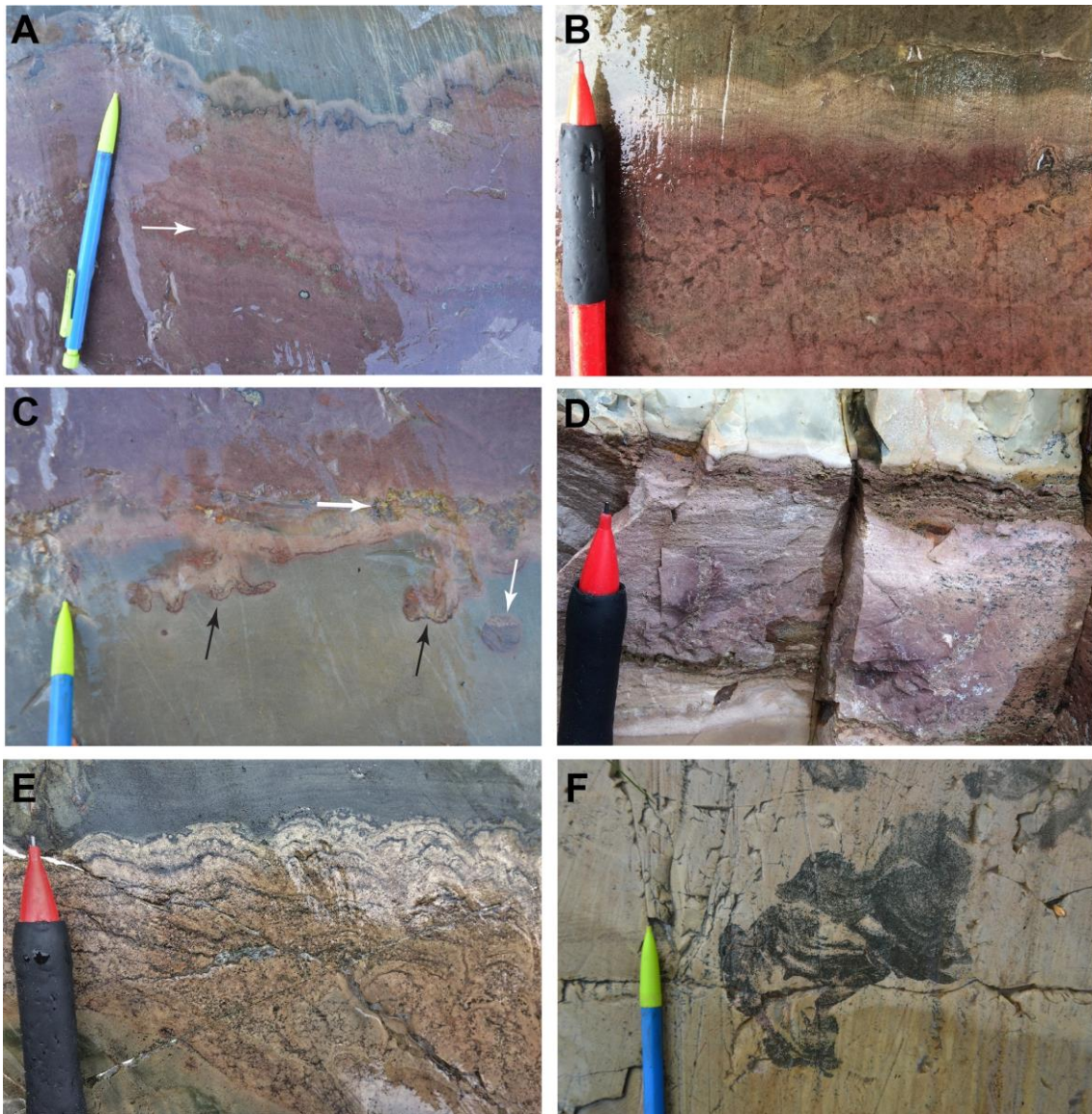


Figure 4.7. Microbial mats and mat chips identified in the Bruce Mines area (oblique sections). A) Laterally and vertically continuous microbial mat with fine, wavy laminations. Note the irregular, undulating surface of the mat and slightly botryoidal horizon (white arrow). B) Close-up of the mat surface from (A) and its botryoidal texture. Photo colour saturation increased to enhance structures. C) Base of microbial mat shown in (A). Note the horizon of sulphide minerals (thick white arrow) and pseudonodules detaching from the base of the biofilm (black arrows). A small, laminated pseudonodule on the right is detached (thin white arrow). D) Fine-grained sandstone bed with wavy laminae and numerous voids (fenestrae?) in the top 2 cm of the bed, interpreted to be a microbial mat. E) Close-up of a second microbial mat displaying wavy to slightly pseudo-columnar appearance. Photo colour saturation increased to enhance structures. F) Small, layered mat-chip with ragged margins. Pencil is 14.5 cm long and 8 mm wide.

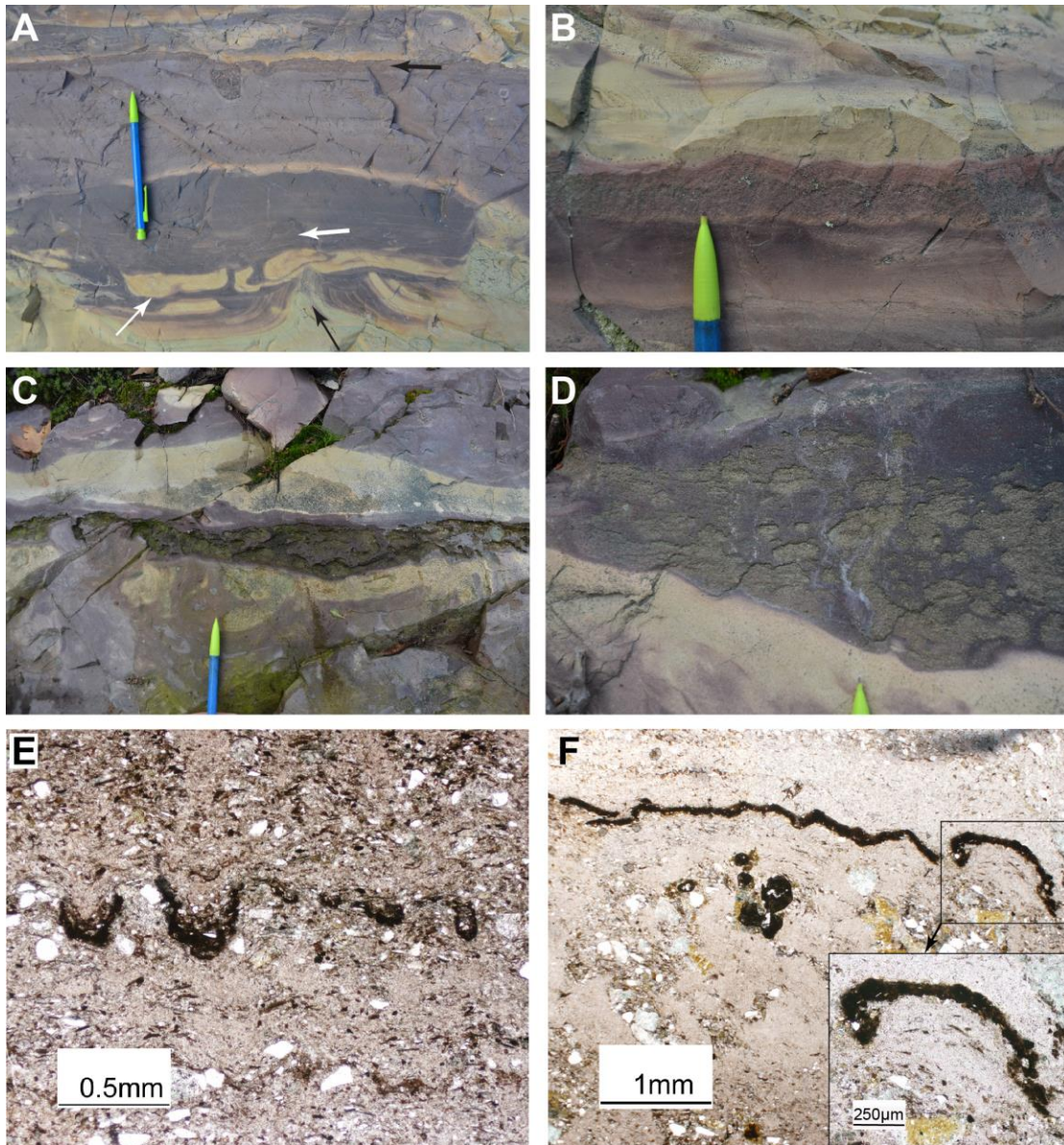


Figure 4.8. Assortment of structures in the middle interval of the outcrop exposure. A) Two examples of load (thin white arrow) and water-escape structures (thin black arrow) in beds beneath a microbially-stabilized event layer (thick black arrow). The interval immediately above the load structures contains convolute laminae (thick white arrow). B) Small, flat to wavy microbial mats within a fine-grained sandstone bed. C) Large mat-chip surrounded by mudstone and siltstone. Note the ragged margins of the chip and the load structures immediately below. D) Close-up of a large mat-chip showing spongy, irregular texture and mat margins. E) Concave-upward carbonaceous laminae. Note the faint horizontal laminations above and below the laminae, which are often defined by trapped sand and silt sized quartz grains. F) Irregular, wavy, carbonaceous laminae. Note the silt grains bound within the laminae. Pencil is 14.5 cm long.

relatively calm conditions in a shallow marine setting. In order for such a large quantity of fine-grained material to be deposited, a shallow shelf or continental slope setting may be appropriate. The sandy beds that sourced the pseudonodules are here interpreted as event deposits, as they are anomalous in the stratigraphy, coarser grained than the overlying and underlying beds, and have abrupt contacts. Minor intra-formational conglomerate and graded beds may have formed during storm events, whereas microbial mats would have colonized during periods of low sediment influx. The top of the exposure contains desiccation cracks and is interpreted as being deposited in a shallow, tidally-influenced setting. This interpretation compares favorably to the tidal flat environment suggested for the deposits of the Gordon Lake Formation in the Flack Lake area (Wood, 1973; Hill et al., 2016). Shallow marine environments are dynamic settings and in this context a variety of trigger mechanisms and driving forces are considered in Section 4.4.3 below.

4.4.2 SSDS elsewhere in the Gordon Lake Fm

A summary of the SSDS found in the Gordon Lake Formation is listed in Table 4.1; the Gordon Lake Formation contains a significantly higher assortment, and likely quantity, of SSDS than other formations in the Huronian Supergroup. Outcrops of the Gordon Lake Formation in the Baie Fine, Flack Lake, and Cobalt plains areas contain neither the same quantity, nor size of SSDS as are present in the study area near Bruce Mines (Young, 1968; Card, 1976; Card, 1978; Chandler, 1986). This is significant as it suggests that the western portion of the basin was either affected by different intensities of sedimentary processes or local events. After the study area, the Baie Fine area contains the next highest abundance of SSDS, followed by only a few observed examples in the Flack Lake and Cobalt plains areas. This suggests that the trigger mechanism(s) may have been restricted to the western and southern portions of the basin, which are interpreted to have been offshore settings. Overall, outcrops in the Baie Fine area contain comparable types of SSDS as to the study area. Clastic dikes and two small-scale syn-sedimentary faults were observed in the Baie Fine and Cobalt plains areas, suggesting that at least one high energy, basin-wide event occurred.

4.4.3 Possible triggers for SSD in the Gordon Lake Fm

In consideration of the structural setting and stratigraphic context of the Gordon Lake Formation, there are six possible triggers for SSDS formation: 1) loading by storm waves (Molina et al., 1998; Alfaro et al., 2002; Chen et al., 2009), 2) impact of breaking waves (Kerr and Eyles, 1991), 3) tsunamis (Takashimizu and Masuda, 2000; Meshram et al., 2011), 4) tidal shear (Greb and Archer, 2007), 5) rapid sediment loading (Postma, 1983; Moretti et al., 2001; Oliveira et al., 2009), and 6) seismic disturbance (Moretti and Sabato, 2007; Roy and Banerjee, 2016).

4.4.3.1 Loading by breaking and storm waves

Breaking waves in shallow water can trap a pocket of air that causes a rapid, high impact force on the bed that is then spread through the sediment (Dalrymple, 1979). Breaking waves can also lead to the compaction of sediment, which decreases the likelihood of liquefaction and deformation (Dalrymple, 1979). Storm waves increase stress through both cyclic, recurrent loading and the abrupt impact of breaking waves (Seed and Rahman, 1978; Owen, 1987). Liquefaction and fluidization occur because the interstitial pore pressure of sediment increases rapidly in response to the pressure differences between the crest and trough of storm waves (Seed and Lee, 1966; Molina et al., 1998) and an increase in wave height (Dalrymple, 1979). In addition, cyclic loading by long period waves can induce liquefaction (Seed and Lee, 1966; Seed and Rahman, 1978; Figueiredo et al., 1982).

Sedimentary structures are frequently obscured in the SSDS-rich lower and middle portions of the Gordon Lake Formation exposure. Those that are visible, in conjunction with the predominance of fine-grained deposits and a paucity of HCS, suggest that deposition occurred in relatively calm water that was unaffected by persistent wave action. The large quantity of SSDS suggests that the sediment in the study area was unconsolidated during and shortly following burial. Impact of breaking waves is, therefore, an unlikely trigger mechanism for the formation of SSDS in the study area.

Many beds in the study area are thicker than the largest deformed beds reported from modern tidal flats (e.g. 30-cm-thick; Greb and Archer, 2007), which suggests that a high-energy, non-tidal related trigger mechanism is responsible for their formation. Outcrops of the Gordon Lake Formation in other areas contain several structures that formed as a result of storm processes (including hummocks) and graded beds were found in the study area. The exposure in this study does not permit the horizontal association of SSDS with HCS or other storm deposits. Locally, flame structures have truncated tops, meaning that they formed near surface and were likely wave induced; however, many modern truncated flame structures have been linked to tsunamis (Matsumoto et al., 2008). Although HCS was not observed in the outcrop, it is probable that recurrent loading by storm waves occurred during deposition and was a trigger for some of the SSDS; a large storm event may have led to the formation of the largest SSDS observed (Figure 4.3c).

4.4.3.2 Tsunamis

High-energy events along a passive margin can also be linked to tsunamis. Unlike storms, tsunami waves typically generate a strong, uninterrupted unidirectional current, which may trigger soft-sediment deformation on runup (Matsumoto et al., 2008). The lack of high amplitude HCS in the study area supports a high-energy, non-storm trigger mechanism for the formation of the SSDS. As such, the sandy event beds may represent tsunami deposits. Alternating coarse- and fine-grained laminae were observed in several pseudonodules that originated from the event deposits, and may indicate multiple surges of water. The plastic nature of many mudstone clasts in the pseudonodules (Figure 4.6c) suggests that the beds were not fully consolidated when the events took place. The lack of structural evidence for prolonged induration also supports a tsunami trigger (Benson et al., 1997), in addition to the lateral variability throughout the exposure, few depositional layers, presence of SSDS, graded beds, and mud rip-up clasts. The event beds are quite thin, however, tsunami event deposit thicknesses of as little as 0.5 cm have been reported (Table 3 in Morton et al., 2007). Perhaps the tsunamis were relatively small-scale events that neither rapidly nor significantly altered the hydrologic regime of the area.

Mud rip-up clasts are more likely to be preserved in tsunami deposits as opposed to storm deposits, as they are subjected to less turbulence and shorter agitation time, which leads to a smaller likelihood of disintegrating (Morton et al., 2007). Rip-up clasts were observed throughout the Gordon Lake Formation exposure and in the event beds. Preservation of a chert pebble in the dewatering pipe also supports a tsunami trigger because a significant amount of energy is needed to transport a pebble from a near shore setting. Modern truncated flame structures have been linked to tsunamis (Matsumoto et al., 2008), and truncated flame structures were observed in the study area. Both storm and tsunami deposits may contain heavy mineral laminae (Morton et al., 2007). In general, storm and tsunami deposits share many similarities and can be difficult to distinguish, particularly if outcrops are not well exposed or if there are no fossils to aid in interpretation, which is the case in the majority of Precambrian successions.

4.4.3.3 Tidal shear and tidal bores

Tidal shear may produce SSDS through a rapid increase in applied stress (Dalrymple, 1979; Greb and Archer, 2007) and must therefore always be evaluated as a potential trigger mechanism for soft-sediment deformation in tidally-influenced settings. For example, an ebb tide coinciding with a rapid water level fall would be favourable for soft-sediment deformation (Dalrymple, 1979). Lateral shear stress from current drag may also trigger deformation in unstable density gradients, leading to the formation of asymmetrical load casts (Moretti et al., 2001).

Greb and Archer (2007) report modern contorted bedding, flow rolls, dish and flame structures, and small dewatering pipes from the macrotidal estuary at Turnagain Arm, Alaska. Flow rolls and contorted beds in that area were previously interpreted as earthquake induced, however the authors observed similar SSDS forming in a single tidal cycle in the absence of a seismic shock (Greb and Archer, 2007). Soft-sediment deformation structures from Cambrian tidal deposits in NW Estonia display an intimate relationship with the tidal sediments and structures (Põldsaar and Ainsaar, 2015); for example, the tips of flame structures indicating opposing flow directions (tidal currents) within consecutive horizons of SSDS. This relationship was not observed in the study

area. If the paleoenvironment of the Gordon Lake Formation was a long, thin, shallow inlet it is possible that some of the SSDS in the study area may have formed from tidal bores, however there is no indication of such a setting. Asymmetric load casts were observed infrequently in the exposure and may have formed as a result of current shear. Overall, it is unlikely that tidal shear was a primary trigger for the SSDS observed in the Gordon Lake Formation near Bruce Mines.

4.4.3.4 Rapid sediment loading and density inversions

A layer of denser sediment deposited on top less dense sediment creates an inverse density gradient. The heavier material tends to sink due to a higher potential energy accumulated during deposition, which causes deformation (Anketell et al., 1970). Similarly, a reduction in the shear strength of a bed can occur when coarser-grained sediments are rapidly deposited on top of finer-grained sediments (Moretti et al., 2001).

The abundance of microbial mats in the study area suggests that sedimentation rates were not high, as extensive microbial mats would have formed only during periods of slow deposition. In addition, slope-related flows are rare, and the dominant SSDS are load structures, therefore rapid sediment loading is not interpreted as a primary trigger mechanism.

The ubiquity of load casts in the outcrop, however, indicate that inverse density gradients probably drove the formation of many SSDS. Relatively simple, undeformed load structures are interpreted to have been induced by density inversion, whereas the more disrupted load structures may have formed in response to overpressuring. Preservation of internal laminae suggests that the sediments remained relatively uniform throughout deformation and were subject to stretching and not turbulence. In addition, flexure of more competent mud intervals during deformation may have caused the interbedded siltstone layers to readjust plastically (Dzulynski and Smith, 1963), resulting in some of the chaotic forms observed in outcrop.

4.4.3.5 Seismic disturbance

A number of SSDS in the Bruce Mines area fulfill some of the six criteria for recognizing seismites, as outlined by Owen and Moretti (2011). These include 1) large areal extent, 2) lateral continuity, 3) vertical repetition, 4) morphology comparable with structures described from seismically-affected beds, 5) proximity to active faults, and 6) zonation of complexity or frequency with short distance from fault.

In general, the Gordon Lake Formation is not well-exposed, thus it is difficult to conclude a large areal extent of the SSDS in the Bruce Mines area. However, SSDS have been observed in other areas where the Gordon Lake Formation is exposed, illustrating that a large area has been affected. Tsunamis and meteorite impacts are also capable of affecting large areas, therefore it is not a reliable criterion for a seismic trigger (Shanmugam, 2016). The longest lateral continuity of SSDS provided in outcrop is approximately 20 m, however SSDS are known to be laterally discontinuous (Alfaro et al., 2002; Greb and Archer, 2007). Vertical repetition of SSDS is easily apparent, as the structures were observed on various scales throughout the entire exposed section. Deformed beds are generally not distinct and the intervening beds show considerable evidence of soft-sediment deformation, which is inconsistent with the expected representation of a seismic trigger.

The large SSDS, highly chaotic and convolute bedding, and abundance of pseudonodules are comparable with structures described throughout the literature as having been induced by earthquakes (e.g. Moretti and Sabato, 2007; Nehyba, 2014; Roy and Banerjee, 2016; van Loon and Dechen, 2013). These structures would have required either a relatively large amount of energy or some considerable component of horizontal stress, or both, during formation, which suggests a seismic interpretation. The main outcrop in this study is located approximately 1.2 km north of the Murray Fault (Figure 4.2), therefore fulfilling the criteria of close proximity to a fault. Because the Murray Fault is interpreted to have undergone normal growth faulting during deposition of the lower Huronian Supergroup (Roscoe, 1969; Card, 1978; Zolnai et al., 1984), it is possible that local

seismic disturbances would have occurred during deposition of the Gordon Lake Formation.

The six criteria outlined above are not diagnostic of seismic triggers and some criteria, such as large areal extent, are difficult to apply on an outcrop scale (Owen and Moretti, 2011). We hesitate to use the term “seismite” here to classify the SSDS, as it holds many problems in application, such as not conveying depositional origin (Shanmugam, 2016).

4.4.3.6 Summary of trigger mechanisms

Given the frequency and various degrees of disruption throughout the outcrop, a combination of trigger mechanisms is suggested for the SSDS of the Gordon Lake Formation in the Bruce Mines area. Loading by long period storm waves and tsunamis appear to be the most likely trigger mechanisms, with seismic shock, inverse density gradients, and overpressuring as possible less common driving forces and trigger mechanisms. Although it is tempting to suggest a direct seismic trigger for the highly deformed beds, these beds are relatively uncommon, and are not evident on the large scale needed to link to significant fault movements. Many of the SSDS are not highly deformed and it is doubtful that seismic disturbances would occur with such a high frequency along a passive margin. Non-seismogenic triggers, such as storm or tsunami waves, would have been more common in such a setting.

In this paper an attempt has been made to elucidate the deformation triggers ultimately responsible for the formation of SSDS in the Gordon Lake Formation in the Bruce Mines area, however it is possible that there is no single “cause”. There are clear challenges in determining the order of events; for example, an earthquake-triggered tsunami can lead to mass wasting that consequently triggers a secondary tsunami (Shanmugam, 2016). In general, caution must be taken when determining the mechanism of SSDS formation in shallow marine environments, as there are multiple possible trigger mechanisms.

4.4.4 Significance of microbial mats

Recognition of microbial mats and mat-related structures in the study area increases the quantity of biosignatures in the Paleoproterozoic Huronian Supergroup and may help

with paleoenvironmental interpretation. Modern microbial mats are most often observed in shallow marine-tidal-supra-tidal settings (Eriksson et al. 2010), however throughout the Precambrian, microbes extensively colonized shallow-marine environments, where they affected sedimentation during and after deposition (Catuneanu, 2007). In general, mat morphologies are reflections of the physical, chemical and biological adjustments made by microbial colonies to local conditions (Eriksson et al. 2010). The lack of evidence for repeated subaerial exposure and low number of destruction-related microbial mat structures in the studied exposure supports a subtidal setting. Flat-wavy laminated microbial mats are frequently associated with intertidal zones, whereas pustular and discrete buildups are associated predominantly with subaqueous settings. In addition, multi-laminated biofilms require weeks to months to form (Gerdes and Klenke, 2003) and must be exposed in an environment with a low-rate of sedimentation, which supports a subtidal paleoenvironment.

In addition to the processes discussed in Section 4.4.3, a number of biological, chemical, and physical forces, such as plant roots, burrows, crystal growth and the desiccation of clays, may also influence the formation of SSDS (Owen, 1987). During the Paleoproterozoic, microbial mats were the only biological agents that could have influenced soft-sediment deformation. Microbial mats can act as permeability barriers and may increase the likelihood of forming SSDS by creating impenetrable seals beneath which pore-pressure increases (Obermeier, 1996; Harazim et al., 2013). The underlying pore fluid is unable to evenly dissipate upwards through the sediment, which results in overpressuring until the fluid is able to perforate the weakest segment(s) of the mat, leading to soft-sediment deformation. Conversely, microbial mats increase the cohesion, and therefore stability, of the sediment they colonize, which often leads to less-pronounced loading, flexible sediment, or rolling-up and folding during soft-sediment deformation (Schieber, 1986; Schieber, 2007; Le Ber et al., 2015). Deformation behaviour of microbially-bound sediment may differ than non-microbially bound sediment, as a portion of the initial mat cohesiveness may be maintained for some time after burial (Schieber, 2004). Extensive vertical growth of microbial mats may also limit the formation of SSDS by creating a relatively rigid framework (Schieber, 2007; Le Ber et al., 2015).

In the study area, the undulating pink beds overlie the relatively coarse-grained event layers that formed many of the small pseudonodules, and may have provided a favorable surface for microbial mats to colonize. A sequence of microbial mats a few cm thick is interpreted to have formed over the pink bed shown in Figure 4.7c, which may have prevented more pseudonodules from forming. There is local evidence for successful and unsuccessful penetration of the overlying mat-bound bed during soft-sediment deformation (Figure 4.6e). Gases produced during microbial mat decay may also leave voids in the sediment through which pore water later escapes (Menon et al., 2016). Microbial mats may have contributed to the morphology and perhaps formation of some SSDS in the study area, but were not likely a predominant mechanism that drove their formation.

It is possible that during growth, microbial mats in the study area were affected by wave or current activity, which could indicate that the small and large, purple mat chips may have formed through tearing, dragging, and erosion by these agents. Conversely, although uncommon, seismically-deformed microbialites and stromatolites have been reported throughout the geologic record in carbonate, siliceous, and siliciclastic rocks (Pratt, 1994; Behr and Röhrlich, 2000; Nogueira et al., 2003; Donaldson and Chiarenzelli, 2007; Martín-Chivelet et al., 2011; Hongshui et al., 2013; van Loon and Dechen, 2013). Similar characteristics are shared between the deformed biofilms in this study and seismically-deformed stromatolites reported from the Mesoproterozoic Wumishan Formation, Changping District, China (van Loon and Dechen, 2013), and the Cambro-Ordovician Nepean Formation, Ottawa, Canada (Donaldson and Chiarenzelli, 2007).

4.5 Conclusion

A large exposure of the Gordon Lake Formation in the Bruce Mines area contains numerous SSDS of varying morphology and size. Many beds were violently disturbed, whereas others show limited deformation. Main trigger mechanisms responsible for the deformation include storm waves and tsunamis, however, proximal earthquakes and overpressuring by means of permeability barriers (biofilms) may have had a minor

influence. Density inversions may have also drove the formation of SSDS. Other outcrops of the Gordon Lake Formation in the Bruce Mines area do not contain the same abundance of soft-sediment deformation features, which may be due to their position in the stratigraphy, a lower degree of water saturation, or absence of driving mechanisms related to soft-sediment deformation. Evidence of microbial colonization in the study area extends the convincing indication of microbial colonization during deposition of the Gordon Lake Formation to two areas.

4.6 References

- Alfaro, P., Delgado, J., Estévez, A., Molina, J.M., Moretti, M., Soria, J.M., 2002. Liquefaction and fluidization structures in Messinian storm deposits (Bajo Segura Basin, Betic Cordillera, southern Spain). *Int. J. Earth Sci.* 91, 505-513.
- Al-Hashim, M.H., 2016. Sedimentology and geochemistry of the mixed carbonate-siliciclastic Espanola Formation, Paleoproterozoic Huronian Supergroup, Bruce Mines-Elliot Lake Area, Ontario, Canada. PhD Thesis. The University of Western Ontario. Electronic Thesis and Dissertation Repository. 4350.
- Allwood, A.C., Walter, M.R., Kamber, B.S., Marshall, C.P., and Burch, I.W., 2006. Stromatolite reef from the Early Archean era of Australia. *Nature* 441, 7094: 714-718.
- Anketell, J.M., Cegla, J., Dzulynski, S., 1970. On the deformational structures in systems with reversed density gradients. *Ann. Soc. Geol. Po.* 40, 3–30.
- Aranha, R.D.J, 2015. Factors controlling the composition and Lithofacies characteristics of the Paleoproterozoic Bar River Formation, Huronian Supergroup. MSc Thesis, The University of Western Ontario. Electronic Thesis and Dissertation Repository. 3321.
- Baumann, S.D.J., Arrospeide, T., Wolosyzn, A.E., 2011. Preliminary redefinition of the Cobalt Group (Huronian Supergroup), the Southern geologic province, Ontario, Canada. In: MIGE Report G-012011-2A.
- Behr, H.-J., Röhricht, C., 2000. Record of seismotectonic events in siliceous cyanobacterial sediments (Magadi cherts), Lake Magadi, Kenya. *Int. J. Earth Sci.* 89, 268-283.
- Bekker, A., Karhu, J.A., Kaufman, A.J., 2006. Carbon isotope record for the onset of the Lomagundi carbon isotope excursion in the Great Lakes area, North America. *Precam. Res.* 148, 145-180.

- Bennett, G., 2006. Geological features and correlation of a dolostone unit in Fenwick Township, northeast of Sault Ste Marie, Ontario. In: *The Huronian Supergroup between Sault Ste Marie and Elliot Lake. Field Trip Guidebook, V.52, Part 4*, pp. 49-50.
- Bennett, G., Dressler, B.O., Robertson, J.A., 1991. The Huronian Supergroup and associated intrusive rocks. In: Thurston, P.C., Williams, H.R., Sutcliffe, R.H., Scott, G.M. (Eds.), *Geology of Ontario, Part 1: Ontario Geological Survey, Special Volume 4*, pp. 549–591.
- Benson, B.E., Grimm, K.A., and Clague, J.J., 1997. Tsunami deposits beneath tidal marshes on Northwestern Vancouver Island, British Columbia. *Quat. Res.* 48, 192-204.
- Berner, R.A., 1984. Sedimentary pyrite formation; an update. *Geochim. Cosmochim. Acta* 48, 605–615.
- Bouougri, E.H., and Porada H., 2011. Biolaminated siliciclastic deposits. In: Reitner, J., Quéric, N.-V., and Arp, G. (Eds.) *Advances in Stromatolite Geobiology, Lecture Notes in Earth Sciences* 131, pp.507-524.
- Card, K.D., 1976. *Geology of the McGregor Bay-Bay of Islands Area, Districts of Sudbury and Manitoulin. Ontario Division of Mines Geoscience, Report 138*, 63p.
- Card, K.D., 1978. *Geology of the Sudbury-Manitoulin area, districts of Sudbury and Manitoulin. Ontario Geological Survey, Geoscience Report, 166*, 238p.
- Card, K.D., 1984. *Geology of the Espanola-Whitefish Falls Area, District of Sudbury, Ontario. Ontario Geological Survey, Report 131*, p. 70. Accompanied by Maps 2311, 2312, and 2 charts.
- Card, K.D., and Lumbers, S.B., 1975. *Sudbury-Cobalt. Ontario Geological Survey, Map 2361*.
- Card, K.D., Innes, D.G., Debicki, R.L., 1977. *Stratigraphy, Sedimentology, and Petrology of the Huronian Supergroup of the Sudbury-Espanola Area. Ontario Division of Mines, Geoscience Study 16*, 99p. Accompanied by 4 charts and one figure.
- Catuneanu, O., 2007. Sequence stratigraphic context of microbial mat features. In: Schieber, J., Bose, P.K., Eriksson, P.G., Banerjee, S., Sarkar, S., Altermann, W., Catuneanu, O. (Eds.), *Atlas of Microbial Mat Features Preserved within the Siliciclastic Rock Record, Atlases in Geoscience 2*. Elsevier, pp. 276-283.
- Chandler, F.W., 1973. Clastic dykes at Whitefish Falls, Ontario and the base of the Huronian Gowganda Formation. In Young, G.M. (Ed.), *Huronian stratigraphy and sedimentation. Geological Association of Canada Special Paper 12*, 199-210.

- Chandler, F.W., 1986. Sedimentology and paleoclimatology of the Huronian (Early Aphebian) Lorrain and Gordon Lake Formations and their bearing on models for sedimentary copper mineralization. In: Geological Survey of Canada Paper 86-1A, pp. 121–132.
- Chandler, F.W., 1988a. Quartz arenites: review and interpretation. *Sediment. Geol.* 58, 105–126.
- Chandler, F.W., 1988b. Diagenesis of sabkha-related, sulphate nodules in the early Proterozoic Gordon Lake Formation, Ontario, Canada. *Carbonates Evaporites* 3, 75–94.
- Chen, J., Chough S.K., Chun, S.S., Han, Z., 2009. Limestone pseudoconglomerates in the Late Cambrian Gushan and Chaomidian Formations (Shandong Province, China): soft-sediment deformation induced by storm-wave loading. *Sedimentology* 56, 1174-1195.
- Chen, J., Lee, H.S., 2013. Soft-sediment deformation structures in Cambrian siliciclastic and carbonate storm deposits (Shandong Province, China): Differential liquefaction and fluidization triggered by storm-wave loading. *Sediment. Geol.* 288, 81-94.
- Corcoran, P.L., 2008. Ordovician paleotopography as evidenced from original dips and differential compaction of dolostone and shale unconformably overlying Precambrian basement on Manitoulin Island, Canada. *Sediment. Geol.* 207, 22–33.
- Corfu, F. and Andrews, A.J. 1986. A U–Pb age for mineralized Nipissing diabase, Gowganda, Ontario. *Can. J. Earth Sci.*, 23(1): 107-109.
- Dalrymple, R.W., 1979. Wave-induced liquefaction: a modern example from the Bay of Fundy. *Sedimentology* 26, 835-844.
- Davenport, C.A., Ringrose, P.S., 1987. Deformation of Scottish Quaternary sediment sequences by strong earthquake motions. In: Jones, M.E., Preston, R.M.F. (Eds.), *Deformation of Sediments and Sedimentary Rocks*, Geological Society Special Publication No. 29, pp. 299-314.
- Donaldson, J.A., Chiarenzelli, J.R., 2007. Disruption of mats by seismic events. In: Schieber, J., Bose, P.K., Eriksson, P.G., Banerjee, S., Sarkar, S., Altermann, W., Catuneanu, O. (Eds.), *Atlas of Microbial Mat Features Preserved within the Siliciclastic Rock Record*, *Atlases in Geoscience* 2. Elsevier, pp. 245-247.
- Dzulynski, S., Smith, A.J., 1963. Convolute lamination, its origin, preservation, and directional significance. *J. Sediment. Petrol.* 33, 3: 616-627.
- Eisbacher, G.H., 1970. Contemporaneous faulting and clastic intrusions in the Quirke Lake Group, Elliot Lake, Ontario. *Can. J. Earth Sci.* 7, 215-225.

- Eisbacher, G.H., and Bielenstein, H.U., 1969. The Flack Lake depression, Elliot Lake area, Ontario (41 J/10). Geological Survey of Canada Paper 69-1, Part B, pp.58-60.
- Eriksson, P.G., Sarkar, S., Samanta, P., Banerjee, S., Porada, H., and Catuneanu, O., 2010. Paleoenvironmental context of microbial mat-related structures in siliciclastic rocks. In: Seckbach, J., and Oren, A. (Eds.) *Microbial Mats: Modern and Ancient microorganisms in stratified systems. Cellular Origin, Life in Extreme Habitats and Astrobiology books series*, v. 14. Springer, pp.73-108.
- Figueiredo, A.G., Sanders, J.E., and Swift, D.J.P., 1982. Storm-graded layers on inner continental shelves: examples from southern Brazil and the Atlantic coast of the central United States. *Sediment. Geol.* 31, 171-190.
- Frarey, M.J., 1977. Geology of the Huronian belt between Sault Ste. Marie and Blind River, Ontario. Geological Survey of Canada Memoir 383, 87p.
- Gerdes, G., 2007. Structures left by modern microbial mats in their host sediments. In: In: Schieber, J., Bose, P.K., Eriksson, P.G., Banerjee, S., Sarkar, S., Altermann, W., Catuneanu, O. (Eds.), *Atlas of Microbial Mat Features Preserved within the Siliciclastic Rock Record, Atlases in Geoscience 2*. Elsevier, pp.5-38.
- Gerdes, G., and Klenke, T., 2003. Geologische Bedeutung ökologischer Zeiträume in biogener Schichtung (Mikrobenmatten, potentielle Stromatolithe). *Mitt. Ges. Geol. Bergbaustud. Österr* 46, 35-49.
- Gerdes, G., Krumbein, W.E., Reineck, H.-E., 1985. The depositional record of sandy, versicolored tidal flats (Mellum Island, southern North Sea). *J. Sediment. Petrol.* 55, 265–278.
- Giblin, P.E., Leahy, E.J., Robertson, J.A., 1979. Sault Ste. Marie-Elliot Lake, Ontario Geological Society Map 2419. Geological Compilation Series.
- Greb, S.F., Archer, A.W., 2007. Soft-sediment deformation produced by tides in a meizoseismic area, Turnagain Arm, Alaska. *Geology* 35, 5: 435-438.
- Harazim, D., Callow, R.H.T., Mcilroy, D., 2013. Microbial mats implicated in the generation of intrastratal shrinkage ('synaeresis') cracks. *Sedimentology* 60, 1621–1638.
- Hill, C., Corcoran, P.L., Aranha, R., and Longstaffe, F.J. 2016. Microbially induced sedimentary structures in the Paleoproterozoic, upper Huronian Supergroup, Canada. *Precambrian Res.* 281, 155-165.
- Hoffman, P.F., 2013. The Great oxidation and a Siderian snowball Earth: MIF-S based correlation of Paleoproterozoic glacial epochs. *Chem. Geol.* 362, 143–156.

- Hofmann, H.J., Pearson, D.A.B., Wilson, B.H., 1980. Stromatolites and fenestral fabric in early Proterozoic Huronian Supergroup, Ontario. *Can. J. Earth Sci.* 17 (10), 1351–1357.
- Hongshui, T., Zhang, Z., Zhang, B., Zhu, J., Sang, Z., Li, H., 2013. Tectonic taphrogenesis and paleoseismic records from the Yishu Fault Zone in the initial stage of the Caledonian movement. *Acta Geol. Sin.-Eng.* 87, 4: 936-947.
- Jackson, S.L., 1994. Geology of the Aberdeen area. Ontario Geological Survey, Open File Report 5903, 69p.
- Jackson, S.L., 2001. On the Structural Geology of the Southern Province between Sault Ste. Marie and Espanola, Ontario. Ontario Geological Survey, Open File Report 5995, 55p.
- Kerr, M., Eyles, N., 1991. Storm-deposited sandstones (tempestites) and related ichnofossils of the Late Ordovician Georgian Bay Formation, southern Ontario, Canada. *Can. J. Earth Sci.* 28, 266-282.
- Ketchum, K.Y., Heaman, L.M., Bennett, G., Hughes, D.J., 2013. Age, petrogenesis and tectonic setting of the Thessalon volcanic rocks, Huronian Supergroup, Canada. *Precambrian Res.*, 233: 144–172.
- Krogh, T.E., Davis, D.W., Corfu, F., 1984. Precise U–Pb zircon and baddeleyite ages for the Sudbury Structure. In: Pye, E.G., Naldrett, A.J., Giblin, P.E. (Eds.), *Geology and Ore Deposits of the Sudbury Structure*, Ontario Geological Survey, Special Volume, pp. 431–446.
- Le Ber, E., Le Heron, D.P., Oxtoby, N.H., 2015. Influence of microbial framework on Cryogenian microbial facies, Rasthof Formation, Namibia. In: Bosence, D.W.J., Gibbons, K.A., Le Heron, D.P., Morgan, W.A., Pritchard, T., Vining, B.A. (Eds.) *Microbial Carbonates in Space and Time: Implications for Global Exploration and Production*. Geological Society, London, Special Publication 418, pp. 111-122.
- Long, D.G.F., 1978. Depositional environments of a thick Proterozoic sandstone, the (Huronian) Mississagi Formation of Ontario, Canada. *Can. J. Earth Sci.* 15, 190–206.
- Long, D.G.F., 2004. The tectonostratigraphic evolution of the Huronian basement and subsequent basin fill: geological constraints on impact models of the Sudbury event. *Precambrian Res.* 129, 203–223.
- Long, D.G.F., 2009. The Huronian Supergroup. In: Rousell, D.H., Brown, G.H. (Eds.), *A Field Guide to the Geology of Sudbury, Ontario*: Ontario Geological Survey Open File Report 6243, pp. 14–30.

- McDowell, J.P., 1957. The sedimentary petrology of the Mississagi quartzite in the Blind River area. Ontario Department of Mines, Geological Circular 6, p. 31.
- Maltman, A., 1994. Introduction and overview. In: Maltman, A. (Ed.), *The Geological Deformation of Sediments*. Chapman and Hall, pp. 1-35.
- Martín-Chivelet, J., Palma, R.M., López-Gómez, J., Kietzmann, D.A., 2011. Earthquake-induced soft-sediment deformation structures in Upper Jurassic open-marine microbialites (Neuquén Basin, Argentina). *Sediment. Geol.* 235, 3-4: 210-221.
- Matsumoto, D., Naruse, H., Fujino, S., Surphawajruksakul, A., Jarupongsakul, T., Sakakura, N., and Murayama, M., 2008. Truncated flame structures within a deposit of the Indian Ocean tsunami: evidence of syn-sedimentary deformation. *Sedimentology* 55, 1559-1570.
- Menon, L.R., McIlroy, D., Liu, A.G., Brasier, M.D., 2016. The dynamic influence of microbial mats on sediments: fluid escape and pseudofossil formation in the Ediacaran Longmyndian Supergroup, UK. *J. Geol. Soc. London* 173, 177-185.
- Meshram, D.C., Sangode, S.J., Gujar, A.R., Ambre, N.V., Dhongle, D., and Porate, S., 2011. Occurrence of soft sediment deformation at Dive Agar beach, west coast of India: possible record of the Indian Ocean tsunami (2004). *Nat. Hazards* 57, 385-393.
- Molina, J.M., Alfaro, P., Moretti, M., Soria, J.M., 1998. Soft-sediment deformation structures induced by cyclic stress of storm waves in tempestites (Miocene, Guadalquivir Basin, Spain). *Terra Nova* 10, 145-150.
- Moretti, M., Sabato, L., 2007. Recognition of trigger mechanisms for soft-sediment deformation in the Pleistocene lacustrine deposits of the Sant' Arcangelo Basin (Southern Italy): Seismic shock vs. overloading. *Sediment. Geol.* 196, 31-45.
- Moretti, M., Soria, J.M., Alfaro, P., Walsh, N., 2001. Asymmetrical soft-sediment deformation structures triggered by rapid sedimentation in turbiditic deposits (Late Miocene, Guadix Basin, Southern Spain). *Facies* 44, 283-294.
- Morton, R.A., Gelfenbaum, G., and Jaffe, B.E., 2007. Physical criteria for distinguishing sandy tsunami and storm deposits using modern examples. *Sediment. Geol.* 200, 184-207.
- Nehyba, S. 2014. Soft-sediment deformation structures in Lower Badenian (Middle Miocene) foreshore sands and their trigger mechanism (Carpathian foredeep basin, Czech Republic). *Austrian J. Earth Sci.* 107, 2: 23-36.
- Noffke, N., 2010. Chapter 3: Classification. In: Noffke, N. (Ed.) *Geobiology: Microbial mats in sandy deposits from the Arhcean Era to today*. Springer-Verlag, Berlin, pp.76-140.

- Noffke, N., Beukes, N., Bower, D., Hazen, R.M., and Swift, D.J.P., 2008. An actualistic perspective into Archean worlds – (cyano-)bacterially induced sedimentary structures in the siliciclastic Nhlazatse Section, 2. Ga Pongola Supergroup, South Africa. *Geobiology* 6, 5-20.
- Nogueira, A.C.R., Riccomini, C., Sial, A.N., Moura, C.A.V., Fairchild, T.R., 2003. Soft-sediment deformation at the base of the Neoproterozoic Puga cap carbonate (southwestern Amazon craton, Brazil): Confirmation of rapid icehouse to greenhouse transition in snowball Earth. *Geology* 31, 7:613-616.
- Obermeier, S.F., 1996. Use of liquefaction-induced features for paleoseismic analysis - an overview of how seismic liquefaction features can be distinguished from other features and how their regional distribution and properties of source sediment can be used to infer the location and strength of Holocene paleo-earthquakes. *Eng. Geol.* 44, 1-76.
- Oliveira, C.M., Hodgson, D.M., Flint, S.S., 2009. Aseismic controls on in situ soft-sediment deformation processes and products in submarine slope deposits of the Karoo Basin, South Africa. *Sedimentology* 56, 1201-1225.
- Owen, G., 1987. Deformation processes in unconsolidated sands. In: Jones, M.E., and Preston, R.M.F. (Eds.), *Deformation of Sediments and Sedimentary Rocks*, Geological Society Special Publication No. 29, pp. 11-24.
- Owen, G., 2003. Load structures: gravity-driven sediment mobilization in the shallow subsurface. In: Van Rensbergen, P., Hillis, R.R., Maltman, A.J. and Morley, C.K., (Eds.), *Subsurface sediment mobilization*. Geological Society, London, Special Publications 216, 21-34.
- Owen, G., Moretti, M., 2011. Identifying triggers for liquefaction-induced soft-sediment deformation in sands. *Sediment. Geol.* 235, 141-147.
- Peredery, W.V., 1991. Geology and ore deposits of the Sudbury Structure, Ontario (Field Trip 7). Geological Survey of Canada Open File Report 2162, p.38.
- Põldsaar, K., Ainsaar, L., 2015. Soft-sediment deformation structures in the Cambrian (Series 2) tidal deposits (NW Estonia): Implications for identifying endogenic triggering mechanisms in ancient sedimentary record. *Palaeoworld* 24, 16-35.
- Postma, G., 1983. Water escape structures in the context of a depositional model of a mass flow dominated conglomeratic fan-delta (Abrioja Formation, Pliocene, Almeria Basin, SE Spain). *Sedimentology* 30, 91-103.
- Pratt, B.R., 1994. Seismites in the Mesoproterozoic Altyn Formation (Belt Supergroup), Montana: a test for tectonic control of peritidal carbonate cyclicity. *Geology* 22, 1091-1094.

- Ramsay, B., and Fralick, P., 2017. Sedimentology and geochemistry of the 2310 Ma Kona Dolomite, Huronian Supergroup, northwestern Ontario and western upper peninsula of Michigan. 63rd Institute on Lake Superior Geology Proceedings, v. 63, Part 1, Program and Abstracts, p. 73-74.
- Rasmussen, B., Bekker, A., Fletcher, I.R., 2013. Correlation of Paleoproterozoic glaciations based on U–Pb zircon ages for tuff beds in the Transvaal and Huronian Supergroups. *Earth Planet. Sci. Lett.* 382, 173–180.
- Rice, R.J., 1986. Regional sedimentation in the Lorrain Formation (Aphebian), central Cobalt Embayment. In: *Summary of Field Work and Other Activities: Ontario Geological Survey, Miscellaneous Paper 137*, 210–216.
- Robertson, J.A., 1976. The Blind River uranium deposits: the ores and their setting. Ontario Division of Mines, *Miscellaneous Paper 65*, 45p.
- Robertson, J.A., 1986. Huronian geology and the Blind River (Elliot Lake) uranium deposits, the Pronto Mine. *Uranium Deposits of Canada, Canadian Institute of Mining and Metallurgy, Special Paper 33*, 43–46.
- Robertson, J.A., Card, K.D., 1988. *Geology and Scenery: North shore of Lake Huron Region. Ontario Geological Survey, Geological Guidebook*, p. 4.
- Roscoe, S.M., 1957. Stratigraphy, Quirke Lake–Elliot Lake Senior, Blind River area, Ontario. *Royal Society of Canada Special Publication Number 6*, pp. 54–58.
- Roscoe, S.M., 1969. Huronian rocks and uraniferous conglomerates. *Geological Survey of Canada Paper*, 68-40.
- Rousell, D.H., Card, K.D., 2009. Sudbury area geology and mineral deposits. In: Rousell, D.H., Brown, G.H. (Eds.), *A Field Guide to the Geology of Sudbury, Ontario, Ontario Geological Survey Open File Report 6243*, pp. 1–6.
- Roy, S.K., Banerjee, S., 2016. Soft sediment deformation structures in the Andaman Flysch Group, Andaman Basin: evidence for Palaeogene seismic activity in the Island Arc. *Berita Sedimentol.* 35, 55-64.
- Rust, B.R., Shields, M.J., 1987. The sedimentology and depositional environments of the Huronian Bar River Formation, Ontario, Grant 189, Geoscience Research Grant Program. Ontario Geological Survey, *Open File Report 5672*, 52p.
- Sarkar, S., Choudhuri, A., Banerjee, S., van Loon, A.J., Bose, P.K., 2014. Seismic and non-seismic soft-sediment deformation structures in the Proterozoic Bhandar Limestone, central India. *Geologos* 20, 2: 89-103.
- Schieber, J., 1986. The possible role of benthic microbial mats during the formation of carbonaceous shales in shallow Proterozoic basins. *Sedimentology* 33, 521-536.

- Schieber, J., 2004. Microbial mats in the siliciclastic rock record: a summary of diagnostic features. In: Eriksson, P.G., Altermann, W., Nelson, D., Mueller, W.U., Catuneanu, O., Strand, K. (Eds.), *The Precambrian Earth: Tempos and Events, Development in Precambrian Geology*, Elsevier, p. 663-672.
- Schieber, J., 2007. Microbial mats on muddy substrates – examples of possible sedimentary features and underlying processes. In: Schieber, J., Bose, P.K., Eriksson, P.G., Banerjee, S., Sarkar, S., Altermann, W., Catuneanu, O. (Eds.), *Atlas of Microbial Mat Features Preserved within the Siliciclastic Rock Record, Atlases in Geoscience 2*. Elsevier, pp. 117–134.
- Seed, H.B., and Lee, K.L., 1966. Liquefaction of saturated sands during cyclic loading. *J. Soil. Mech. Found. Div., PASCE* 92:6, 105-134.
- Seed, H.B., and Rahman, M.S., 1978. Wave-induced pore pressure in relation to ocean floor stability of cohesionless soils. *Mar. Geotechnol.* 3:2, 123-150.
- Shanmugam, G., 2016. The seismite problem. *J. Palaeogeogr.* 5(4), 318-362.
- Stárková, M., Martínek, K., Mikuláš, R., 2015. Types of soft-sediment deformation structures in a lacustrine Ploužnice member (Stephanian, Gzhelian, Pennsylvanian, Bohemian Massif), their timing, and possible trigger mechanism. *Int. J. Earth Sci.* 104, 1277-1298.
- Takashimizu, Y., and Masuda, F., 2000. Depositional facies and sedimentary successions of earthquake-induced tsunami deposits in Upper Pleistocene incised valley fills, central Japan. *Sediment. Geol.* 135, 231-239.
- van Loon, A.J., 2009. Soft-sediment deformation structures in siliciclastic sediments: an overview. *Geologos* 15, 1: 3-55.
- van Loon, A.J., Dechen, S., 2013. Deformed stromatolites in marbles of the Mesoproterozoic Wumishan Formation as evidence for synsedimentary seismic activity. *J. Palaeogeogr.* 2, 4: 390-401.
- Wood, J., 1973. Stratigraphy and depositional environments of upper Huronian rocks of the Rawhide Lake-Flack Lake area, Ontario. In: *The Geological Association of Canada Special Paper Number 12*, pp. 73–95.
- Young, G.M., 1968. Sedimentary structures in Huronian rocks of Ontario. *Palaeogeogr. Palaeoclimatol. Palaeoecol.* 4, 125-153.
- Young, G.M., 1983. Tectono-sedimentary history of early Proterozoic rocks of the northern Great Lakes Region. *Geological Society of America Memoirs* 160, 15-32.
- Young, G.M., 2014. Contradictory correlations of Paleoproterozoic glacial deposits: local, regional or global controls? *Precambrian Res.* 247, 33–44.

- Young, G.M., Nesbitt, H.W., 1985. The lower Gowganda Formation in the southern part of the Huronian outcrop belt, Ontario, Canada: stratigraphy, depositional environments and tectonic setting. *Precambrian Res.* 29, 265–301.
- Young, G.M., Long, D.G.F., Fedo, C.M., Nesbitt, H.W., 2001. Proterozoic Huronian basin: product of a Wilson cycle punctuated by glaciations and a meteorite impact. *Sediment. Geol.* 141–142, 233–254.
- Zhou, L., McKenna, C.A., Long, D.G.F., Kamber, B.S., 2017. LA-ICP-MS elemental mapping of pyrite: An application to the Palaeoproterozoic atmosphere. *Precambrian Res.* 297, 33-55.
- Zolnai, A.I., Price, R.A., Helmstaedt, H., 1984. Regional cross section of the Southern Province adjacent to Lake Huron, Ontario: implications for the tectonic significance of the Murray Fault Zone. *Can. J. Earth Sci.* 21, 447-456.

Chapter 5

5 New U-Pb geochronology evidence for 2.3 Ga detrital zircon grains in the youngest Huronian Supergroup formations, Canada

5.1 Introduction

The Huronian Supergroup is a thick, well-exposed record of the Paleoproterozoic (Figure 5.1) and has been studied extensively throughout the past century (see summary in Young et al., 2001). The succession records minor initial volcanism and extensive clastic sediment deposition over a span of approximately 230 m.y. based on reported U-Pb ages of ~2.45 Ga from basal volcanic rocks (e.g. Krogh et al., 1984; Ketchum et al., 2013) and ~2.22 Ga from gabbro intrusions that cut the entire succession (e.g. Corfu and Andrews, 1986; Noble and Lightfoot, 1992). Direct dating of the rocks of the Huronian Supergroup is difficult due to a lack of intercalated volcanic rocks in the section (Figure 5.1b).

Krogh et al. (1984) were the first to conduct U-Pb dating of zircon grains from the Copper Cliff Formation rhyolite at the base of the Huronian Supergroup (Figure 5.1b), for which they determined an U-Pb age of $2450 \pm 25/-10$ Ma. Several additional U-Pb analyses of zircon, baddeleyite and titanite from lower intrusive rocks interpreted to be cogenetic with the volcanic rocks of the Huronian Supergroup, the Thessalon Formation, and of zircon from the Copper Cliff Formation have since been dated (Table 5.1). A minimum U-Pb age of ca. 2.22 Ga is often cited, based on baddeleyite and rutile in the Nipissing gabbro, as determined by Corfu and Andrews (1986; $2219.4 \pm 3.6/-3.5$ Ma), and others (Table 5.1). Rasmussen et al. (2013) analyzed zircon from tuff beds in the Gordon Lake Formation, which produced U-Pb ages of 2308 ± 8 Ma, 2308 ± 10 Ma, and 2311 ± 11 Ma. No other workers, however, have identified tuff beds in the Gordon Lake Formation. The intent of this short research communication is to present new detrital zircon U-Pb ages for sedimentary samples from the Gordon Lake and Bar River formations in the Flack Lake area, Ontario, in order to contribute to the understanding of the depositional history of the upper Huronian Supergroup and its maximum depositional age. The Gordon Lake Formation is composed primarily of mudstone, siltstone and fine-

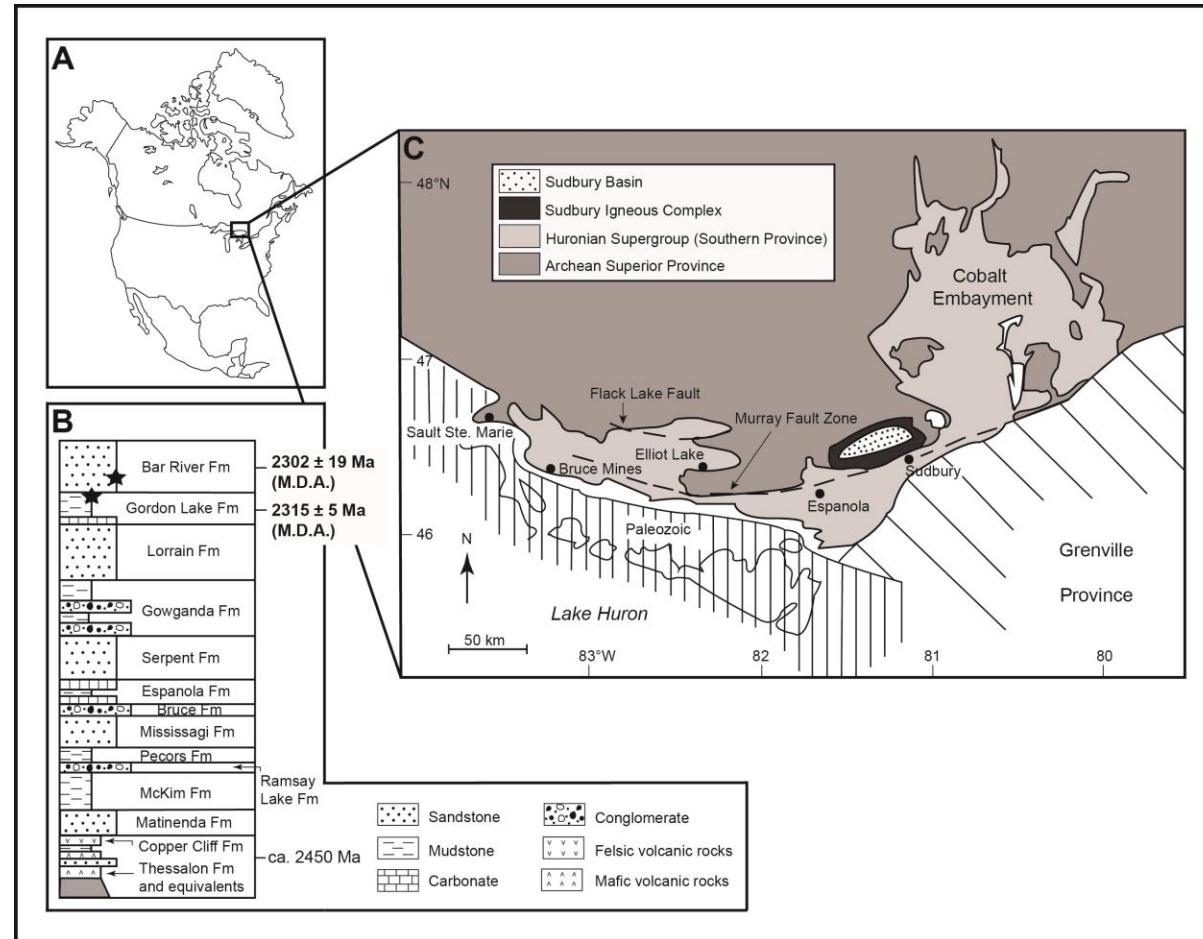


Figure 5.1. Distribution and stratigraphy of the Huronian Supergroup north of Lake Huron. A) Location of study area in Ontario, Canada. B) General stratigraphy of the Huronian Supergroup. Location of samples shown with black stars. Maximum depositional ages (M.D.A.) from this study are shown in bold. Lower age from Krogh et al. (1984) and Ketchum et al. (2013). C) Simplified geologic map of the distribution of the Huronian Supergroup, modified from Young et al. (2001). Gordon Lake Formation sample collected at 46°36'17.1"N 82°46'13.2"W and Bar River Formation sample collected at 46°35'52.7"N 82°45'33.7"W.

Table 5.1. Summary of reported upper and lower age limits for the Huronian Supergroup.

	Formation/Unit	U-Pb age	Reference
Lower age limit	Gabbro-anorthosite intrusion (East Bull Lake)	2472.2 ± 0.8 Ma	Clough and Hamilton, 2017
	Gabbro-anorthosite-syenite intrusion (East Bull Lake)	2475.1 ± 1.2 Ma	Heaman, 2007
	Granophyre intrusion (Agnew Lake)	2491 ± 5 Ma	Krogh et al., 1984
	River Valley pluton	2475 +2/-1 Ma	Easton et al., 1999
	Hearst dikes	2445.8 +2.9/-2.6 Ma	Heaman, 1997
	Murray granite	2460 ± 6 Ma	Bleeker et al., 2015
	Opx–hornblendite (GFTZ*)	2468 ± 5 Ma	Corfu and Easton, 2000
	Granitic intrusions (GFTZ)	2475 +25/-15 Ma 2460 ± 20 Ma	Corfu and Easton, 2000
	Copper Cliff Fm (rhyolite)	2450 +25/-10 Ma	Krogh et al., 1984
	Copper Cliff Fm (rhyolite)	2452.5 ± 6.2 Ma	Ketchum et al., 2013
	Copper Cliff Fm (rhyolite)	2455 ± 3 Ma	Bleeker et al., 2013
	Livingstone Creek Fm (sst**)	2497 ± 10 Ma	Rainbird and Davis, 2006; Craddock et al., 2013
	Matinenda Fm (sst)	2648.5 ± 6.3 Ma 2638.5 ± 5.2 Ma	Easton and Heaman, 2011
	Mississagi Fm (sst)	2445 ± 9 Ma 2451 ± 6 Ma	Rainbird and Davis, 2006; Craddock et al., 2013
Upper age limit	Senneterre dikes	2216 +8/-4 Ma	Buchan et al., 1998
	Nipissing gabbro	2217 ± 1.6 Ma	Andrews et al., 1986
	Nipissing gabbro	2219.4 +3.6/-3.5 Ma	Corfu and Andrews, 1986
	Nipissing gabbro	2217.8 +6/-3 Ma	Buchan et al., 1994
	Nipissing gabbro	2215 ± 1 Ma	Bleeker et al., 2015
	Nipissing gabbro suite (Kerns and Triangle Mtn intrusions)	2217.2 ± 4 Ma 2209.6 ± 3.5 Ma	Noble and Lightfoot, 1992
	Gordon Lake Fm (tuff)	2308 ± 8 Ma 2308 ± 10 Ma 2311 ± 11 Ma	Rasmussen et al., 2013
	Gordon Lake Fm (sst) Bar River Fm (claystone)	2315 ± 5 Ma 2302 ± 19 Ma	This paper This paper

*GFTZ = Grenville Front Tectonic Zone; **sst = sandstone

grained sandstone, with minor intraformational conglomerate. Based on sedimentary structures, such as interference ripples and microbially induced sedimentary structures (MISS), the Gordon Lake Formation was deposited in a tidally influenced depositional setting (Hill et al., 2016; Hill and Corcoran, 2018). The overlying Bar River Formation is a 900 m thick quartz arenite succession that contains evidence of marine and tidal influence, such as herringbone cross-stratification, and is interpreted to have been deposited in a tidal channel or sand shoal setting (Aranha, 2015). Chandler (1986; 1988) suggested a coastal sabkha setting for the Gordon Lake Formation from evaporite nodules at the base of the formation, a view supported by Wood (1973). Wood (1973) also used hematite oolites and abundant, often bimodal cross-bedding to advance a tidal flat and beach origin for the Gordon Lake and Bar River formations, respectively.

5.2 Methods

Uranium-lead age data were determined from detrital zircon in sandstone sample CH-14-50 collected from the Gordon Lake Formation and claystone sample RA-14-79 collected from the Bar River Formation, in the Flack Lake area. Sample preparation and analyses were conducted at the Jack Satterly Geochronology Laboratory, University of Toronto. Samples were crushed using a jaw crusher followed by a disk mill. Initial separation of heavy minerals was carried out with a Wilfley table. This was followed by paramagnetic separations with the Frantz isodynamic separator and density separations using bromoform and methylene iodide. Final sample selection for geochronology was by hand picking under a microscope, choosing the freshest, least cracked zircon grains.

Grains were mounted on double sided tape and ablated on natural (unpolished) surfaces using a New Wave 213 nm laser with diameters of 12-25 microns at 5 Hz and 5 J/cm² fluence. Data were collected on 88Sr (10 ms), 206Pb (30 ms), 207Pb (70 ms), 232Th (10 ms) and 238U (20 ms) using a VG Series 2 Plasmaquad ICPMS. Sensitivity was enhanced by the use of a 75 l/sec rotary pump (S-option) connected to the expansion chamber. Immediately prior to each analysis, the spot was pre-ablated over a larger area than the beam diameter for about 10 seconds to clean the surface and remove any surface alteration. Following a 10 second period of baseline accumulation, the laser sampling beam was turned on and data were collected for 35 seconds followed by a 50 second

washout period. About 150 measurement cycles per sample were produced and ablation pits were about 15 microns deep. In some cases, data profiles show rapidly varying emission due to chemical zoning of zircon. Instability was dampened through the use of a 75 ml mixing chamber in-line with the He flow transporting the ablated sample to the plasma. Data were edited and reduced using custom VBA software (UTILLAZ program) written by D.W. Davis. $^{206}\text{Pb}/^{238}\text{U}$ ratios show only slight fractionation caused by hole depth through the run and most of the $^{207}\text{Pb}/^{206}\text{Pb}$ and $^{206}\text{Pb}/^{238}\text{U}$ data can be averaged. No corrections were made for common Pb, because this peak was too small to be measured precisely. Common Pb should be negligible in fresh zircon, but would have the effect of pushing data to the right away from the concordia curve, if present. It is therefore insignificant for concordant data. ^{88}Sr was monitored from zircon in order to detect intersection of the beam with zones of alteration or inclusions, or penetration of the beam through the sample. Pb-U data were rejected from areas with excess ^{88}Sr signal. The Th/U ratio of zircon can be a useful petrogenetic indicator and was also measured, although it is only a rough estimate because the ratio is not constant in the standard. Zircon from sample DD91-1, a monzodiorite from the Pontiac province of Quebec dated at 2682 ± 1 Ma (Davis, 2002) was used as a standard. Sets of 3 sample measurements are bracketed by measurements on standards.

Backscattered electron (BSE) and cathodoluminescence (CL) imaging were carried out on the zircon grains. The images are available in Appendix C; BSE images are on the left and CL images on the right for sample CH-14-50. Zircons in sample RA-14-79 were imaged in BSE and the first group was also imaged in CL.

5.3 Results

5.3.1 CH-14-50 Sandstone, Gordon Lake Formation

CH-14-50 is a fine- to medium-grained, pink sandstone that yielded moderately abundant zircon. All grains are rounded or subrounded and most are stubby (Figures 5.2b and 5.3a). A subpopulation of long prismatic grains was also mounted and analyzed (Figures 5.2c and 5.3a). U-Pb analyses of 75 grains were all concordant or near-concordant.

Concordia data for zircon are plotted in Figure 5.3b using the Isoplot program of Ludwig (1998, 2003). The majority of ages (75%) are late Archean and many of these cluster within error with an average age of 2689 ± 6 Ma (Figure 5.3b). Many of the long prismatic grains are Paleoproterozoic and the 14 youngest $^{207}\text{Pb}/^{206}\text{Pb}$ ages are considered to comprise a single population with an average age of 2315 ± 10 Ma (MSWD – 0.9). The U-Pb age data for detrital zircons from the Gordon Lake and Bar River formations is presented in the supplementary material in Appendix D.

5.3.2 RA-14-79 Claystone, Bar River Formation

Sample RA-14-79 is composed of green claystone with very fine-grained, quartz-rich lenses. The sample yielded only a small amount of zircon, consisting mostly of small, rounded, stubby grains with a few long prisms (Figures 5.2a and 5.4a). U-Pb analyses of 27 grains are all concordant or near-concordant (Figure 5.4b), clustering into three or four groups. The four youngest grains yield data that overlap, giving an average $^{207}\text{Pb}/^{206}\text{Pb}$ age of 2302 ± 19 Ma (MSWD – 0.7). A slightly older group also clusters within error with an average age of 2364 ± 16 Ma (5 data, MSWD – 0.5). It is difficult to know whether these ages correspond to distinct units that formed significant components of provenance, but the youngest agrees with the youngest age cluster from the Gordon Lake Formation sample. Three of the long prisms are in the youngest age group. An intermediate aged cluster of 6 grains gives an average age of 2525 ± 15 Ma. Detrital grains with ages around 2500 Ma are also present in sample CH-14-50 (Figure 5.3b). Several analyses give late-Archean ages whereas the oldest, which is somewhat discordant, gives a $^{207}\text{Pb}/^{206}\text{Pb}$ age of 3158 Ma.

5.4 Discussion and Conclusion

Detrital zircon ages from samples of the Gordon Lake and Bar River formations, upper Huronian Supergroup, yield late Archean ages (61%), but also a significant contribution from source rocks that formed at ca. 2500 Ma and ca. 2300 Ma (Figure 5.5). The proportion of post-Archean material is greater in the Bar River Formation (RA-14-79) sample than in the Gordon Lake Formation (CH-14-50) sample, which may be a result of

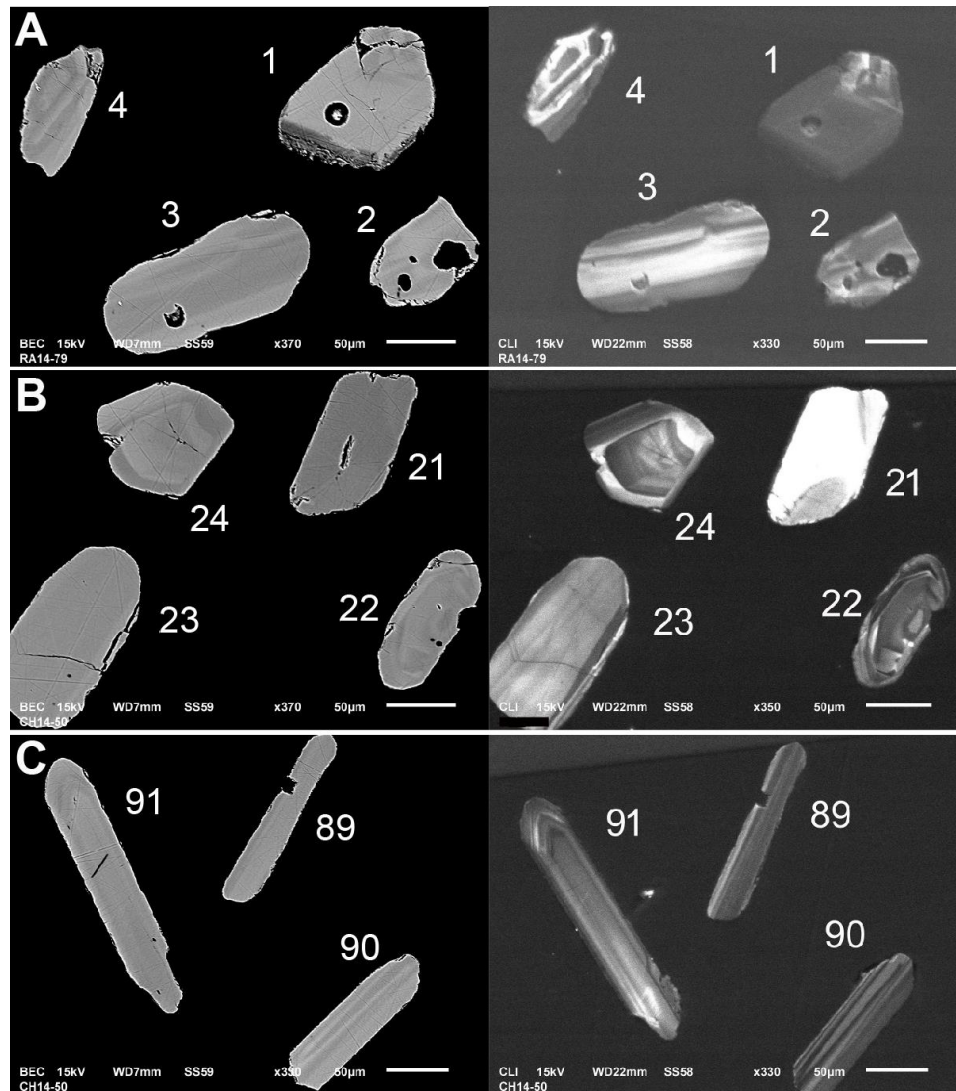


Figure 5.2. Backscattered electron (left) and cathodoluminescence (right) images of representative zircon grains from the different age populations in the Gordon Lake and Bar River formations. A) Four zircons from the Bar River Formation. Grains 1, 2 and 4 have an age of ca. 2300 Ma and grain 3 has an age of ca. 2700. B) Four zircons from the Gordon Lake Formation. Grains 21 and 22 have an age of ca. 2700 Ma and grains 23 and 24 have an age of ca. 2500 Ma. C) Three long prismatic zircons from the Gordon Lake Formation with an age of ca. 2300 Ma.

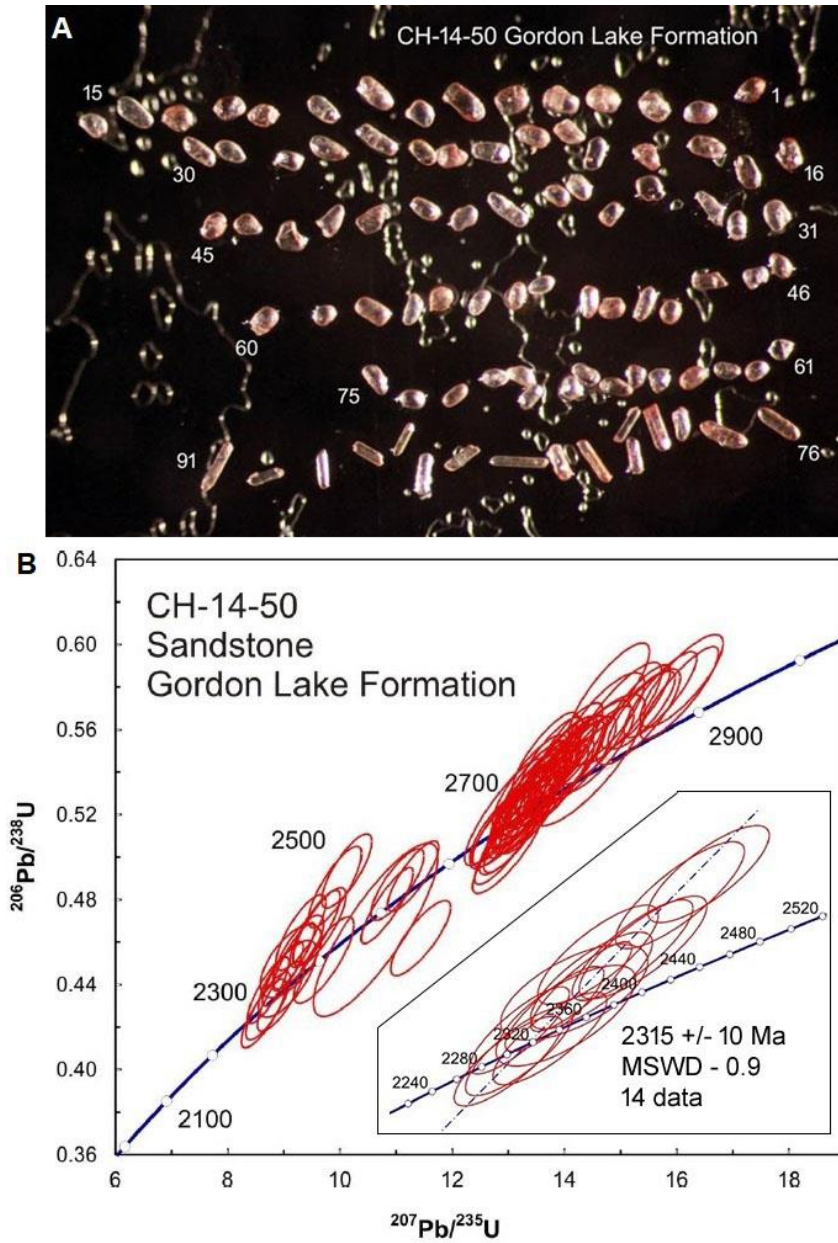


Figure 5.3. U-Pb data from the Gordon Lake Formation. A) 91 zircon grains, 75 of which were used for radiometric dating. B) U-Pb concordia plot showing data on 75 detrital zircons from quartz-rich sandstone sample CH-14-50 in the Gordon Lake Formation. The inset shows the youngest data.

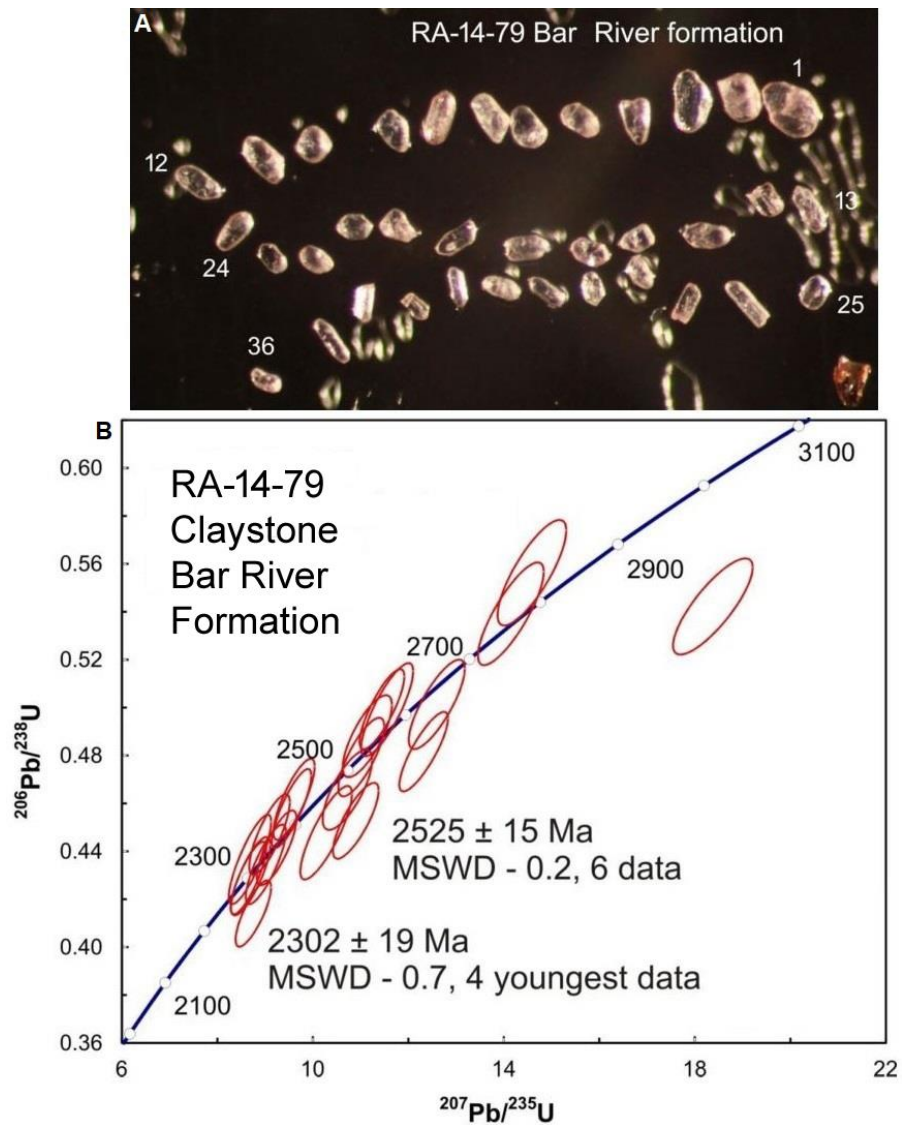


Figure 5.4. U-Pb data from the Bar River Formation. A) 36 zircon grains, 27 of which were used for radiometric dating. B) U-Pb concordia plot showing data on the detrital zircons from sample BR-14-79 in the Bar River Formation.

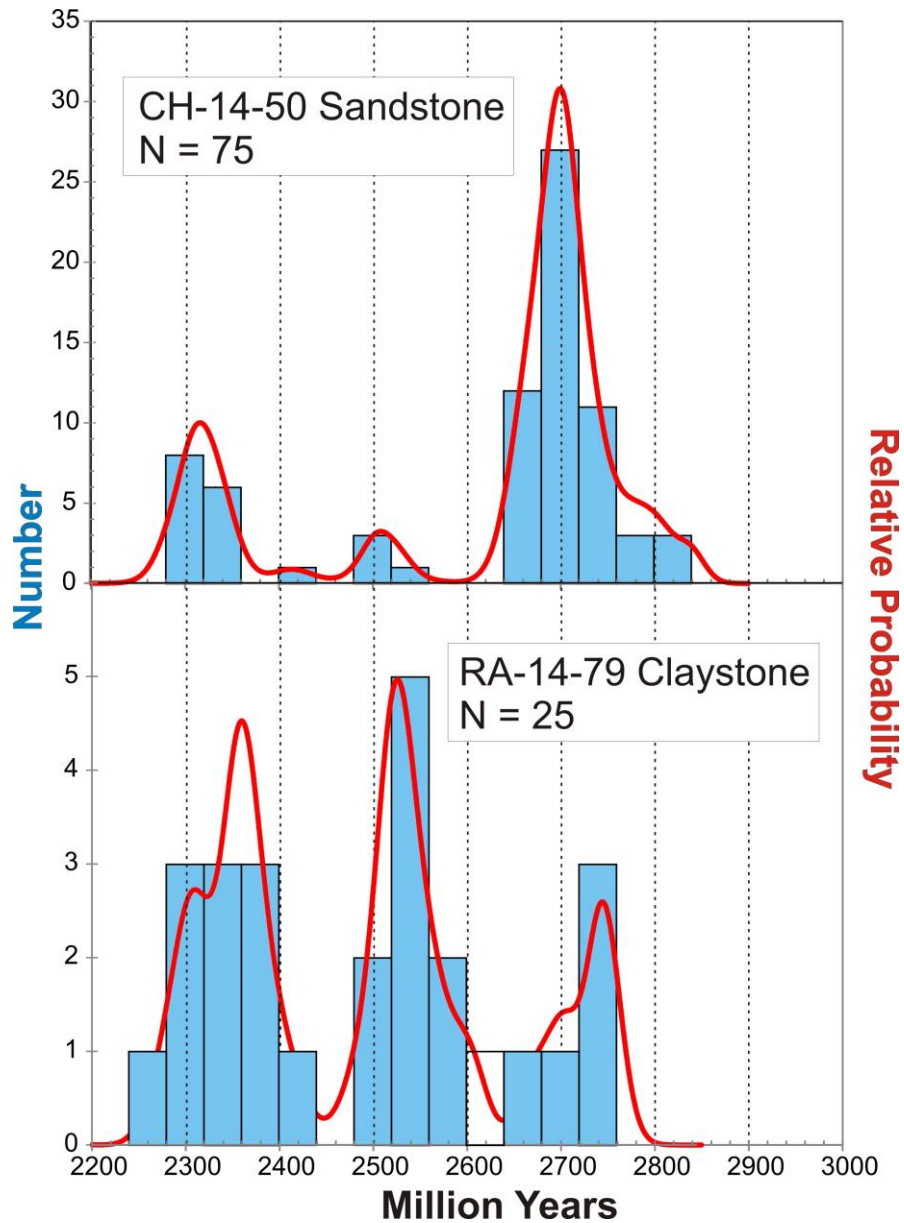


Figure 5.5. Age probability density diagrams with superimposed histograms for $^{207}\text{Pb}/^{206}\text{Pb}$ ages on detrital zircon grains from sample CH-14-50 of the Gordon Lake Formation (top), and sample BR-14-79 of the Bar River Formation (bottom), Huronian Supergroup.

the grain size of the sample and dilution of coarser-grained material. The best constrained age on the youngest detrital grains puts a time limit on deposition of the upper part of the Huronian Supergroup between 2315 ± 5 Ma and intrusion of the Nipissing gabbro at about 2220 Ma (Corfu and Andrews, 1986).

The youngest ages determined for the Gordon Lake Formation sample (CH-14-50) coincide with those determined by Rasmussen et al. (2013) (2311 ± 11 Ma and 2308 ± 10 Ma). Both the samples analyzed by Rasmussen et al. (2013) and CH-14-50 were collected from the Flack Lake area, but the exact coordinates of samples HU372, GLF-FL, FL-GLF and JT98/4 from Rasmussen et al. (2013) are unknown (coordinates for our study can be found in Figure 5.1 caption). The authors collected samples from purported tuff beds in the Gordon Lake Formation and interpret that the main age peak of ca. 2310 Ma represents the timing of felsic volcanism. We were unable to identify tuff beds in the Gordon Lake Formation in the Flack Lake area. The zircons in CH-14-50 are rounded, however some of the long and prismatic grains that cluster around 2315 ± 5 Ma are more euhedral, which may represent a volcanic component, but this is impossible to prove. In general, the high energy nature of the Gordon Lake and Bar River formations decreases the likelihood of preserving a tuff. Rasmussen et al. (2013) interpret zircons younger than 2310 Ma to have undergone post-depositional resetting, however the zircon grains that are also older than Nipissing gabbro (2220 Ma) may represent the youngest detrital grains in the rock, as opposed to being metamorphosed.

Rainbird and Davis (2006) dated detrital zircon grains from sandstone samples throughout the Huronian succession. The authors' age probability density diagram for $^{207}\text{Pb}/^{206}\text{Pb}$ ages from the Bar River Formation differs significantly from our diagram for the Bar River Formation claystone (cf. Rainbird and Davis, 2006). This may be due to sample collection in different parts of the basin. A large cluster is present at ca. 2700 Ma, which is more aligned with our data from the Gordon Lake Formation. Vallini et al. (2006) determined an age of 2317 ± 6 Ma for the youngest detrital zircon populations in the glaciogenic Enchantment Lake Formation of the Chocoyay Group, Marquette Range Supergroup. The stratigraphically higher Sturgeon Quartzite has a maximum depositional age of 2306 ± 9 Ma (Vallini et al., 2006). The Sunday Quartzite, which is equivalent to

the Sturgeon Quartzite, is correlative to the Lorrain Formation of the Huronian Supergroup. Overall, these data generally agree with our maximum depositional age for the Gordon Lake Formation.

The data reveal that the zircon grains in this study were derived from at least three sources. Potential sources include significant contribution from Archean basement rocks of the Superior Province, in addition to two younger sources with ages of ca. 2500 and 2300 Ma. The lowermost volcanic units of the Huronian Supergroup and associated intrusions may have provided the ca. 2500 Ma zircons. The source of the ca. 2300 Ma zircons is more problematic as there are few known sources of zircons that age in the Superior Province. An age of 2376.3 ± 2.3 Ma was determined for the younger of two phases of the Creighton granite (Smith, 2002), which is found in the Sudbury region, approximately 120 km east of the study area. However, it may be inferred from the presence of the ca. 2300 Ma long, prismatic zircons in the Gordon Lake Formation sample that these grains were locally derived from volcanic material and not heavily reworked. In addition, oscillatory zoning present in several long prismatic zircons supports a magmatic interpretation (Figure 5.2c). Vallini et al. (2006) obtained similar results from the Chocoy Group in Michigan and suggest that sequences of ca. 2300 Ma sedimentary-volcanic material may have existed at the time of deposition and are now largely removed; a portion of this material is preserved as detrital zircon grains in the lower units of the Chocoy Group. The authors infer that the ca. 2300 Ma source was restricted to the eastern side of the basin, which places it closer to the Huronian basin. Several of the analyzed zircon grains from the Bar River and Gordon Lake formations also display crosscutting of original zoning obtained during erosion, suggesting a polycyclic history for several zircons. Other internal structures of the analyzed zircon grains include sector and weak zoning.

5.5 References

Andrews, A.J., Masliwec, A., Morris, W.A., Owsiacki, L., and York, D., 1986. The silver deposits at Cobalt and Gowganda, Ontario. II: an experiment in age determinations employing radiometric and paleomagnetic measurements. *Can. J. Earth Sci.* 23, 1507-1518.

- Aranha, R.D.J., 2015. Factors controlling the composition and lithofacies characteristics of the Paleoproterozoic Bar River Formation, Huronian Supergroup. MSc Thesis, The University of Western Ontario. *Electronic Thesis and Dissertation Repository*. 3321.
- Bleeker, W., Kamo, S., and Ames, D., 2013. New field observations and U-Pb age data for footwall (target) rocks at Sudbury: towards a detailed cross-section through the Sudbury Structure. *Large Meteorite Impacts and Planetary Evolution V*, Geol. Soc. Am. Special Papers, 3112.
- Bleeker, W., Kamo, S.L., Ames, D.E., and Davis, D., 2015. New field observations and U-Pb ages in the Sudbury area: toward a detailed cross-section through the deformed Sudbury Structure. In: *Targeted Geoscience Initiative 4: Canadian Nickel-Copper Platinum Group Elements-Chromium Ore Systems – Fertility, Pathfinders, New and Revised Models*, Geological Survey of Canada Open File 7856, 153-166.
- Buchan, K.L., Mortensen, J.K., and Card, K.D., 1994. Integrated paleomagnetic and U-Pb geochronologic studies of mafic intrusions in the southern Canadian Shield: implications for the Early Proterozoic polar wander path. *Precambrian Res.* 69, 1-10.
- Buchan, K.L., Mortensen, J.K., and Card, K.D., and Percival, J.A., 1998. Paleomagnetism and U-Pb geochronology of diabase dyke swarms of Minto block, Superior Province, Quebec, Canada. *Can. J. Earth Sci.* 35, 1054-1069.
- Chandler, F.W., 1986. Sedimentology and paleoclimatology of the Huronian (Early Aphebian) Lorrain and Gordon Lake Formations and their bearing on models for sedimentary copper mineralization. In: *Geological Survey of Canada Paper 86-1A*, pp. 121–132.
- Chandler, F.W., 1988. Diagenesis of sabkha-related, sulphate nodules in the early Proterozoic Gordon Lake Formation, Ontario, Canada. *Carbonates Evaporites* 3, 75–94.
- Clough, C.E., and Hamilton, M.A., 2017. Matachewan LIP revisited: A revised, high-resolution U-Pb age for the East Bull Lake intrusion and associated units. In: *GAC-MAC Technical Program, T3: Archean Cratons and Their Rifted Margins: Stratigraphic Systems, Tectonics, Secular Evolution and Metallogeny (Poster)*, Kingston, ON.
- Corfu, F., and Andrews, A.J., 1986. A U–Pb age for mineralized Nipissing diabase, Gowganda, Ontario. *Can. J. of Earth Sci.* 23(1): 107-109.
- Corfu, F., and Easton, R.M., 2000. U–Pb evidence for polymetamorphic history of Huronian rocks in the Grenville Front Tectonic Zone east of Sudbury, Ontario, Canada. *Chem. Geol.* 172, 149-171.

- Craddock, J.P., Rainbird, R.H., Davis, W.J., Davidson, C., Vervoort, J.D., Konstantinou, A., Boerboom, T., Vorhies, S., Kerber, L., and Lundquist, B., 2013. Detrital zircon geochronology and provenance of the Paleoproterozoic Huron (~2.4-2.2 Ga) and Animikie (~2.2-1.8 Ga) basins, southern Superior Province. *J. Geol.* 121, 623-644.
- Davis, D.W., 2002. U-Pb geochronology of Archean metasediments in the Pontiac and Abitibi subprovinces, Quebec, constraints on timing, provenance and regional tectonics. *Precambrian Research* 115: 97-117.
- Easton, R.M., Davidson, A., and Murphy, E.I., 1999. Transects across the Southern-Grenville Province Boundary near Sudbury, Ontario. Geological Association of Canada, Sudbury '99, Guidebook #A2, 52 p.
- Easton, R.M., and Heaman, L.M., 2011. Detrital zircon geochronology of Matinenda Formation sandstones (Huronian Supergroup) at Elliot Lake, Ontario: Implications for uranium mineralization. In: *Proceedings of the 57th ILSG Annual Meeting – Part 1*, pp. 31-32.
- Heaman, L., 1997. Global mafic magmatism at 2.45 Ga: Remnants of an ancient large igneous province? *Geology* 25, 4: 299-302.
- Heaman, L., 2007. Proterozoic large igneous provinces and the latest in dating accessories. Presented at Geological Association of Canada NUNA Conference, Sudbury, ON.
- Hill, C.M., and Corcoran, P.L., 2018. Processes responsible for the development of soft-sediment deformation structures (SSDS) in the Paleoproterozoic Gordon Lake Formation, Huronian Supergroup, Canada. *Precambrian Res.* 310, 63-75.
- Hill, C., Corcoran, P.L., Aranha, R., and Longstaffe, F.J., 2016. Microbially induced sedimentary structures in the Paleoproterozoic, upper Huronian Supergroup, Canada. *Precambrian Res.* 281, 155-165.
- Ketchum, K.Y., Heaman, L.M., Bennett, G., and Hughes, D.J., 2013. Age, petrogenesis and tectonic setting of the Thessalon volcanic rocks, Huronian Supergroup, Canada. *Precambrian Res.* 233, 144–172.
- Krogh, T.E., Davis, D.W., and Corfu, F., 1984. Precise U–Pb zircon and baddeleyite ages for the Sudbury Structure. In: Pye, E.G., Naldrett, A.J., Giblin, P.E. (Eds.), *Geology and Ore Deposits of the Sudbury Structure*, Ontario Geological Survey, vol. 1, pp. 431–446.
- Ludwig, K.R., 1998. On the treatment of concordant uranium-lead ages. *Geochim. Cosmochim. Acta* 62: 665-676.
- Ludwig, K.R., 2003. User's manual for Isoplot 3.00 a geochronological toolkit for Excel. Berkeley Geochronological Center Special Publication 4, 71 p.

- Noble, S.R., and Lightfoot, P.C., 1992. U-Pb baddeleyite ages of the Kerns and Triangle Mountain intrusions, Nipissing Diabase, Ontario. *Can. J. Earth Sci* 29, 1424-1429.
- Rainbird, R.H., and Davis, W.J., 2006. Detrital zircon geochronology of the western Huronian basin. In: *Proceedings of the 52nd ILSG Annual Meeting – Part 1*, pp. 55-56.
- Rasmussen, B., Bekker, A., and Fletcher, I.R., 2013. Correlation of Paleoproterozoic glaciations based on U–Pb zircon ages for tuff beds in the Transvaal and Huronian Supergroups. *Earth Planet. Sci. Lett.* 382, 173–180.
- Smith, M.D., 2002. The timing and petrogenesis of the Creighton pluton, Ontario: an example of felsic magmatism associated with Matachewan igneous events. M.Sc. thesis, The University of Alberta, Edmonton, AB.
- Vallini, D.A., Cannon, W.F., and Shulz, K.J., 2006. Age constraints for Paleoproterozoic glaciation in the Lake Superior Region: detrital zircon and hydrothermal xenotime ages for the Chocoday Group, Marquette Range Supergroup. *Can J. Earth Sci.* 43, 571-591.
- Wood, J., 1973. Stratigraphy and depositional environments of upper Huronian rocks of the Rawhide Lake-Flack Lake area, Ontario. In: Young, G.M. (Ed.), *Huronian Stratigraphy and sedimentation*, Geological Association of Canada Special Paper Number 12, pp. 73–95.
- Young, G.M., Long, D.G.F., Fedo, C.M., and Nesbitt, H.W., 2001. Proterozoic Huronian basin: product of a Wilson cycle punctuated by glaciations and a meteorite impact. *Sediment. Geol.* 141–142, 233–254.

Chapter 6

6 Conclusions

This thesis investigated the lithostratigraphic, sedimentological, and geochronological characteristics of the Paleoproterozoic Gordon Lake Formation, Huronian Supergroup, Ontario, Canada. The main ideas presented here provide insight into the paleodepositional setting represented by the formation, and allow inferences to be made about basin tectonism. This thesis also evaluated the maximum depositional age of the Gordon Lake Formation using U-Pb detrital zircon geochronology in order to contribute to the understanding of the depositional history of the Huronian Supergroup. This chapter summarizes the results of this project and offers suggestions for future research.

6.1 Lithofacies and lithofacies associations

Four study areas were chosen for sedimentary facies analysis based on outcrop exposure, and are located near Bruce Mines, near Flack Lake, in Lady Evelyn-Smoothwater Provincial Park, and in Baie Fine and Killarney Provincial Park. Seven distinct lithofacies were identified in the four study areas: very fine- to fine-grained sandstone (LF1), fine- to medium-grained sandstone (LF2), carbonate (LF3), interlaminated to interbedded mudstone and fine-grained sandstone (LF4), coarse-grained sandstone (LF5), intraformational granular to pebbly sandstone and conglomerate (LF6a and b), and mudstone (LF7). These lithofacies were grouped into three lithofacies associations, in ascending order: subtidal nearshore (LFA1), subtidal to offshore transition (LFA2), and mixed intertidal flats (LFA3).

Lithofacies association 1 is composed of very fine- to fine-grained sandstone (LF1), fine- to medium-grained sandstone (LF2), and coarse-grained sandstone (LF5), with a minor amount of mudstone (LF7). Characteristic sedimentary structures include planar laminae, massive bedding, and planar and trough cross-bedding, with local ripples, SSDS, and synaeresis cracks. The LFA1 is interpreted to have been deposited in a subtidal nearshore environment, possibly the lower shoreface.

Lithofacies association 2 is composed of a series of distinct storm deposits, that include fining-upward intervals of intraformational granule to pebbly sandstone and conglomerate (LF6a), very fine- to fine-grained sandstone (LF1), and mudstone (LF7) or interlaminated to interbedded mudstone and fine-grained sandstone (LF4); tabular, thin to medium bedded sandstone (LF1 and LF2) and mudstone beds (LF7) that contain synaeresis cracks and HCS; stacked interlaminated to interbedded mudstone and sandstone (LF1, with minor LF4) that are characterized by SSDS of varying size and type, and normally graded beds. This lithofacies association is interpreted to have been deposited in the subtidal to offshore transition zone.

Lithofacies association 3 is composed of interlaminated to interbedded mudstone and fine-grained sandstone (LF4), alternating with fine-grained sandstone (LF1), and mudstone (LF7). Characteristic sedimentary structures include flaser and lenticular bedding, wave and interference ripples, ripple cross- and planar laminae, bipolar-opposed ripples separated by mudstone drapes, desiccation cracks and MISS. The LFA3 is interpreted to have been deposited as mixed intertidal flats.

6.2 Microbial influence on sedimentation

Fossil evidence of early life was observed in the Bruce Mines, Flack Lake, and Lady Evelyn-Smoothwater Provincial Park study areas, and include microbial mat fragments and stromatolites. A biological origin for the structures is supported by their similarities to documented examples of MISS and stromatolites in both modern and ancient successions, the sand-dominated (MISS) and calcareous-dominated (stromatolites) nature of the substrate in which they are preserved, and key microtextures identified in thin section. Microtextures include curled, frayed and layered mat chips, carbonaceous laminae, oriented grains, concentrated heavy minerals, and fenestrae. The types of MISS identified in the Gordon Lake Formation support the interpretation of an intertidal to subtidal depositional environment. Although fossil evidence of life is rare in the rocks of the Huronian Supergroup, identification of MISS in the Flack Lake area, stromatolites in Lady Evelyn-Smoothwater Provincial Park, and microbial mat fragments in the Bruce Mines area, provides a significant and convincing indication of microbial colonization at the time of deposition. Microbial mats increased the cohesion, and therefore preservation

potential, of sedimentary structures in the Gordon Lake Formation, and may have been partially responsible for the preservation of the large quantity of fine-grained sediment.

6.3 Other influences on sedimentation

A significant quantity of interpreted tide- and storm-generated sedimentary structures and deposits are present in the Gordon Lake Formation. These were observed in all four study areas; tide-generated deposits are preserved throughout the succession and storm-generated deposits are most abundant towards the middle of the formation. Characteristic tide-generated sedimentary structures include mudstone drapes, bipolar-opposed cross-bedding and ripple cross-laminae, flaser and lenticular bedding, interference ripples and desiccation cracks. Characteristic sedimentary structures formed by storm currents and waves include SSDS, HCS, graded beds, and upward-fining units. The primary trigger mechanism of the SSDS is proposed to be storm or tsunami activity, however earthquakes, overloading brought about by density inversions or microbial mats, or a combination of these processes, may have influenced the formation of SSDS to a lesser degree. Seismic events may have influenced local parts of the basin during deposition, as the underlying extensional faults would still have been active during deposition of the upper formations. The lack of barrier deposits and evidence of open marine conditions and strong tidal currents, supports the interpretation that the Gordon Lake Formation represents a macrotidal- to shallow shelf, characterized by microbial, tide, and storm activity.

6.4 Timing of deposition

A maximum depositional age of 2315 ± 5 Ma was determined from detrital zircon grains in a sandstone sample from the Flack Lake area. This age constrains the timing of deposition of the upper part of the Huronian Supergroup between ca. 2315 Ma and intrusion of gabbro approximately 95 m.y. later. Sediment was derived predominantly from Archean rocks of the Superior Province, with relatively minor contributions from basal volcanic rocks of the Huronian Supergroup (age ca. 2500 Ma), and an unknown source with an age of ca. 2300 Ma.

6.5 Future studies

In order to establish a more complete understanding of the paleodepositional settings of the upper Huronian Supergroup, further work is needed to elucidate the depositional histories of the under- and overlying, Lorrain and Bar River formations, respectively. Future research recommendations for the Gordon Lake Formation (GLF) include: 1) isotope geochemistry of the different types of nodules and chert and their use as environmental indicators, 2) whole rock major, trace, and rare earth element geochemical investigations of the GLF and their relation to climate, provenance, diagenesis, and recycling, 3) lithostratigraphic analysis of the relationships between the GLF and the underlying Lorrain and overlying Bar River formations, 4) study of why the GLF is highly siliceous compared to the other formations in the Huronian Supergroup, 5) investigation of the different colours of the GLF strata to determine primary vs. diagenetic signatures, and 6) assessment of mechanisms of MISS formation from petrographic study.

Appendices

Appendix A: Outcrop locations with coordinates.

Region	Station number	Coordinates
Bruce Mines area	224	46°24'16.09"N, 83°50'22.67"W
	225	46°24'15.70"N, 83°50'16.37"W
	226	46°24'7.88"N, 83°49'20.17"W
	374	46°23'57.08"N, 83°47'58.56"W
	375	46°23'52.44"N, 83°47'55.54"W
	376	46°24'34.67"N, 83°52'46.20"W
	377	46°23'9.42"N, 83°46'22.40"W
	378	46°25'36.70"N, 83°54'49.07"W
	379	46°25'1.99"N, 83°54'24.59"W
	380	46°24'55.40"N, 83°54'46.40"W
	381	46°26'58.56"N, 83°57'28.08"W
	382	46°26'53.05"N, 83°57'16.56"W
	383	46°26'51.47"N, 83°57'4.25"W
	384	46°26'20.40"N, 83°51'54.65"W
	385	46°25'0.77"N, 83°54'49.54"W
Flack Lake area	200	46°36'13.93"N, 82°47'25.73"W
	221	46°36'30.38"N, 82°47'17.12"W
	220	46°37'42.49"N, 82°48'27.47"W
	230	46°35'55.00"N, 82°46'27.26"W
	240	46°35'14.17"N, 82°57'51.98"W
	241	46°35'18.67"N, 82°57'59.40"W
	243	46°35'25.80"N, 82°58'26.58"W
	244	46°37'30.97"N, 82°50'1.90"W
	248	46°37'49.69"N, 82°49'2.68"W
	255	46°36'26.57"N, 82°47'1.39"W
	256	46°36'24.70"N, 82°46'53.98"W
	258	46°36'16.99"N, 82°46'15.49"W
	279	46°36'24.70"N, 82°46'51.89"W
	281	46°36'15.19"N, 82°46'7.00"W
	Lady Evelyn-Smoothwater Provincial Park	4
5		47°20'15.86"N, 80°27'26.46"W
	6	47°20'41.71"N, 80°26'59.96"W
	300	47°22'45.70"N, 80°31'51.38"W
	301	47°22'49.08"N, 80°31'54.08"W
	302	47°22'29.78"N, 80°31'16.97"W
	303	47°21'48.78"N, 80°31'2.06"W
	305	47°23'22.85"N, 80°31'4.15"W
	306	47°22'26.65"N, 80°30'46.44"W
	309	47°22'29.96"N, 80°30'49.50"W
	669	47°23'39.30"N, 80°41'10.00"W
	670	47°23'39.30"N, 80°41'11.58"W
	671	47°23'14.06"N, 80°41'30.70"W
	672	47°22'9.37"N, 80°41'26.38"W
	673	47°22'59.77"N, 80°40'10.09"W
	674	47°23'9.28"N, 80°40'4.69"W
	675	47°23'59.50"N, 80°41'15.40"W
	676	47°24'38.99"N, 80°41'10.68"W
	677	47°24'38.30"N, 80°41'11.60"W
	678	47°24'38.09"N, 80°41'14.10"W
	679	47°24'38.10"N, 80°41'14.10"W

	680	47°24'40.79"N, 80°41'9.17"W
	681	47°24'38.99"N, 80°41'3.19"W
	682	47°24'39.38"N, 80°41'1.28"W
	683	47°24'51.08"N, 80°40'46.78"W
Baie Fine-Killarney Provincial Park	313	46° 1'45.62"N, 81°30'55.87"W
	314	46° 1'46.52"N, 81°30'53.71"W
	315	46° 1'45.95"N, 81°30'50.90"W
	316	46° 1'46.13"N, 81°30'49.28"W
	317	46° 1'46.96"N, 81°30'46.03"W
	318	46° 1'48.05"N, 81°30'45.29"W
	319	46° 1'50.05"N, 81°30'35.86"W
	320	46° 1'51.17"N, 81°30'25.02"W
	321	46° 1'51.60"N, 81°30'19.58"W
	322	46° 1'55.88"N, 81°30'18.47"W
	323	46° 2'2.87"N, 81°30'17.64"W
	324	46° 2'14.93"N, 81°31'37.52"W
	325	46° 2'14.42"N, 81°31'49.37"W
	326	46° 2'22.78"N, 81°30'57.75"W
	327	46° 2'23.24"N, 81°31'5.41"W
	328	46° 2'20.18"N, 81°31'13.33"W
	329	46° 2'13.74"N, 81°31'12.11"W
	330	46° 2'14.03"N, 81°31'9.41"W
	331	46° 2'3.37"N, 81°30'18.61"W
	332	46° 2'4.88"N, 81°30'15.95"W
	333	46° 2'8.41"N, 81°30'19.69"W
	334	46° 2'8.77"N, 81°30'22.25"W
	335	46° 2'13.99"N, 81°30'36.14"W
	336	46° 2'12.91"N, 81°31'15.60"W
	337	46° 2'16.33"N, 81°30'37.66"W
	338	46° 2'18.38"N, 81°30'34.06"W
	339	46° 2'24.00"N, 81°30'34.31"W
	340	46° 2'21.70"N, 81°30'29.38"W
	341	46° 2'24.79"N, 81°30'35.89"W
	342	46° 2'24.54"N, 81°30'42.88"W
	343	46° 2'36.64"N, 81°30'43.63"W
	344	46° 2'29.65"N, 81°30'50.36"W
	345	46° 2'26.23"N, 81°30'47.45"W
	346	46° 2'22.52"N, 81°30'58.46"W
	347	46° 2'5.32"N, 81°31'43.18"W
	348	46° 1'56.57"N, 81°32'5.28"W
	349	46° 1'33.31"N, 81°32'6.76"W
	350	46° 1'43.86"N, 81°31'6.71"W
	351	46° 1'24.38"N, 81°34'21.18"W
	352	46° 1'57.10"N, 81°34'34.20"W
	353	46° 1'57.70"N, 81°34'35.18"W
	354	46° 1'47.53"N, 81°35'33.50"W
	355	46° 1'21.68"N, 81°35'26.52"W
	356	46° 1'2.32"N, 81°38'31.56"W
	357	46° 0'57.92"N, 81°39'5.29"W
	358	46° 0'51.30"N, 81°39'17.64"W
	359	46° 0'42.44"N, 81°38'49.88"W
	360	46° 0'34.77"N, 81°38'27.24"W
	361	46° 0'37.94"N, 81°38'29.18"W
	363	46° 0'50.22"N, 81°38'16.33"W
	364	46° 0'55.37"N, 81°38'17.95"W
	365	46° 0'52.69"N, 81°38'3.46"W
	366	46° 0'57.74"N, 81°37'39.79"W
	367	46° 1'7.07"N, 81°37'26.11"W
	368	46° 1'7.03"N, 81°36'46.87"W

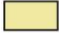







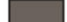







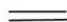



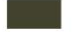





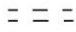



















369	46° 1'10.49"N, 81°36'45.00"W
370	46° 1'12.54"N, 81°36'40.72"W
371	46° 1'14.59"N, 81°36'20.92"W
372	46° 1'11.71"N, 81°36'8.14"W
463	46° 3'13.36"N, 81°23'13.24"W
464	46° 3'12.24"N, 81°23'20.22"W
465	46° 3'11.48"N, 81°23'21.77"W
466	46° 3'9.18"N, 81°23'27.06"W
467	46° 3'7.60"N, 81°23'34.58"W
468	46° 3'6.44"N, 81°23'38.54"W
469	46° 3'3.71"N, 81°23'25.12"W
470	46° 2'59.14"N, 81°23'19.93"W
471	46° 2'58.92"N, 81°23'18.96"W
472	46° 2'57.62"N, 81°23'18.20"W
473	46° 3'17.57"N, 81°23'5.57"W
474	46° 3'31.10"N, 81°23'5.57"W
475	46° 3'31.50"N, 81°23'5.35"W
476	46° 3'33.95"N, 81°23'6.07"W
477	46° 3'34.34"N, 81°23'8.95"W
478	46° 3'36.07"N, 81°23'6.29"W
479	46° 3'40.64"N, 81°23'8.30"W
480	46° 3'31.25"N, 81°23'15.47"W
481	46° 3'29.30"N, 81°23'37.72"W
482	46° 3'31.93"N, 81°23'46.03"W
483	46° 3'15.05"N, 81°23'48.05"W
484	46° 3'22.14"N, 81°24'0.94"W
485	46° 3'17.53"N, 81°23'56.62"W
486	46° 3'12.96"N, 81°23'57.77"W
487	46° 3'4.57"N, 81°23'48.00"W
488	46° 3'3.71"N, 81°23'48.62"W
489	46° 3'5.08"N, 81°24'2.00"W
491	46° 3'14.04"N, 81°21'59.44"W
492	46° 3'21.13"N, 81°21'59.44"W
494	46° 3'17.96"N, 81°21'53.82"W
495	46° 3'15.34"N, 81°22'10.02"W
496	46° 3'12.28"N, 81°22'9.23"W
497	46° 3'9.25"N, 81°22'0.48"W
498	46° 3'10.01"N, 81°21'53.10"W
499	46° 3'7.42"N, 81°21'43.88"W
501	46° 3'16.34"N, 81°21'39.17"W
502	46° 3'17.68"N, 81°21'45.97"W
503	46° 3'17.82"N, 81°21'49.14"W
504	46° 3'28.91"N, 81°21'46.87"W
505	46° 3'28.04"N, 81°21'52.70"W
507	46° 3'30.42"N, 81°21'56.66"W
508	46° 3'32.54"N, 81°21'59.58"W
509	46° 3'34.78"N, 81°22'4.87"W
510	46° 3'34.63"N, 81°22'7.14"W
511	46° 3'34.99"N, 81°22'10.78"W
512	46° 3'37.08"N, 81°22'14.56"W
513	46° 3'37.76"N, 81°22'26.44"W
514	46° 3'39.67"N, 81°22'28.45"W
515	46° 3'41.29"N, 81°22'23.74"W
516	46° 3'42.62"N, 81°22'18.88"W
517	46° 3'45.11"N, 81°22'14.99"W
518	46° 3'48.85"N, 81°22'5.16"W
519	46° 3'51.77"N, 81°21'58.54"W
520	46° 3'56.34"N, 81°21'56.99"W
521	46° 3'55.84"N, 81°21'34.52"W

522	46° 3'53.10"N, 81°21'27.50"W
523	46° 3'52.78"N, 81°21'24.66"W
525	46° 3'50.83"N, 81°21'20.63"W
527	46° 3'47.05"N, 81°21'17.21"W
529	46° 3'49.07"N, 81°21'12.35"W
530	46° 3'50.80"N, 81°21'4.39"W
531	46° 3'56.23"N, 81°21'11.95"W
532	46° 3'59.94"N, 81°21'14.44"W
533	46° 3'54.14"N, 81°21'39.17"W
534	46° 3'50.04"N, 81°21'40.72"W
535	46° 3'45.94"N, 81°21'38.84"W
536	46° 3'43.38"N, 81°21'39.89"W
537	46° 3'38.74"N, 81°21'37.69"W
538	46° 3'34.09"N, 81°21'32.44"W
539	46° 3'29.20"N, 81°21'28.08"W
540	46° 3'25.42"N, 81°21'28.08"W
541	46° 3'27.29"N, 81°21'34.52"W
542	46° 3'26.71"N, 81°21'43.60"W
543	46° 3'24.62"N, 81°21'51.70"W
544	46° 3'5.18"N, 81°21'47.20"W
545	46° 3'2.99"N, 81°21'43.96"W
546	46° 2'56.40"N, 81°21'41.87"W
548	46° 2'54.56"N, 81°21'32.94"W
550	46° 2'51.61"N, 81°21'29.27"W
551	46° 2'51.18"N, 81°21'34.45"W
552	46° 2'52.22"N, 81°21'40.39"W
553	46° 2'53.48"N, 81°21'46.62"W
555	46° 2'46.54"N, 81°21'35.75"W
556	46° 2'46.79"N, 81°21'31.97"W
557	46° 2'46.25"N, 81°21'26.28"W
558	46° 2'44.34"N, 81°21'22.03"W
559	46° 2'53.88"N, 81°21'27.00"W
561	46° 2'59.24"N, 81°21'35.93"W
562	46° 3'1.12"N, 81°21'29.12"W
563	46° 3'5.54"N, 81°21'27.58"W
564	46° 3'8.50"N, 81°21'31.28"W
565	46° 3'12.17"N, 81°21'32.76"W
566	46° 3'13.32"N, 81°21'33.55"W
567	46° 3'20.52"N, 81°21'48.35"W
568	46° 3'15.30"N, 81°26'19.68"W
569	46° 3'11.23"N, 81°26'24.22"W
570	46° 3'13.93"N, 81°26'26.02"W
571	46° 3'13.90"N, 81°26'30.55"W
572	46° 3'11.88"N, 81°26'32.17"W
573	46° 3'9.11"N, 81°26'34.51"W
574	46° 3'8.46"N, 81°26'28.10"W
575	46° 3'7.45"N, 81°26'27.46"W
576	46° 3'5.80"N, 81°26'23.93"W
577	46° 3'6.62"N, 81°26'15.54"W
578	46° 3'6.55"N, 81°26'6.04"W
579	46° 3'5.58"N, 81°25'56.75"W
580	46° 3'4.46"N, 81°25'48.47"W
581	46° 3'10.37"N, 81°25'40.94"W
582	46° 3'13.00"N, 81°25'41.34"W
583	46° 3'27.68"N, 81°25'31.55"W
584	46° 3'29.95"N, 81°25'28.45"W
585	46° 3'32.51"N, 81°25'4.01"W
586	46° 3'33.44"N, 81°24'58.25"W
587	46° 3'35.21"N, 81°24'45.83"W

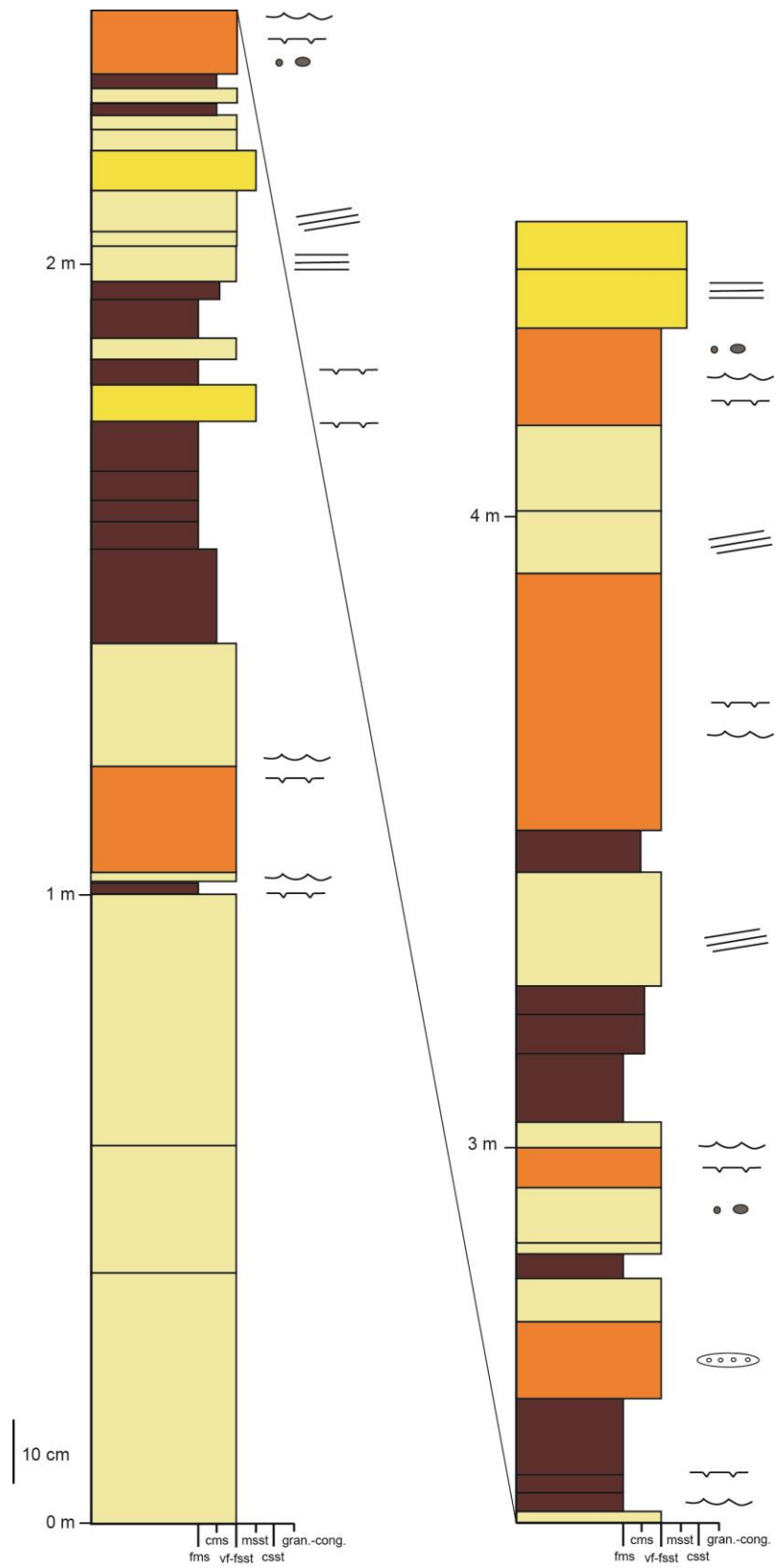
588	46° 3'35.21"N, 81°24'42.44"W
589	46° 3'37.33"N, 81°24'41.54"W
590	46° 3'33.16"N, 81°24'35.14"W
591	46° 3'30.92"N, 81°24'9.70"W
592	46° 3'26.46"N, 81°24'19.98"W
593	46° 3'27.50"N, 81°24'21.85"W
594	46° 3'16.85"N, 81°24'22.18"W
595	46° 3'13.00"N, 81°24'24.34"W
596	46° 3'15.62"N, 81°24'26.64"W
597	46° 3'19.51"N, 81°24'29.56"W
598	46° 3'24.30"N, 81°24'36.76"W
599	46° 2'56.15"N, 81°28'5.70"W
600	46° 3'1.01"N, 81°28'2.46"W
601	46° 3'5.08"N, 81°28'3.83"W
602	46° 3'7.70"N, 81°27'54.94"W
603	46° 3'10.40"N, 81°27'55.48"W
604	46° 3'9.47"N, 81°27'44.93"W
605	46° 3'13.90"N, 81°27'42.34"W
606	46° 3'11.45"N, 81°27'32.33"W
607	46° 3'16.20"N, 81°27'28.87"W
608	46° 3'19.33"N, 81°26'52.58"W
609	46° 3'22.14"N, 81°26'47.65"W
610	46° 3'19.37"N, 81°26'41.75"W
611	46° 3'23.11"N, 81°26'36.13"W
612	46° 3'13.10"N, 81°26'11.33"W
613	46° 3'12.10"N, 81°26'6.25"W
614	46° 3'11.84"N, 81°25'54.55"W
615	46° 3'12.67"N, 81°25'45.23"W
616	46° 3'29.95"N, 81°24'46.33"W
617	46° 3'24.55"N, 81°24'37.73"W
618	46° 3'18.43"N, 81°24'46.15"W
619	46° 3'16.67"N, 81°24'46.66"W
620	46° 3'7.99"N, 81°24'31.57"W
621	46° 3'8.50"N, 81°24'18.94"W
622	46° 3'19.76"N, 81°24'30.53"W
623	46° 3'27.32"N, 81°24'51.20"W
624	46° 3'25.45"N, 81°25'2.60"W
625	46° 3'24.05"N, 81°25'25.57"W
626	46° 2'57.77"N, 81°28'43.18"W
627	46° 2'59.24"N, 81°29'0.02"W
628	46° 2'57.84"N, 81°29'2.18"W
629	46° 2'54.64"N, 81°28'53.04"W
630	46° 2'56.58"N, 81°28'50.20"W
631	46° 2'54.02"N, 81°28'52.39"W
632	46° 2'53.81"N, 81°28'45.66"W
633	46° 2'57.08"N, 81°28'36.52"W
634	46° 2'52.69"N, 81°28'43.97"W
635	46° 2'48.48"N, 81°28'34.97"W
636	46° 2'53.81"N, 81°28'55.16"W
637	46° 2'52.22"N, 81°28'58.94"W
638	46° 2'51.18"N, 81°28'58.94"W
639	46° 2'51.18"N, 81°29'8.02"W
640	46° 2'51.18"N, 81°29'8.84"W
641	46° 2'48.88"N, 81°29'17.27"W
642	46° 2'46.61"N, 81°29'26.77"W
643	46° 2'46.61"N, 81°29'28.03"W
644	46° 2'44.92"N, 81°29'37.75"W
645	46° 2'44.52"N, 81°29'40.85"W
646	46° 2'43.87"N, 81°29'45.38"W

	647	46° 2'43.19"N, 81°29'50.24"W
	648	46° 2'40.06"N, 81°30'1.19"W
	649	46° 2'37.61"N, 81°30'17.17"W
	650	46° 2'35.70"N, 81°30'22.86"W
	651	46° 2'36.10"N, 81°30'30.64"W
	652	46° 2'30.95"N, 81°30'38.34"W
	653	46° 2'31.31"N, 81°30'43.92"W
	654	46° 2'39.23"N, 81°30'31.93"W
	655	46° 2'42.79"N, 81°30'22.18"W
	656	46° 2'45.31"N, 81°30'13.46"W
	657	46° 2'50.53"N, 81°29'39.01"W
	658	46° 2'43.51"N, 81°28'36.91"W
	659	46° 2'39.55"N, 81°28'31.40"W
	660	46° 2'38.87"N, 81°28'27.12"W
	661	46° 2'41.46"N, 81°28'48.25"W

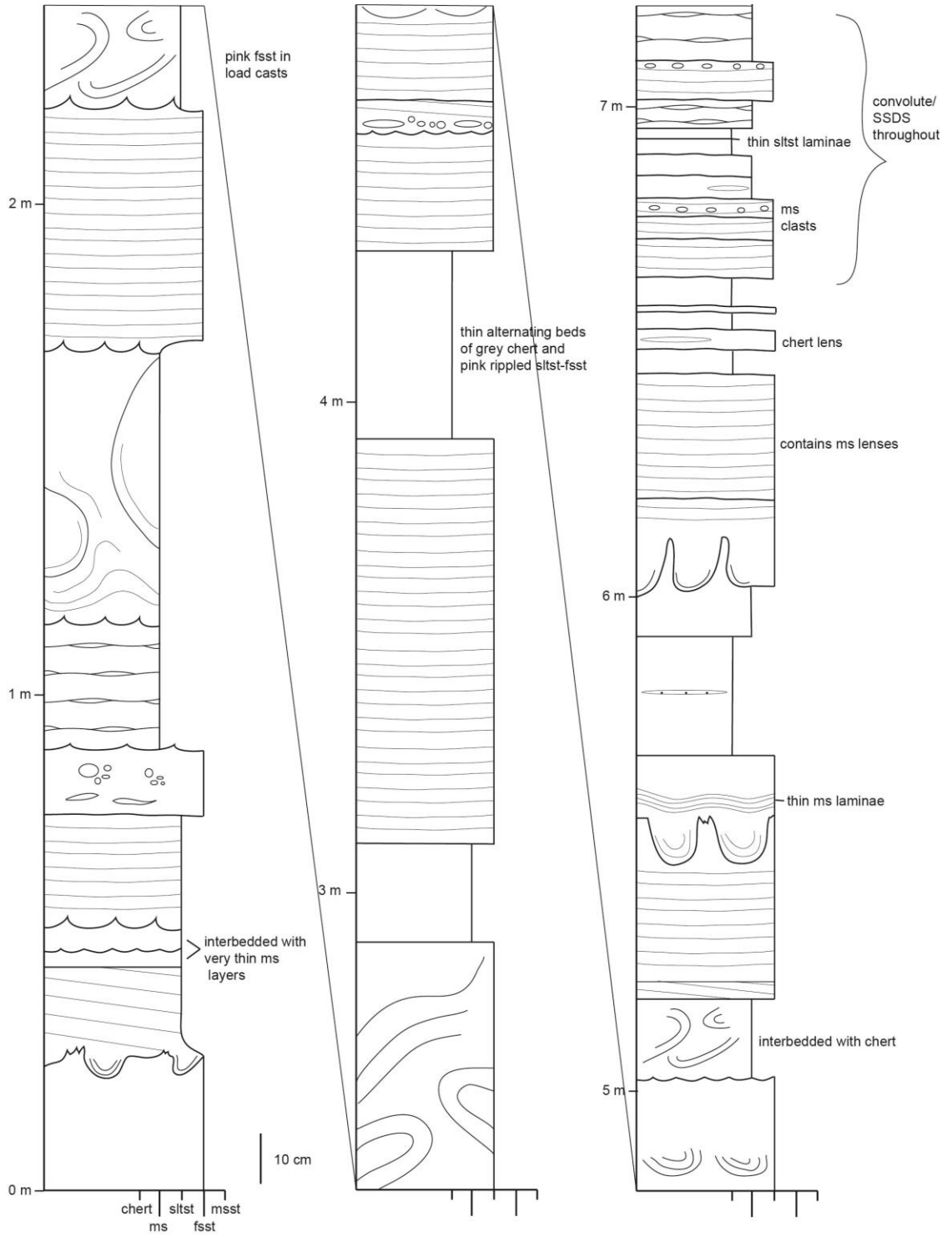
Appendix B: Supplementary stratigraphic sections. Refer to legend below.

Legend					
	LF1		large ball structure		shrinkage cracks
	LF2		load structures		pinch-and-swell
	LF3		convolute bedding		mudstone
	LF4		mudstone laminae		mudstone lens
	LF5		fg sandstone lens		synaeresis cracks
	LF6a		planar to wavy laminae		cg sandstone lens
	LF6b		pseudonodules		gabbro intrusion
	LF7		microbial mat		trough cross-bedding
	flame and load cast		HCS		massive to faintly laminated
	low angle cross-laminae		microbial mat chip		flaser bedding
	ripples		scoured surface		sandstone intrusion
	flames		graded bed		sugary quartz nodules
	wavy laminae		pink granules		pebble lens
	mudstone clasts		secondary sulphides		ripple cross-laminae
	lenticular bedding		conglomerate clast with sulphide stains		mudstone drape
					quartz nodules

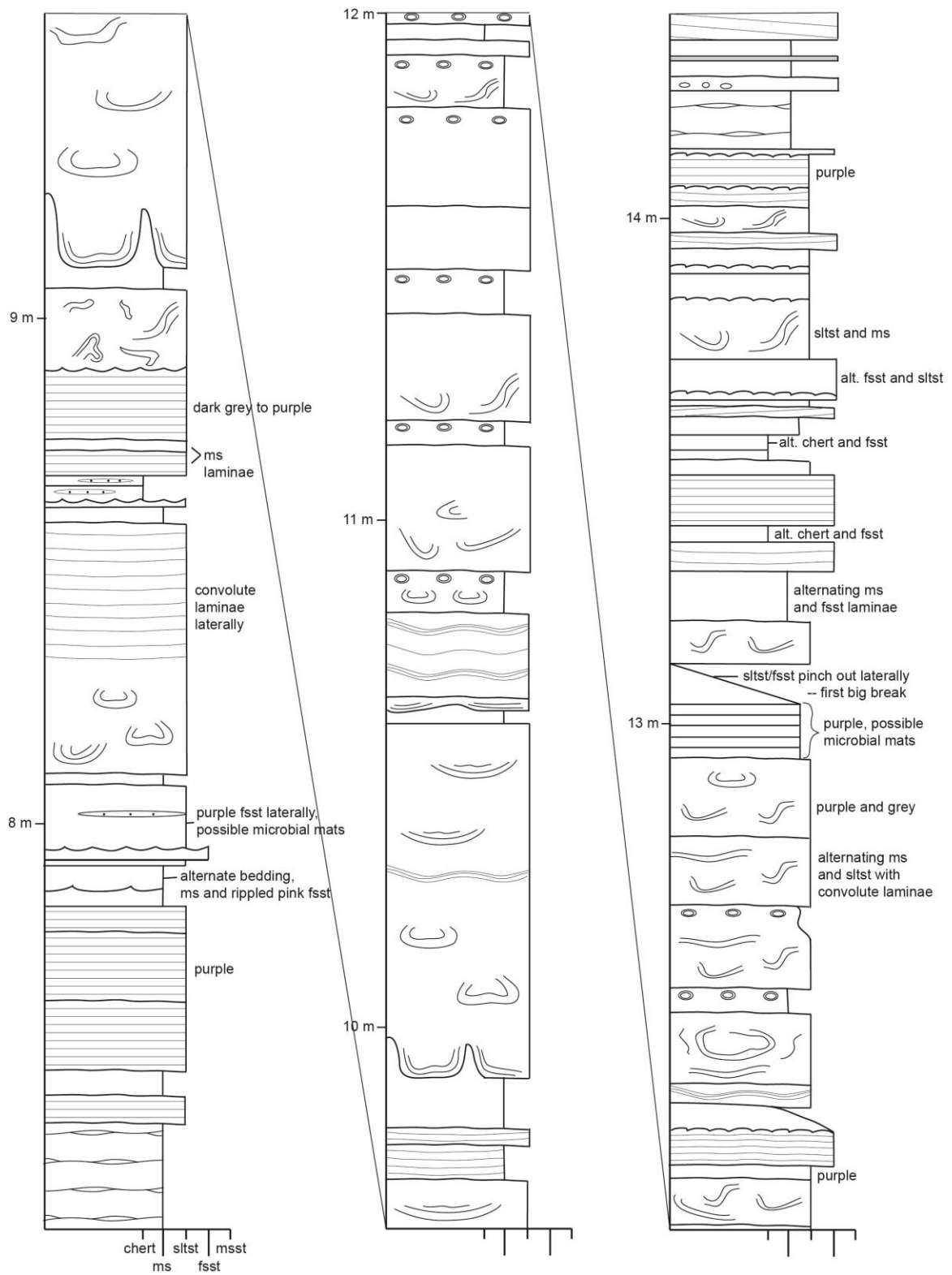
#200



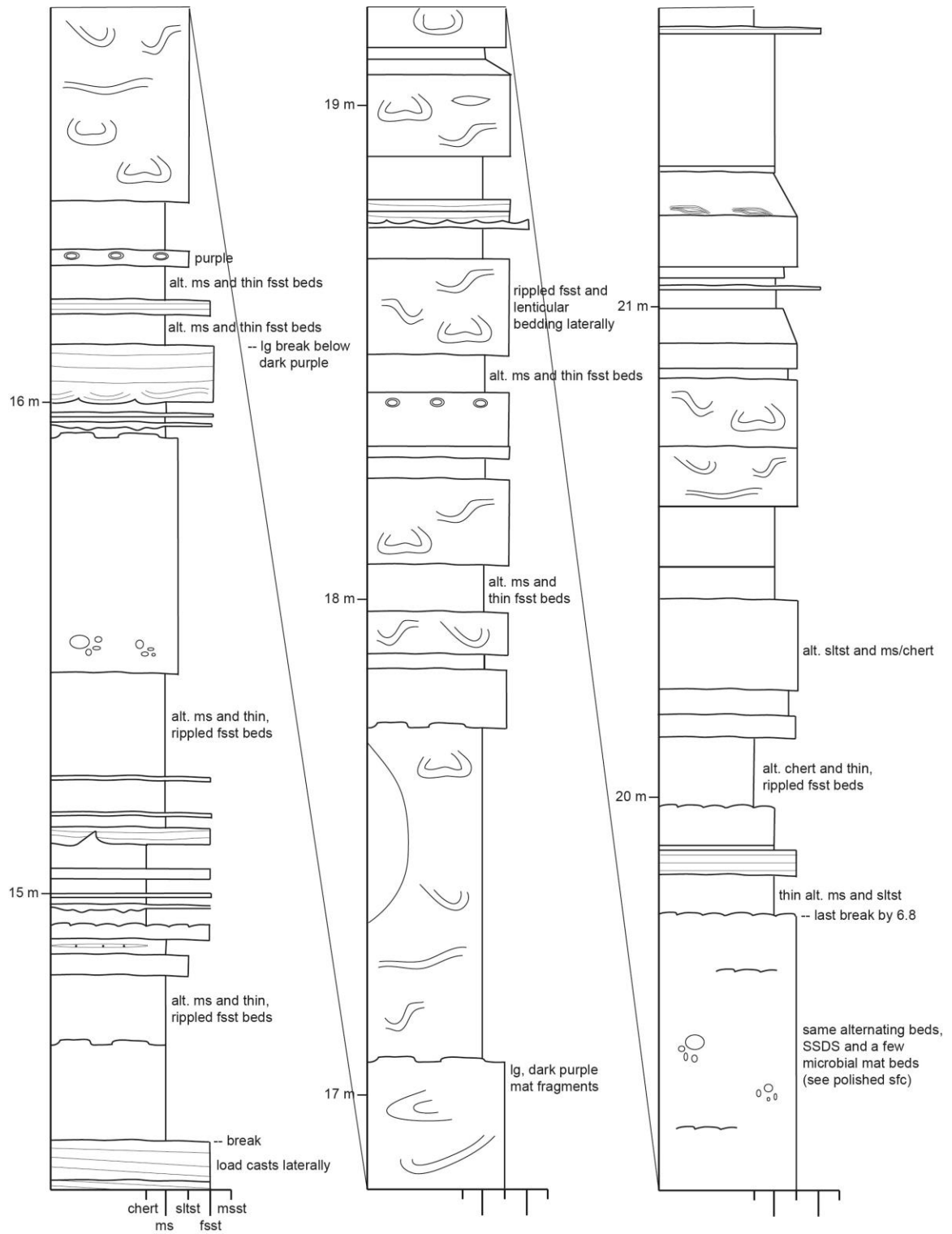
#226 – Note that chert is silicified mudstone in this section.



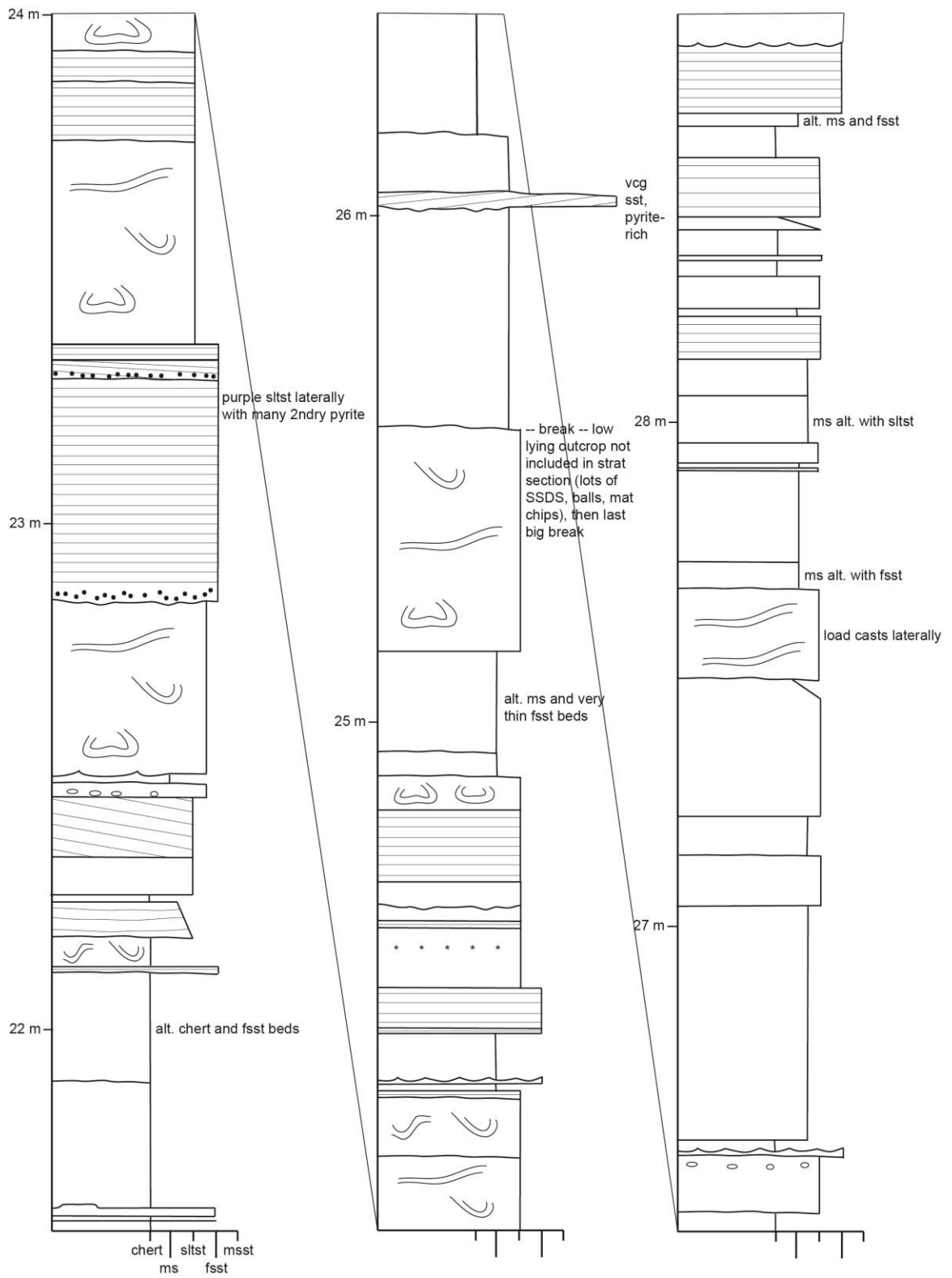
#226 continued



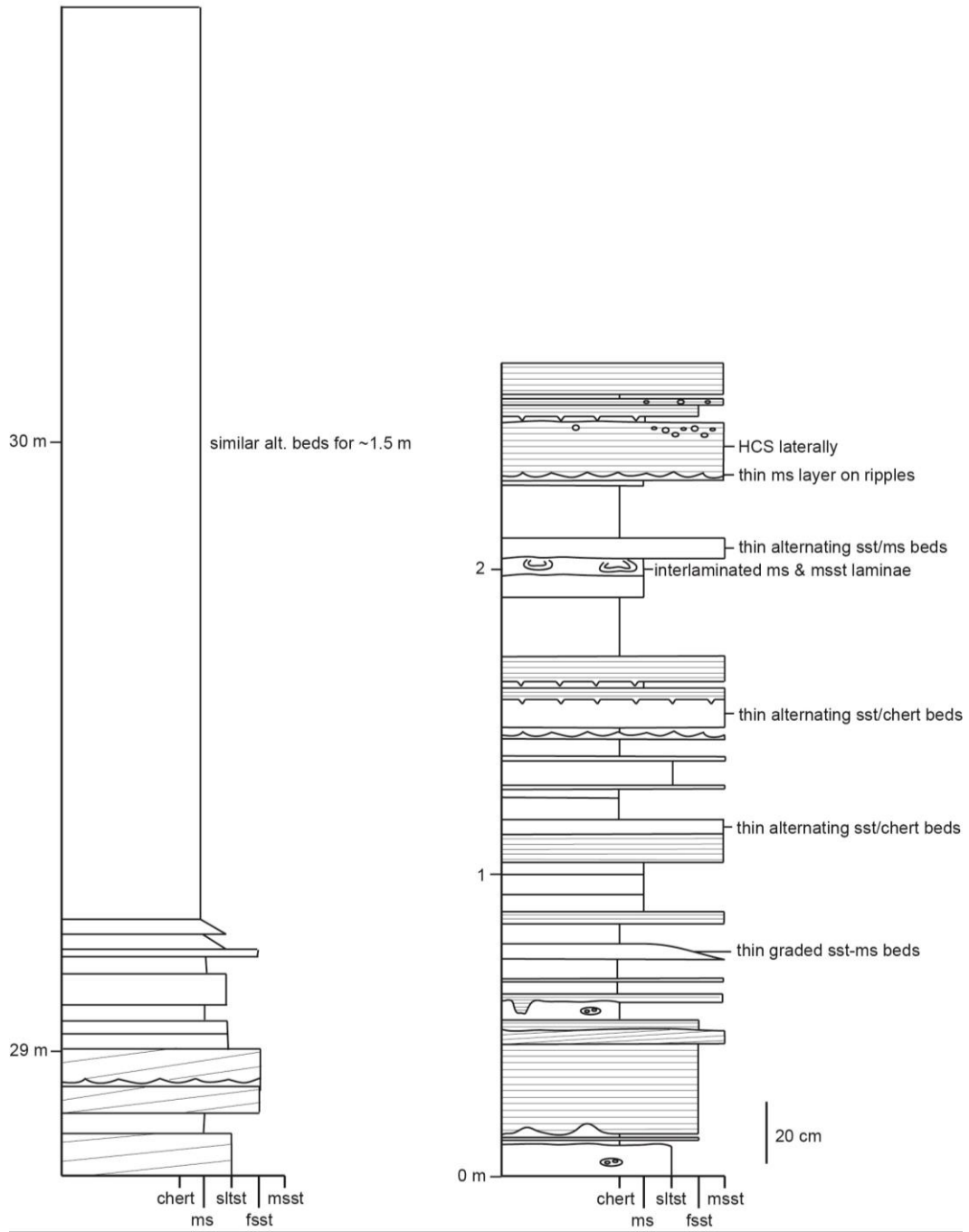
#226 continued



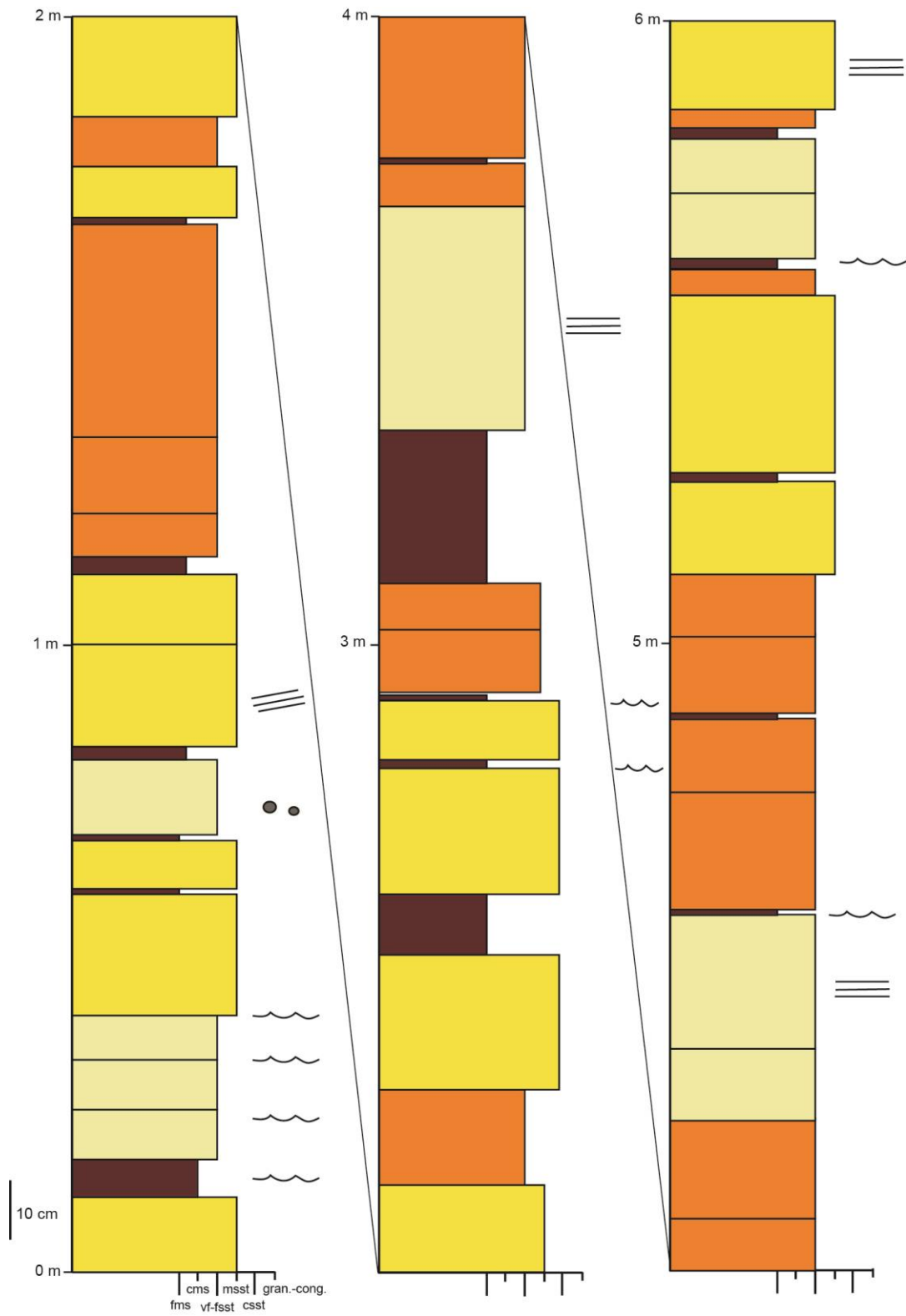
#226 continued



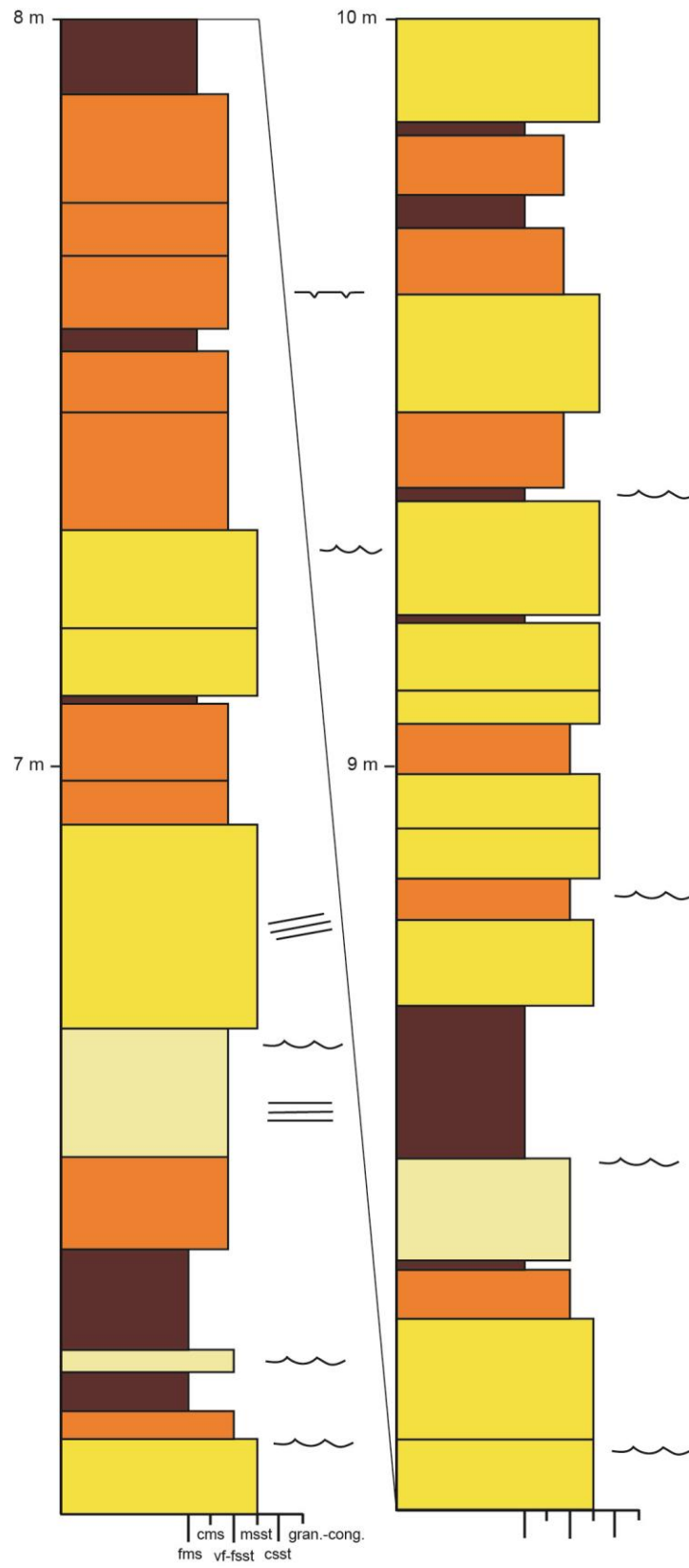
#226 continued



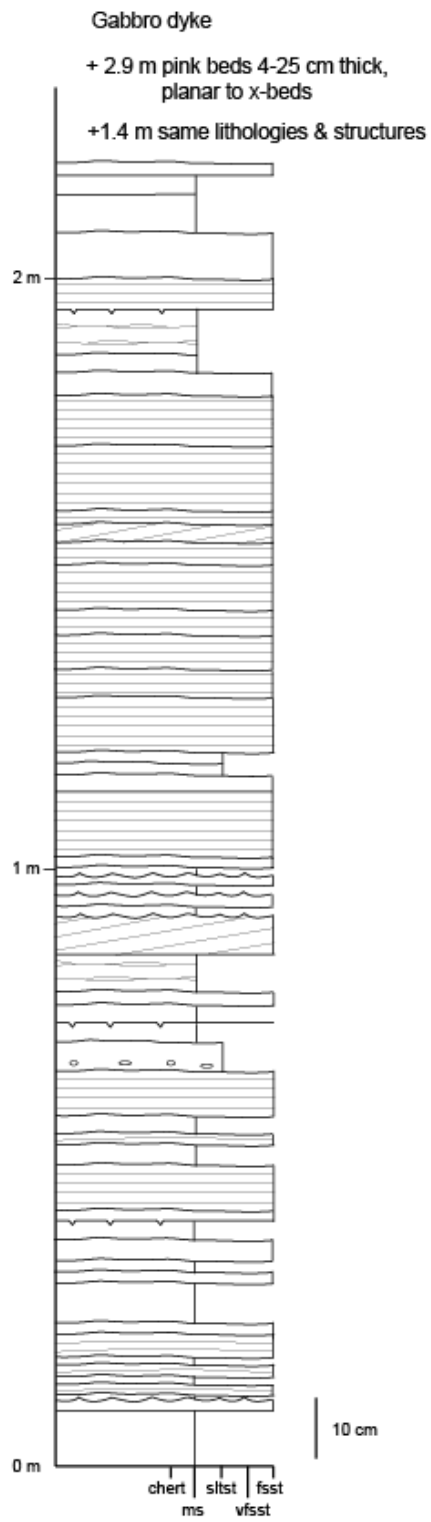
#377



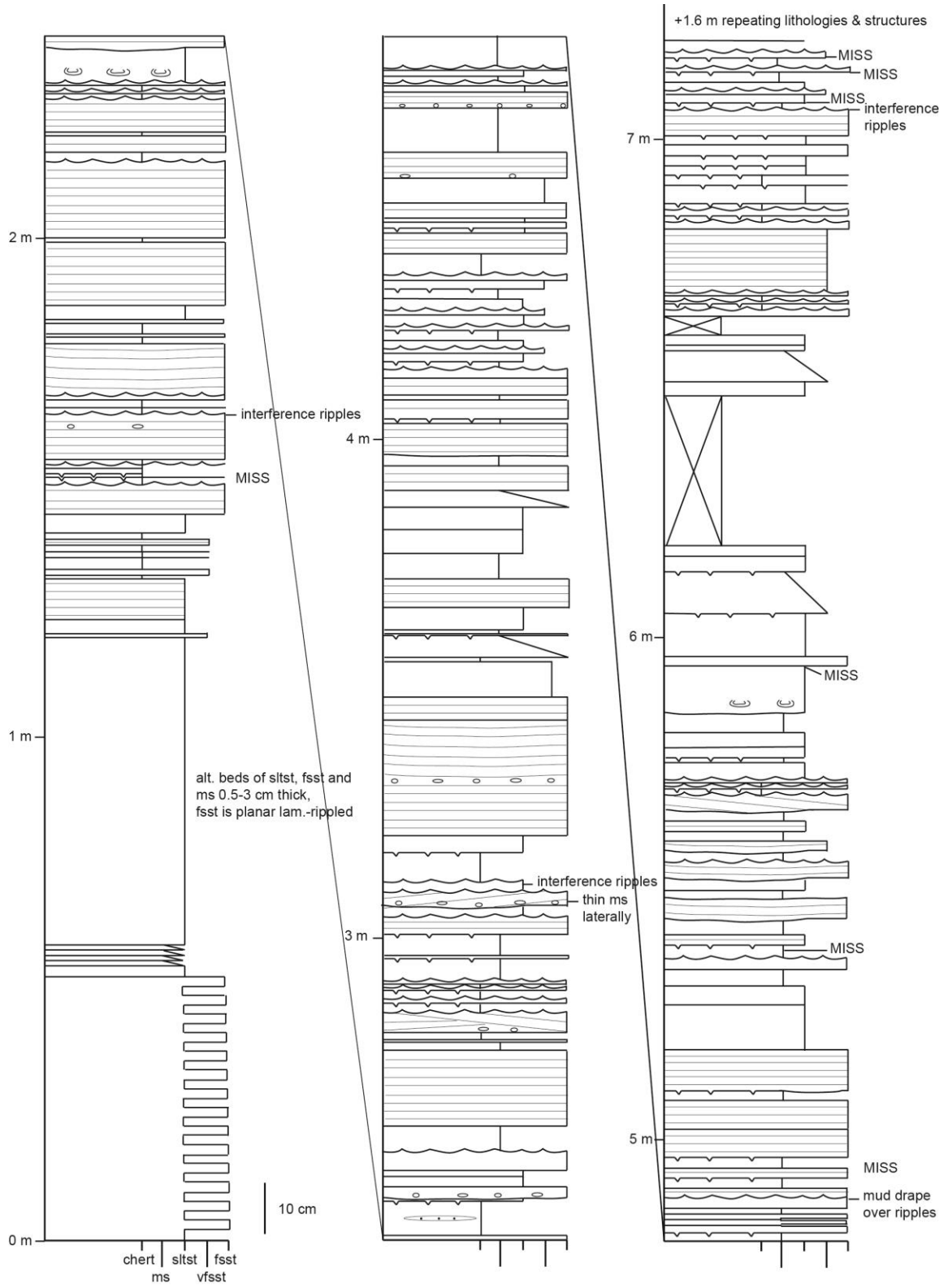
#377 continued



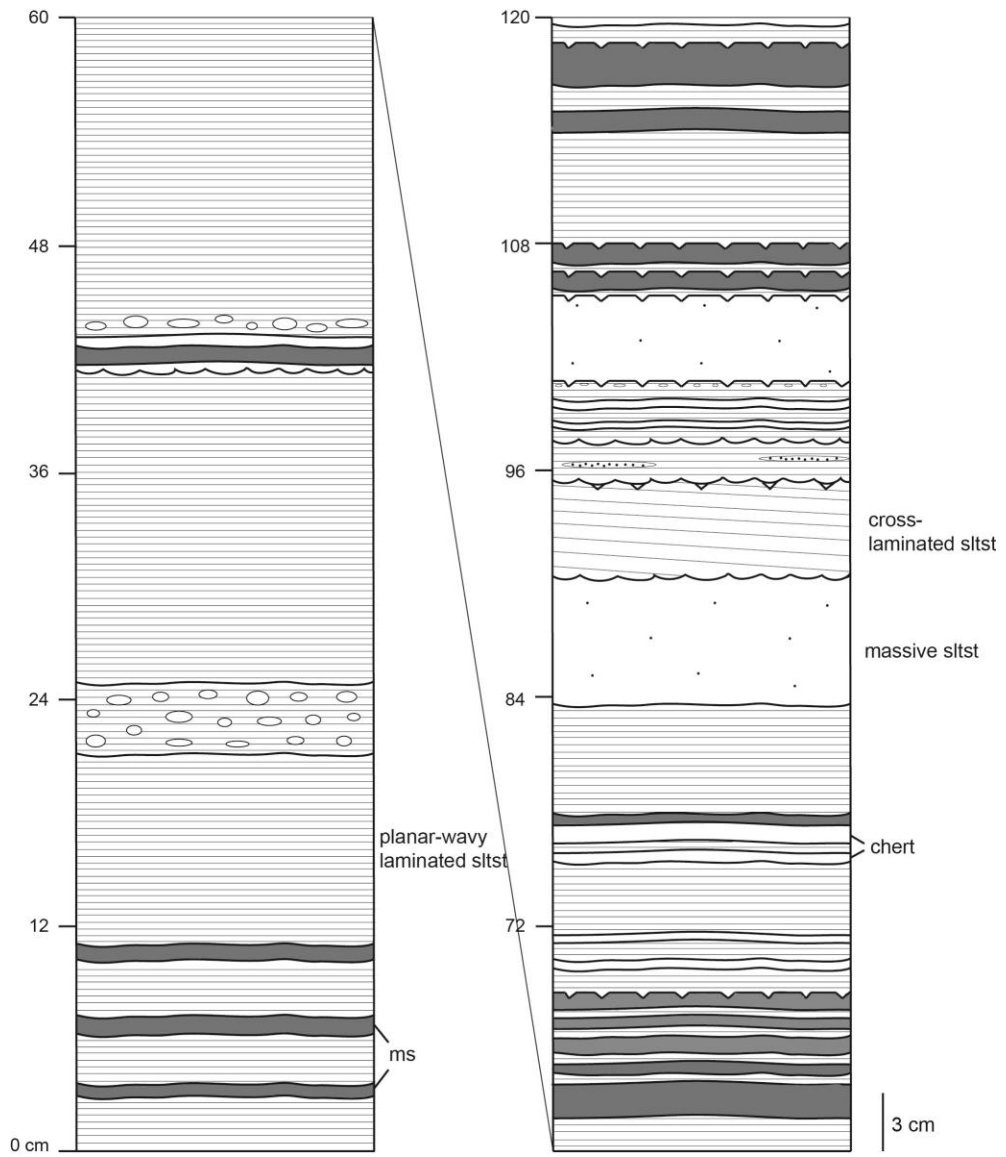
#230



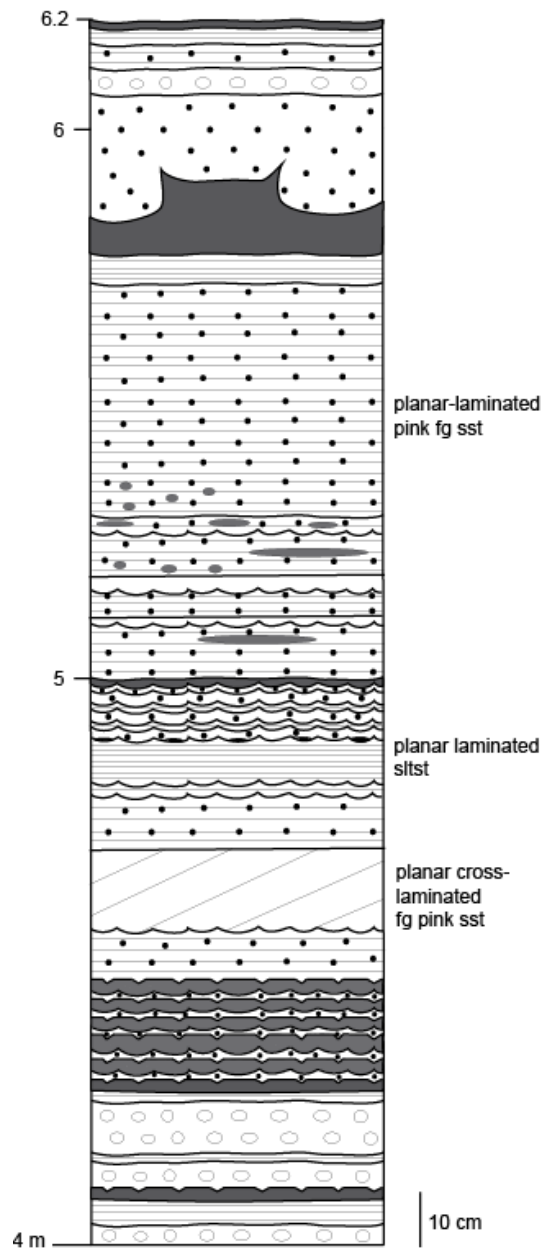
#221



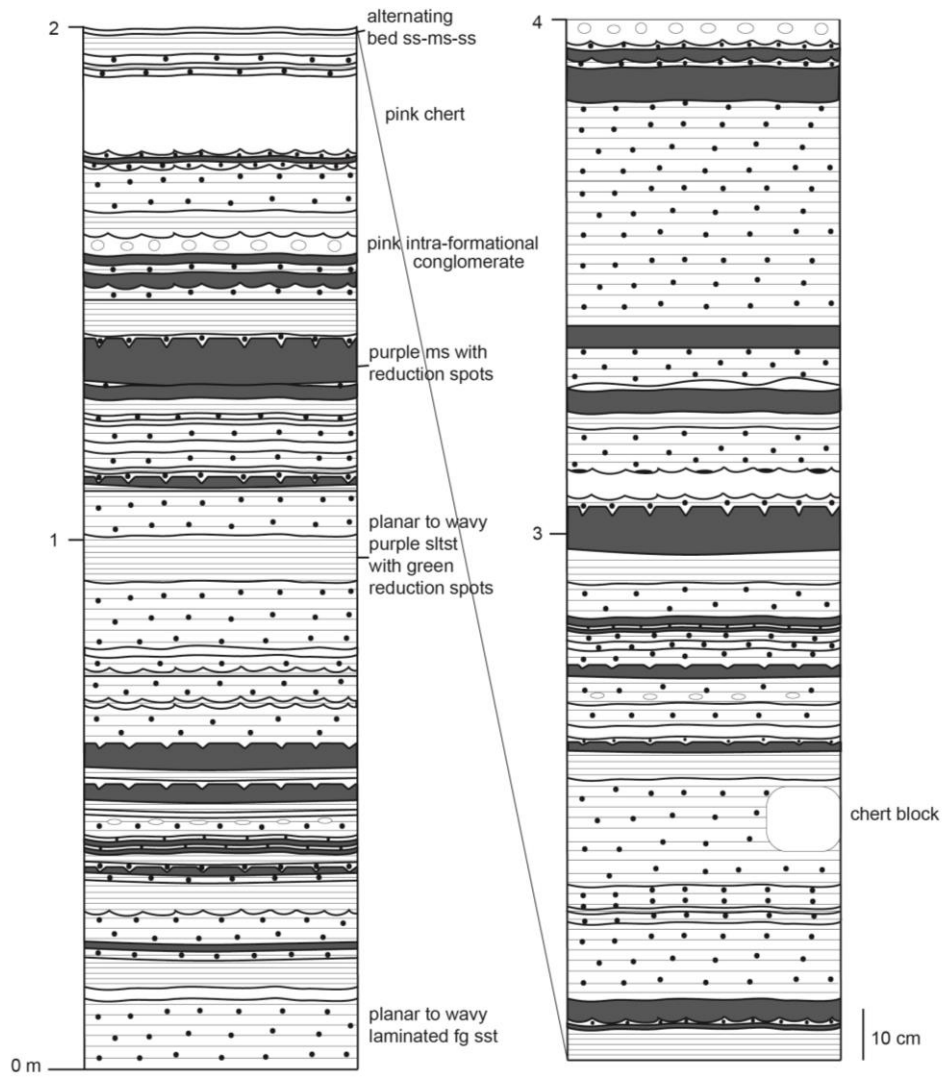
#255



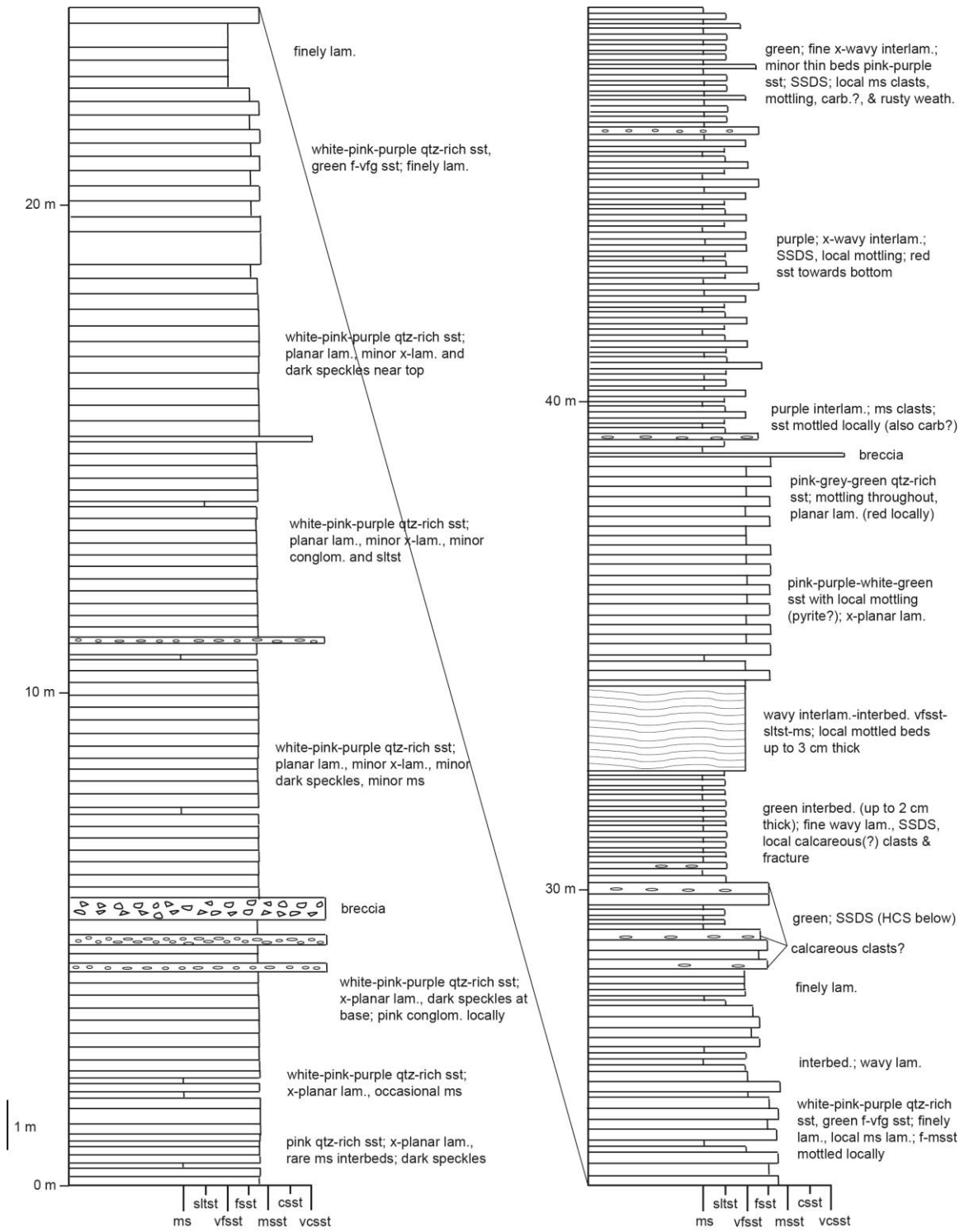
#256



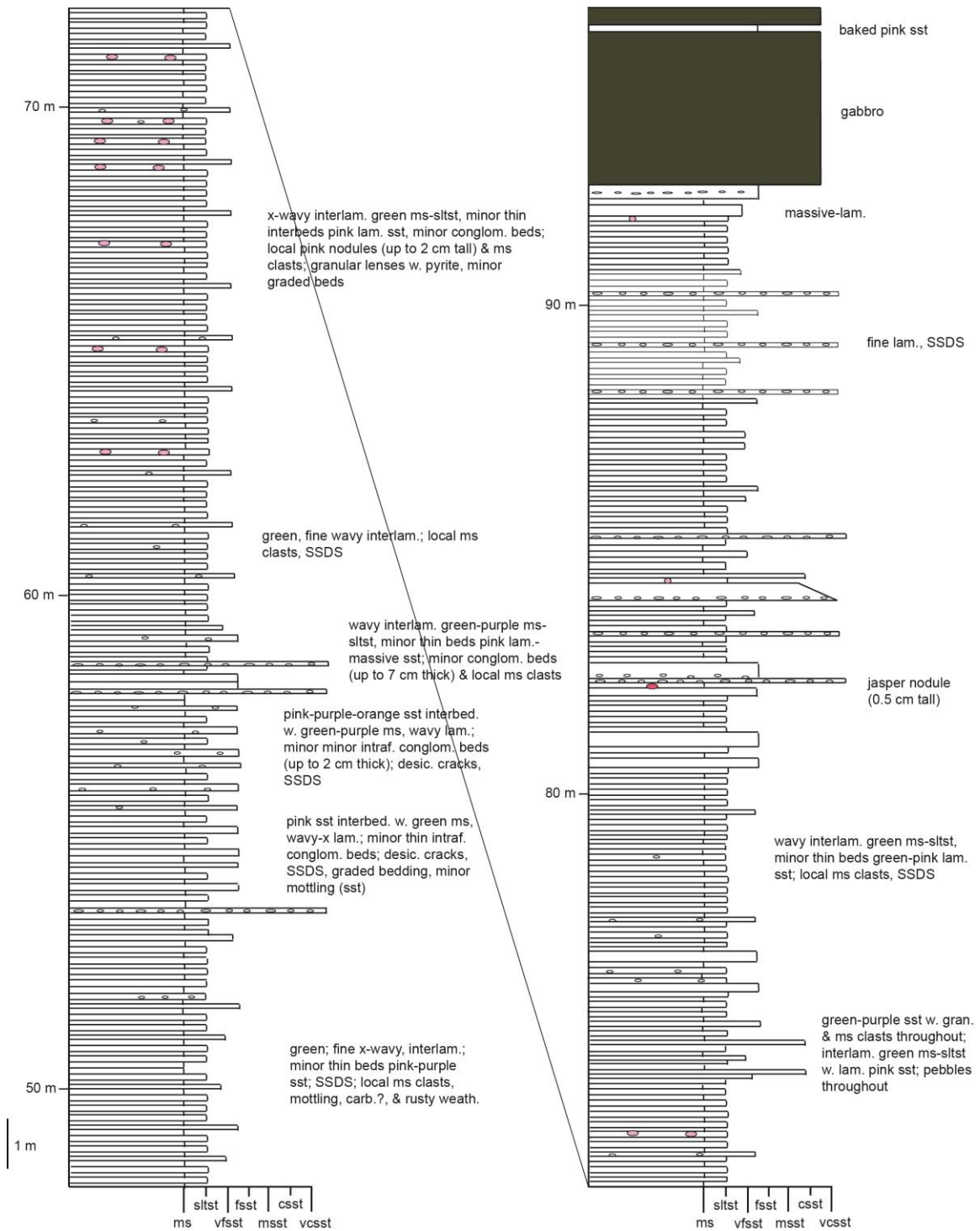
#258



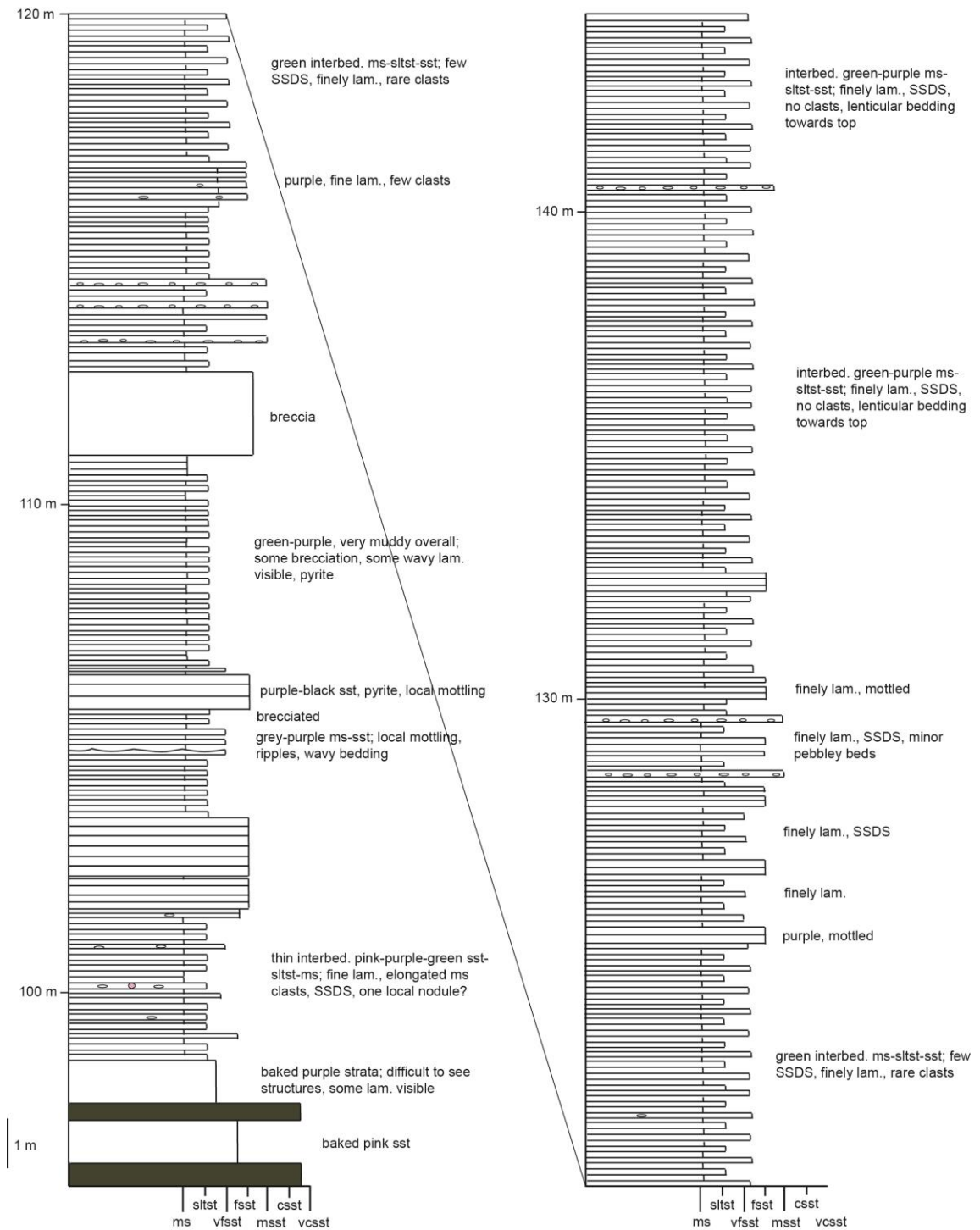
CJM core 68-1



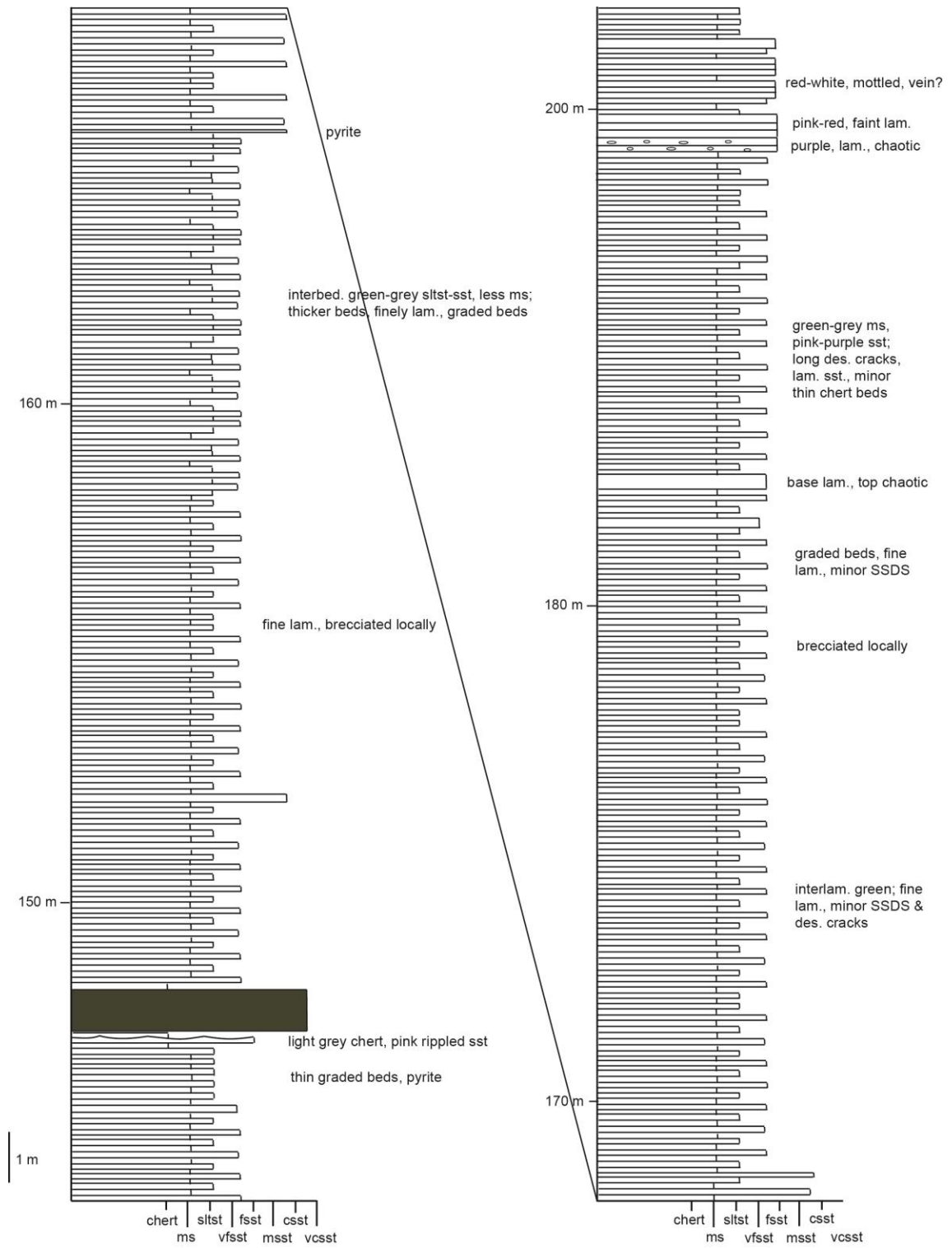
CJM core 68-1 continued



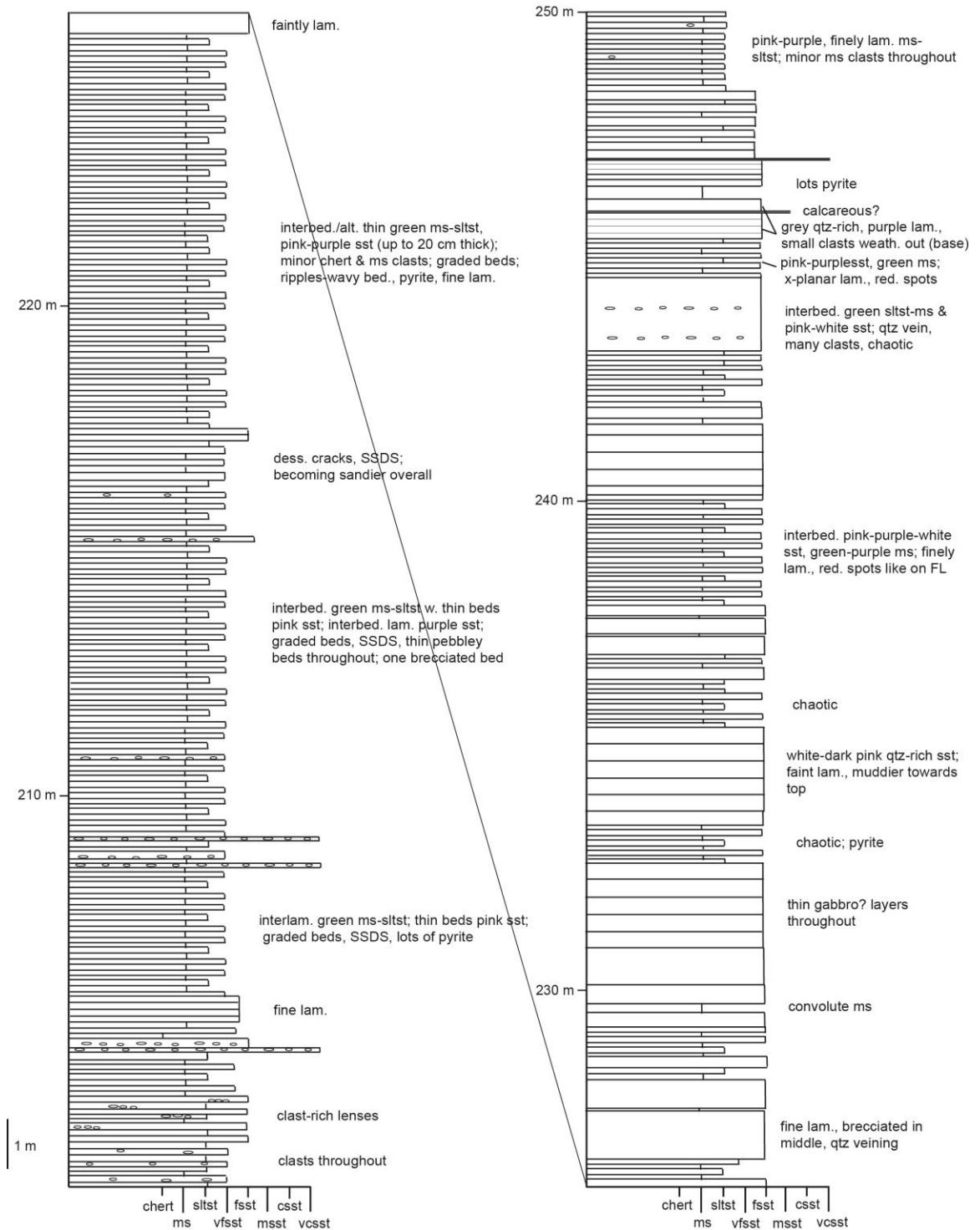
CJM core 68-1 continued



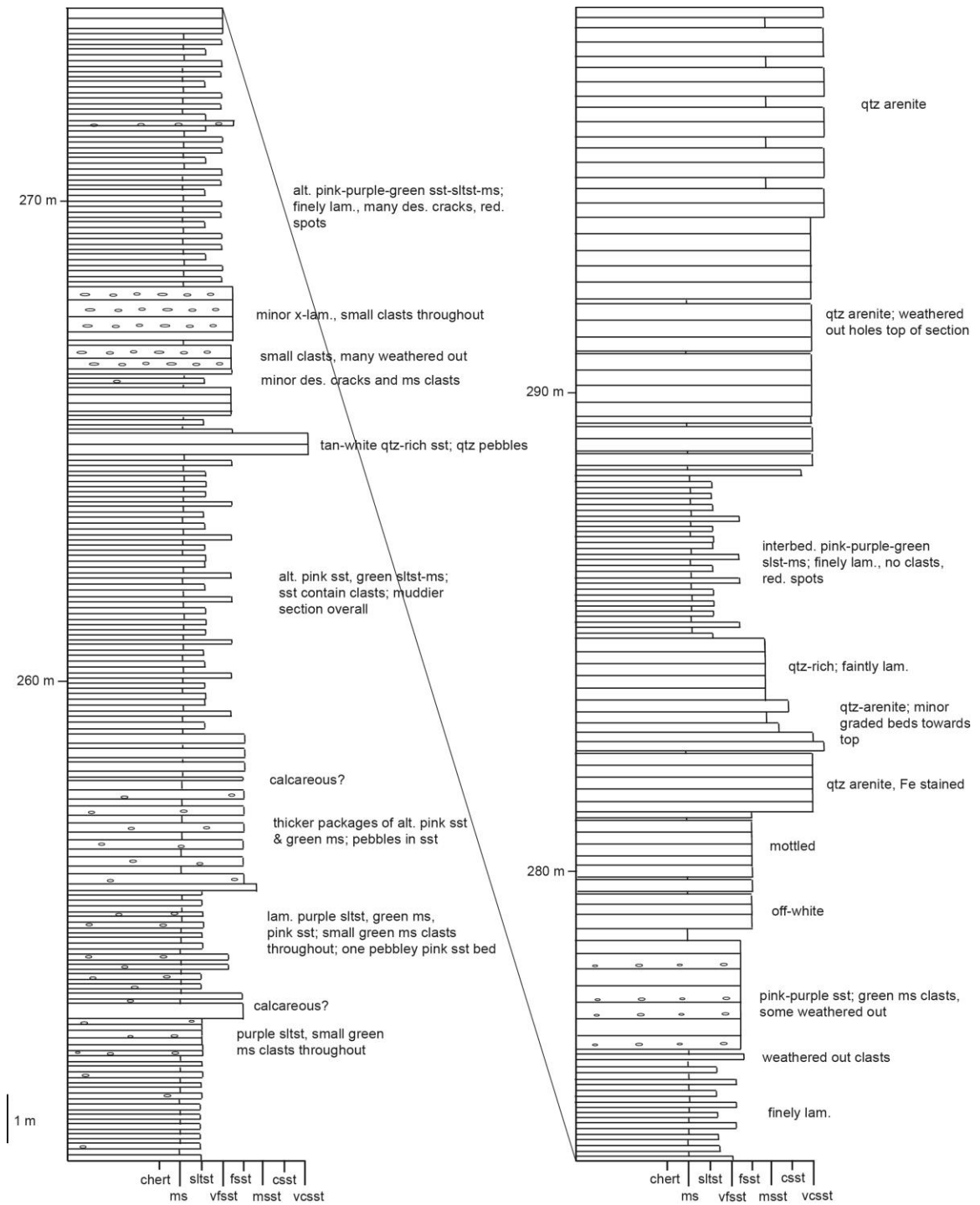
CJM core 68-1 continued



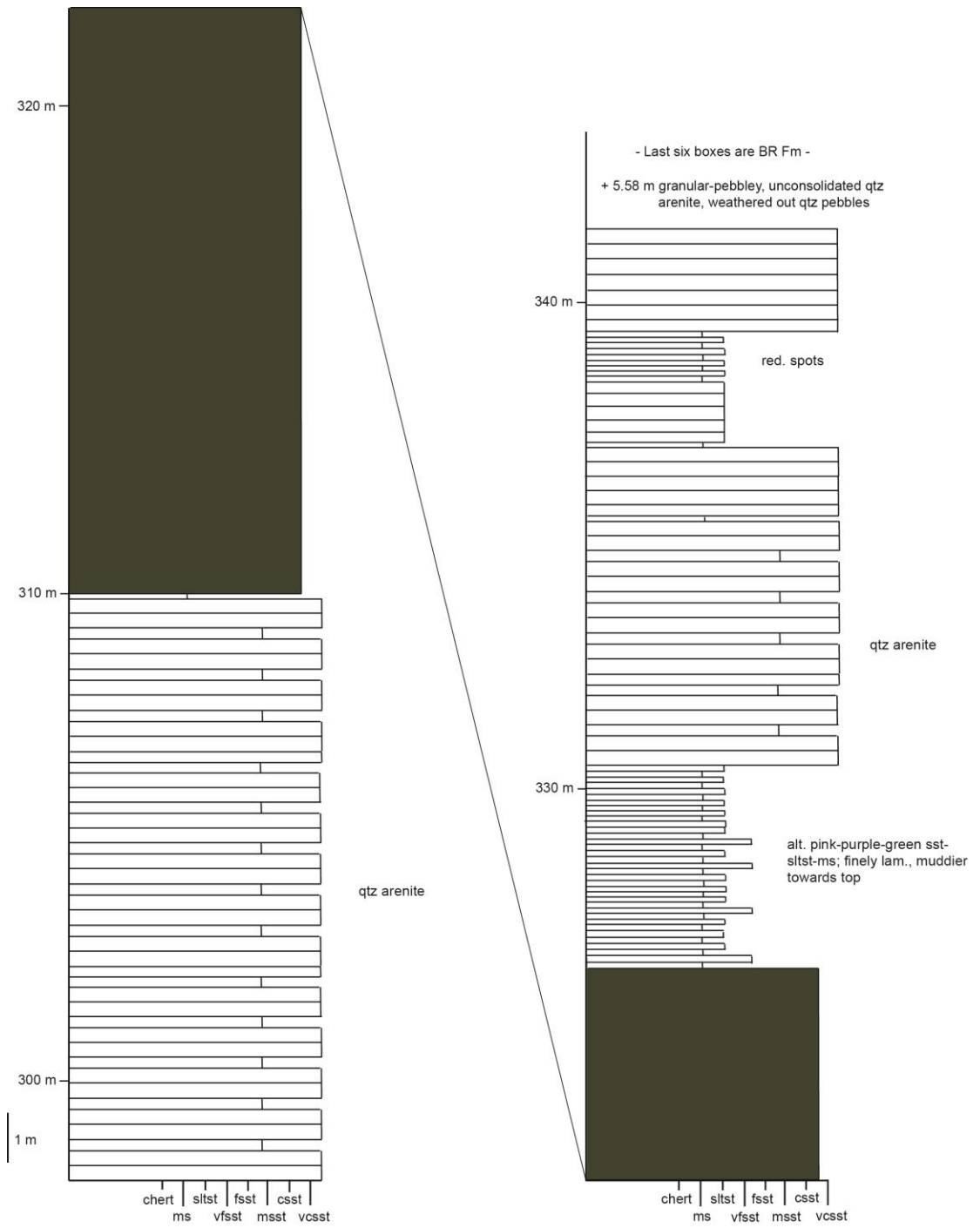
CJM core 68-1 continued



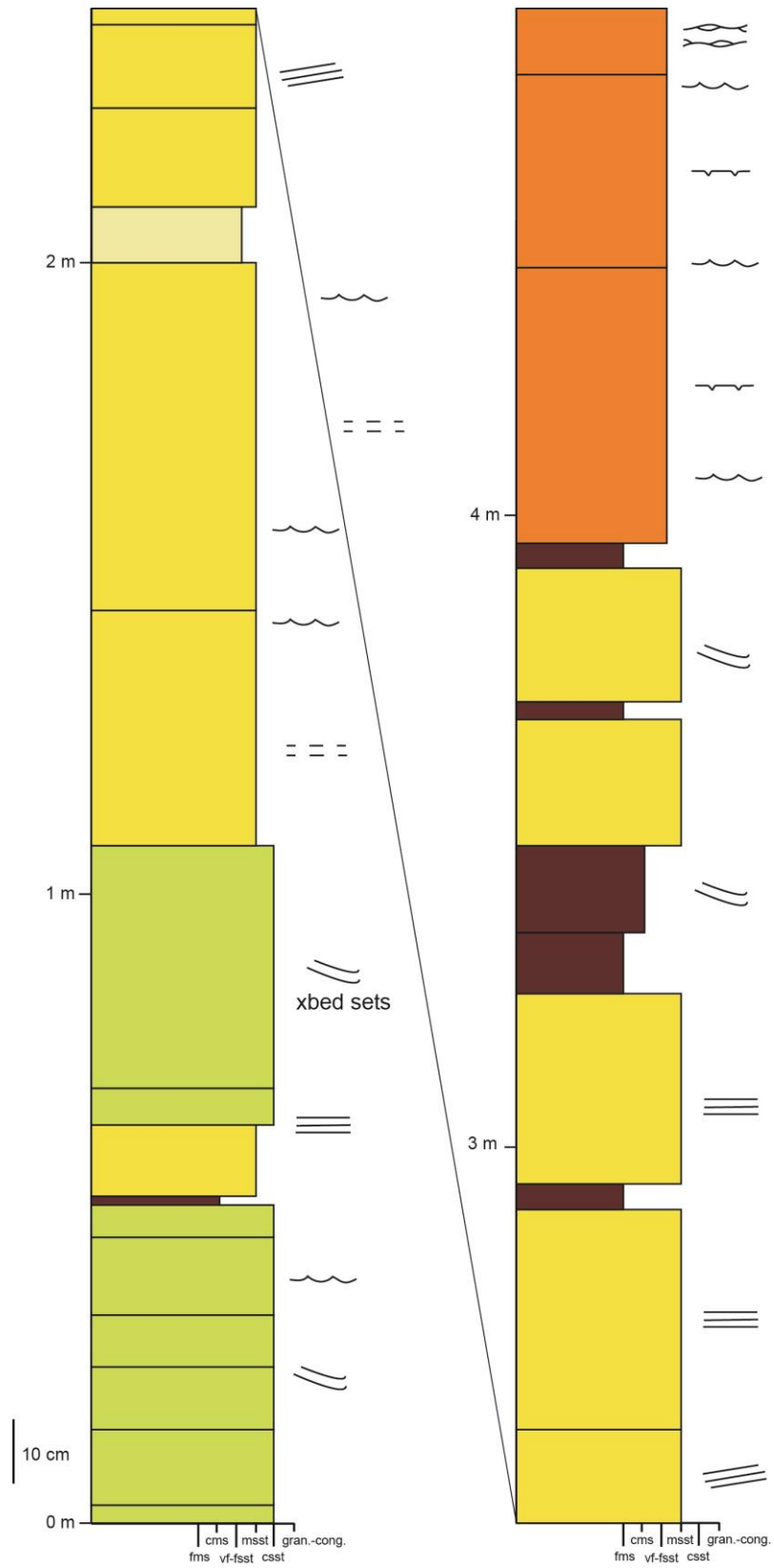
CJM core 68-1 continued



CJM core 68-1 continued



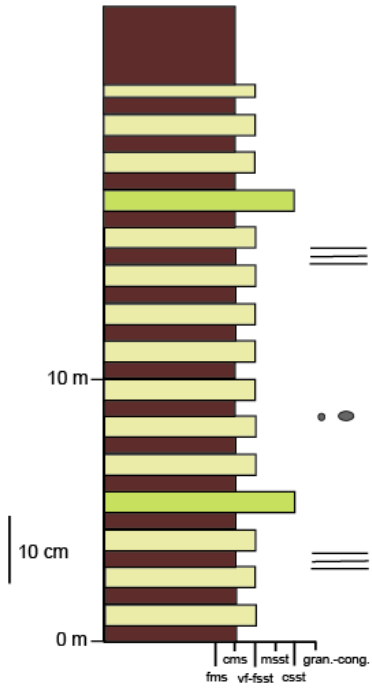
#305



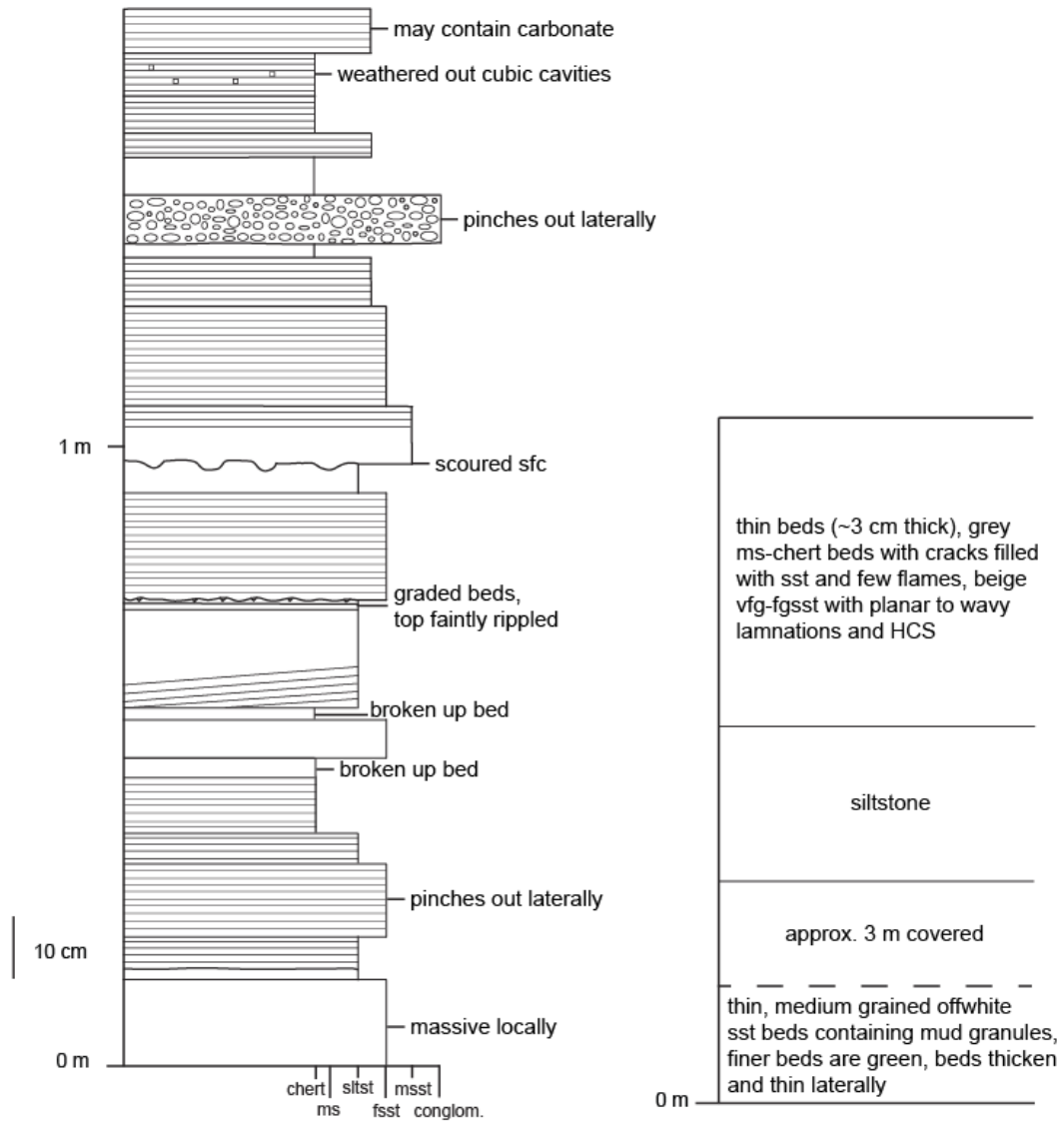
#305 continued



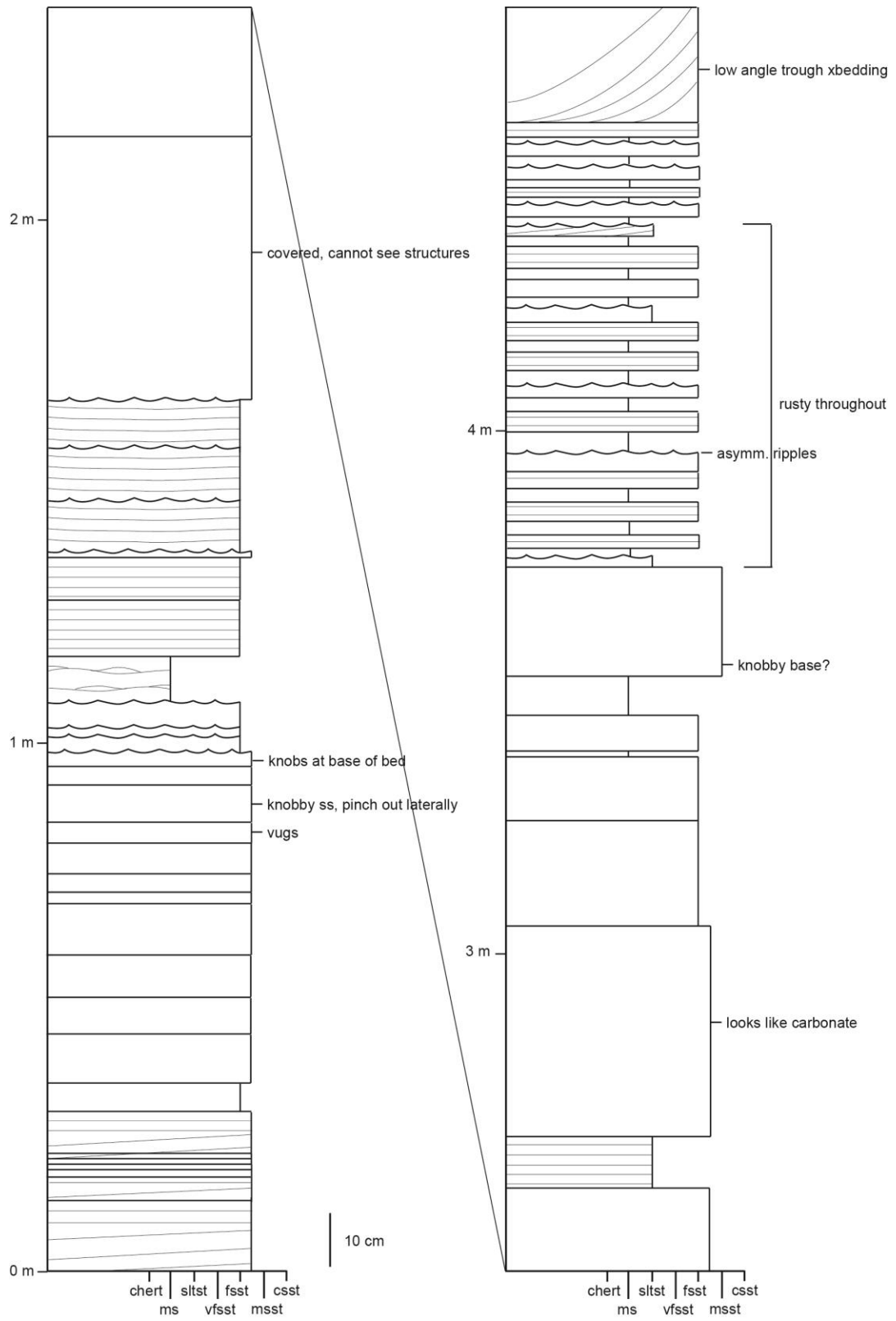
#305 continued



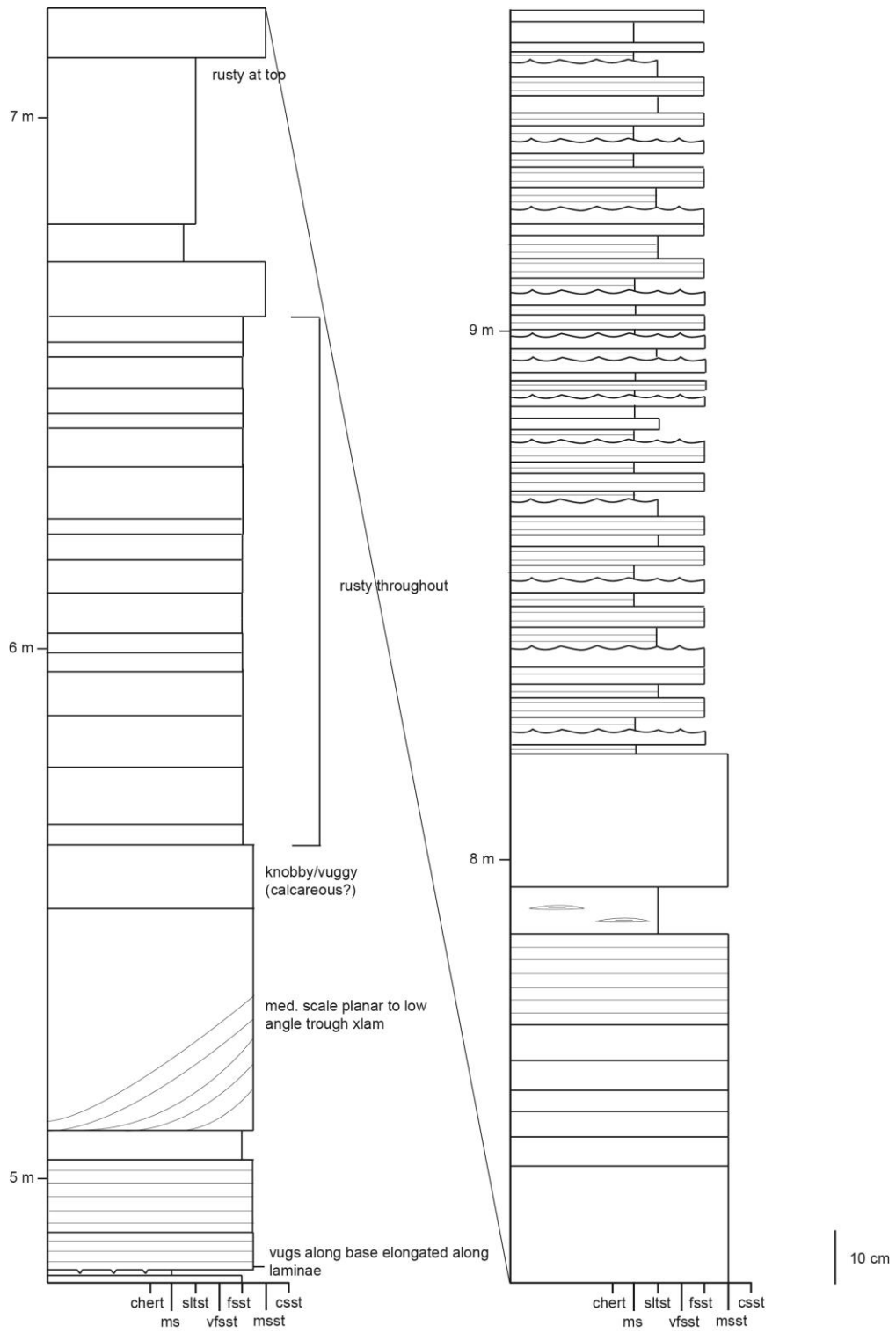
#306 (right) and 309 (left). Note that chert in these sections is silicified mudstone.



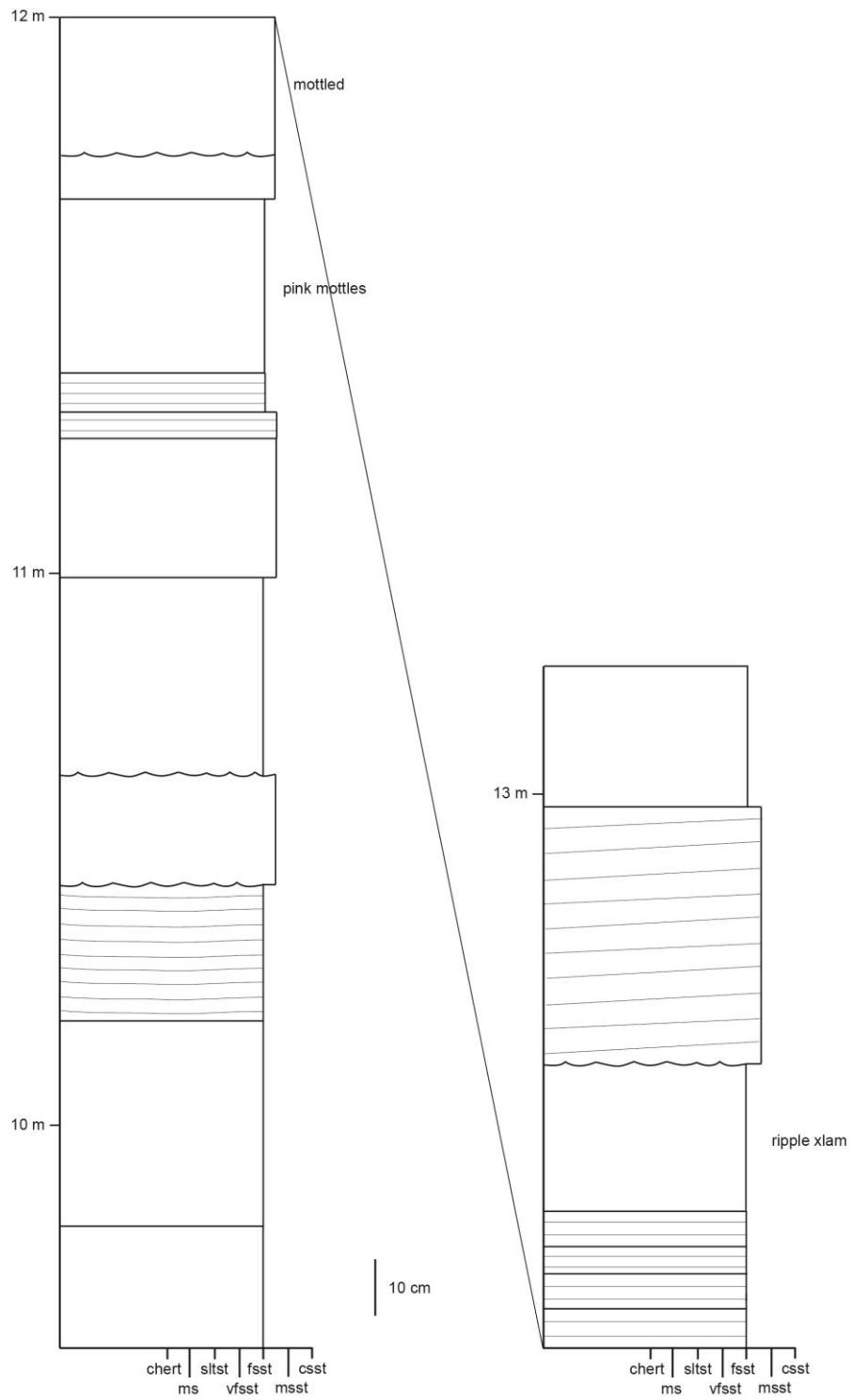
#6



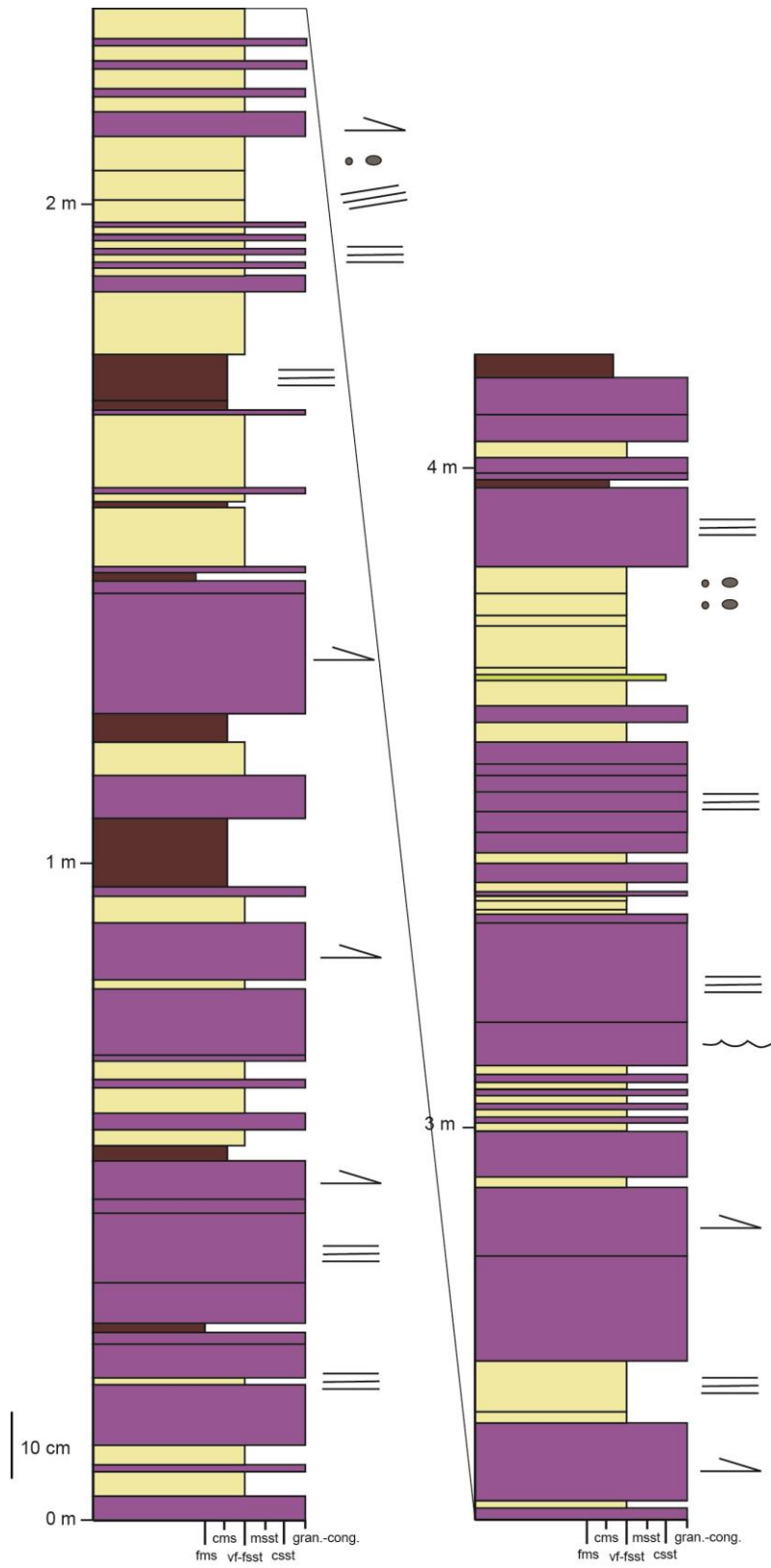
#6 continued



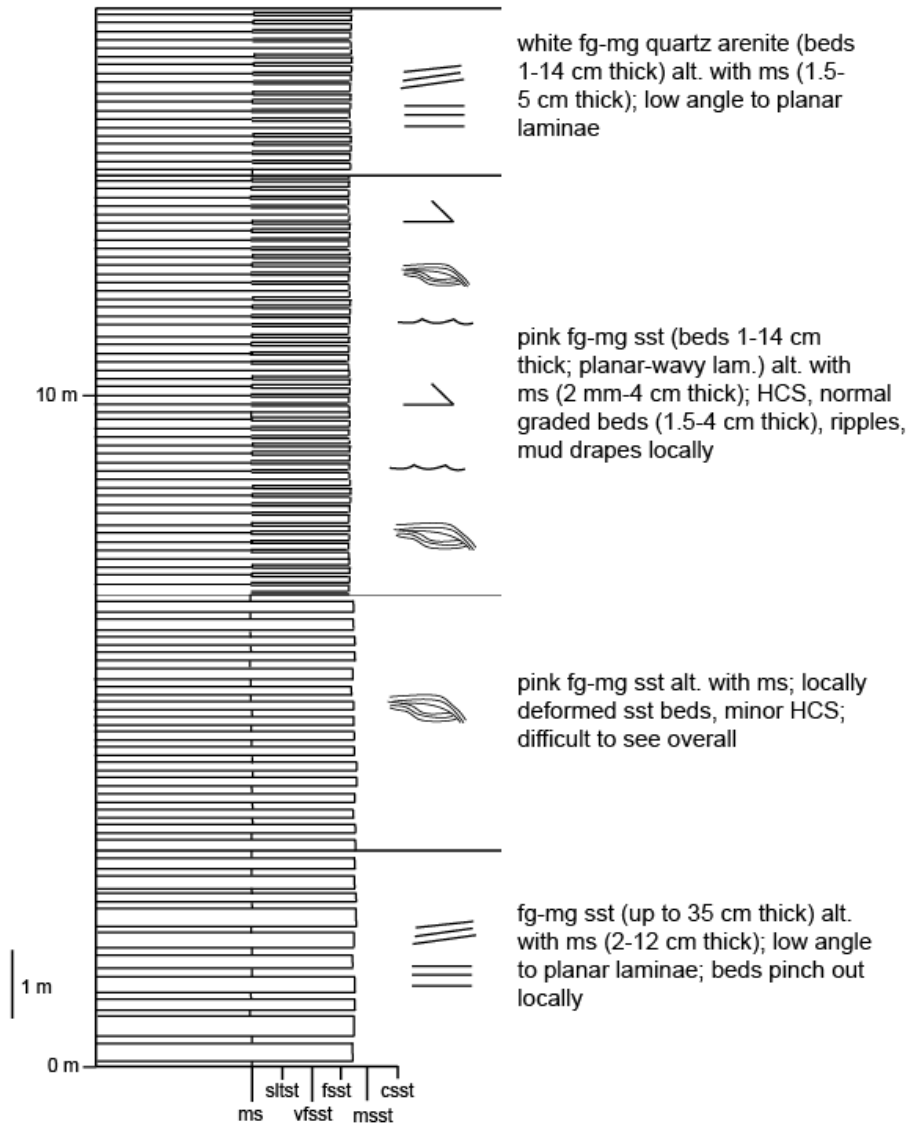
#6 continued



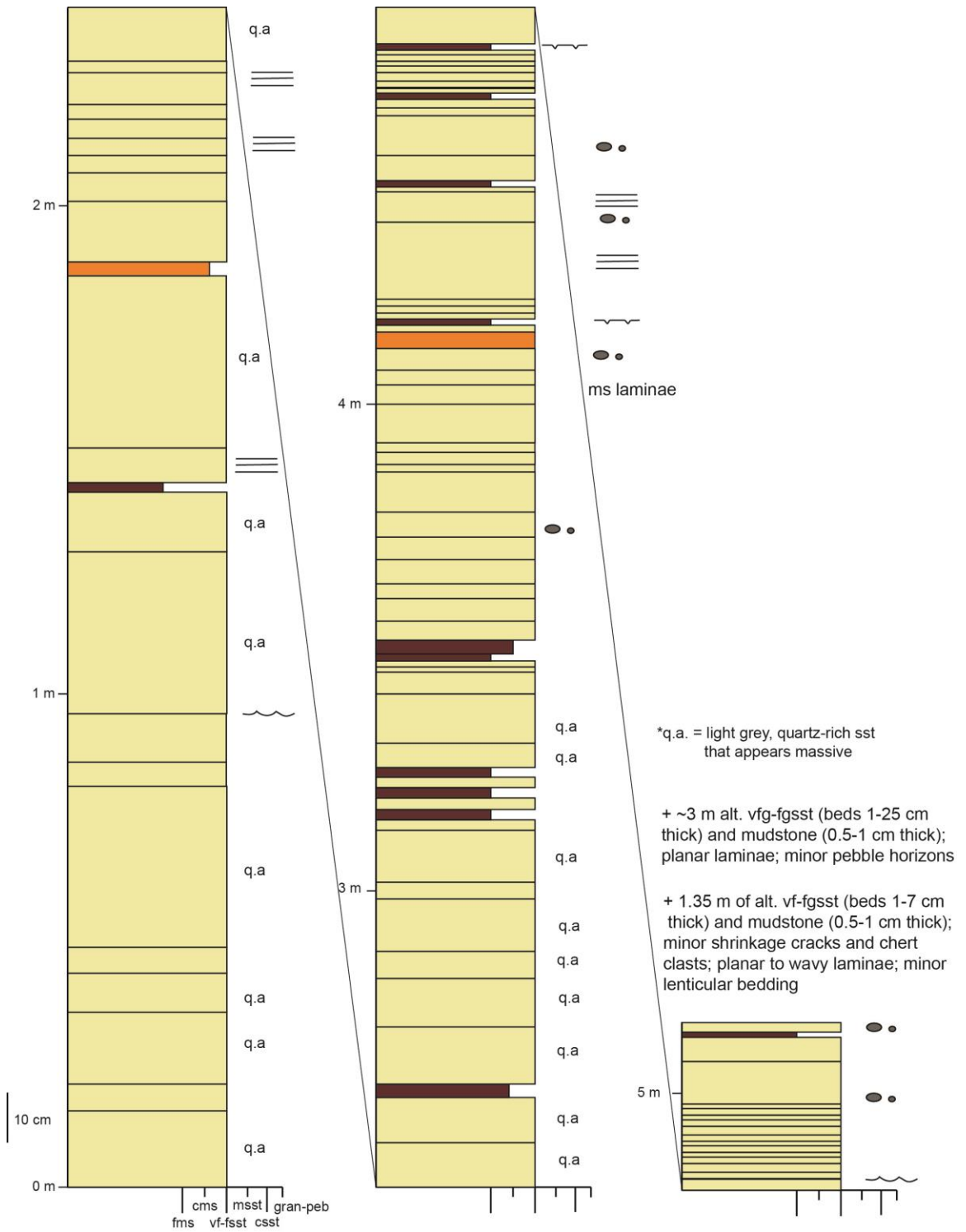
#684



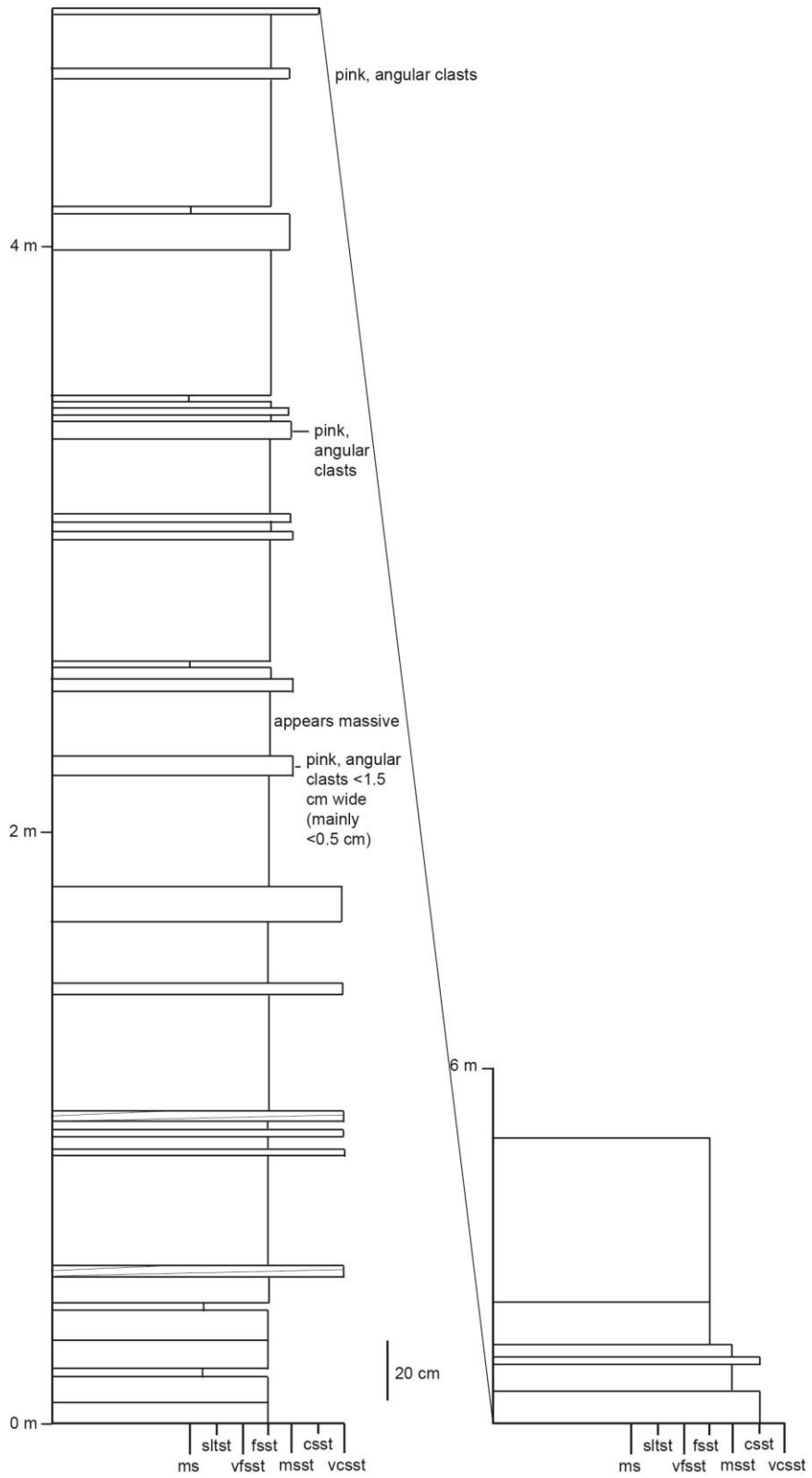
#322



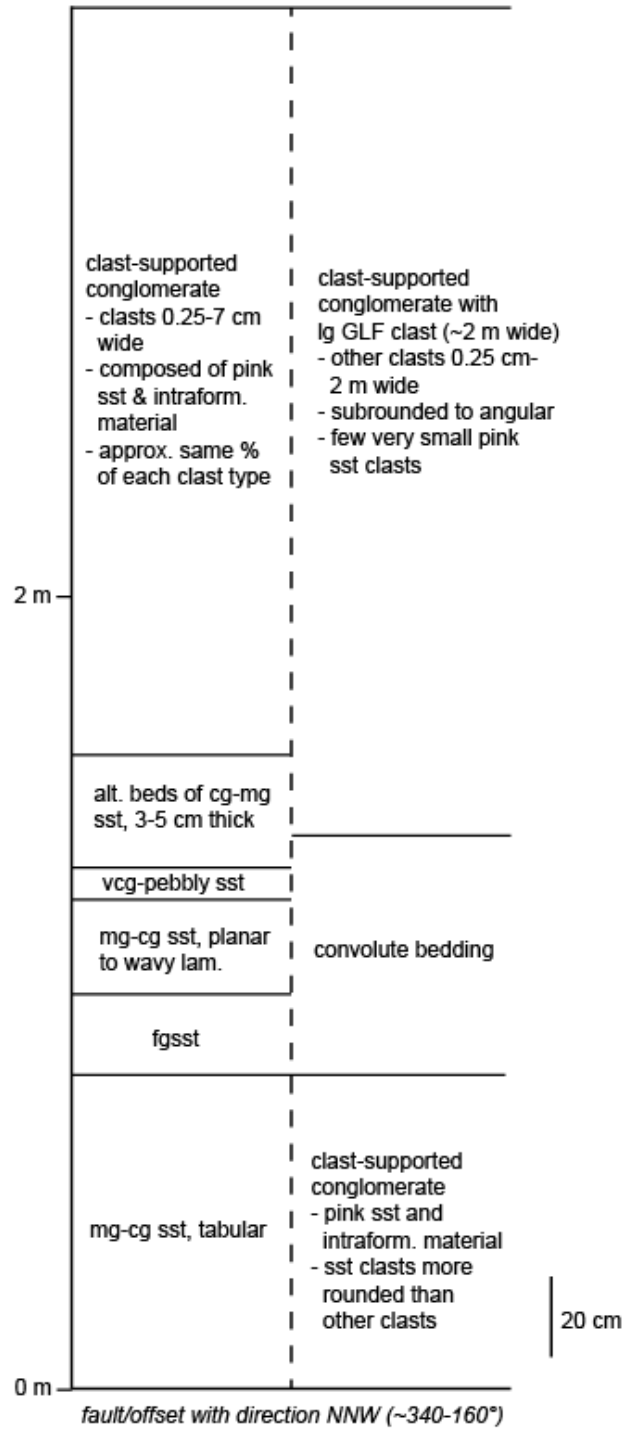
#323



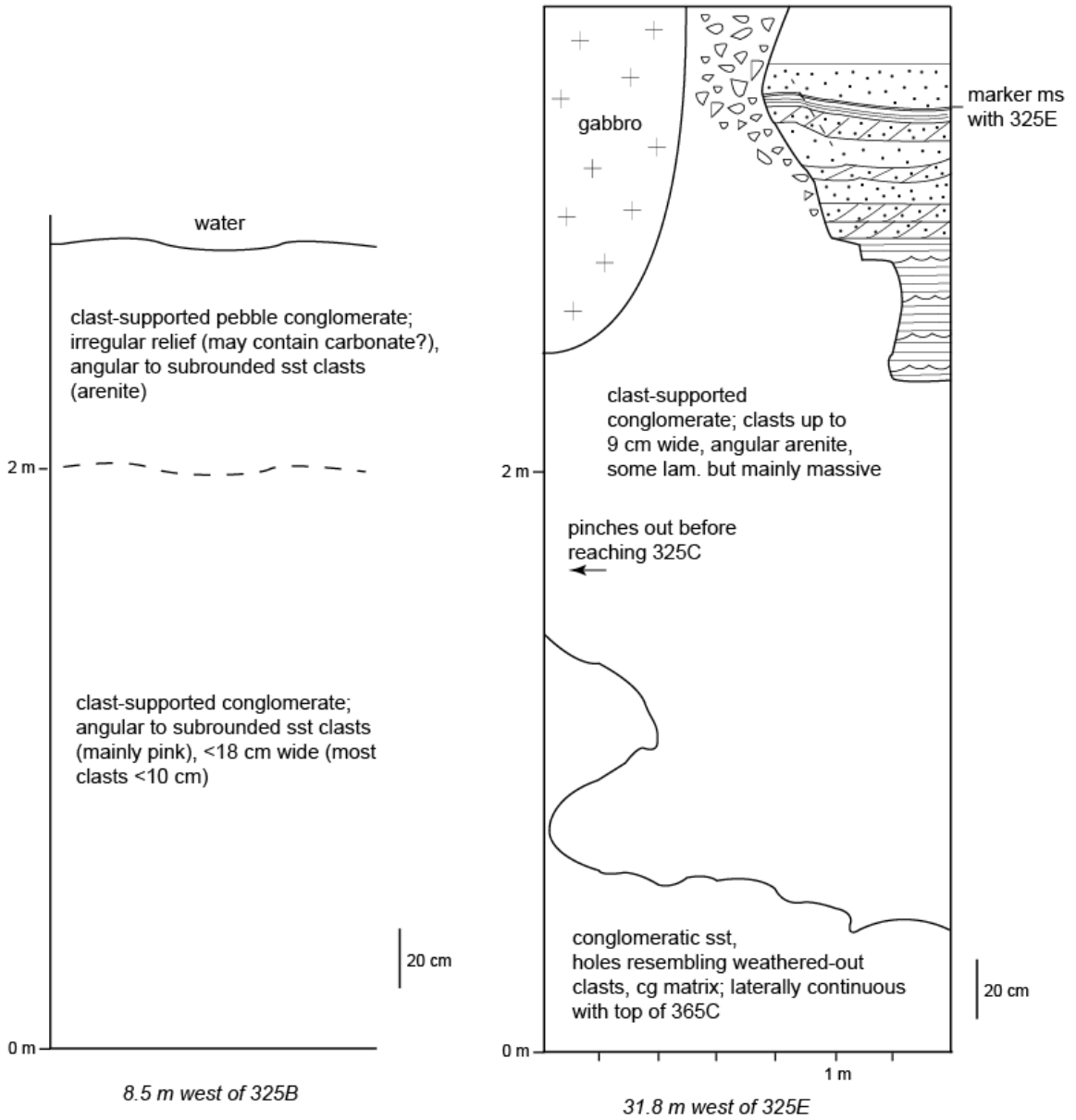
#325A



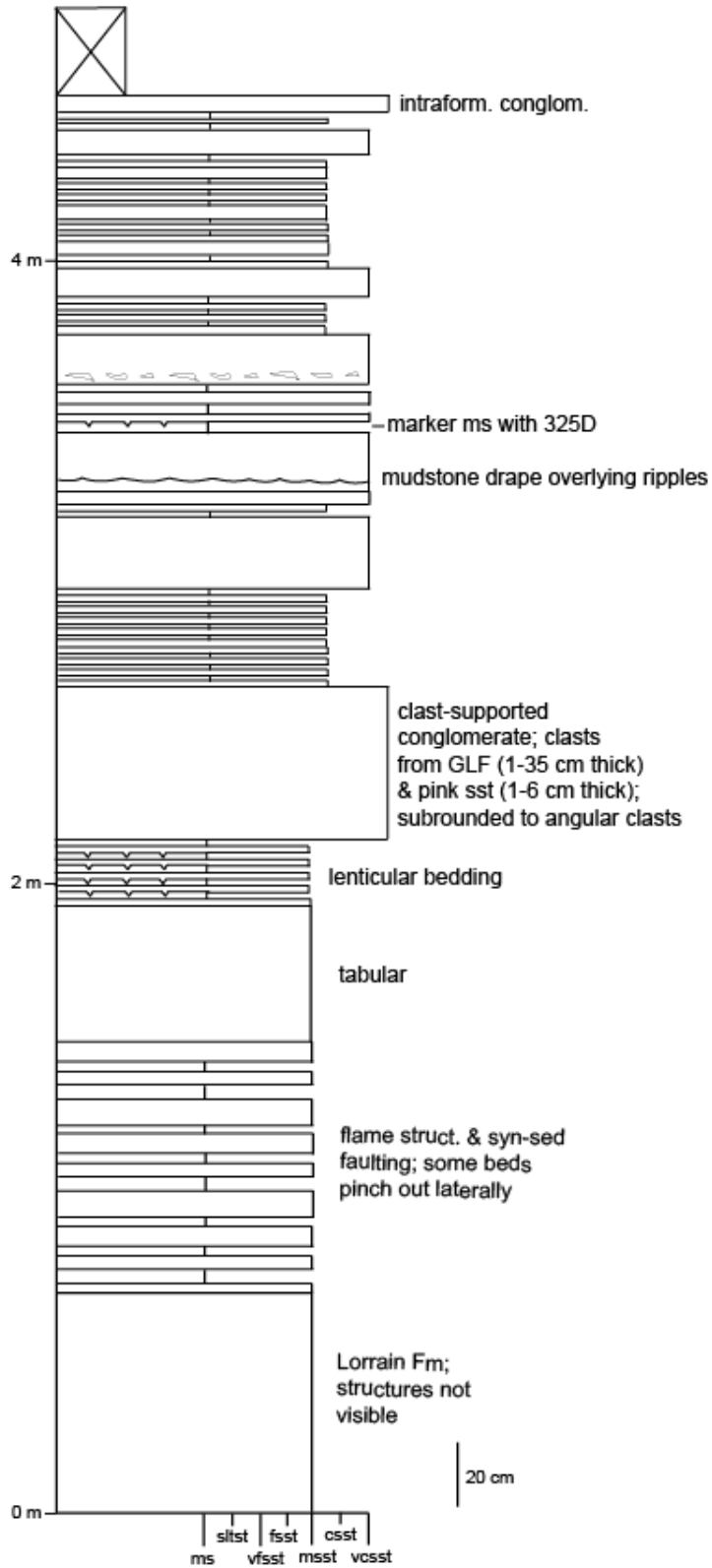
#325B



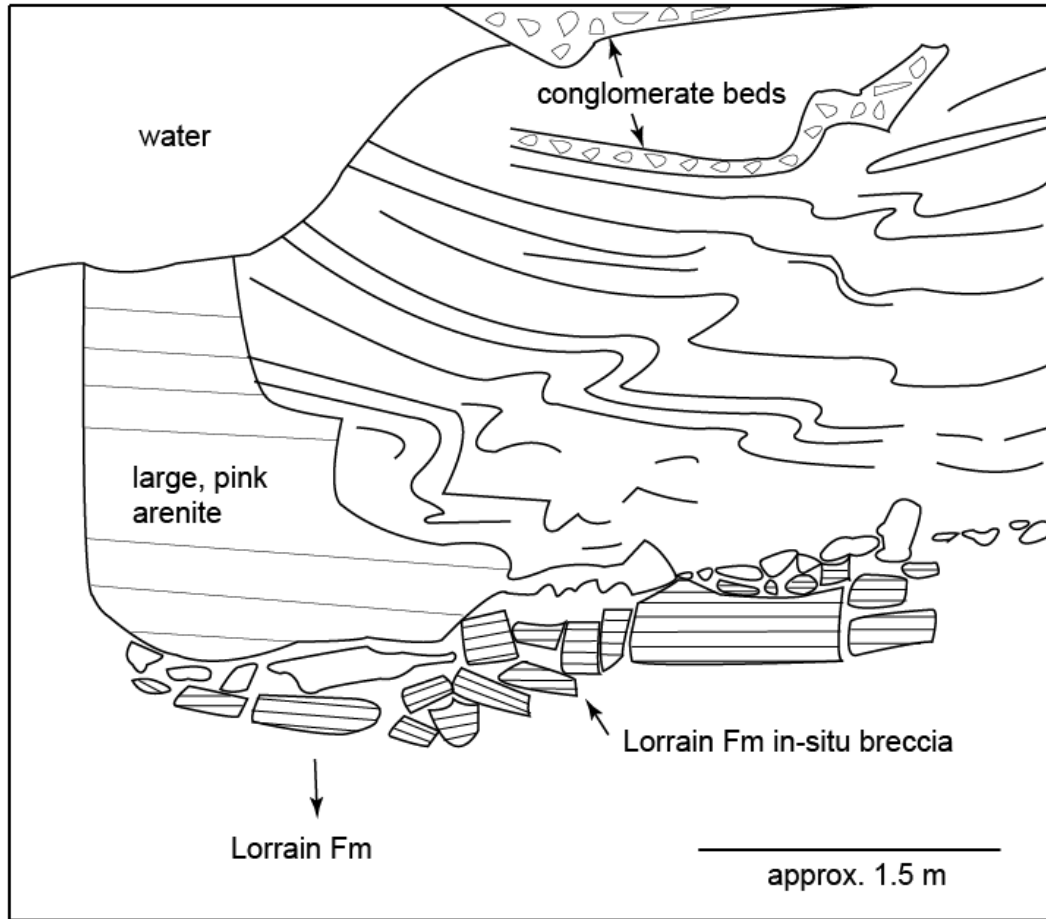
#325C (left) and #325D (right)



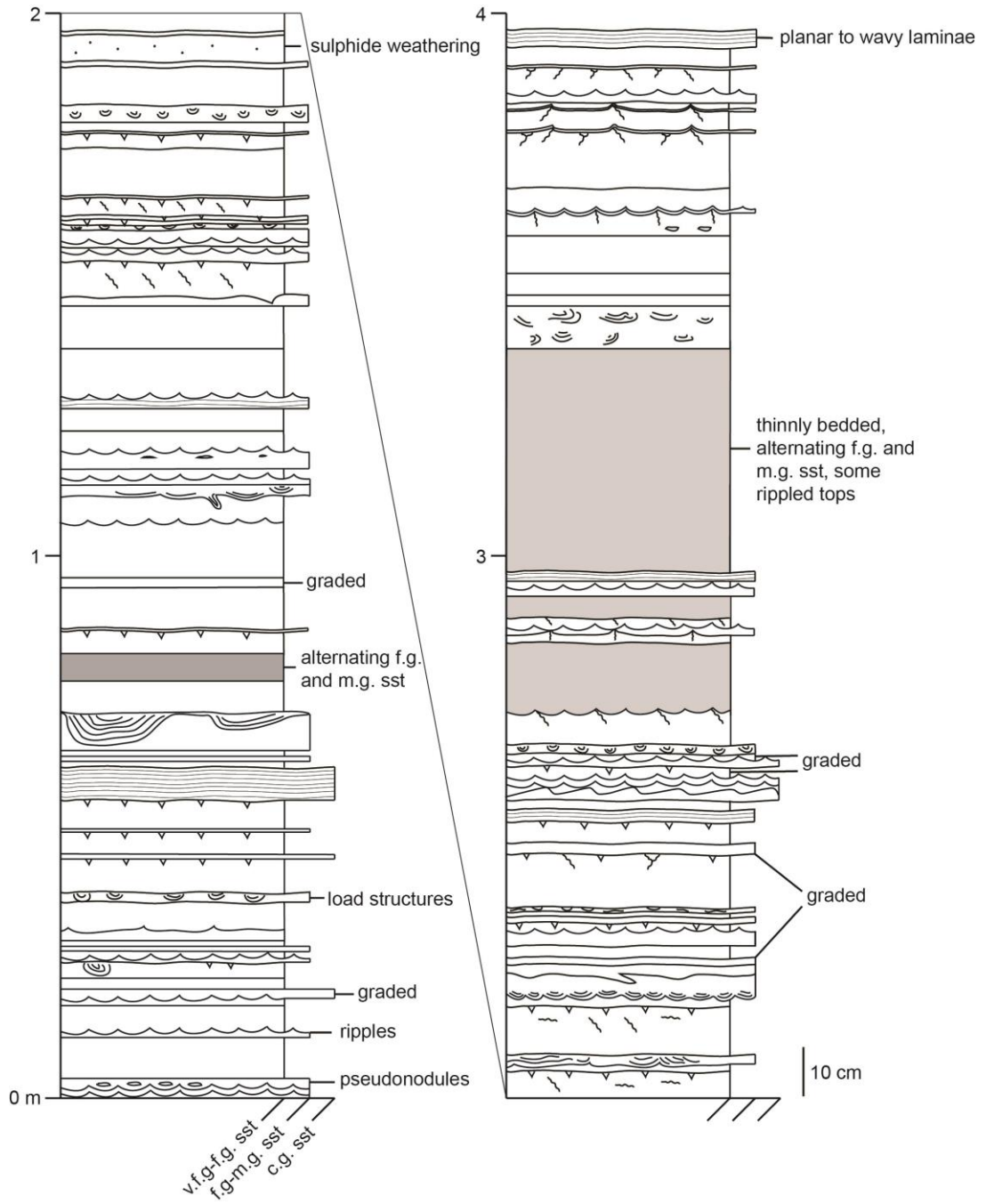
#325E



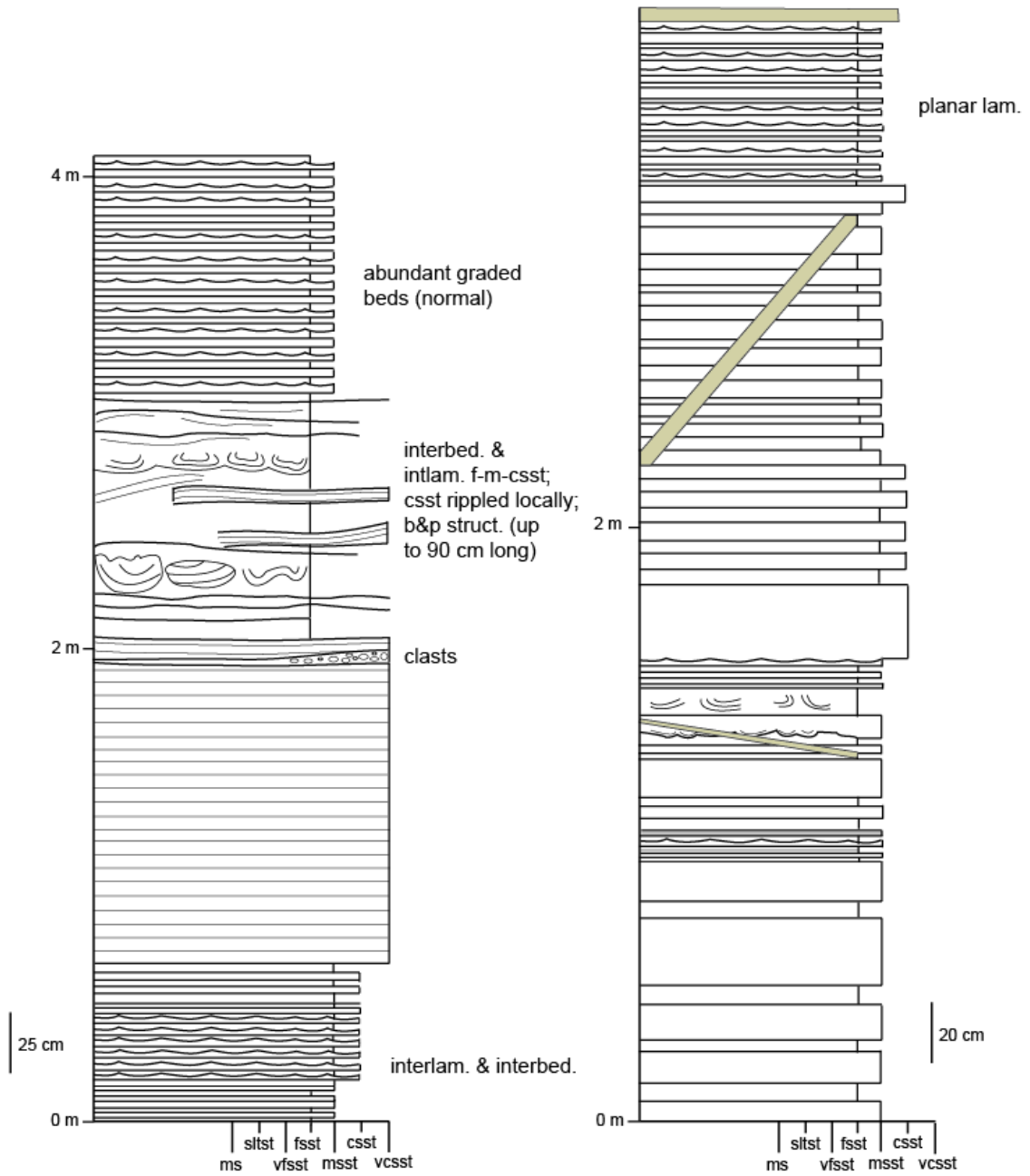
#325F



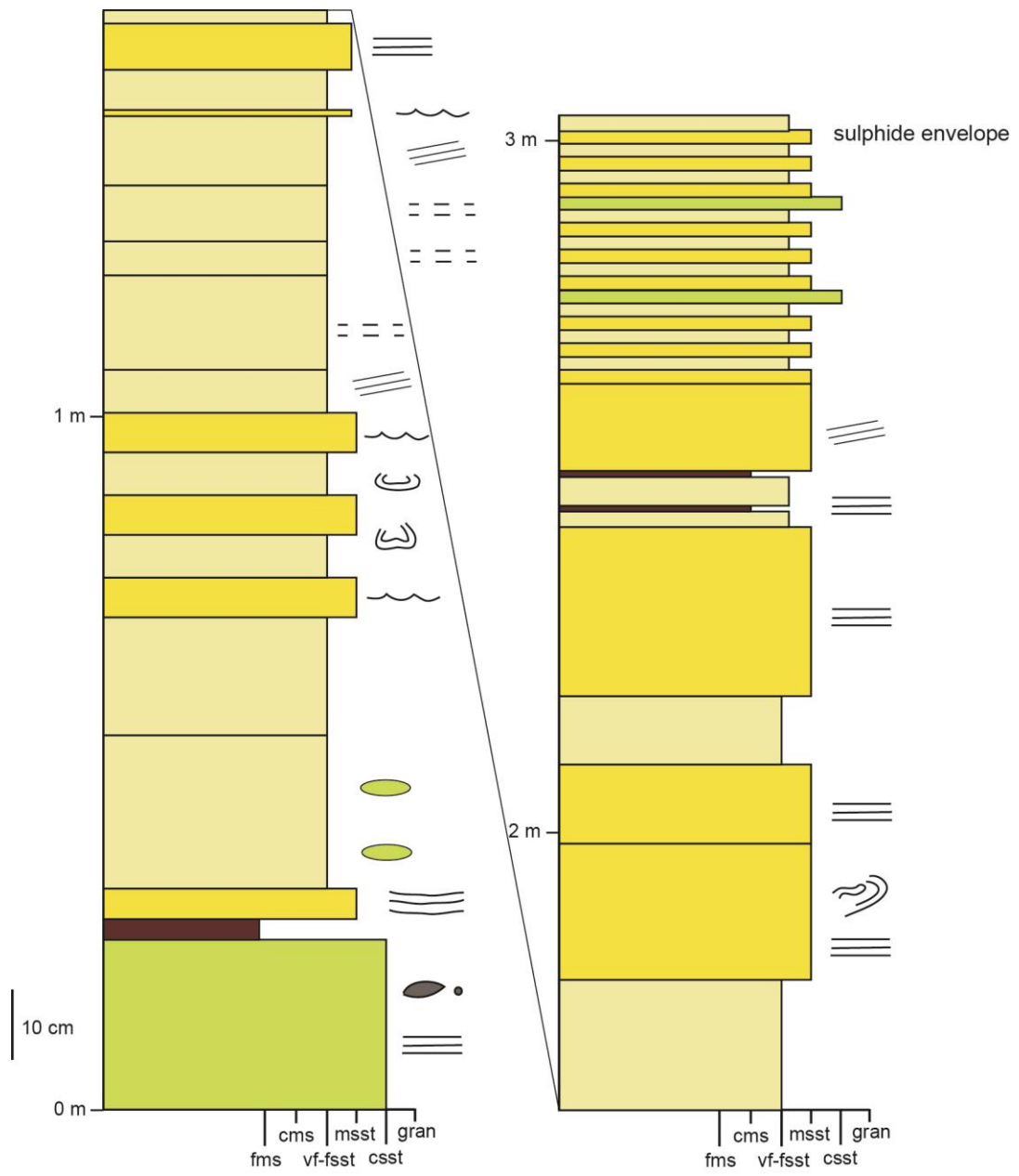
#335 lower



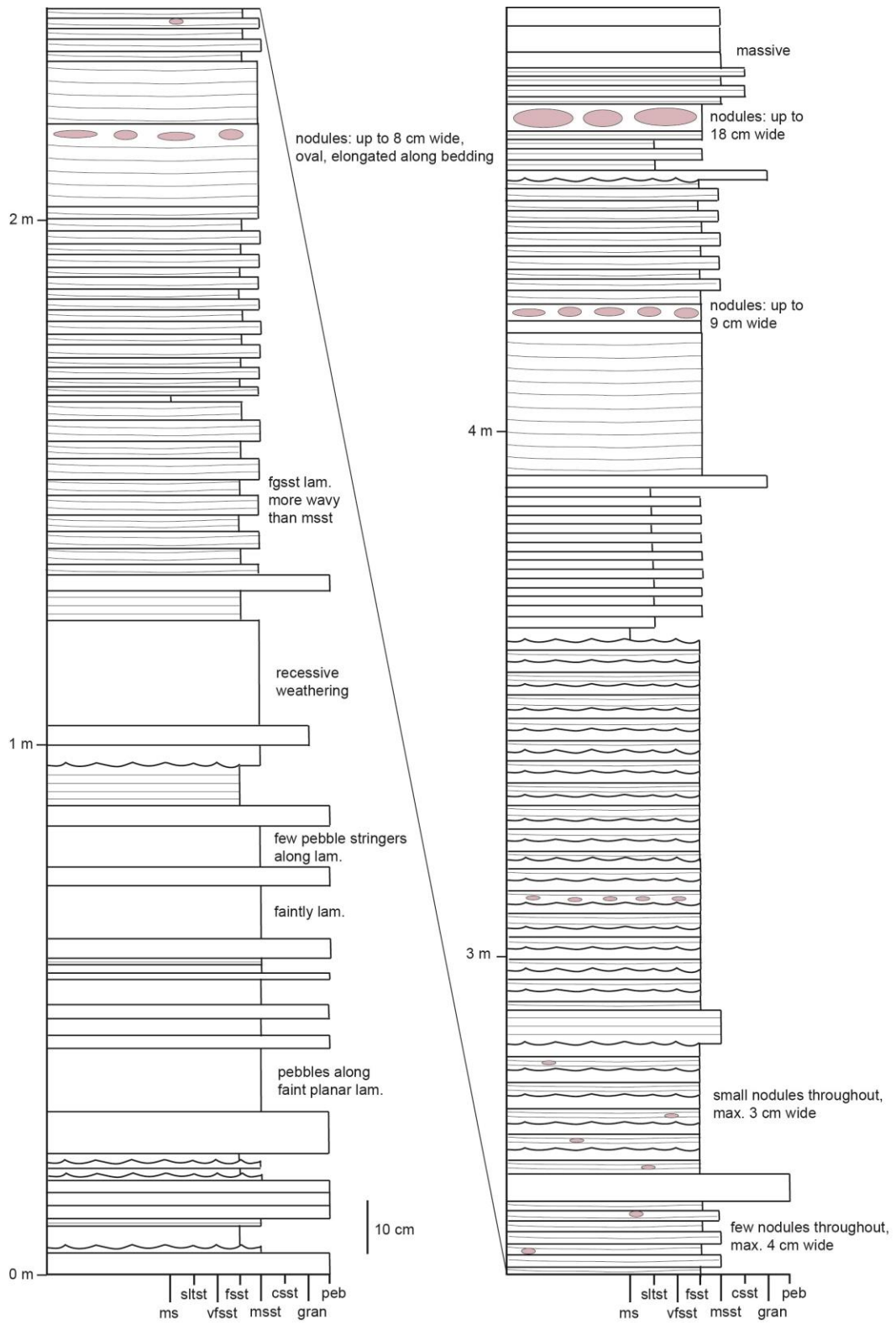
#339 lower (left) and upper (right)



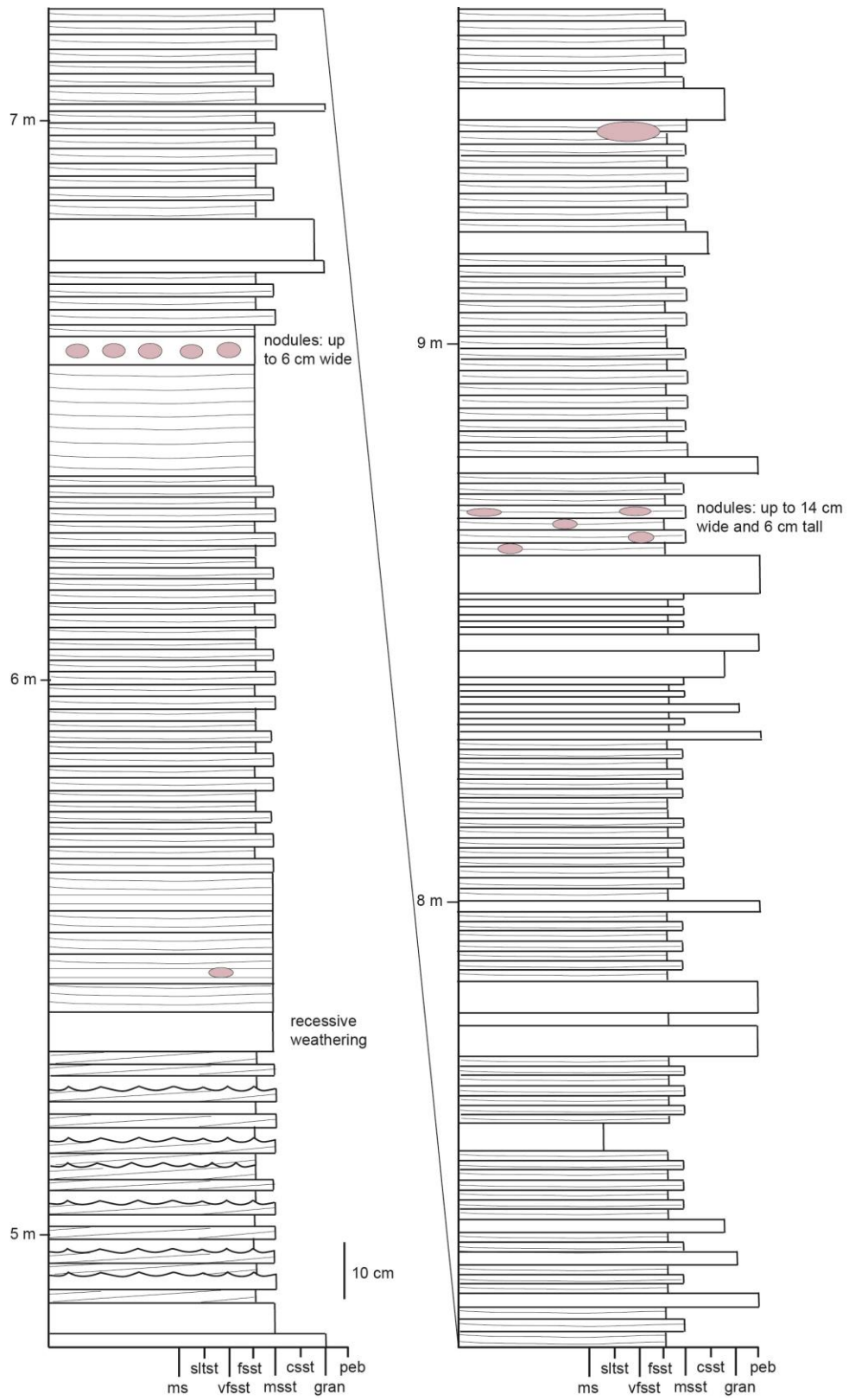
#340



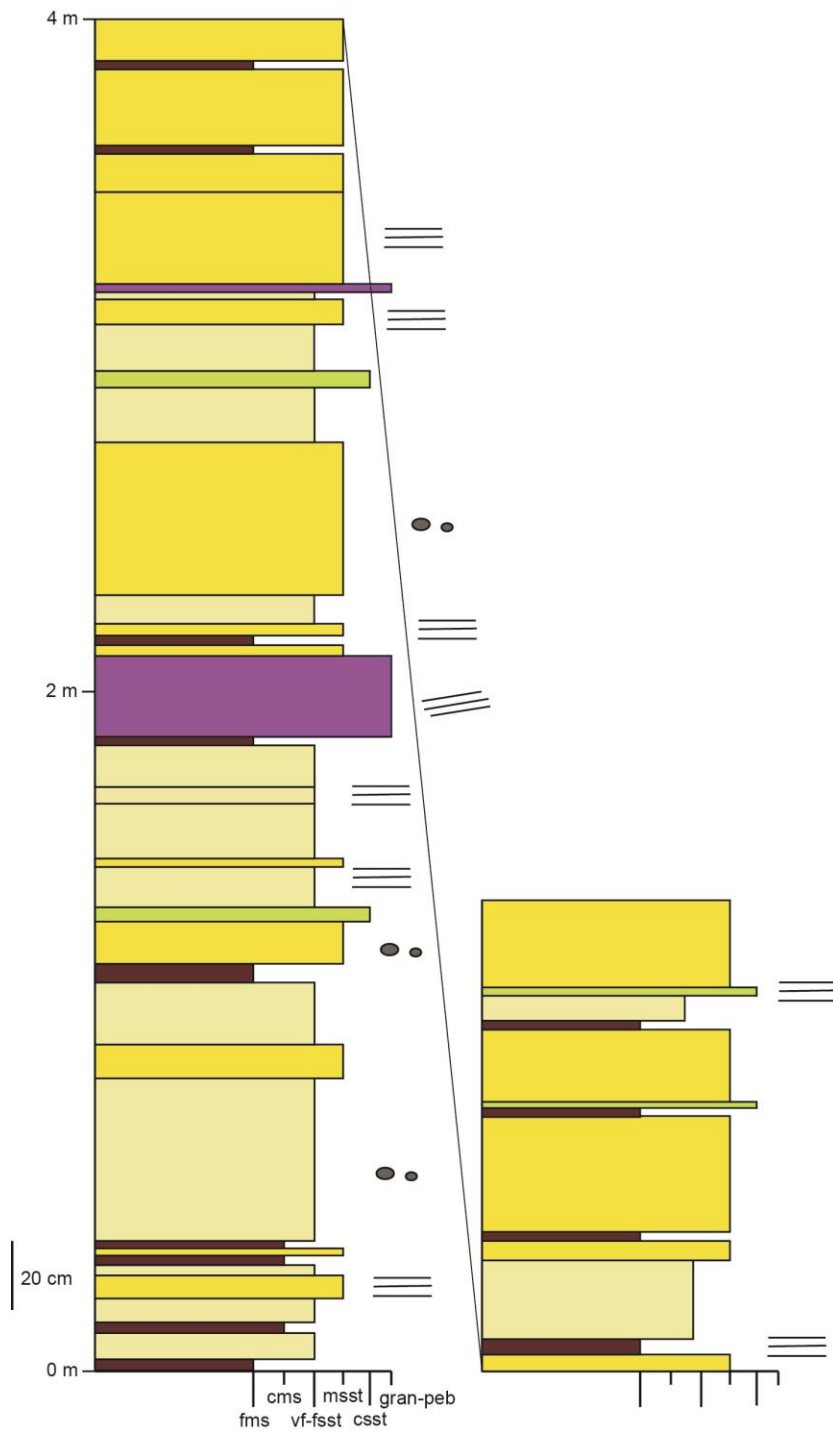
#342



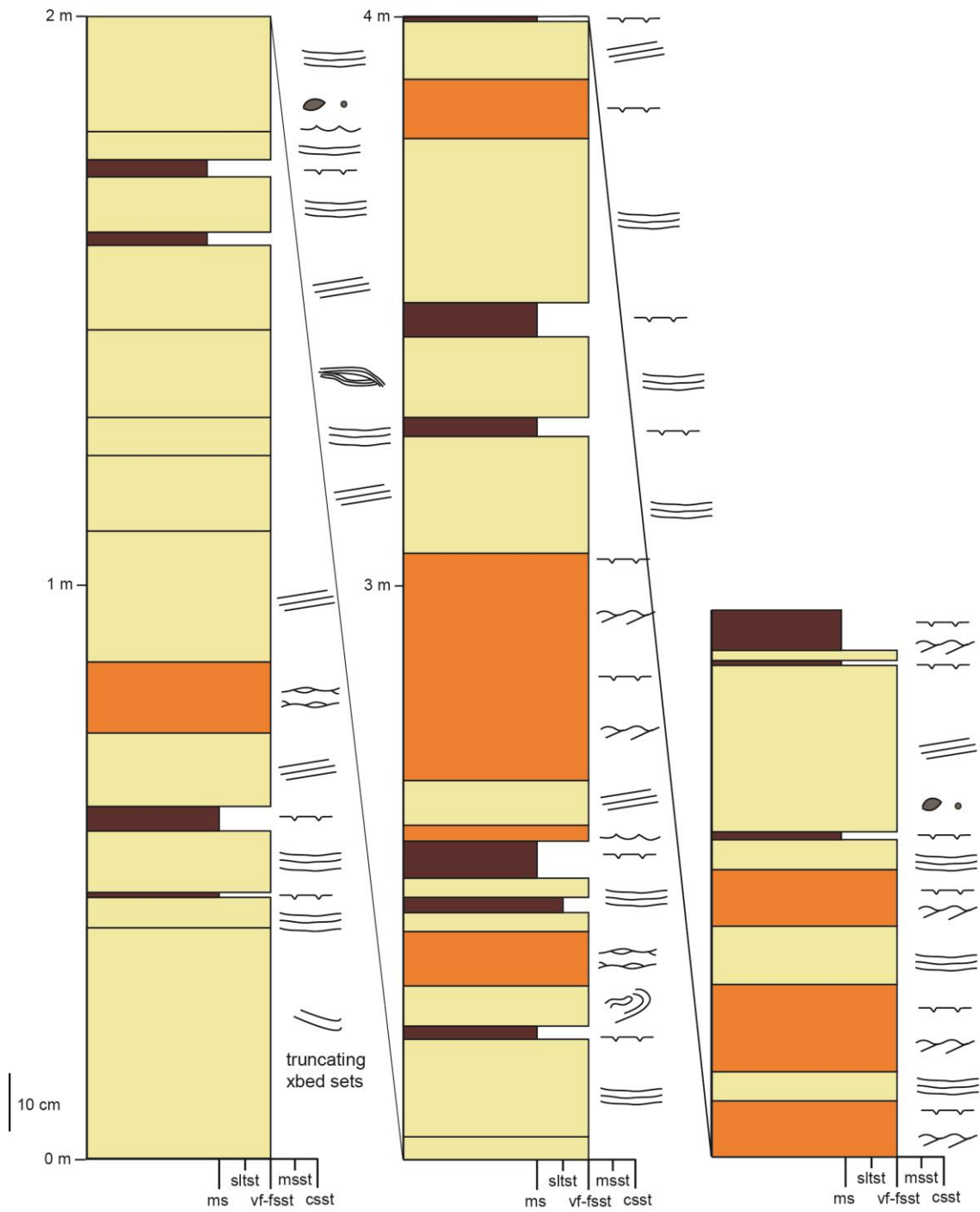
#342 continued



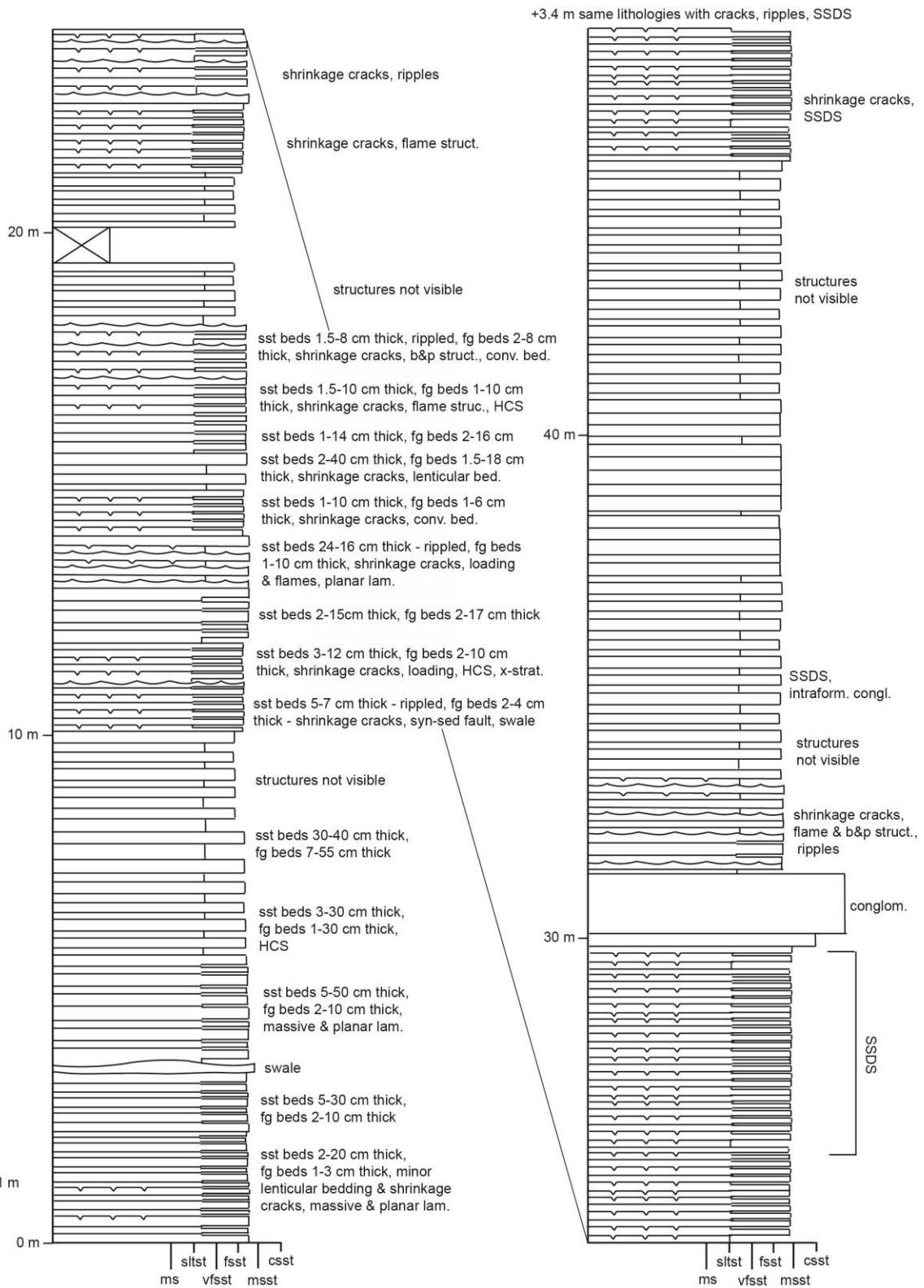
#345



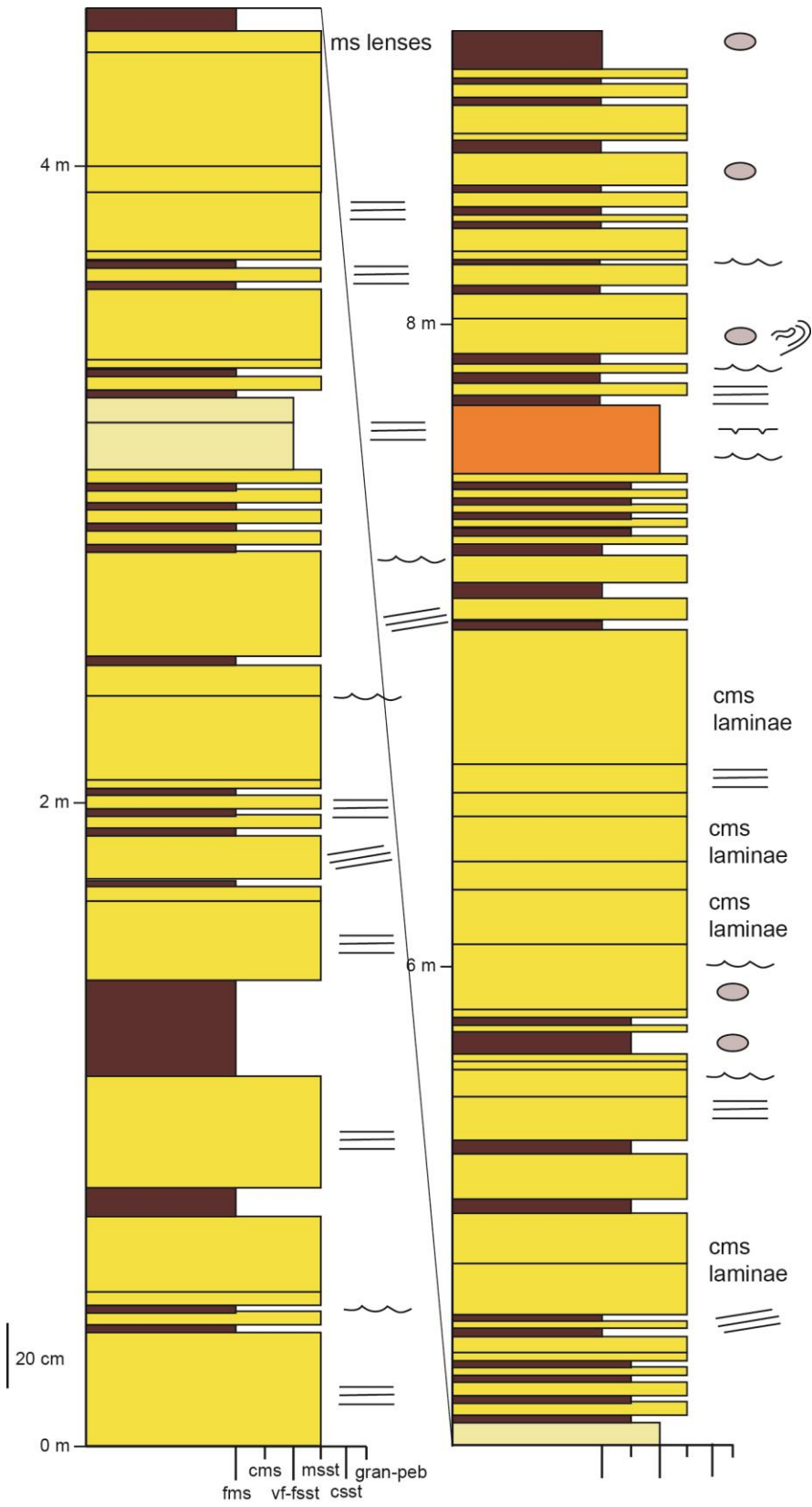
#349



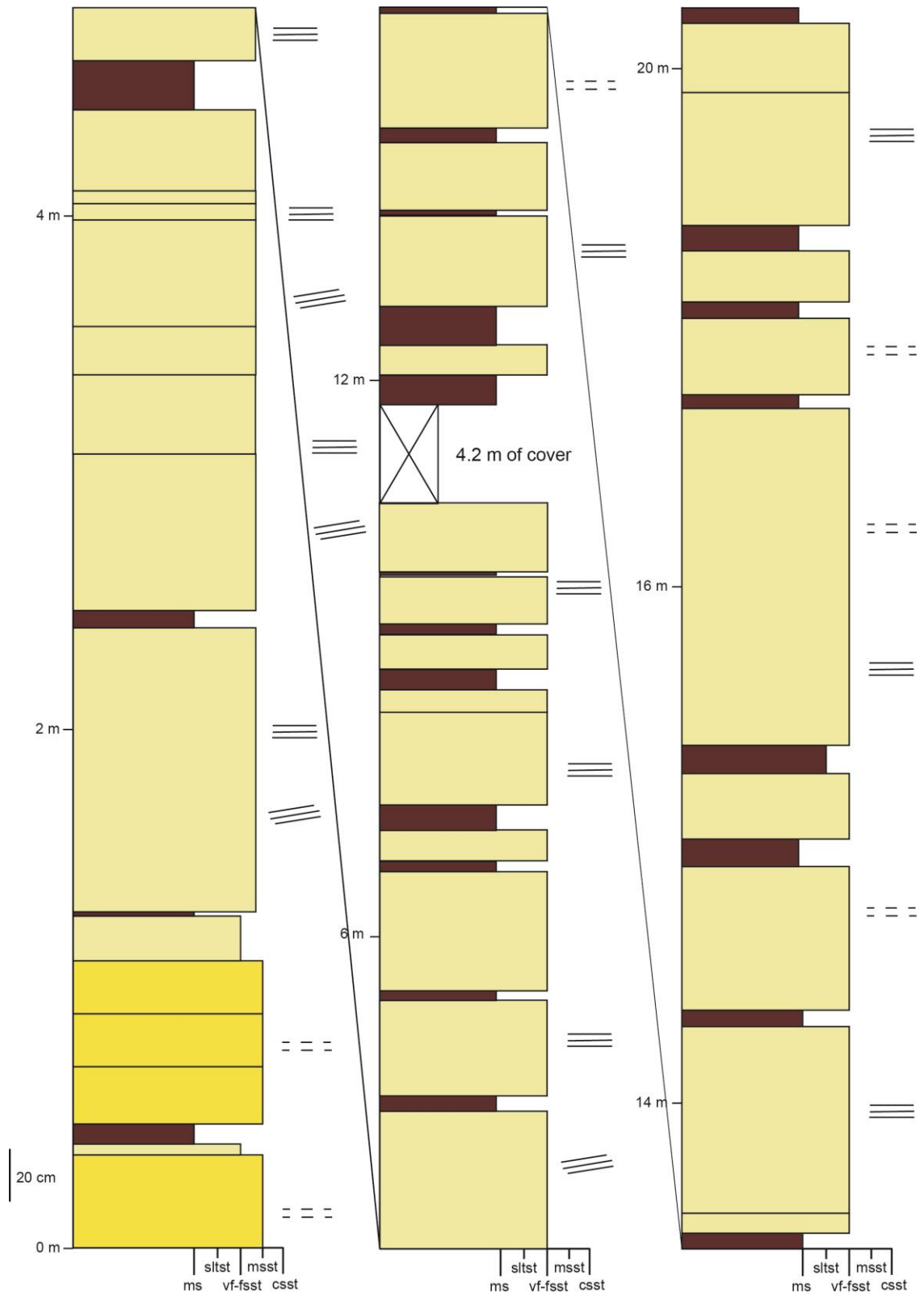
#350



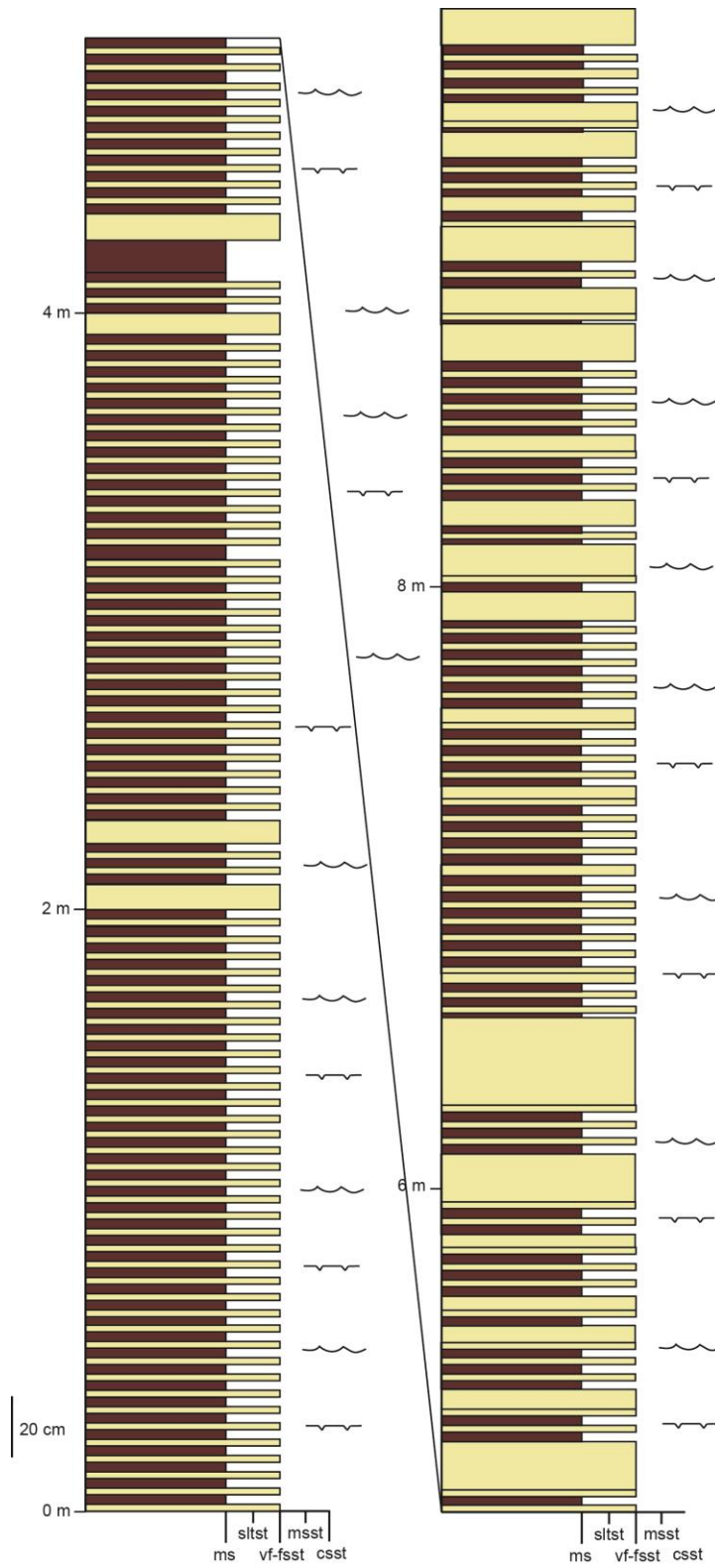
#353



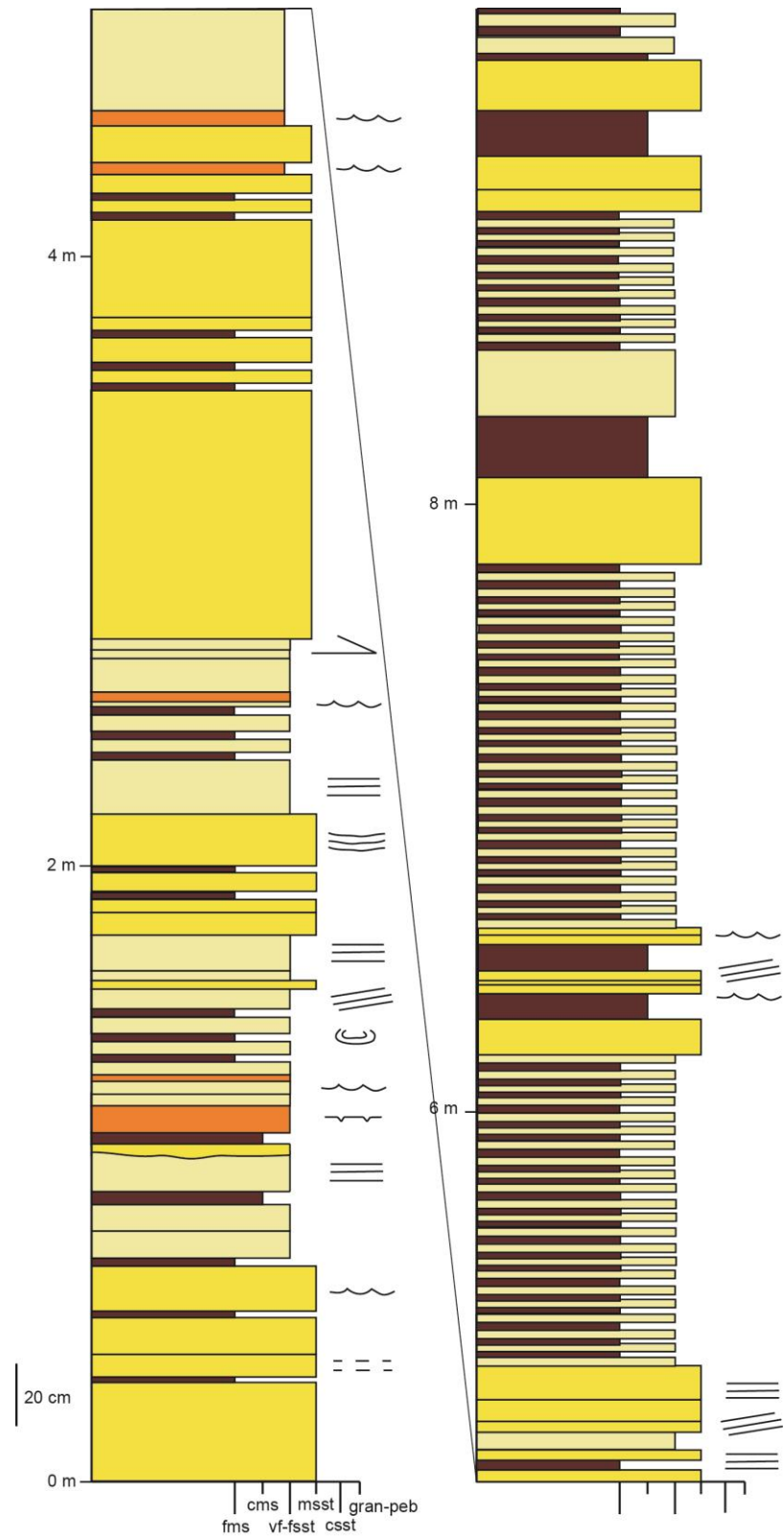
#361



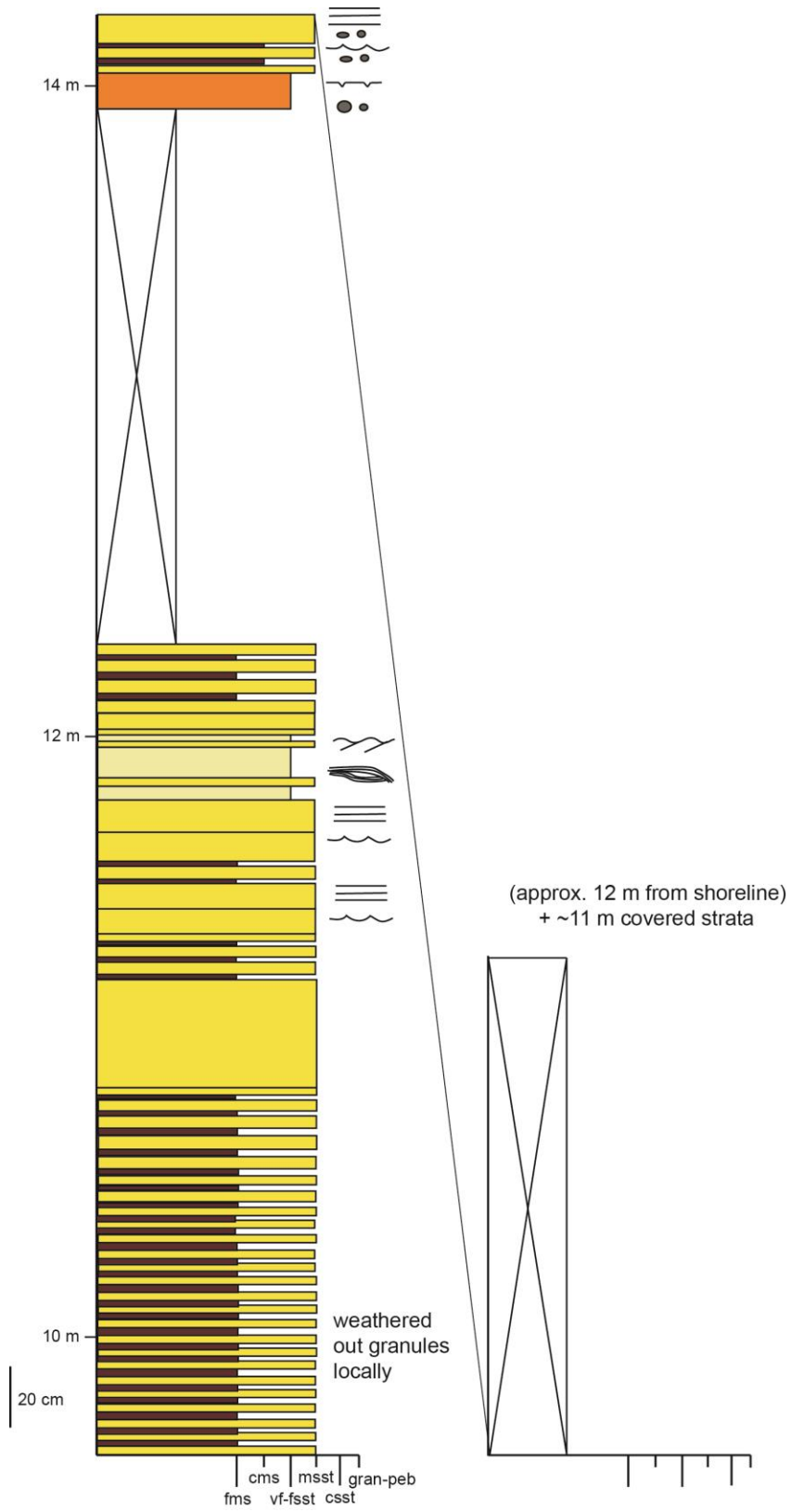
#364



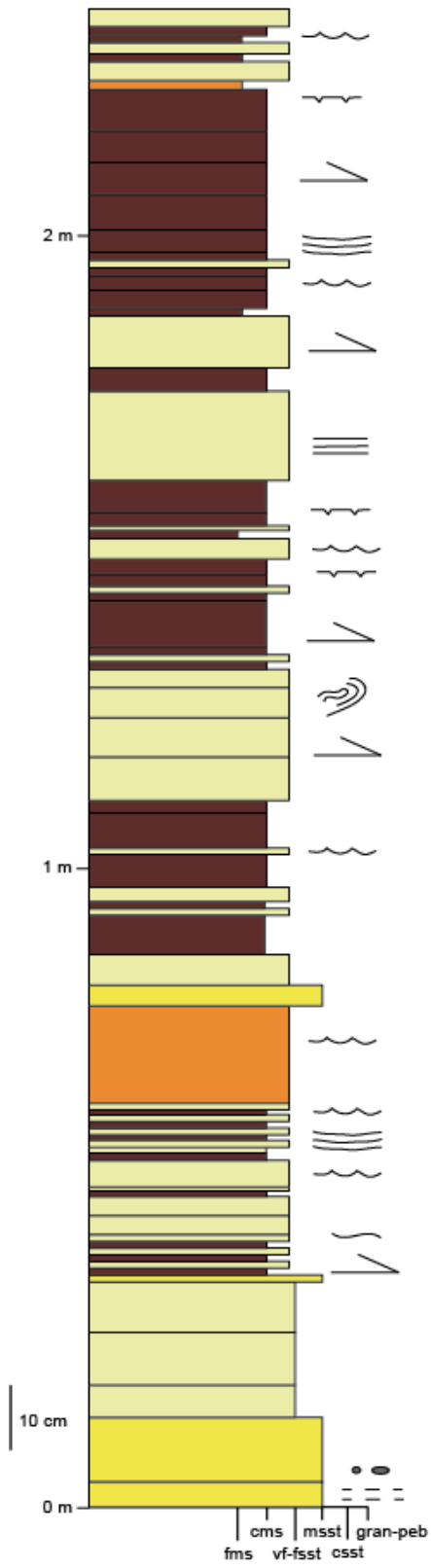
#467



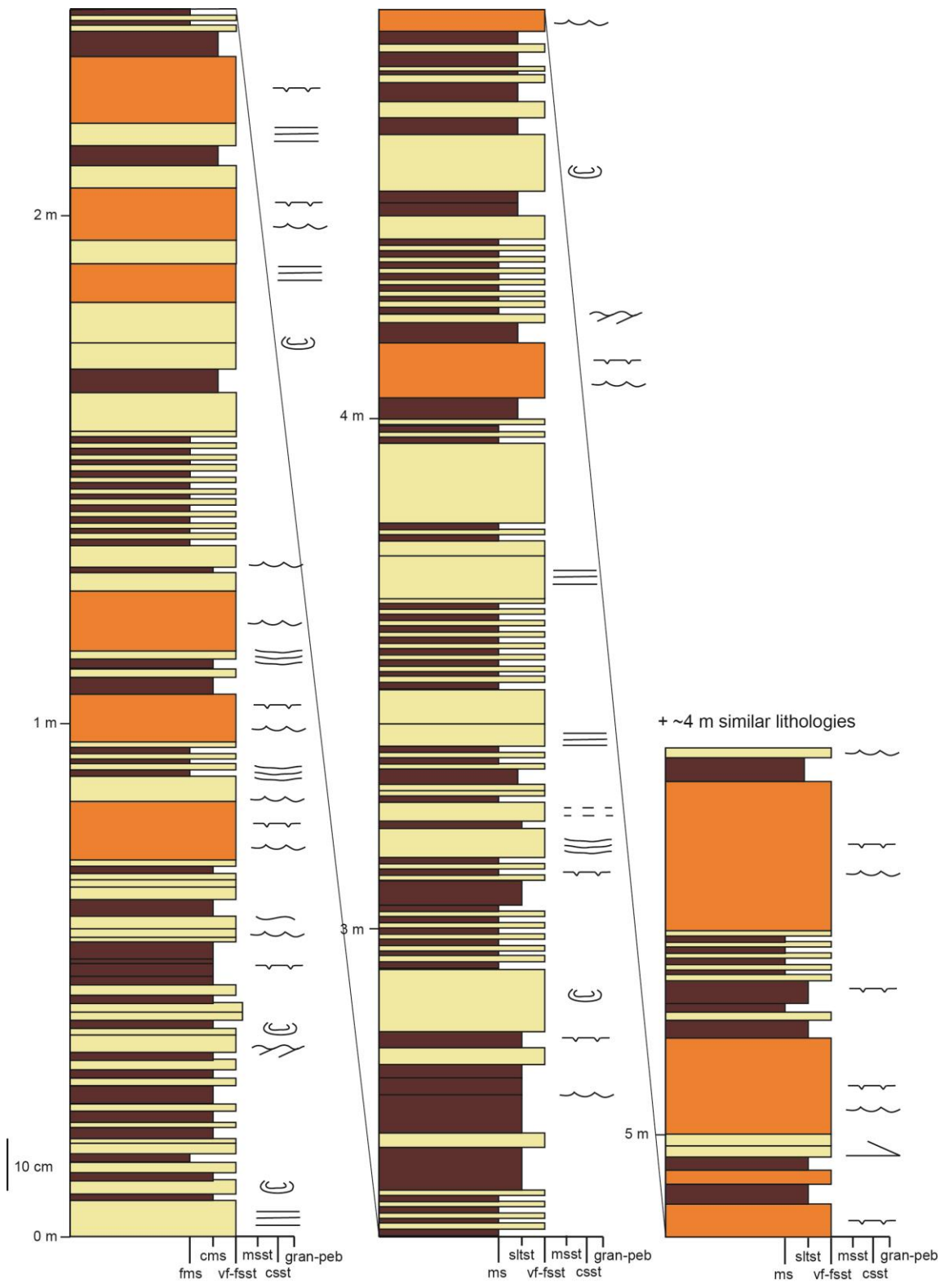
#467 continued



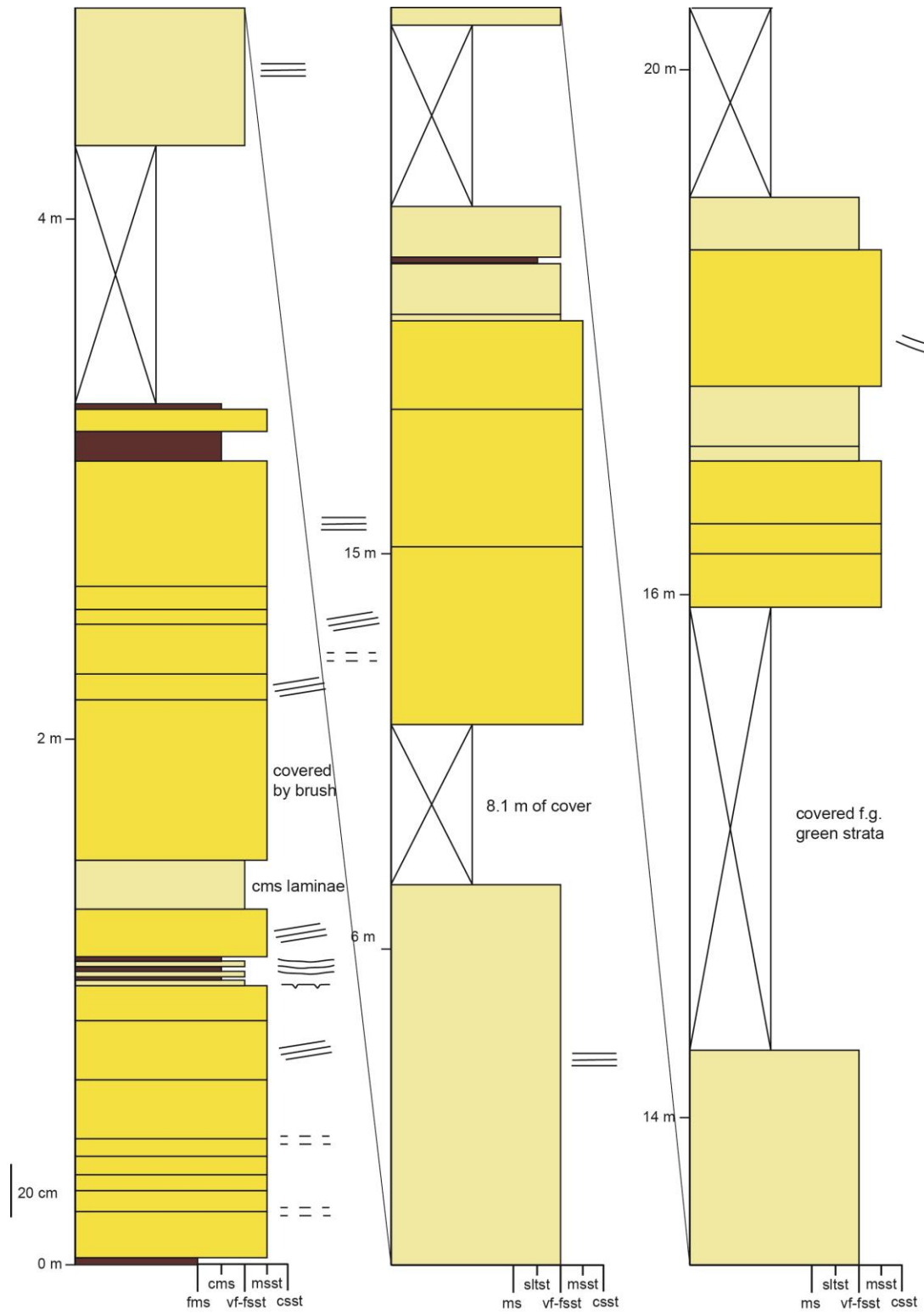
#569



#575

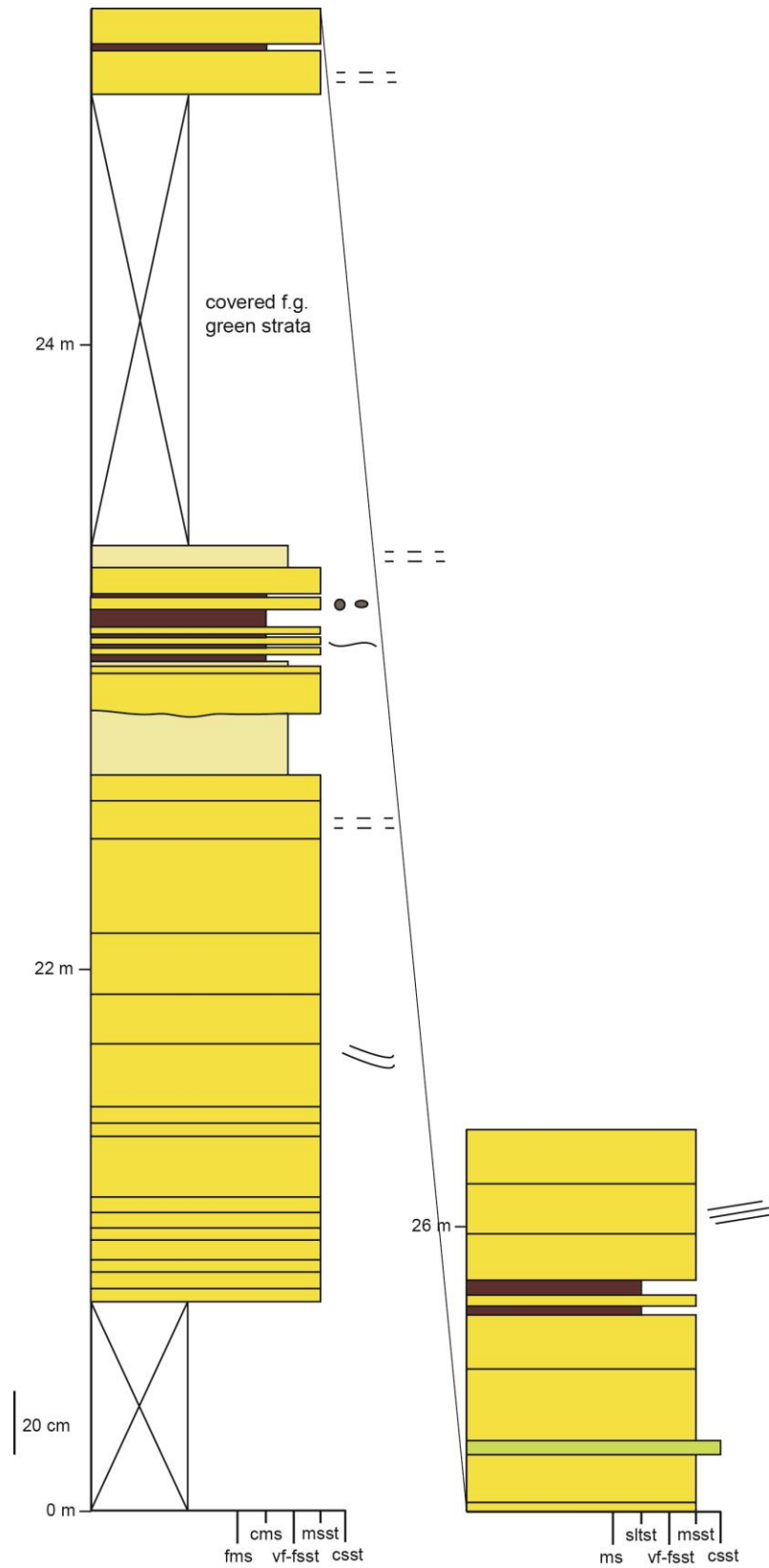


#580

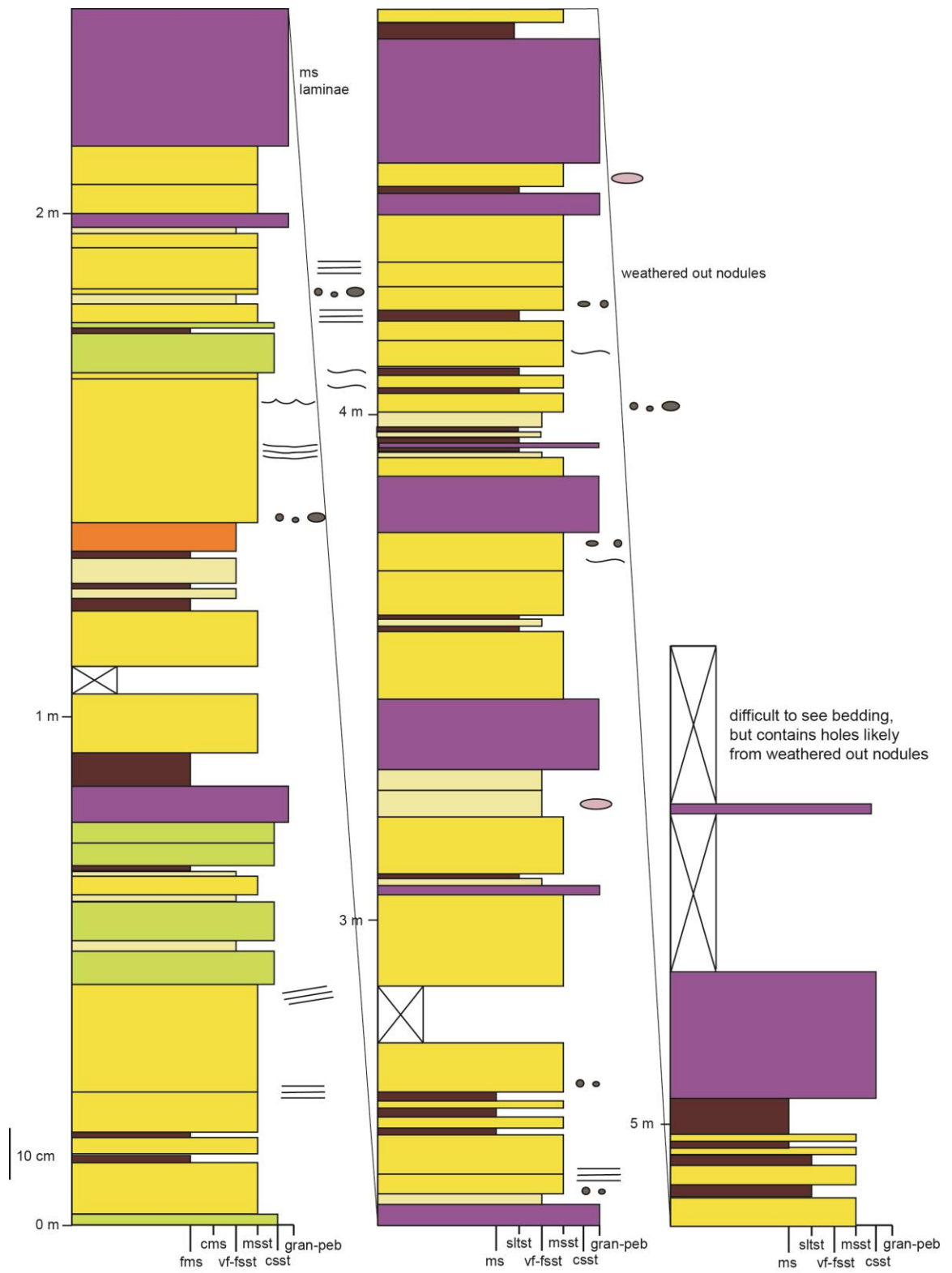


underlain by ~4m very covered thinly bedded, green f.g. sst and ms beds; shrinkage cracks, ripples

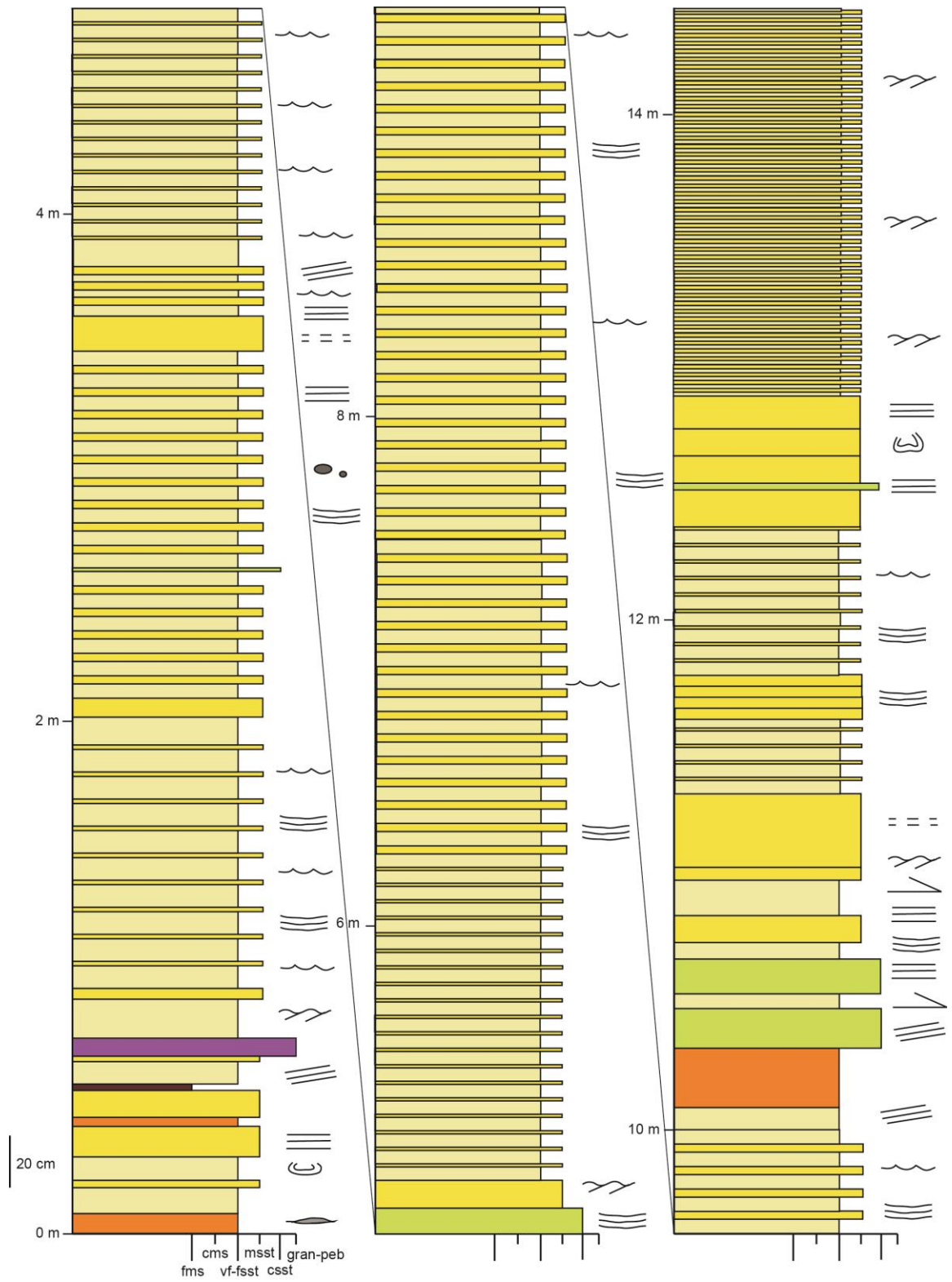
#580 continued



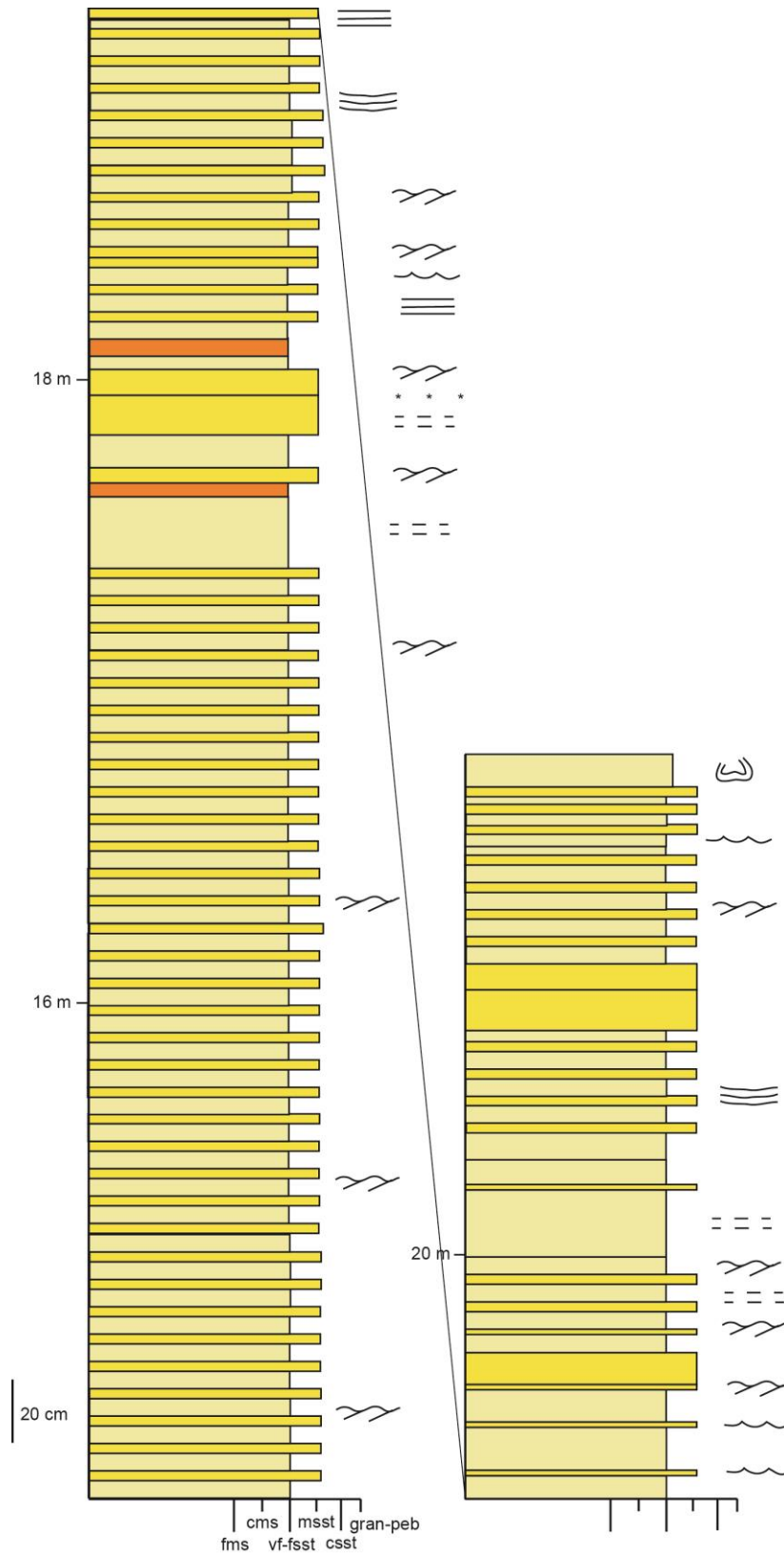
#603



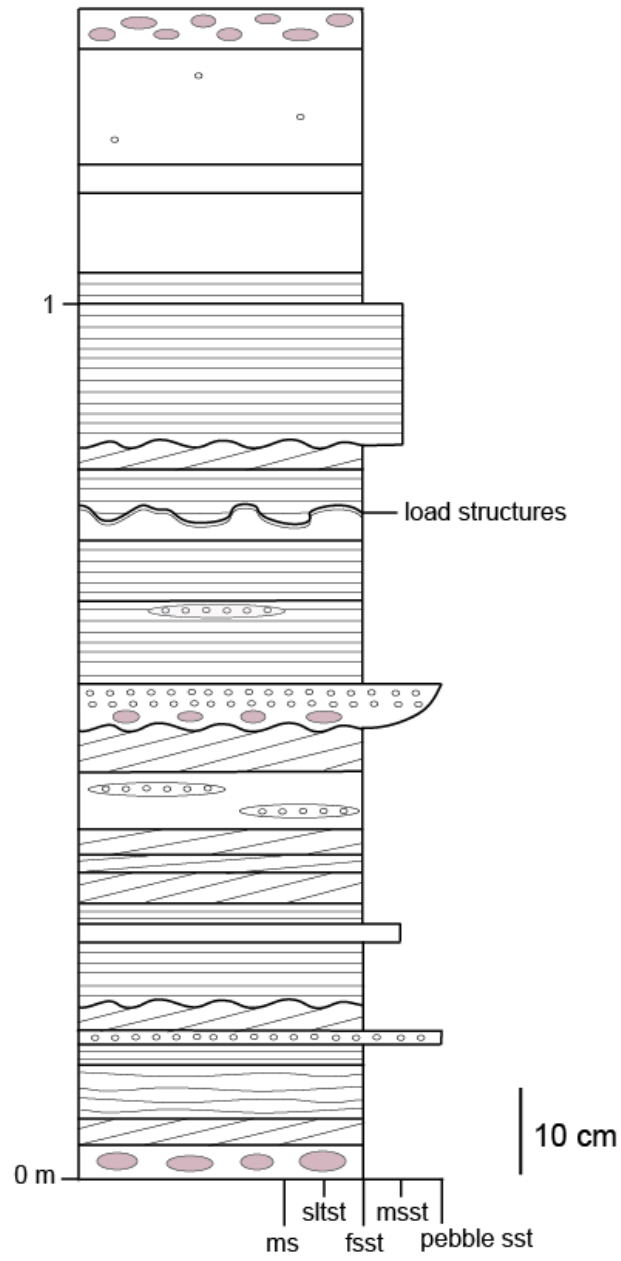
#617



#617 continued



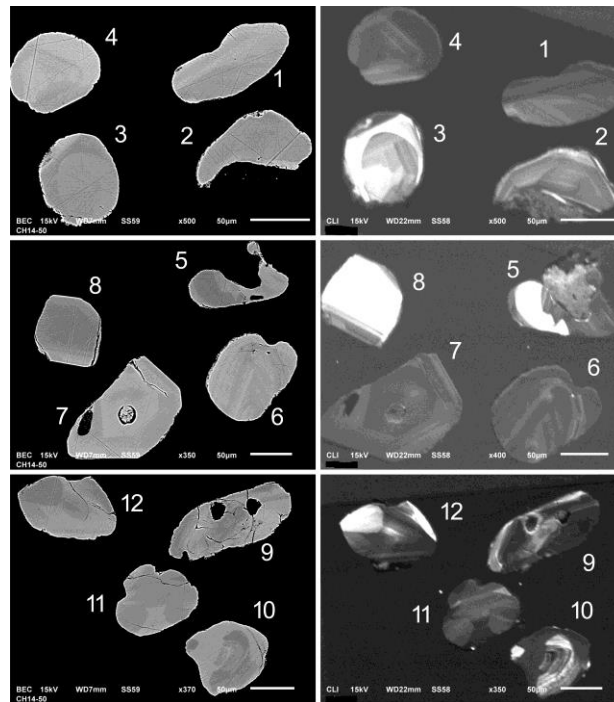
#626



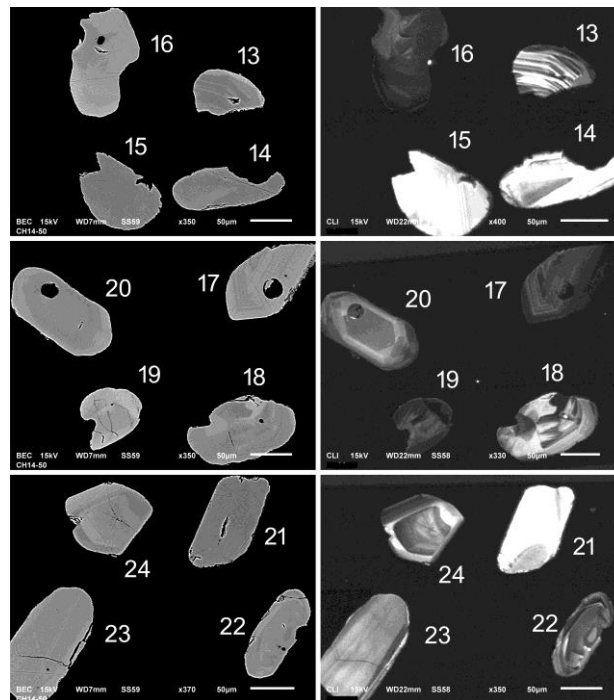
#652



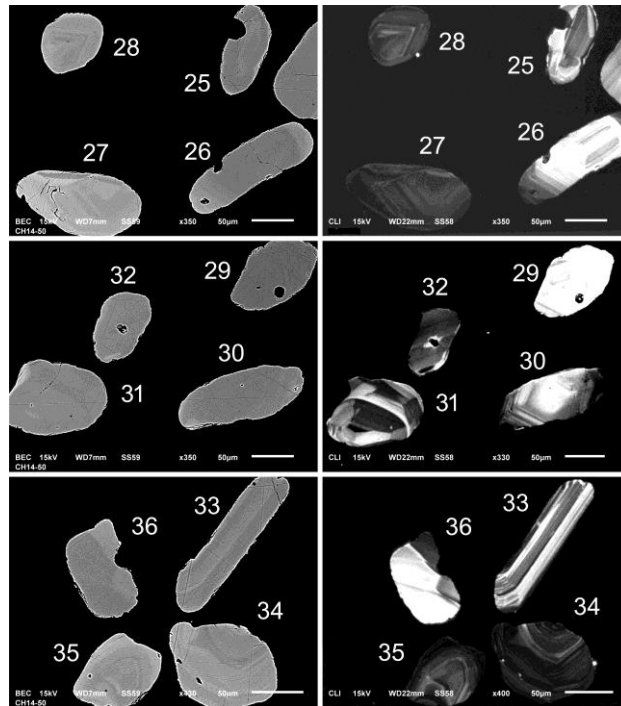
Appendix C: Supplementary back-scattered electron (BSE; left) and cathodoluminescence (CL; right) images of detrital zircon grains from the Gordon Lake and Bar River formations.



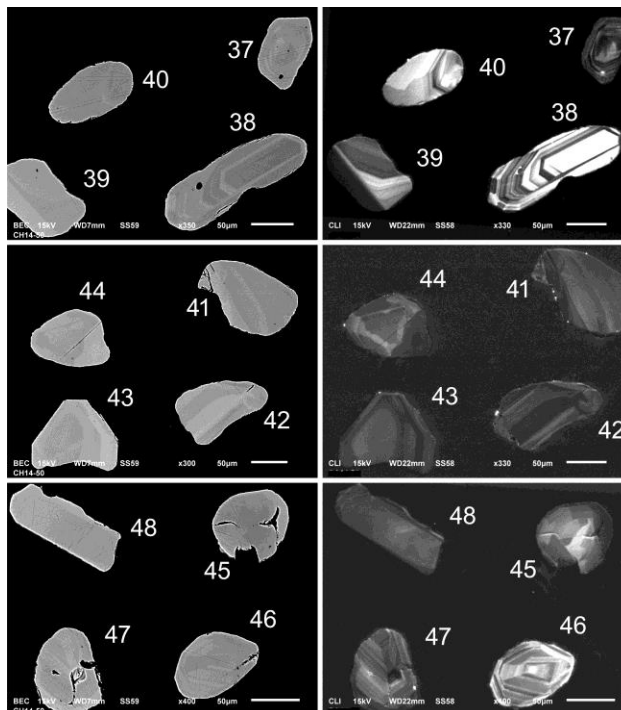
CH-14-50, zircon grains 1-12



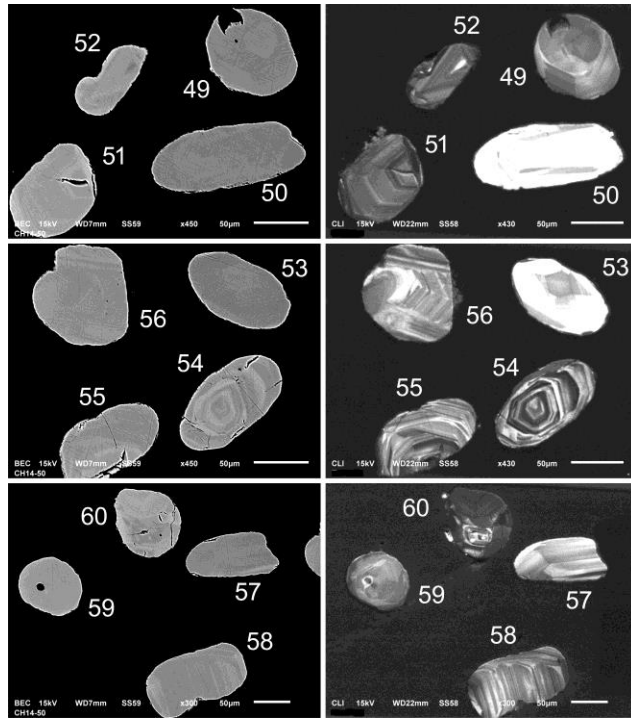
CH-14-50, zircon grains 13-24



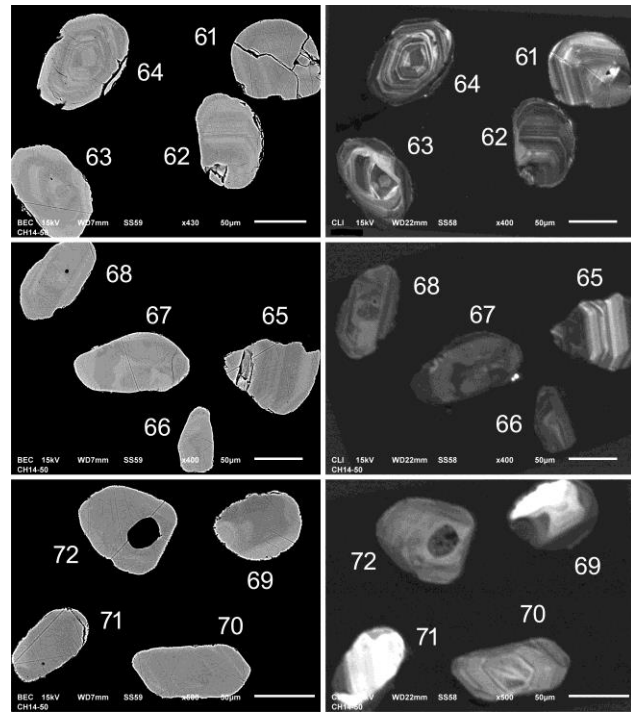
CH-14-50, zircon grains 25-36



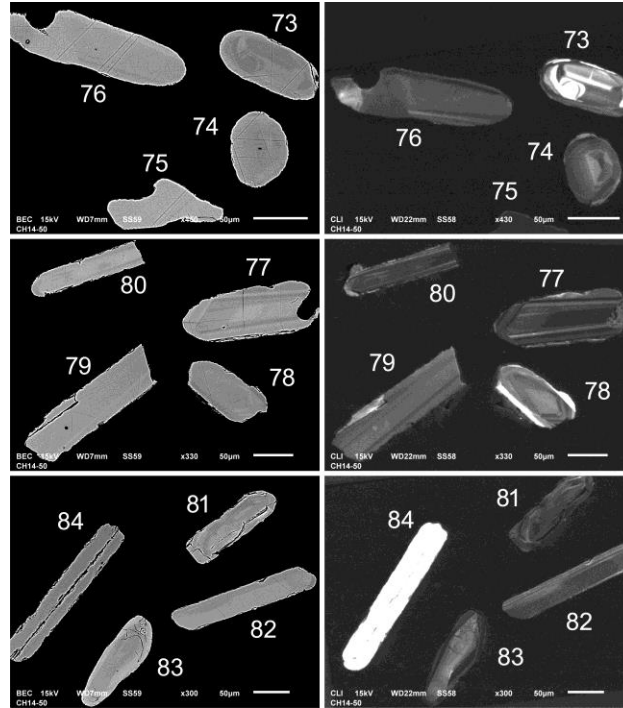
CH-14-50, zircon grains 37-48



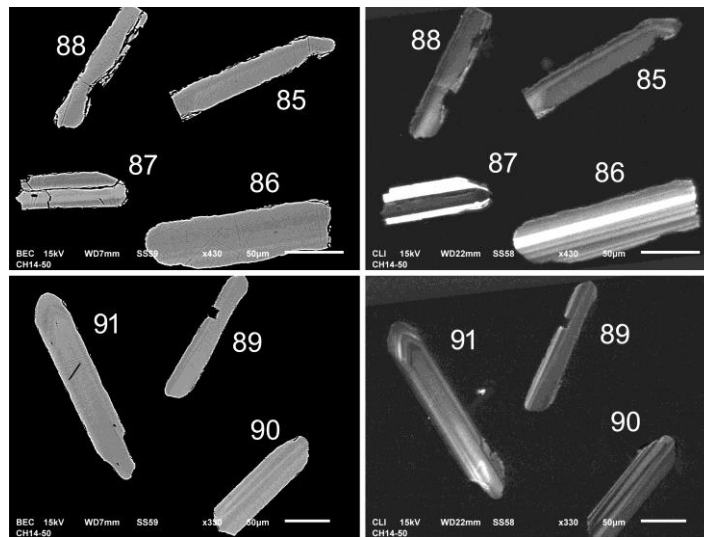
CH-14-50, zircon grains 49-60



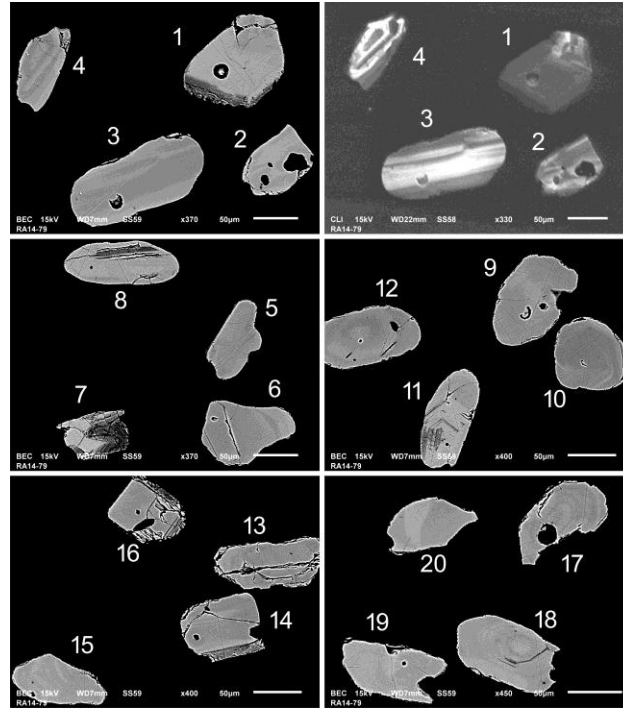
CH-14-50, zircon grains 61-72



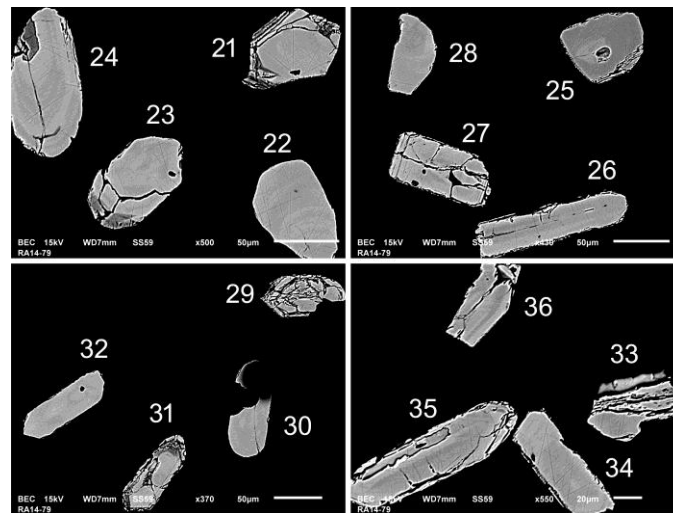
CH-14-50, zircon grains 73-84



CH-14-50, zircon grains 85-91



RA-14-79, zircon grains 1-20 (only grains 1-4 imaged in CL; the rest imaged in BSE)



RA-14-79, zircon grains 21-36 (imaged in BSE)

Appendix D: Laser-ablation inductively coupled plasma mass spectroscopy (LA-ICP-MS) data from detrital zircons in the Gordon Lake and Bar River formations.

	Spot	U (ppm)	Pb ²⁰⁶	Th/U	$\frac{^{207}\text{Pb}}{^{235}\text{U}}$	1 Sig	$\frac{^{206}\text{Pb}}{^{238}\text{U}}$	1 Sig	Err. Correl.	$\frac{^{207}\text{Pb}/^{206}\text{Pb}}$ Age (Ma)	1 Sig	$\frac{^{207}\text{Pb}/^{235}\text{Pb}}$ Age (Ma)	1 Sig	$\frac{^{206}\text{Pb}/^{238}\text{U}}$ Age (Ma)	1 Sig	Disc. (%)
1^a	CH-14-50	Sandstone, Gordon Lake Formation														
1	CH14-50-55rnd	50	22	0.6	8.724	0.151	0.4373	0.0064	0.8431	2284	16	2310	16	2339	29	-3
2	CH14-50-82srd, lpr	198	92	0.8	9.305	0.182	0.4645	0.0073	0.8012	2291	20	2369	18	2459	32	-9
3	CH14-50-77srd	168	75	0.8	8.984	0.149	0.4451	0.0062	0.8420	2304	15	2336	15	2373	28	-4
4	CH14-50-84srd, lpr	39	18	2.2	9.129	0.222	0.4511	0.0070	0.6400	2309	32	2351	22	2400	31	-5
5	CH14-50-17srd, st	224	101	0.8	9.182	0.152	0.4531	0.0066	0.8730	2311	14	2356	15	2409	29	-5
6	CH14-50-81srd, st	272	116	1.3	8.642	0.163	0.4263	0.0066	0.8173	2311	19	2301	17	2289	30	1
7	CH14-50-79srd, lpr	35	15	0.5	8.723	0.162	0.4299	0.0065	0.8142	2313	18	2310	17	2305	29	0
8	CH14-50-91srd, lpr	207	94	0.6	9.257	0.184	0.4552	0.0071	0.7839	2317	21	2364	18	2419	31	-5
9	CH14-50-88srd, lpr	424	206	2.7	9.910	0.194	0.4859	0.0078	0.8220	2322	19	2426	18	2553	34	-12
10	CH14-50-29srd, st	12	5	1.6	9.068	0.211	0.4426	0.0074	0.7176	2330	27	2345	21	2362	33	-2
11	CH14-50-90srd, lpr	354	165	0.4	9.560	0.182	0.4662	0.0074	0.8317	2331	18	2393	17	2467	32	-7
12	CH14-50-89srd, lpr	303	149	0.8	10.121	0.183	0.4934	0.0071	0.7973	2332	19	2446	17	2586	31	-13
13	CH14-50-9srd, st	36	16	0.5	8.950	0.172	0.4345	0.0068	0.8131	2339	19	2333	17	2326	30	1
14	CH14-50-85srd, lpr	154	72	0.9	9.638	0.193	0.4671	0.0075	0.8059	2342	20	2401	18	2471	33	-7

15	CH14-50-27rnd	931	420	0.1	9.716	0.218	0.4515	0.0083	0.8166	2414	22	2408	21	2402	37	1
16	CH14-50-24srd, st	58	28	0.6	11.025	0.192	0.4870	0.0069	0.8066	2499	17	2525	16	2558	30	-3
17	CH14-50-7srd, st	146	69	0.8	10.843	0.190	0.4772	0.0073	0.8719	2506	14	2510	16	2515	32	0
18	CH14-50-16srd	116	54	0.8	10.639	0.453	0.4657	0.0167	0.8405	2514	38	2492	39	2465	73	2
19	CH14-50-48srd	140	69	0.7	11.304	0.187	0.4910	0.0067	0.8304	2528	15	2549	15	2575	29	-2
20	CH14-50-4rnd, st	103	43	1.2	10.410	0.251	0.4218	0.0087	0.8507	2643	21	2472	22	2269	39	17
21	CH14-50-80srd, lpr	385	178	3.2	11.437	0.218	0.4618	0.0072	0.8171	2649	18	2559	18	2448	32	9
22	CH14-50-83rnd, lpr	738	384	0.4	12.937	0.292	0.5211	0.0103	0.8745	2653	18	2675	21	2704	43	-2
23	CH14-50-23rnd, st	90	35	2.0	9.657	0.156	0.3888	0.0051	0.8197	2654	15	2403	15	2117	24	24
24	CH14-50-43srd, st	124	68	0.6	13.653	0.238	0.5484	0.0080	0.8394	2658	16	2726	16	2818	33	-7
25	CH14-50-60srd	78	40	2.0	12.845	0.216	0.5143	0.0071	0.8267	2663	16	2668	16	2675	30	-1
26	CH14-50-57srd, st	20	11	1.4	13.381	0.272	0.5350	0.0092	0.8466	2666	18	2707	19	2763	39	-4
27	CH14-50-19srd	419	215	0.4	12.867	0.223	0.5125	0.0074	0.8298	2672	16	2670	16	2667	31	0
28	CH14-50-41srd, st	74	39	0.9	13.253	0.211	0.5267	0.0070	0.8366	2675	14	2698	15	2728	30	-2
29	CH14-50-26rnd	44	24	0.7	13.766	0.232	0.5471	0.0077	0.8332	2676	15	2734	16	2813	32	-6
30	CH14-50-40rnd	17	9	1.2	13.473	0.239	0.5353	0.0078	0.8149	2676	17	2713	17	2764	33	-4
31	CH14-50-8srd, st	24	13	1.1	12.976	0.251	0.5153	0.0082	0.8183	2677	18	2678	18	2679	35	0
32	CH14-50-15srd	36	19	1.2	13.482	0.264	0.5342	0.0085	0.8117	2681	19	2714	18	2759	36	-4

	Spot	U (ppm)	Pb ²⁰⁶	Th/U	$\frac{^{207}\text{Pb}}{^{235}\text{U}}$	1 Sig	$\frac{^{206}\text{Pb}}{^{238}\text{U}}$	1 Sig	Err. Correl.	$\frac{^{207}\text{Pb}/^{206}\text{Pb}}{\text{Age (Ma)}}$	1 Sig	$\frac{^{207}\text{Pb}/^{235}\text{Pb}}{\text{Age (Ma)}}$	1 Sig	$\frac{^{206}\text{Pb}/^{238}\text{U}}{\text{Age (Ma)}}$	1 Sig	Disc. (%)	
1^a	CH-14-50	Sandstone, Gordon Lake Formation															
33	CH14-50-11srd, st	118	62	1.3	13.265	0.237	0.5238	0.0078	0.8318	2686	16	2699	17	2715	33	-1	
34	CH14-50-3rnd, st	31	16	1.2	13.359	0.283	0.5269	0.0092	0.8273	2688	20	2705	20	2728	39	-2	
35	CH14-50-49rnd	27	15	1.6	13.552	0.247	0.5344	0.0079	0.8083	2689	18	2719	17	2760	33	-3	
36	CH14-50-31rnd, st	19	10	1.1	13.451	0.276	0.5299	0.0089	0.8186	2690	19	2712	19	2741	37	-2	
37	CH14-50-56srd, st	25	13	0.8	13.292	0.226	0.5234	0.0073	0.8177	2691	16	2701	16	2714	31	-1	
38	CH14-50-12srd, st	280	146	0.6	13.313	0.251	0.5239	0.0083	0.8360	2692	17	2702	18	2716	35	-1	
39	CH14-50-47rnd	99	52	1.1	13.466	0.218	0.5295	0.0071	0.8236	2693	15	2713	15	2739	30	-2	
40	CH14-50-30srd	37	19	1.0	13.174	0.233	0.5180	0.0075	0.8189	2693	17	2692	17	2691	32	0	
41	CH14-50-18srd	56	31	1.4	14.111	0.232	0.5542	0.0075	0.8220	2695	15	2757	16	2842	31	-7	
42	CH14-50-59rnd	36	19	0.8	13.707	0.235	0.5378	0.0077	0.8372	2697	15	2730	16	2774	32	-4	
43	CH14-50-35srd, st	57	30	1.1	13.712	0.239	0.5378	0.0076	0.8129	2697	17	2730	16	2774	32	-4	
44	CH14-50-1rnd, st	140	76	1.3	13.905	0.255	0.5452	0.0084	0.8441	2698	16	2743	17	2805	35	-5	
45	CH14-50-22srd, st	100	53	2.0	13.470	0.229	0.5278	0.0074	0.8287	2699	16	2713	16	2732	31	-1	
46	CH14-50-42srd, st	91	48	0.5	13.568	0.223	0.5314	0.0073	0.8349	2700	15	2720	15	2747	31	-2	
47	CH14-50-76rnd, lpr	57	29	0.7	13.288	0.236	0.5198	0.0075	0.8183	2702	17	2700	17	2698	32	0	
48	CH14-50-6rnd	91	50	0.8	13.972	0.249	0.5462	0.0081	0.8349	2703	16	2748	17	2809	34	-5	

49	CH14-50-45rnd	46	24	1.2	13.017	0.219	0.5089	0.0070	0.8173	2703	16	2681	16	2652	30	2
50	CH14-50-20srd, st	89	48	1.4	13.726	0.214	0.5365	0.0071	0.8428	2703	14	2731	15	2769	30	-3
51	CH14-50-32srd, st	51	26	0.7	12.902	0.207	0.5038	0.0068	0.8430	2705	14	2673	15	2630	29	3
52	CH14-50-44rnd	78	45	0.5	14.794	0.295	0.5773	0.0096	0.8319	2706	18	2802	19	2938	39	-11
53	CH14-50-58srd, st	36	19	0.6	13.337	0.234	0.5203	0.0075	0.8251	2706	16	2704	17	2700	32	0
54	CH14-50-2rnd, st	64	33	1.1	13.107	0.221	0.5106	0.0073	0.8503	2709	15	2687	16	2659	31	2
55	CH14-50-37srd, st	55	29	0.9	13.424	0.240	0.5208	0.0079	0.8476	2715	16	2710	17	2703	33	1
56	CH14-50-51rnd, st	54	30	1.0	14.124	0.236	0.5479	0.0077	0.8435	2716	15	2758	16	2816	32	-5
57	CH14-50-33srd, lpr	52	26	0.3	12.994	0.259	0.5037	0.0085	0.8492	2717	17	2679	19	2629	36	4
58	CH14-50-50rnd	15	8	0.2	13.795	0.257	0.5340	0.0079	0.7977	2719	18	2736	18	2758	33	-2
59	CH14-50-34rnd, st	100	55	1.5	14.105	0.269	0.5450	0.0087	0.8421	2722	17	2757	18	2804	36	-4
60	CH14-50-38srd	30	16	0.5	13.826	0.243	0.5333	0.0078	0.8286	2725	16	2738	17	2755	33	-1
61	CH14-50-28rnd, st	206	112	1.3	14.091	0.262	0.5432	0.0084	0.8319	2726	17	2756	18	2797	35	-3
62	CH14-50-86srd, lpr	100	56	2	14.697	0.298	0.5645	0.0090	0.7893	2732	20	2796	19	2885	37	-7
63	CH14-50-54rnd	60	32	1.2	13.980	0.225	0.5368	0.0074	0.8597	2732	14	2748	15	2770	31	-2
64	CH14-50-36srd, st	24	13	1.3	14.280	0.263	0.5458	0.0082	0.8221	2740	17	2769	17	2808	34	-3
65	CH14-50-21srd, st	43	24	0.5	14.532	0.264	0.5540	0.0080	0.8005	2744	18	2785	17	2842	33	-4
66	CH14-50-87srd, lpr	59	24	3	10.525	0.331	0.4005	0.0093	0.7358	2747	35	2482	29	2171	43	25

	Spot	U (ppm)	Pb ²⁰⁶	Th/U	$\frac{^{207}\text{Pb}}{^{235}\text{U}}$	1 Sig	$\frac{^{206}\text{Pb}}{^{238}\text{U}}$	1 Sig	Err. Correl.	$\frac{^{207}\text{Pb}/^{206}\text{Pb}}$ Age (Ma)	1 Sig	$\frac{^{207}\text{Pb}/^{235}\text{Pb}}$ Age (Ma)	1 Sig	$\frac{^{206}\text{Pb}/^{238}\text{U}}$ Age (Ma)	1 Sig	Disc. (%)
1^a	CH-14-50	Sandstone, Gordon Lake Formation														
67	CH14-50-25srd, st	29	16	0.8	14.966	0.313	0.5675	0.0098	0.8284	2753	19	2813	20	2897	40	-7
68	CH14-50-10srd	72	39	0.5	14.426	0.414	0.5456	0.0126	0.8074	2757	28	2778	27	2807	53	-2
69	CH14-50-46rnd, st	21	12	0.5	14.578	0.270	0.5506	0.0083	0.8180	2760	17	2788	18	2828	35	-3
70	CH14-50-52rnd	49	28	1.0	15.270	0.251	0.5707	0.0080	0.8556	2777	14	2832	16	2911	33	-6
71	CH14-50-53rnd	27	15	1.5	15.376	0.244	0.5691	0.0074	0.8257	2793	15	2839	15	2904	31	-5
72	CH14-50-14srd	27	15	0.7	15.315	0.306	0.5659	0.0092	0.8174	2795	19	2835	19	2891	38	-4
73	CH14-50-39rnd, st	59	34	0.0	15.708	0.264	0.5763	0.0082	0.8517	2807	14	2859	16	2934	34	-6
74	CH14-50-13srd	123	72	0.9	16.087	0.302	0.5829	0.0089	0.8139	2828	18	2882	18	2960	36	-6
75	CH14-50-5rnd	84	49	0.3	16.048	0.285	0.5772	0.0089	0.8682	2840	14	2880	17	2937	36	-4
2^a	RA-14-79	Claystone, Bar River Formation														
1	RA14-79-26srd, lpr	123	54	0.3	8.686	0.181	0.4366	0.0076	0.8384	2279	19	2306	19	2335	34	-3
2	RA14-79-24rnd, st	274	117	0.6	8.651	0.152	0.4288	0.0062	0.8186	2304	17	2302	16	2300	28	0

3	RA14-79-32srd, lpr	149	64	0.6	8.699	0.168	0.4296	0.0067	0.8027	2310	20	2307	18	2304	30	0
4	RA14-79-30rnd	79	35	0.4	9.094	0.173	0.4470	0.0068	0.8028	2318	19	2348	17	2382	30	-3
5	RA14-79-9rnd, st	84	37	0.4	9.018	0.172	0.4345	0.0068	0.8209	2352	19	2340	17	2326	30	1
6	RA14-79-11rnd	223	51	0.4	4.743	0.223	0.2283	0.0104	0.9726	2354	19	1775	39	1326	55	48
7	RA14-79-18srd, st	152	70	0.5	9.608	0.177	0.4617	0.0069	0.8141	2357	18	2398	17	2447	30	-5
8	RA14-79-22rnd, st	185	85	0.5	9.555	0.169	0.4578	0.0067	0.8333	2362	17	2393	16	2430	30	-3
9	RA14-79-1rnd, st	141	62	0.2	9.245	0.169	0.4414	0.0064	0.7889	2368	19	2363	17	2357	28	1
10	RA14-79-2rnd, st	128	53	1.2	8.755	0.151	0.4140	0.0057	0.7893	2384	18	2313	16	2233	26	7
11	RA14-79-21srd, st	289	117	0.5	8.692	0.242	0.4051	0.0101	0.8948	2409	21	2306	25	2192	46	11
12	RA14-79-27srd, st	129	37	0.6	6.550	0.165	0.2915	0.0062	0.8492	2487	22	2053	22	1649	31	38
13	RA14-79-25srd, st	44	22	1.0	11.143	0.210	0.4880	0.0070	0.7592	2514	21	2535	18	2562	30	-2
14	RA14-79-16srd, st	78	39	0.6	11.449	0.191	0.4993	0.0068	0.8202	2521	16	2560	16	2611	29	-4
15	RA14-79-23rnd, st	190	85	0.6	10.280	0.221	0.4477	0.0080	0.8297	2523	20	2460	20	2385	35	7
16	RA14-79-34srd, lpr	163	78	0.6	11.016	0.196	0.4793	0.0067	0.7842	2525	19	2524	17	2524	29	0
17	RA14-79-10rnd	27	12	0.8	10.726	0.212	0.4656	0.0068	0.7427	2529	22	2500	18	2464	30	3
18	RA14-79-6rnd, st	130	65	0.5	11.558	0.223	0.4991	0.0079	0.8252	2537	18	2569	18	2610	34	-3
19	RA14-79-17srd, st	104	45	1.2	10.047	0.236	0.4278	0.0085	0.8448	2561	21	2439	22	2296	38	12
20	RA14-79-33srd, st	313	86	1.2	6.450	0.160	0.2740	0.0058	0.8590	2565	21	2039	22	1561	29	44
21	RA14-79-5rnd, st	131	59	0.6	10.901	0.195	0.4527	0.0065	0.7983	2603	18	2515	17	2407	29	9
22	RA14-79-12rnd, st	33	17	1.2	12.597	0.240	0.5013	0.0076	0.7990	2674	19	2650	18	2619	33	2

23	RA14-79-15rnd	73	35	0.6	12.323	0.208	0.4816	0.0068	0.8335	2703	15	2629	16	2534	29	8
24	RA14-79-3rnd	59	33	1.3	14.590	0.294	0.5562	0.0090	0.8028	2744	20	2789	19	2851	37	-5
25	RA14-79-14srd, st	272	17	0.8	1.662	0.039	0.0633	0.0013	0.9106	2745	16	994	15	396	8	88
26	RA14-79-35rnd, lpr	117	63	0.6	14.149	0.281	0.5391	0.0088	0.8164	2745	19	2760	19	2780	37	-2
27	RA14-79-4srd	135	73	0.9	18.379	0.341	0.5421	0.0082	0.8142	3158	17	3010	18	2792	34	14

NOTES:

Samples are individually sorted from lowest to highest $^{207}\text{Pb}/^{206}\text{Pb}$ age

rnd - rounded, srd - subrounded, lpr - long prismatic, st - stubby

Err. Correl. - Error correlation coefficient for concordia coordinates

Disc. - Discordance

Relation between ages and concordia coordinates: $Y = ^{206}\text{Pb}/^{238}\text{U} = \text{EXP}(L238*(206-238\text{Age})) - 1$;

$X = ^{207}\text{Pb}/^{235}\text{U} = \text{EXP}(L235*(207-235\text{Age})) - 1$

$^{207}\text{Pb}/^{206}\text{Pb} = 137.88*X/Y$; U decay constants (L238 & L235) from Jaffey et al. (1971).

^aAnalysis number refers to the order in which the grains were analyzed. The grains are numbered (spot) according to the numbering on the whole-grain mount LA140919.

Curriculum Vitae

Name: Carolyn M. Hill

Post-secondary Education and Degrees: The University of Western Ontario
London, Ontario, Canada
2014-present; Ph.D. Candidate in Geology

The University of Western Ontario
London, Ontario, Canada
2009-2015; B.Sc.

Honours and Awards: Robert and Ruth Lumsden Graduate Award in Earth Sciences
2019
20th International Sedimentological Congress Student Travel Grant
2018
Western Graduate Research Scholarship
2014-2016, 2018
Ontario Graduate Scholarship
2017-2018
GAC-MAC Student Travel Grant
2017
Queen Elizabeth II Graduate Scholarship in Science & Technology
2016-2017
Gordon Dixon Award, Department of Earth Sciences
2013-2014

Related Work Experience: Lecturer for ES3314B: Sedimentary Petrology
The University of Western Ontario
2017-2019

Teaching Assistant
The University of Western Ontario
2014-2018

Peer Reviewed Publications:

Hill, C.M., Davis, D.W., and Corcoran, P.L. (2018). New U-Pb geochronology evidence for 2.3 Ga detrital zircon grains in the youngest Huronian Supergroup formations, Canada. *Precambrian Research* 314: 428-433.

Hill, C.M. and Corcoran, P.L. (2018). Processes responsible for the development of soft-sediment deformation structures (SSDS) in the Paleoproterozoic Gordon Lake Formation, Huronian Supergroup, Canada. *Precambrian Research* 310: 63-75.

Hill, C., Corcoran, P.L., Aranha, R., and Longstaffe, F.J. (2016) Microbially induced sedimentary structures in the Paleoproterozoic, upper Huronian Supergroup, Canada. *Precambrian Research* 281: 155-165.

Conference abstracts (8 total):

Hill, C.M., and Corcoran, P.L. (accepted) A Paleoproterozoic macro-tidal to shallow marine shelf characterized by microbial, tide, and storm activity: the Gordon Lake Formation, Huronian Supergroup. Geological Association of Canada-Mineralogical Association of Canada-International Association of Hydrogeologists (GAC-MAC-IAH), Joint Annual Meeting; Québec City, QC, May 12-15.

Hill, C.M., and Corcoran, P.L. (2018) Development of soft-sediment deformation structures in the Paleoproterozoic Gordon Lake Formation, Huronian Supergroup, Canada. 20th International Sedimentological Congress (ISC), Book of Abstracts 1-343; Québec City, QC, August 13-17.

Hill, C.M., and Corcoran, P.L. (2015) Microbially induced sedimentary structures (MISS) from the Paleoproterozoic Gordon Lake Formation, Huronian Supergroup, Canada. Geological Society of America (GSA) Annual Meeting, Abstracts with Programs Vol. 47, No. 7, pg. 177; Baltimore, MD., November 1-4.